

A key to the genera and species of the transversely-dividing Flabellidae (Anthozoa, Scleractinia, Flabellidae), with a guide to the literature, and the description of two new species

Stephen D. Cairns¹

¹ Department of Invertebrate Zoology, National Museum of Natural History, Smithsonian Institution, Washington, DC 20560, USA

Corresponding author: Stephen D. Cairns (cairnss@si.edu)

Academic editor: B. W. Hoeksema | Received 24 November 2015 | Accepted 12 January 2016 | Published 10 February 2016

<http://zoobank.org/D11C6C1E-6EE7-4C8D-A560-331E75947EC8>

Citation: Cairns SD (2016) A key to the genera and species of the transversely-dividing Flabellidae (Anthozoa, Scleractinia, Flabellidae), with a guide to the literature, and the description of two new species. ZooKeys 562: 1–48. doi: 10.3897/zookeys.562.7310

Abstract

The transversely-dividing flabellids consist of five genera (*Truncatoflabellum*, *Placotrochides*, *Blastotrochus*, *Placotrochus*, and *Falcatoflabellum*) and 45 species. A dichotomous key is provided for these five genera as well as the species of the genus *Truncatoflabellum* and *Placotrochides*, the other three genera being monotypic. A tabular key is also provided for the 38 species of *Truncatoflabellum*. Two new combinations are suggested (*T. gambiense* and *T. sphenodeum*) and two new species are described (*T. duncani* and *T. mozambiquensis*). All but one species are illustrated and accompanied by their known distribution and a guide to the pertinent literature for the species. New records of 19 of the 45 species are listed. The transversely-dividing flabellids range from the Middle Eocene to the Recent at depths of 2–3010 m, and constitute 60% of the 65 known extant species of transversely-dividing Scleractinia.

Keywords

Flabellidae, *Truncatoflabellum*, *Placotrochides*, *Blastotrochus*, *Placotrochus*, *Falcatoflabellum*, transversely dividing, key, asexual reproduction

Introduction

Confronted with a large collection of *Truncatoflabellum* during a recent (2014) trip to Taiwan, it became apparent that the literature on the species of this genus was scattered and not well organized. Although there were some keys to the species, they were regional in nature, i.e., Philippine region (Cairns 1989b), southwest Indian Ocean (Cairns and Keller 1993), North Pacific (Cairns 1994), and Western Australia (Cairns 1998). No unified key or comparative table existed to update that of Cairns (1989b). *Truncatoflabellum* is the seventh largest Holocene genus among the approximately 240 living scleractinian genera, and thus a key to the species and guide to the pertinent literature was thought appropriate. (The most speciose Holocene scleractinian genera are (Hoeksema and Cairns 2015): *Acropora* – about 120 living species, *Caryophyllia* – 75 species, *Balanophyllia* – 59 species, *Montipora* – about 56 species, *Flabellum* – 42 species, *Porites* – about 41 species, and then *Truncatoflabellum*, with 32 living species). The four other truncate flabellid genera are included for completeness: *Blastotrochus*, *Placotrochides*, *Placotrochus*, and *Falcatoflabellum*. Of the 120 living azooxanthellate genera (Roberts et al. 2009), 17 of them (14.2% of the genera) and 65 of the approximately 725 azooxanthellate species (or 9.0% of the species) represent transversely-dividing species: i.e., the five flabellid genera previously listed and: *Anthemiphyllia* (in part), *Australocyathus*, *Bourneotrochus*, *Caryophyllia* (in part), *Dunocyathus*, *Endopachys*, *Idiotrochus*, *Kionotrochus*, *Notophyllia*, *Peponocyathus*, *Trochocyathus* (in part), and *Truncatoguyunia*.

Fossil Truncatoflabellum: Because of the easily diagnosed aspect of the anthocya thus basal scar, fossil *Truncatoflabellum* are easily distinguished, even though most have been attributed to the genus *Flabellum*. Most fossil flabellids cannot be correlated to Recent species, but on the other hand, several have been described as discrete species. The earliest record of a transversely-dividing fossil flabellid was that of Duncan (1864), who reported three truncate species from southern Australia: *F. victoriae* (= *T. victoriae*) from Muddy Creek (Middle Miocene), Victoria; *F. gambierense* (= *T. gambierense*) from Mount Gambier, S. Australia (Middle Miocene), and *F. candeanum* (= *T. duncani*, herein) from the “Murray Tertiaries”, Victoria; these specimens are deposited in the BM. These records were reiterated by Duncan (1870), with the slight addition of several more specimens. Tenison-Woods (1878b) reported additional fossil records of *F. gambierense* and *F. victoriae* from Cape Otway, Victoria (Middle Miocene) and Muddy Creek, Victoria (Middle Miocene), respectively. Specimens from that paper were deposited primarily in the Macleayan Museum, Sydney. The first fossil *Truncatoflabellum* from New Zealand were reported by Tenison-Woods (1880) from the Upper Oligocene Pareora beds: *T. corbicula*, *T. sphenodeum*, and *T. simplex* (types deposited at NZGS, now the GNS). Dennant (1899) added another Miocene species to the Australian fauna, *F. gippslandicum*, from the Gippsland Lake region of Victoria, a species quite similar to *T. victoriae*. The types from that paper were deposited at the NMV. Gerth (1921) reported three *Truncatoflabellum* from the Lower Miocene to Pliocene of Java, all of which can be related to living species (specimens deposited at the RGM). Umb-

grove (1938) reported eight specimens as *Flabellum rubrum* from the Pleistocene of Talaud, Celebes, one of which is *T. aculeatum*, four of which are unidentifiable to species, and three are *Trochocyathus*. Although not illustrated by Umbgrove (1938), these specimens are also deposited at the RGM (35461). Umbgrove (1950) also reported two *Truncatoflabellum* species from the Lower Pleistocene of the Putjangan Beds of Java, part of one of which has been re-identified as *T. carinatum* (see Cairns, 1989b). Those specimens were deposited at the Institute of Mines at Delft in 1989. Various species of *Truncatoflabellum* from the Pliocene of Taiwan and Plio-Pleistocene of the Ryukyu Islands were reported by Yabe and Eguchi (1942a, b) under the rubric of *F. rubrum*. Most of these specimens, deposited at the TIUS, were examined by the author and re-identified in Cairns (1989b). Yabe and Eguchi (1941) also reported one fossil *Truncatoflabellum* (= *T. spheniscus*) from the “Neogene” of Java. Squires (1958: pl. 12, figs 6-7) illustrated two *Truncatoflabellum* from the Altonian (Lower Miocene) of New Zealand as *Flabellum rubrum rubrum*, but these are certainly not *F. rubrum* and have not been subsequently re-identified. Most specimens from that paper are deposited at the AUC. Hayward reported *F. sphenodeum* (= *T. sphenodeum*) from the Lower Miocene of North Auckland, New Zealand; these specimens are also deposited at the AUC. Wells (1984) reported two species from the Late Pleistocene deposits of Kere River, Santo, Vanuatu: *F. vanuatu* (= *T. vanuatu*) and *F. paripavoninum* (= *T. mortenseni*); these specimens are deposited at the NMNH. Finally, Hu (1987) reported two truncate flabellids from the Maanshan Mudstone (Plio-Pleistocene) of Hengchun Peninsula, southern Taiwan: *Flabellum transversale* (= *T. carinatum*) and *Flabellum elongatum* (= *Placotrochides scaphula*); these specimens are deposited at the National Museum of Natural Science, Taichung, Taiwan, and seen by the author in 2014. Hu (1988) also reported *Flabellum rubrum stokesii* from the Tunghsiao and Lungkang Pleistocene formations of the Miaoli District, northern Taiwan, some of which are probably *T. carinatum*.

It should be noted that in a comprehensive phylogenetic analysis of the Scleractinia using the CO1 gene (Kitahara et al. 2010), in which 65 additional deep-water species were included to the data base, *Truncatoflabellum* was found to be polyphyletic and always ancestral to species within the genus *Flabellum*. Both genera have their earliest records in the Eocene.

Methods

This is not a taxonomic revision or a phylogenetic or morphometric analysis. It is a key to facilitate identification of a species-rich group, accompanied with a guide to the literature. The synonymies are not exhaustive, but include the original description and those papers that were found useful in identification of the species, especially those that contain useful illustrations, descriptions and/or extended synonymy. Furthermore, the key incorporates exclusively fossil species that occur in the respective genera. Since the key is intended to serve a practical purpose and include fossil species, molecular sequencing was not employed.

In an effort to discuss and illustrate morphologically similar species in adjacent text, and to facilitate their identification through keys, the text and illustrations are arranged in the order in which they occur in the key.

The key is based primarily on the morphology of the (free-living) anthocyathus stage of each species, the founding (attached) anthocaulus stage rarely being collected and usually of generic morphology. The shape of the anthocyathus contains the primary distinguishing set of characters for these genera, the shape most accurately defined by the thecal edge and face angles (Fig. 1). These two measurements geometrically define the GCD:LCD, and thus that index is not an independent one, but is presented in Table 2 because of its ease in visualization. The H:GCD is a general measure of the height of the corallum, but is dependent on the size (maturity) of the corallum, thus adult specimens are best measured for this characteristic. The maximum greater scar diameter (GSD), on the other hand, is fairly constant, being the same size for juvenile or large specimens; however, the ratio of GSD:GCD is dependent on the size of the corallum. In addition to shape criteria, the number of pairs of thecal edge spines seems to be relatively constant, some species having none, others one basal pair, others four or more pairs, and still others two or three pairs. The purpose of the thecal edge spines is unknown, however Tokuda et al. (2010) suggest that they function to stabilize “the life position” of the anthocyathus after transverse division. Several species have crests instead of spines. Other characters useful in differentiating species are: number and symmetry of the septa, nature of the upper outer edges of the septa as they meet the theca (e.g., notched, attenuate, abrupt), and corallum color. Geography, fossil occurrence, and even depth distribution may also be used as circumstantial characters.

Of the 45 species of truncate flabellids, 41 are represented in the NMNH collections, including types of 27 of those species. Of those four species not represented in the NMNH collections, photographs were obtained of three (*T. inconstans*, *T. gipp-landicum*, and *T. sphenodeum*); only *T. trapezoideum* (known only from one specimen deposited in Moscow) was not re-examined and not illustrated herein. Whenever possible, five views of a typical anthocyathus of each species is presented in a vertical arrangement, top to bottom: lateral face, edge, basal scar, calice, and oblique calice.

Abbreviations used in the text include

| | |
|----------------|---|
| AUC | Auckland University College (Dept. of Geology), New Zealand |
| BM | British Museum, London (The Natural History Museum) |
| EAN | Edge Angle: angle formed by two lateral edges of an anthocyathus (Fig. 1) |
| FAN | Face Angle: angle formed by two faces of an anthocyathus (Fig. 1) |
| GCD | Greater calicular diameter of anthocyathus (Fig. 1) |
| GCD:LCD | Ratio of greater calicular diameter to lesser calicular diameter of an anthocyathus |
| GNS | Institute of Geological and Nuclear Sciences, Lower Hutt, New Zealand |
| GSD | Greater scar diameter of anthocyathus (Fig. 1) |

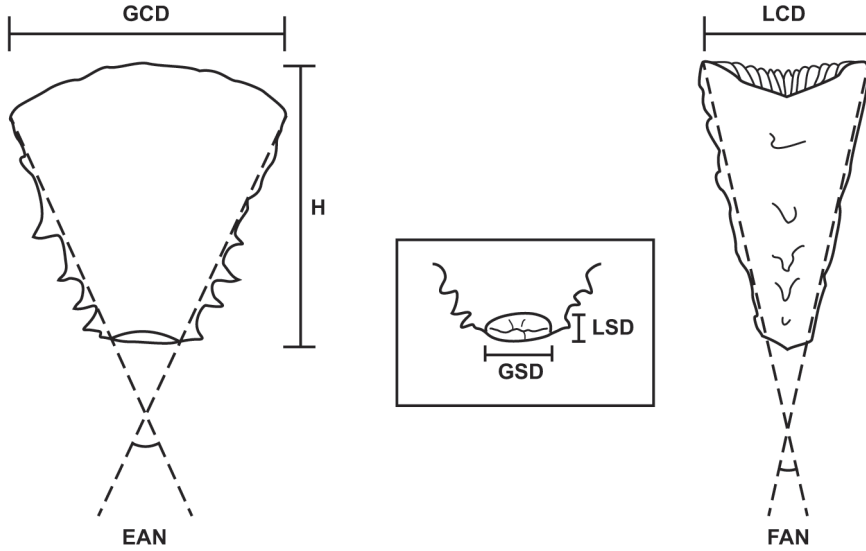


Figure 1. Diagram showing abbreviations of geometric terms used to describe truncate flabellids. Left: lateral view of an anthocyathus; center: basal scar of an anthocyathus; right: edge view of an anthocyathus. Abbreviations defined in Materials section.

- GSD:GCD** Ratio of basal greater scar diameter to greater calicular diameter of anthocyathus
- H** Height of corallum (Fig. 1)
- H:GCD** Ratio of corallum height to greater calicular diameter (Fig. 1)
- IOM** Institute of Okeanology, Moscow
- IWP** Indo-West Pacific
- LCD** Lesser calicular diameter of anthocyathus (Fig. 1)
- LSD** Lesser scar diameter of anthocyathus (Fig. 1)
- NMNH** National Museum of Natural History, Smithsonian Institution, Washington, DC
- NMV** National Museum of Victoria, Victoria, Australia
- NZGS** New Zealand Geological Survey (now the GNS), Lower Hutt, New Zealand
- RGM** National Museum of Geology and Mineralogy (at present Naturalis Biodiversity Center, Leiden)
- SAM** South African Museum, Cape Town
- SIPHILEXP** Smithsonian Institution Philippines Expedition
- SWIO** Southwest Indian Ocean
- S_x, C_x, P_x** Cycle of septa, costae, or pali, respectively, designated by numerical subscript
- S_x>S_y** In the context of a septal formula, septa of cycle x are wider than those of cycle y

| | |
|-------------------|---|
| Sx°>Sy° | In the context of a septal formula, septa size class x are wider than those of size class y |
| TIUS | Institute of Geology and Paleontology, Tohoku (Imperial) University, Sendai, Japan |
| USNM | United States National Museum (now the NMNH) |

Key to the Transversely-Dividing Flabellid Genera

- 1 Columella rudimentary (trabecular) or absent..... **2**
- 1' Columella lamellar or fascicular **4**
- 2 Anthocyathus buds only from a basal anthocaulus **3**
- 2' Anthocyathi bud from basal anthocaulus (transverse division) and from lateral edges of anthocaulus (forming anthoblasts) *Blastotrochus* (1 species)
- 3 Anthocyathus usually fan-shaped with divergent thecal edges, but if compressed-cylindrical in shape, the latter bear edge spines; base of anthocaulus not stereome-reinforced..... *Truncatoflabellum* (38 species)
- 3' Anthocyathus compressed-cylindrical in shape (edge angle 0-5°), lacking lateral spines; base of anthocaulus stereome-reinforced..... *Placotrochides* (4 species)
- 4 Columella lamellar..... *Placotrochus* (1 species)
- 4' Columella fascicular..... *Falcatoflabellum* (1 species)

Guide to the literature, distribution, and remarks

Family Flabellidae Bourne, 1905

Genus *Truncatoflabellum* Cairns, 1989b

Flabellum: Milne Edwards and Haime 1848: 257, 259 (in part: *flabelline tronquees*).—Vaughan and Wells 1943: 226-227 (in part).—Wells 1956: F432 (in part).—Zibrowius 1974: 19 (in part: group 2, but not *B. nutrix*).

Truncatoflabellum Cairns, 1989b: 60–61; 1994: 75; 1995: 113.—Cairns and Kitahara 2012: 14 (key to genus).

Diagnosis. Asexual reproduction by apical transverse division of corallum, resulting in distal anthocyathus and basal anthocaulus. Corallum usually laterally compressed and fan shaped, having one or more pairs of thecal edge spines or crests; some species compressed-cylindrical in shape but these always laterally spinose, whereas some fan-shaped coralla lack spines and crests. Columella absent or represented by a fusion of the lower, axial edges of larger septa. Anthocaulus not stereome-reinforced.

Discussion. The taxonomic history of this genus extends long before it was officially described, and is recounted and discussed by Cairns (1989b). To briefly re-

iterate, even as early as 1848 Milne Edwards and Haime (1848) placed these species in a section (=subgenus) they called the “*flabelline tronquees*”. Squires (1963: 10, 25) strongly felt that this group of species should be separated as a genus different from *Flabellum* but ultimately did not take an action, waiting for more biological justification. In Zibrowius’ (1974) revision of the family Flabellidae, he placed the transversely-dividing *Flabellum* as one of three “groups” in the larger conventional genus *Flabellum*. Finally, in a paper about the various modes of asexual reproduction, Cairns (1989a) suggested that transverse division represented a key innovation that led to an adaptive advantage for living on soft substrates, justifying the naming of a new genus. But, it was not until later in that year that Cairns (1989b) proposed the name *Truncatoflabellum*. As of this paper, there are 38 known species in the genus, six of these known only as fossils (Table 1).

Distribution. Middle Eocene (Bortonian) of New Zealand to Recent: cosmopolitan, except for the Antarctic, northeast Pacific and western Atlantic (generally low species diversity in Atlantic), 2–3010 m.

Type species. *Euphyllia spheniscus* Dana, 1846, by original designation.

Key to the species of *Truncatoflabellum* (characteristics pertain to the anthocyathus stage unless otherwise stated; + exclusively fossil species)

- | | | |
|----|---|---------------------------------|
| 1 | One or more pairs of thecal edge spines present | 2 |
| 1' | Thecal edge spines not present | 28 |
| 2 | Corallum compressed-cylindrical (edge angle 0–15°) | 3 |
| 2' | Corallum compressed-conical or fan-shaped (edge angle >15°) | 5 |
| 3 | Corallum small (GCD < 4.5 mm); rejuvenescence common, resulting in a high H:GCD (e.g., up to 4.3); corallum brown; 32 or less septa.... <i>T. phoenix</i> (Fig. 2A) | |
| 3' | Corallum larger (GCD >10 mm); rejuvenescence not common (H:GCD = 1–2); corallum white; 48 or more septa | 4 |
| 4 | Corallum with more than 48 septa (e.g., 76).... + <i>T. gippslandicum</i> (Fig. 2B) | |
| 4' | Corallum with 48 septa | + <i>T. victoriae</i> (Fig. 2C) |
| 5 | GCD < 12 mm..... | 6 |
| 5' | GCD > 12 mm..... | 9 |
| 6 | Tendency for anthocyathus to remain attached to anthocaulus | 7 |
| 6' | Anthocyathus and anthocaulus always detached | 8 |
| 7 | Thecal face angle low (14–18°), resulting in a high GCD:LCD (1.7–2.3); bimodal edge angle; IWP in distribution | <i>T. dens</i> (Fig. 2D) |
| 7' | Face angle higher (18–22°), resulting in a lower GCD:LCD (1.4–1.8); angle of thecal edges not bimodal; SWIO..... | <i>T. zuluense</i> (Fig. 3A) |
| 8 | Thecal edge angle low (14–18°), resulting in a small GCD:LCD (e.g., 1.4–1.7) | <i>T. pusillum</i> (Fig. 3B) |
| 8' | Thecal edge angle higher (28–52°), resulting in a higher GCD:LCD (e.g., 1.85–2.3)..... | <i>T. angustum</i> (Fig. 3C) |

9 One (basal) pair of thecal edge spines present **10**

9' Two or three pairs of thecal edge spines present **19**

9'' Four or more pairs of thecal edge spines present **26**

10 Thecal edge angle >80°; upper calicular edge strongly arched; S7 often present **11**

10' Thecal edge angle 15–80°; calicular edge not strongly arched; S7 never present **13**

11 Basal scar quite small (less than 4.3 mm in length), GSD:GCD < 0.1 *T. angiostrum* (Fig. 3D)

11' Basal scar large (up to 30 mm in length), GSD:GCD = 0.35–0.55 12

12 Thecal edge angle small (55–85°); GCD:LCD = 2.5–3.1 *T. macroeschara* (Fig. 4A)

12' Thecal edge angle larger (95–127°); GCD:LCD = 3.0–4.8 *T. veroni* (Fig. 4B)

13 H:GCD > 1; thecal edge angle 15–30° 14

13' H:GCD < 1; thecal edge angle 30–80° **17**

14 Anthocaulus and anthocyathus remain attached to each other; anthocaulus elongate, narrow, and often bent; Miocene of S. Australia and Victoria + *T. gambierense* (Fig. 4C)

14' Anthocaulus and anthocyathus detach from each other; anthocaulus not elongate; Recent of IWP **15**

15 Septa hexamerally arranged in three or four size classes (S1–2>S2>S4>S5); upper outer septal margin not notched **16**

15' Septa arranged in three size classes, but not hexamerally (e.g., 16–18: 16–18: 32–36); upper outer septal margin slightly notched ... *T. irregularare* (Fig. 4D)

16 Scar diameter up to 10 mm; Lower Miocene to Recent *T. incrustatum* (Fig. 5A)

16' Scar diameter less than 4 mm; Middle Eocene to Middle Miocene + *T. sphenodeum* (Fig. 5B)

17 GSD:GCD < 0.3 *T. crassum* (Fig. 5C)

17' GSD:GCD > 0.3 **18**

18 Corallum white; GSD up to 15 mm *T. aculeatum* (Fig. 5D)

18' Corallum striped reddish-brown; GSD less than 7 mm *T. mortenseni* (Fig. 6A)

19 Calicular margin scalloped **20**

19' Calicular margin straight (not scalloped) **21**

20 Basal scar large (up to 8.6 in GSD); thecal face angle low (18–28°), resulting in a large GCD:LCD (1.9–2.4); Western Australia *T. australiensis* (Fig. 6B)

20' Basal scar smaller (less than 5.7 mm in GSD); thecal face angle higher (30–41°), resulting in a lower GCD:LCD (1.6–2.0); IWP *T. candeanum* (Fig. 6C)

21 Septal symmetry hexameral, up to sixth cycle **22**

21' Septal symmetry not hexameral, but in three size classes **24**

22 Basal scar large (up to 13.7 mm in length); GSD:GCD > 0.35; theca white ... *T. compressum* (Fig. 6D)

- 22' Basal scar smaller (less than 10 mm in length); GSD:GCD < 0.3; theca blackish **23**
- 23 GSD:GCD = 0.28–0.30; three pairs of thecal edge spines; thecal edges acute; H:GCD = 0.83–1.0 *T. martensii* (Fig. 7A)
- 23' GSD:GCD = 0.19–0.26; one (often two) short thecal edge spines; thecal edges rounded; H:GCD = 1.0–1.4 *T. mozambiquensis* (Fig. 7B)
- 24 Septal symmetry in multiples of 20; theca striped reddish-brown; GSD:GCD < 0.15 *T. vigintifarium* (Fig. 7C)
- 24' Septal symmetry in multiples of 16 or 18; theca white; GSD:GCD > 0.3 .. 25
- 25 GCD:LCD = 2.3–3.6 thecal edge angle 82–90° *T. spheniscus* (Fig. 7D)
- 25' GCD:LCD = 1.8–2.0; thecal edge angle 31–44° *T. cumingi* (Fig. 8A)
- 26 Thecal edge angle 41–56°; H:GCD < 1.0; theca brown; axial edges of septa sinuous; SWIO **27**
- 26' Thecal edge angle 20–27°; H:GCD = 1.7–2.0; theca white; central Pacific ...
..... *T. vanuatu* (Fig. 8B)
- 27 Upper outer edges of S1–3 attenuate gracefully to meet theca; Miocene of S. Australia + *T. duncani* (Fig. 8C)
- 27' Upper outer septal edges not attenuate; Recent of IWP
..... *T. multispinosum* (Fig. 8D)
- 28 Thecal edges rounded or acute, but never crested **29**
- 28' Thecal edges discontinuously crested **34**
- 29 Thecal edge angle = 65–138°; thecal face angle = 32–82°; axial septal edges straight *T. paripavoninum* (Fig. 9A)
- 29' Thecal edge angle < 70°; thecal face angle < 38°; axial septal edges sinuous **30**
- 30 GSD:GCD < 0.2 **31**
- 30' GSD:GCD > 0.25 **32**
- 31 Thecal edge angle 60–90°; H:GCD = 0.7–1.1; deep water (786–3010 m)
..... *T. stabile* (Fig. 9B)
- 31' Thecal edge angle 40–50°; H:GCD = 1.0–1.5; shallow water (100 m)
..... *T. inconstans* (Fig. 9C)
- 32 Costae (C1–3) ribbed; thecal edge angle 45–80° **33**
- 32' Costae not ribbed; thecal edge angle less than 20°; fossil from New Zealand
..... + *T. corbicula* (Fig. 9D)
- 33 H:GCD = 0.9–1.2; C1–3 ribbed; southeastern Pacific *T. truncum* (Fig. 10A)
- 33' H:GCD = 0.7; C1–2 ribbed; mid-Pacific *T. trapezoideum*
- 34 Septal symmetry in multiples of 20 (e.g., 20: 20: 20: 80)
..... *T. formosum* (Fig. 10B)
- 34' Septal symmetry hexameral in four to five cycles **35**
- 35 Five cycles of septa and part of sixth; H:GCD < 1.2 *T. carinatum* (Fig. 10C)
- 35' Four cycles of septa and part of fifth; H:GCD > 1.3 **36**
- 36 H:GCD = 1.3–1.9; GCD:LCD = 1.3–1.5 *T. gardineri* (Fig. 10D)
- 36' H:GCD = 2.9–3.5; GCD:LCD = 1.8–2.6 *T. arcuatum* (Fig. 11A)

Table 1. Transversely dividing flabellids, arranged by predominant geographic region (+ = fossil).

| Philippines and Indonesia |
|---|
| <i>Truncatoflabellum</i> Cairns, 1989 (38 spp, including 6 exclusively fossil) |
| <i>compressum</i> (Lamarck, 1816) |
| = <i>stokesii</i> (Milne Edwards & Haime, 1848) |
| = <i>Flabellum oweni</i> Milne Edwards & Haime, 1848 |
| <i>spheniscus</i> (Dana, 1846) |
| = <i>Flabellum debile</i> Milne Edwards & Haime, 1848 |
| = <i>Flabellum affine</i> Milne Edwards & Haime, 1848 |
| = <i>Flabellum bairdi</i> Milne Edwards & Haime, 1848 |
| = <i>Flabellum profundum</i> Milne Edwards & Haime, 1848 |
| = <i>Flabellum sumatrense</i> Milne Edwards & Haime, 1848 |
| = <i>Flabellum crenulatum</i> Milne Edwards & Haime, 1848 |
| = <i>Flabellum elongatum</i> Milne Edwards & Haime, 1848 |
| =+ <i>variable sensu</i> Gerth, 1921 (new synonymy) |
| <i>aculeatum</i> (Milne Edwards & Haime, 1848) |
| =? <i>Flabellum spinosum</i> Milne Edwards & Haime, 1848 |
| =? <i>Flabellum variable</i> Semper, 1872 |
| <i>crassum</i> (Milne Edwards & Haime, 1848) |
| <i>candeanum</i> (Milne Edwards & Haime, 1848) |
| = <i>Flabellum elegans</i> Milne Edwards & Haime, 1848 |
| <i>cumingi</i> (Milne Edwards & Haime, 1848) |
| = <i>F. irregulare</i> Tenison-Woods, 1878: 313 (junior homonym of Semper's 1872, but no need of new name since it is a junior synonym) |
| <i>irregulare</i> (Semper, 1872) |
| <i>paripavoninum</i> (Alcock, 1894) |
| <i>dens</i> (Alcock, 1902) |
| <i>incrustatum</i> Cairns, 1989 |
| =+ <i>irregulare sensu</i> Gerth, 1921:402 (new synonymy) |
| <i>formosum</i> Cairns, 1989 |
| = <i>T. sp. n. sensu</i> Cairns, 1989:73 |
| <i>pusillum</i> Cairns, 1989 |
| <i>carinatum</i> Cairns, 1989 |
| ?+ <i>variable alta</i> Gerth, 1921, if so, name is <i>altum</i> |
| <i>angustum</i> Cairns & Zibrowius, 1997 |
| Central and eastern Pacific |
| <i>trapezoideum</i> (Keller, 1981) |
| <i>truncum</i> (Cairns, 1982) |
| Vanuatu, Wallis and Futuna, New Caledonia |
| <i>martensii</i> (Studer, 1878) |
| =+ <i>paripavoninum sensu</i> Wells, 1984 |
| <i>mortenseni</i> Cairns & Zibrowius, 1997 |
| <i>vanuatu</i> (Wells, 1984) |
| <i>vigintifarium</i> Cairns, 1999 |

New Zealand and Kermadecs

arcuatum Cairns, 1995*phoenix* Cairns, 1995= *T. sp. B sensu* Cairns, 1994

Western Australia

angiosomum (Folkeson, 1919)*australiensis* Cairns, 1998*veroni* Cairns, 1998*macroeschara* Cairns, 1998

Western Indian Ocean/S. Africa

stabile (Marenzeller, 1904)= *Truncatoflabellum sp. A sensu* Cairns, 1994: 79=? *T. sp.* Zibrowius & Gili, 1990*inconstans* (Marenzeller, 1904)*gardineri* Cairns in Cairns & Keller, 1993*zuluense* Cairns in Cairns & Keller, 1993*multispinosum* Cairns in Cairns & Keller, 1993*mozambiquensis* sp. n.

South Australian exclusively fossil species

+ *victoriae* (Duncan, 1864)=? *F. simplex* Tenison-Woods, 1878+ *gambierense* (Duncan, 1864) (new combination)+ *corbicula* (Tenison-Woods, 1880)+ *sphenodeum* (Tenison Woods, 1880) (new comb.)+? *Flabellum attenuatum* Tenison-Woods, 1880+ *gippslandicum* (Dennant, 1899)+ *duncani* sp. n.= *candeanum sensu* Duncan 1870*Blastotrochus* Milne Edwards & Haime, 1848*nutrix* Milne Edwards & Haime, 1848+ *proliferus* d'Archiardi, 1866 (= ?*Cladocora*)*Placotrochides* Alcock, 1902*scaphula* Alcock, 1902= + *Flabellum elongatum* Hu, 1987 (junior homonym of ME and H, 1848)*frustum* Cairns, 1979*cylindrica* Cairns, 2004*minuta* Cairns, 2004= *minima (lapsus calumni) sensu* Cairns, 2006*Placotrochus* Milne Edwards & Haime, 1848*laevis* Milne Edwards & Haime, 1848= *P. candeanus* Milne Edwards & Haime, 1848= *P. pedicellatus* Tenison-Woods, 1879*Falcatoflabellum* Cairns, 1995*rauolensis* Cairns, 1995

Table 2. Tabular key to all species of *Truncatoflabellum* (pr = pair, NC = New Caledonia; NZ = New Zealand; IWP = Indo-West Pacific)

| | Thecal Edge Ornamentation | Edge angle; Face angle | GCD:LCD | H:GCD | GCD max. | Color | GSD:GCD; GSD max. | Septal symmetry (max number of septa) | Upper outer septal margin notched | Unique features | Distribution; depth |
|----------------------|------------------------------|---------------------------|---------|-----------|-------------|--------------------------|-----------------------|---|--|--|--|
| <i>phoenix</i> | 1–2+ pr spines | 0–10°; 0° | 1.3–2.3 | up to 4.3 | 5.9 mm | Lt. brown | 0.86–1.0; 4.3 mm | S1-2>S3>S4 (24–32) | No | Corallum often elongated by rejuvenescence | Japan to Kermadec; 18–441 m |
| <i>gippslandicum</i> | 1 basal pr spines | 0–10°; 10° | 2.3 | 1.9 | 16 mm | Fossil | 0.71; 10 mm | S1-3>S4>S5 (76) | No | | Miocene; Victoria |
| <i>victoriae</i> | 1 basal pr spines | 15–20°; 11–16° | 1.4 | 1.3 | 11.8 mm | Fossil | 0.64; 7.6 mm | S1-2>S3>S4 (32–40) | No | | Oligocene to M. Miocene; Victoria |
| <i>dens</i> | Small crests | Bimodal; 14–18° | 1.7–2.3 | 1.5–1.7 | 13.8 mm | Red- brown | 0.18–0.19; 1.6 mm | S1>S2>S3° (56) | No | Anthocaulus often remains attached | Philippines to NZ; 286–555 m |
| <i>zuluense</i> | 0–1 basal pr spines | 28–38°; 18–22° | 1.4–1.8 | 0.8 | 13.2 mm | Striped | 0.52; 6.5 mm | S1-2>S3>S4> S5 (56) | No | Anthocaulus often remains attached | South Africa; 62–84 m |
| <i>pusillum</i> | 2–4 pr spines | 14–18°; 18–20° | 1.4–1.7 | 1.5–1.6 | 8.4 mm | Striped | 0.41–0.48; 3.2 mm | S1-2>S3>S4 (32–48) | No | | IWP; 85–460 m |
| <i>angustum</i> | 3–4 pr spines | 28–52°; 17–22° | 1.8–2.3 | 1.2–1.7 | 14 mm | Red- brown basally | 0.3; 2.5 mm | S1-2>S3>S4>S5 (56) | Yes | | Philippines to Queensland; 195–530 m |
| <i>angostomum</i> | 1 pr basal spines | 105–200°; 15–25° | 2.9–3.2 | 0.67–0.81 | 63 mm | White | 0.08–0.09; 4.3 mm | S1-4>S5>S6>S7 (268) | Yes | Calice arched | North and west Australia; 15–176 m |
| <i>macrochaeta</i> | 1 pr basal spines | 55–87°; 22–27° | 2.5–3.1 | 0.64–1.0 | 46 mm | White | 0.35–0.53; 30.4 mm | S1-4>S5>S6>S7 (192) | No | | Australia; 18–201 m |
| <i>veroni</i> | 1 pr basal spines | 94–127°; 23–32° | 3.0–4.8 | 0.5–0.56 | 57 mm | White | 0.33; 27 mm | S1-4>S5>S6>S7 (192–212) | Yes | | Australia; 15–176 m |
| <i>gambierense</i> | 1 pr spines | 30–38°; 15–20° | 1.6–3.2 | 1.4–1.8 | 14.5 mm | Fossil | 0.52–0.67; 7.2 mm | S1-2>S3>S4;S5 (56) | No | Anthocaulus slender, remains attached | Middle Miocene; Victoria |
| <i>incrustatum</i> | 1 pr basal spines | 23–32°; 15–19° | 1.6–2.1 | 1.2–1.5 | 28 mm | Blackish | 0.24–0.38; 10 mm | S1-2>S3>S4>S5 (96) | No | | Japan to Philippines; 30–315 m |
| <i>sphenodeum</i> | 1 basal pr spines | 32°; 18° | 1.67 | 1.33 | 15 mm | Fossil | 0.25–0.33; 3.5 mm | S1-3>S4>S5 (60–75) | No | | M. Eocene to M. Miocene; NZ |

| | Thecal Edge Ornamentation | Edge angle; Face angle | GCD:LCD | H:GCD | GCD max. | Color | GSD;GCD; GSD max. | Septal symmetry (max number of septa) | Upper outer septal margin notched | Unique features | Distribution; depth |
|-----------------------|---------------------------|------------------------|-----------|-----------|----------|--------------|--------------------|---------------------------------------|-----------------------------------|-------------------------------------|---|
| <i>irregularis</i> | 1 pr basal spines | 36–43°; 19° | 1.6–2.0 | 1.4 | 28 mm | White | 0.32–0.5; 4 mm | S1°>S2°>S3° (72–80) | Yes | | Japan to Philippines; 11–55 m |
| <i>crassum</i> | 1 pr basal spines | 40–50°; 18–28° | 1.3–1.8 | 0.75–0.85 | 29 mm | White | 0.21–0.29; 6.3 mm | S1-2>S3>S4>S5>S6 (114) | Yes | | IWP; 31–430 m |
| <i>aculeatum</i> | 1 pr basal spines | 31–82°; 17–31° | 1.8–3.7 | 0.56–0.71 | 41 mm | Milky white | 0.35–0.44; 15 mm | S1°>S2°>S3° (50–72) | Yes | | Japan to w. Australia; 11–132 m |
| <i>mortenseni</i> | 1 pr spines | 49–61°; 23–31° | 1.65–1.85 | 0.75–0.81 | 23 mm | Striped | 0.32–0.40; 7 mm | S1-3>S4>S5 (96) | Yes | Anthocyathus often remains attached | Philippines to New Caledonia; 50–455 m |
| <i>australiensis</i> | 2–3 pr spines | 44–73°; 18–28° | 1.9–2.4 | 0.64–0.83 | 25 mm | Striped | 0.36–0.48; 8.6 mm | S1-3>S4>S5 (96) | No | | W. Australia; 90–220 m |
| <i>candeanum</i> | 3 long pr spines | 40–80°; 30–41° | 1.6–2.0 | 0.73–0.76 | 32 mm | Striped | 0.26–0.29; 5.7 mm | S1°>S2°>S3° (72–96) | No | | Japan to Philippines; NC; 70–290 m |
| <i>compressum</i> | 2–3 pr spines | 53–67°; 24–29° | 1.9–3.1 | 0.6–0.8 | 40 mm | White | 0.37–0.43; 13.7 mm | S1-4>S5>S6 (192) | Yes | | Philippines to Indian Ocean; 12–256 m |
| <i>martensii</i> | 3 pr spines | 40–105°; 14–19° | 2.0–2.4 | 0.83–1.0 | 29 mm | Red or brown | 0.28–0.30; 9.3 mm | S1-3>S4>S5>S6 (126) | No | Thecal edges acute | New Caledonia to Andaman Sea; 139–275 m |
| <i>mozambiquensis</i> | 1–2 pr spines | 39–60°; 22–32° | 1.4–2.2 | 0.97–1.4 | 27 mm | Blackish | 0.19–0.26; 6.9 mm | S1-2>S4>S5 (96) | No | C1–3 ribbed | Mozambique; 106–112 m |
| <i>vignitifarium</i> | 2–3 pr spines | 67–84°; 25–30° | 1.95–2.40 | 0.84–0.91 | 27 mm | Striped | 0.13; 3.6 mm | S1°>S2°>S3° (80) | No | | New Caledonia, Queensland; 179–1050 m |
| <i>spheniscus</i> | 1 basal pr spines | 65–118°; 16–31° | 2.8–4.1 | 0.76–0.81 | 50 mm | Striped | 0.22–0.49; 18 mm | 1°>2°>3°>4° (190) | Yes | Calice arched | Japan to Australia; 2–174 m |
| <i>cuningi</i> | 2–3 pr spines | 31–44°; 18–236 | 1.8–2.0 | 1.0–1.13 | 20 mm | White | 0.37–0.41; 9 mm | S1°>S2°>S3° (72) | No | | Philippines to W. Australia; 46–132 m |
| <i>vanuatu</i> | 4–5 pr spines | 20–27°; 12–17° | 1.6–1.8 | 1.7–1.9 | 26 mm | White | 0.22–0.29; 4.9 mm | S1°>S2°>S3° (80) | No | Axial septal edges straight | Vanuatu, NC; 240–335 m |
| <i>duncani</i> | 5 pr spines | 54–72°; 27° | 1.4–1.7 | 0.93–1.04 | 31 mm | Fossil | 0.27–0.29; 10.5 mm | S1-3>S4>S5>S6 (104) | | Attenuate | L. Oligocene–M. Miocene; Victoria |

| | Thecal Edge Ornamentation | Edge angle; Face angle | GCD:LCD | H:GCD | GCD max. | Color | GSD;GCD; GSD max. | Septal symmetry (max number of septa) | Upper outer septal margin notched | Unique features | Distribution; depth |
|-----------------------|----------------------------|------------------------|---------|-----------|----------|------------------|--------------------|---------------------------------------|-----------------------------------|---------------------------------|---|
| <i>multispinosum</i> | 5–7 pr spines | 41–56°; 19–32° | 1.7–2.1 | 0.93–1.02 | 32 mm | Brown | 0.23–0.30; 7.3 mm | S1-3>S4>S5>S6 (100) | No | | W. Indian Ocean, NC; 62–183 m |
| <i>pariparvovinum</i> | None, thecal edges acute | 65–138°; 32–62° | 1.4–2.0 | 0.77–1.0 | 62 mm | Lt brown | 0.17–0.34; 14.5 mm | S1-3>S4>S5>S6 (192) | No | | Philippines to Laccadive Sea; 394–1450 m |
| <i>stabile</i> | None, thecal edges rounded | 59–90°; 40–60° | 1.4–1.7 | 1.0–1.15 | 52 mm | White | 0.14–0.28; 7 mm | S1-3>S4>S5>S6 (104) | No | Costae ribbed | Japan, Mozambique, Cape Verde; 786–3010 m |
| <i>inconstans</i> | None, thecal edges rounded | 38–52°; 25° | 1.5–2.5 | 0.10–1.5 | 44 mm | White | 0.13–0.18; 5 mm | S1-3>S4>S5>S6 (171) | No | C1–3 ribbed | South Africa; 23–130 m |
| <i>orbicula</i> | None, thecal edges rounded | 16–21°; 15° | 1.5–2.2 | 0.97 | 19 mm | Fossil | 0.64–0.67; 12 mm | S1-2>S3>S4 (48) | No | | L. Oligocene, New Zealand |
| <i>truncum</i> | None, thecal edges rounded | 45–70°; 22–38° | 1.4–2.2 | 0.9–1.2 | 38 mm | White | 0.25–0.27; 9.5 mm | S1-3>S4>S5 (96) | No | C1–3 ribbed | Peru to Falklands; 595–1896 m |
| <i>trapesoideum</i> | None, thecal edges rounded | 80°; ? | 1.35 | 0.69 | 28 mm | White | 0.29; 8.1 mm | S1-2>S3>S4>S5 (88) | No | C1–2 ribbed | Marcus-Necker Ridge; 1630 m |
| <i>formosum</i> | 2 pr crests | 37–59°; 18–31° | 1.4–1.9 | 1.05–1.2 | 27 mm | Striped | 0.26; 5.5 mm | S1<S2<S3<S3° (80) | Attenuate | | Philippines to SW Indian Ocean; 42–933 m |
| <i>carinatum</i> | Disjunct crests | 35–57°; 18–32° | 1.6–1.9 | 0.88–1.2 | 23 mm | Red-brown | 0.22–0.24; 5.2 mm | S1-3>S4>S5>S6 (104) | No | | S. China Sea to Mozambique; 30–274 m |
| <i>gardineri</i> | Crests | 21–35°; 14–18° | 1.3–1.5 | 1.3–1.9 | 20 mm | White or striped | 0.37–0.49; 5.3 mm | S1-2>S3>S4 (48) | No | | Japan, S. Africa; 100–144 m |
| <i>arcuatum</i> | Low crests | 14–15°; 8–11° | 1.8–2.6 | 2.9–3.5 | 12 mm | White | 0.50–0.55; 5.9 mm | S1-2>S3>S4>S5 (60) | No | Axial septal edges very sinuous | North of New Zealand; 350–364 m |

***Truncatoflabellum phoenix* Cairns, 1995**

Fig. 2A

Truncatoflabellum sp. B. Cairns, 1994: 75, 79, pl. 33i, l.*Truncatoflabellum phoenix* Cairns, 1995: 115–116, pl. 37i, 38a-f.—Cairns and Zibrowius 1997: 171.—Cairns 1999: 121.—Ogawa 2006: 16, pl. 2, fig. 5a-b.

New records. USGS 25734, Vanuatu, Espiritu Santo Island, Late Pleistocene, 1 specimen, USNM 100175; Ryukyu Islands, Okinawa, Horseshoe Cliffs, 1 km NNW Onna Village (26°30'N, 127°50'54"E), 67-79 m, 6 specimens, USNM 87712, 88380, 88382, 88383, and 100674.

Distribution. Late Pleistocene: Vanuatu. Holocene: southern Japan, Philippines, Indonesia, Wallis and Futuna, New Caledonia, Kermadec Islands, 18-441 m.

Remarks. This is the smallest of the *Truncatoflabellum* species, having a GCD rarely more than 5 mm, but capable of multiple apical regeneration (Fig. 2A, top) resulting in coralla as long as 17.5 mm.

***Truncatoflabellum gippslandicum* (Dennant, 1899)**

Fig. 2B

Flabellum gippslandicum Dennant, 1899: 112–113, pl. 2, figs 1a–b.—Felix 1927: 409.—Bell 1981: 11 (type deposition).—Fitzgerald and Schmidt: 3 (color fig).*Truncatoflabellum gippslandicus* (*sic*): Cairns 1989b: 61.

Distribution. Miocene: Gippsland Lake area of Victoria, Australia; Middle Miocene of Beaumaris, Victoria.

Remarks. The two syntypes of *T. gippslandicum* were reported by Bell (1981) from the NMV (P27064). No other records of this species are known, and the information presented in the key and comparative Table 2 is taken from the original description.

***Truncatoflabellum victoriae* (Duncan, 1864)**

Fig. 2C

Flabellum victoriae Duncan, 1864: 162–163, pl. 5, fig. 2a–c; 1870: 299, 312, pl. 19, fig. 11.—Tenison-Woods 1878b: 312.—Felix 1927: 415 (synonymy).? *Flabellum simplex* Tenison-Woods, 1878: 13.—Squires 1958: 66 (type lost).*Truncatoflabellum victoriae*: Cairns, 1989b: 61, pl. 37i.

New records. Muddy Creek, near Hamilton, Victoria, Australia, Balcombian (Middle Miocene), 13 specimens, USNM 67962 and 68005; Balcombe's Bay, Port Phillip, Victoria, Balcombian (Middle Miocene), 11 specimens, USNM 68000 and M353582;

Balcombe's Bay, Mornington, Balcombian (Middle Miocene), 3 specimens, USNM M353583; Spring Creek, Torquay, Victoria, Janjukian (Late Oligocene), 8 specimens, USNM 1283656.

Distribution. Late Oligocene (Janjukian), Victoria; Middle Miocene (Balcombian), Muddy Creek, Geelong, Victoria, and Balcombe's Bay, Victoria.

***Truncatoflabellum dens* (Alcock, 1902)**

Fig. 2D

Flabellum dens Alcock, 1902: 32, pl. 4, figs 30, 30a.—Cairns 1989b: 54, Table 6, pl. 28g–k.

Truncatoflabellum dens: Cairns 1995: 114–115 (in part: pl. 37g).—Cairns and Zibrowius 1997: 170–171, 173.—Cairns 1999: 120, fig. 20a.

Distribution. Philippines, Indonesia, New Caledonia, Vanuatu, Wallis and Futuna, New Zealand, 286–555 m.

***Truncatoflabellum zuluense* Cairns in Cairns & Keller, 1993**

Fig. 3A

Truncatoflabellum zuluense Cairns in Cairns & Keller, 1993: 267–268, figs 11F–G.—Cairns 1995: 115 (comparison to *T. dens*).

Distribution. Off Natal, South Africa, 62–84 m.

***Truncatoflabellum pusillum* Cairns, 1989b**

Fig. 3B

Truncatoflabellum pusillum Cairns, 1989b: 71_72, Table 6, pl. 37a–e.—Cairns and Keller 1993: 265, fig. 11E.—Cairns 1995: 115 (comparison to *T. dens*).—Cairns and Zibrowius 1997: 170.—Cairns 1999: 120, fig. 20a

Distribution. Philippines, Indonesia, Vanuatu, New Caledonia, southwest Indian Ocean off Mozambique, 85–460 m.

***Truncatoflabellum angustum* Cairns & Zibrowius, 1997**

Fig. 3C

Truncatoflabellum dens: Cairns 1995: in part (pl. 37f, h).



Figure 2. **A** *Truncatoflabellum phoenix*, paratypes, USNM 82010, Kermadec Ridge **B** *T. gippslandicum*: upper lateral and edge views, NMV P133990; lower lateral and calicular views, syntype, NMV P27064, Miocene of Gippsland lake region of Victoria **C** *T. victoriae*, USNM 67962, Muddy Creek, Victoria (Balcombian = Middle Miocene) **D** *T. dens*, USNM 98889, MUSORSTOM 7-569, Vanuatu. Scale bars: 2 mm (**A**); 10 mm (**B**); 5 mm (**C-D**).

Truncatoflabellum angustum Cairns & Zibrowius, 1997: 172–173, figs 23c–f.—Cairns 1999: 121, fig. 20b.—Cairns 2004: 308.

Distribution. Philippines, Indonesia, Vanuatu, Wallis and Futuna, Kermadec Islands, off Queensland, 195–530 m.

***Truncatoflabellum angiosomum* (Folkesson, 1919)**

Fig. 3D

Flabellum angiosomum Folkesson, 1919: 5, pl. 1, figs 1–3.

Truncatoflabellum angiosomum: Cairns 1998: 395–396, Table 4, figs 7a–c, 8a; 2004: 308 (synonymy).

New records. SIPHILEXP M-21, 8°45'S, 145°05'08"E (off mouth of Fly River, Bramble Island, Papua New Guinea), 55 m, USNM 1130683; Karubar 65, 9°14'01"S, 132°28'28"E, 174–176 m, 1, USNM 97256.

Distribution. Western and Northern Australia, Papua New Guinea, 15–176 m.

***Truncatoflabellum macroeschara* Cairns, 1998**

Fig. 4A

Truncatoflabellum macroeschara Cairns, 1998: 401, Table 4, figs 8d–e, g–1; 2004: 309 (synonymy).—Kitahara et al. 2010: fig. 1.

Distribution. Off Western Australia and Queensland, 18–201 m.

Remarks. *T. macroeschara* belongs to a group of three western Australian species that have very large coralla, often including some S7, the other two species being *T. veroni* and *T. angiosomum*. It differs from those two species as well as all others in the genus by having a very large scar diameter.

***Truncatoflabellum veroni* Cairns, 1998**

Fig. 4B

Truncatoflabellum spheniscus: Cairns and Zibrowius: 165–166 (in part: USNM 93197 and USNM 97499).

Truncatoflabellum veroni Cairns, 1998: 400, Figs 7g–i, 8c; 2004: 309 (synonymy).

Distribution. Off Western and Northern Australia, off Queensland, 15–176 m.

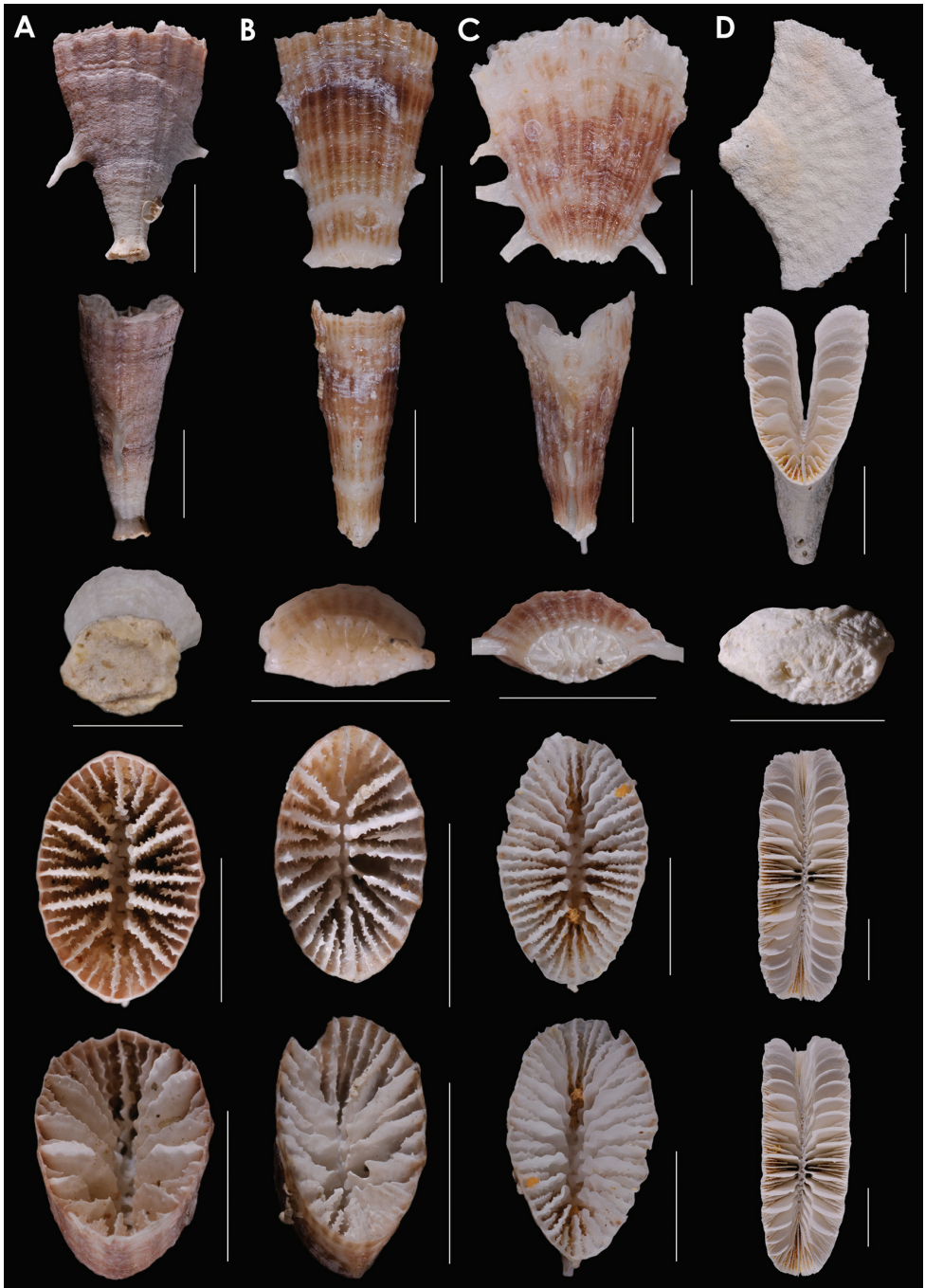


Figure 3. **A** *Truncatoflabellum zuluense*, paratype, USNM 91751, MD ZK-20, South Africa **B** *T. pusillum*, holotype, USNM 81978, Albatross 5178, Philippines **C** *T. angustum*, USNM 98894, MUSOR-STOM 8-1016, Vanuatu **D** *T. angiosotum*, USNM 96643, Cape Jaubert, Western Australia. Scale bars: all 10 mm, except for basal scar views, which are 5 mm.

***Truncatoflabellum gambierense* (Duncan, 1864), comb. n.**

Fig. 4C

Flabellum gambierense Duncan, 1864: 163, pl. 5, fig. 3a-c; 1870: 299–300, 308, 310, 312, pl. 19, figs 9–10.—Tenison-Woods 1878b: 312.—Felix 1927: 409.—Fitzgerald and Schmidt: 3 (color figure).

New records. Spined coralla: USGS 10809, Balcombe's Bay, Mornington, Victoria (Balcombian, Middle Miocene), 2 specimens, USNM 1295473. Non-spined coralla: Muddy Creek, Victoria (Balcombian, Middle Miocene), 9 specimens, USNM 67958, 353989, and M353589; Balcombe's Bay, Mornington, Victoria (Balcombian, Middle Miocene), 6 specimens, USNM M353581 and M353580.

Distribution. Middle Miocene: Mount Gambier, S. Australia; Cape Otway, Balcombe's Bay, Mornington, and Beaumaris, Victoria.

Remarks. In the original description, Duncan (1864) described the species as not having thecal edge spines, but in 1870 said that the coral has “often small spines nearer the calice than the pedicel.” Indeed, some specimens of this distinctively-shaped species have spines (traditional *Truncatoflabellum*) and others do not (see New Records). Ordinarily, if a species of *Truncatoflabellum* bears thecal edge spines then all specimens of that species will bear spines. Thus, this variation in character is unusual and may be indicative of the early evolution in the genus when spination and transverse division were still experimental, as *T. gambierense* is one of those species that shows a crescentric transverse weakness in its corallum but the anthocyathus usually remains attached to the anthocaulus, possibly the ancestral condition for the species.

***Truncatoflabellum irregulare* (Semper, 1872)**

Fig. 4D

Flabellum irregulare Semper, 1872: 242–245, figs 1–3, pl. 16, figs 7–17.

Not *Flabellum irregulare* Tenison-Woods, 1878b: 313, pl. 4, Fig. 2 (junior homonym, = *T. cumingi*).

Truncatoflabellum irregulare: Cairns 1989b: 67–68, Table 6, pls. 34i–k, 35a–c (synonymy). —Cairns and Zibrowius 1997: 168.

New record. Ryukyu Islands, Horseshoe Cliffs (26°30'00"N, 127°50'54"E), 55 m, 1 specimen, USNM 87710.

Distribution. Philippines, Indonesia, Ryukyu Islands, 11–55 m.

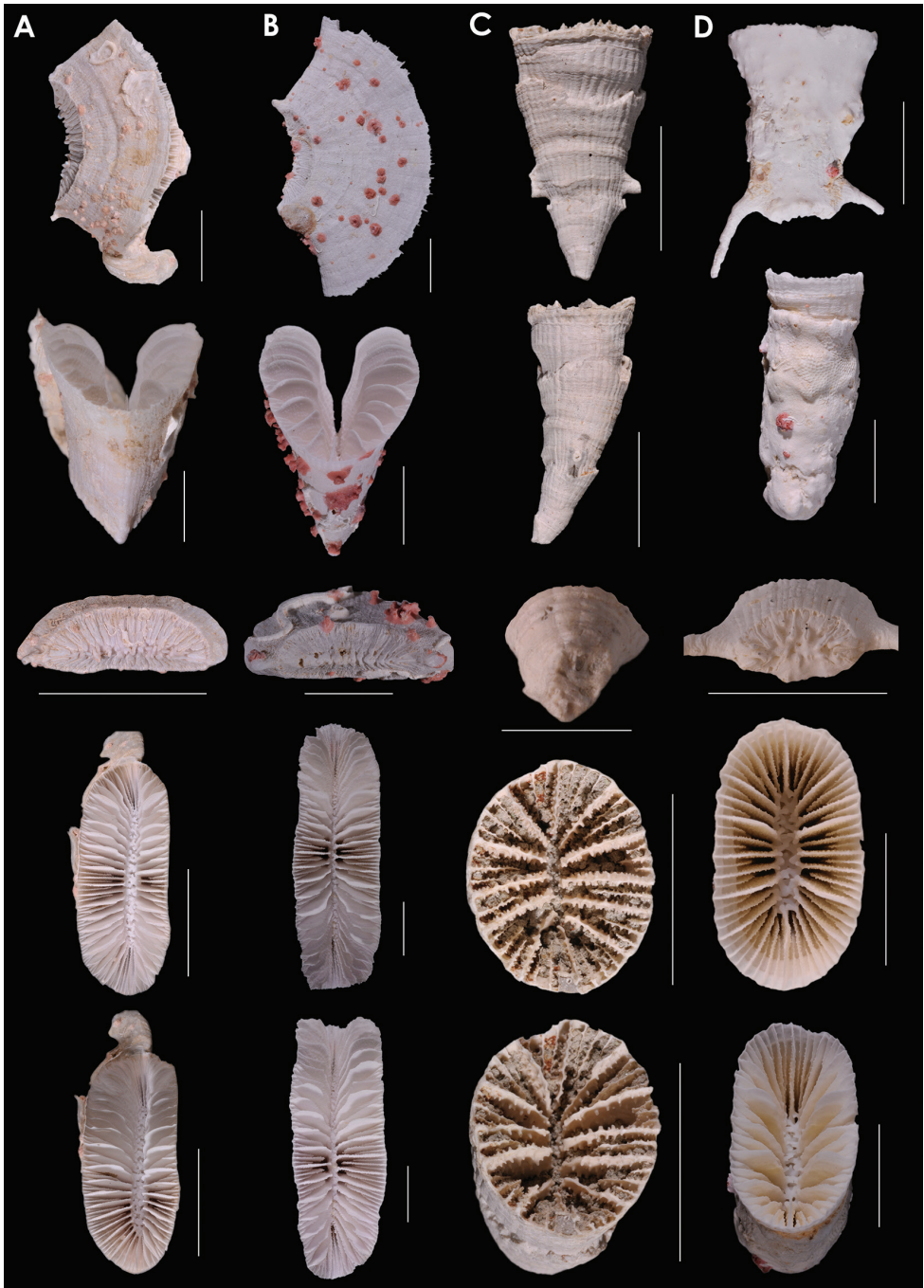


Figure 4. **A** *Truncatoflabellum macroeschara*, paratype, USNM 96661, Onslow Island, Western Australia **B** *T. veroni*, paratype, USNM 96655, Soela 54A, Western Australia **C** *T. gambierense*, USNM 1295473, USGS 10809, Balcombe's Bay, Victoria (Balcombian = Middle Miocene) **D** *T. irregulare*, USNM 87713, Japan. Scale bars: all 10 mm.

***Truncatoflabellum incrustatum* Cairns, 1989b**

Fig. 5A

Flabellum irregulare: Gerth 1921: 402, pl. 57, fig. 15.—Cairns 1989b: 63, Table 6, pl. 37f.

Truncatoflabellum incrustatum Cairns, 1989b: 68–69, Table 6, pl. 35d–e.—Cairns and Zibrowius 1997: 168.

New record. *Tansei Maru* KT9202-YT1, 30°14'48"N, 130°46'06"E, 80–88 m, 5 specimens, USNM 92788.

Distribution. Lower Miocene of Java (Gerth, 1921). Holocene: Philippines; Indonesia; Ryukyu Islands, Japan, 30–315 m.

***Truncatoflabellum sphenodeum* (Tenison-Woods, 1880), comb. n.**

Fig. 5B

Flabellum sphenodeum Tenison-Woods, 1880: 14, figs 12a–c.—?Hayward, 1977: 105–106, fig. 8.

?*Flabellum attenuatum* Tenison-Woods, 1880: 15, fig. 15.

Flabellum rubrum sphenodeum: Squires 1958: 66–67, pl. 11, figs 21–25 (lectotype designated).

?*Flabellum* sp. A Hayward, 1977: 106, fig. 9.

New record. Junction of Porter and Thomas Rivers, New Zealand, S66/74, NZGS 3350, Duntroonian (early Oligocene), 3 specimens, USNM 67908.

Distribution. Middle Eocene (Bortonian) to Middle Miocene (Waiauian) of New Zealand (Squires 1958).

Remarks. According to the records of Squires (1958), this would be the oldest *Truncatoflabellum*, being reported from the Bortonian (Middle Eocene) of New Zealand.

The specimens reported by Hayward (1977) as “*Flabellum*” *sphenodeum* and “*Flabellum*” sp. A have much larger basal scars and shorter coralla than typical *F. sphenodeum* and are thus not included with this species. Specimens in the NMNH that may be the same are USNM 67932 and 67928, and may represent an undescribed species.

***Truncatoflabellum crassum* (Milne Edwards & Haime, 1848)**

Fig. 5C

Flabellum crassum Milne Edwards & Haime, 1848: 276–277, pl. 8, figs 8, 8a.

Flabellum stokesi: Scheer and Pillai 1974: 62–63, pl. 29, figs 1–2.

Truncatoflabellum crassum: Cairns 1989b: 64–65, Table 6, pl. 32d–f (synonymy).



Figure 5. **A** *Truncatoflabellum incrustatum*, holotype, USNM 40774, *Albatross* 5251, Philippines **B** *T. sphenodeum*, lectotype, NZGS CO 681, Trilissick Basin, New Zealand (Duntroonian = Lower Oligocene) **C** *T. crassum*, USNM 1130686, *Albatross* 5270, Philippines **D** *T. aculeatum*, USNM 40781, *Albatross* 5156, Philippines. Scale bars: all 10 mm.

New records. *Albatross* 5091, 35°04'10"N, 139°38'12"E, 366 m, 1 specimen, USNM 92812; *Albatross* 5270, 13°35'45"N, 120°58'30"E, 430 m, 1 specimen, USNM 1130686; *Anton Bruun* 1–38, 14°07'N, 95°05'E, 69–73 m, 1 specimen, USNM 1015342; *Anton Bruun* 260A, 26°15'N, 56°46'E, 91 m, 1 specimen, USNM 1015348; *Anton Bruun* 9–447, 10°00'N, 51°15'E, 59–61 m, 1 specimen, USNM 1015346; *Anton Bruun* 9–451, 11°04'N, 51°15'E, 76–80 m, 14 specimens, USNM 98977; *Anton Bruun* 9–453, 11°11'N, 51°14'E, 47–49 m, approx.. 200 specimens, USNM 77040; *Anton Bruun* 9–456, 11°14'N, 51°08'E, 27–31 m, 1 specimen, USNM 1015285; 11°15'N, 51°12'E, 50 m, 10 specimens, USNM 1015170.

Distribution. Philippines, Sagami Bay (Japan), Gulf of Aden, Persian Gulf, Great Nicobar, Andaman Islands, 31–430 m.

Truncatoflabellum aculeatum (Milne Edwards & Haime, 1848)

Fig. 5D

Flabellum aculeatum Milne Edwards & Haime, 1848: 272, pl. 8, figs 3, 3a.—Cairns 1989a: 643, fig. 1 (lower).

Flabellum spinosum Milne Edwards & Haime, 1848: 271, pl. 8, fig. 4.

Flabellum variable Semper, 1872: 245–251, pl. 17, pl. 18, figs 1–10.

Flabellum rubrum: Umbgrove 1938: 264 (in part).

Truncatoflabellum aculeatum: Cairns 1989b: 61–64, Table 6, pl. 31h-l, 32a-c.—Cairns and Zibrowius 1997: 166–167.—Cairns 1998: 399–400, Table 4; 1999: 123; 2004: 308 (synonymy).

New records. *Tansei Maru* KT9202, YT1, 30°14'48"N, 130°46'06"E, 80–88 m, 2 specimens, USNM 92790; Singapore, depth unknown, 1 specimen, USNM 1279597.

Distribution. Pleistocene: Indonesia. Holocene: Okinawa, Philippines, Indonesia, Vanuatu, off Queensland, Northern Territory and Western Australia, 11–132 m.

Truncatoflabellum mortenseni Cairns & Zibrowius, 1997

Fig. 6A

Truncatoflabellum mortenseni Cairns & Zibrowius, 1997: 171–172, figs 22g-h.—Cairns 1999: 122–123.

Distribution. Philippines, Indonesia, Vanuatu, Wallis and Futuna, New Caledonia, 50–455 m.

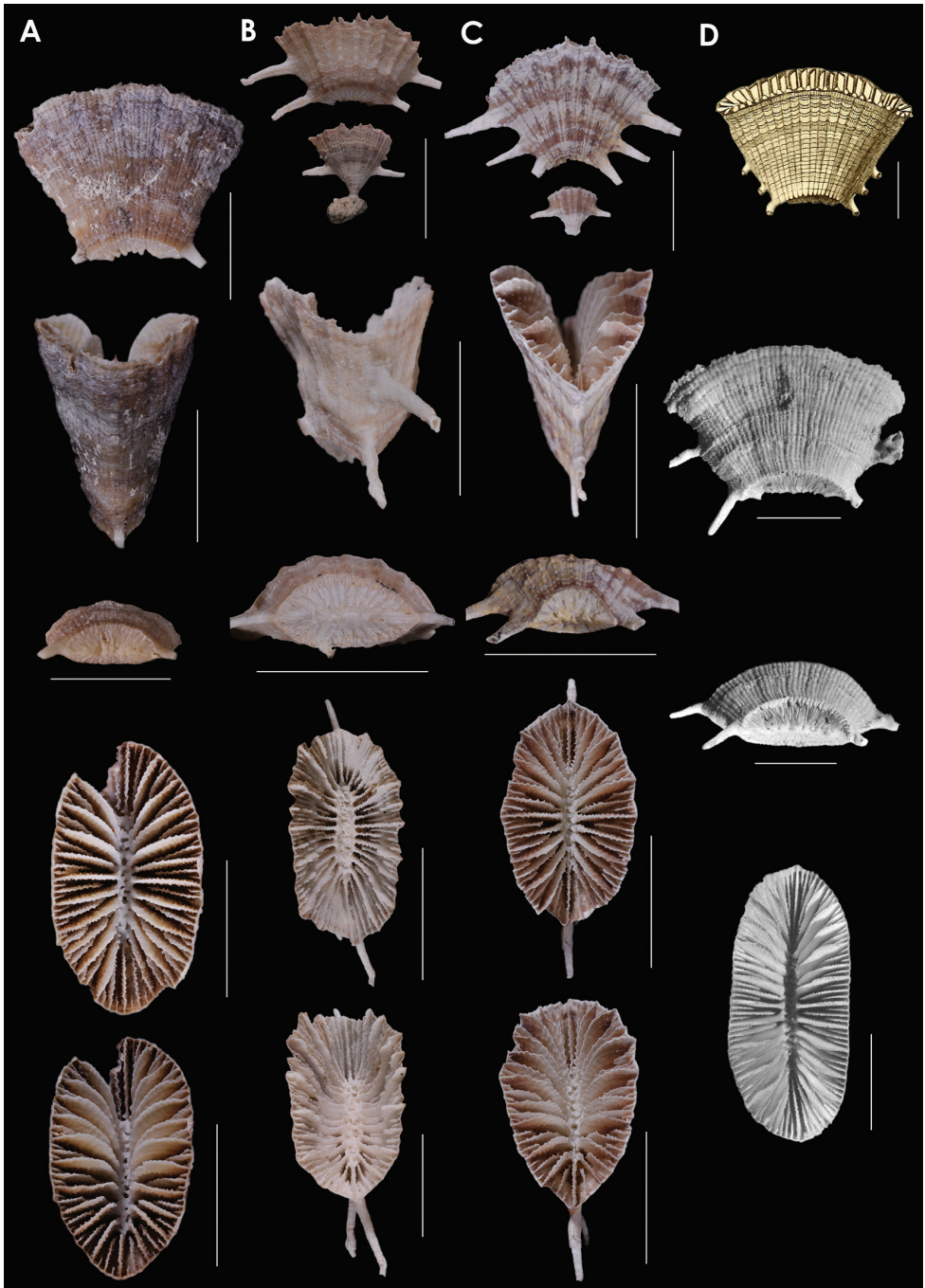


Figure 6. **A** *Truncatoflabellum mortenseni*, USNM 97522, paratype, Philippines **B** *T. australiensis*, paratype (including anthocaulus), USNM 96652, Western Australia **C** *T. candeanum*, neotype, including anthocaulus, USNM 81963, *Albatross* 5369, Philippines **D** *T. compressum*, upper figure, illustration of type from Lesson (1827); other views from *Challenger* 190, BM 1880.11.25.78. Scale bars: all 10 mm.

***Truncatoflabellum australiensis* Cairns, 1998**

Fig. 6B

Truncatoflabellum australiensis Cairns, 1998: 396–399, Table 4, figs 7d-f, 8b; 2004: 308.—Kitahara et al. 2010: fig. 1.

Distribution. Western Australia, 90–220 m.

***Truncatoflabellum candeanum* (Milne Edwards & Haime, 1848)**

Fig. 6C

Flabellum candeanum Milne Edwards & Haime, 1848: 278, pl. 8, fig. 13.—Not Duncan, 1864: 163 (= *T. duncani*, herein).

Flabellum elegans Milne Edwards & Haime, 1848: 277.

Truncatoflabellum candeanum: Cairns 1989b: 70–71, Table 6, pl. 36d-h (synonymy, neotype designated); 1994: 76–77, pl. 33e-f.—Cairns and Zibrowius 1997: 167.—Cairns 1999: 123–124.—Kitahara et al. 2010: fig. 1.

Distribution. Southern Japan, Philippines, Indonesia, Vanuatu, New Caledonia, 70–290 m.

***Truncatoflabellum compressum* (Lamarck, 1816)**

Fig. 6D

Fungia compressa Lamarck, 1816: 235; 1827: pl. 483, fig. 2.

Flabellum compressum: Milne Edwards & Haime, 1848: 273–274 (synonymy).—Duncan 1864: 167.

Flabellum stokesii Milne Edwards & Haime, 1848: 278, pl. 8, fig. 12.—Moseley 1881: 172–173 (in part: *Challenger* 190).—Gerth 1921: 402, pl. 567, fig. 14.—Not Umbgrove 1950: 640.—Not Scheer and Pillai 1974: 62 (= *T. crassum*).

Flabellum oweni Milne Edwards & Haime, 1848: 279, pl. 8, fig. 9.

Truncatoflabellum stokesi: Cairns 1989b: 66, Table 6, pl. 33b-h, j (synonymy).

Truncatoflabellum compressum: Cairns 1989b: 61 (listed).

Distribution. Miocene: Java. Holocene: Philippines, Indonesia, “Indian Ocean” (Lamarck, 1816), 12–256 m.

Remarks. This species, with a name overlooked since 1864, was beautifully illustrated by Lamarck (1827). Its description and illustration (Fig. 6D, top) leave little doubt that it is the species that has become known as *T. stokesi*.

***Truncatoflabellum martensii* (Studer, 1878)**

Fig. 7A

Flabellum martensii Studer, 1878: 630–631, pl. 1, figs 4a-b.*Flabellum paripavoninum*: Wells 1984: 214–215, fig. 4, 6–7.*Truncatoflabellum martensii*: Cairns 1989b: 61, Table 6, pl. 37, figs g–h; 1999: 124, figs 21a–f (synonymy); 2004: 309.*Truncatoflabellum* sp. Cairns & Kitahara, 2012, pl. 23, figs C–F.**New records.** *Anton Bruun* 1–22A, 10°39'N, 97°06'E, 275 m, 5 specimens, USNM 1015345; *Anton Bruun* 4B–230B, 23°31'N, 66°55'E, 88 m, 1 specimen, USNM 1015347.**Distribution.** Late Pleistocene: Vanuatu (Wells, 1984). Holocene: New Caledonia, Vanuatu, off Brisbane, Andaman Sea, 139–275 m.***Truncatoflabellum mozambiquensis* sp. n.**<http://zoobank.org/5F659B28-7F5B-45D0-9E87-0CD7D9DC7731>

Fig. 7B

Types. Holotype: *Anton Bruun* 7–372L, 25°07'S, 34°34'E, 112 m, grey sandy mud, USNM 91764. Paratypes: *Anton Bruun* 7–372L, 232 coralla, USNM 1283832; *Anton Bruun* 7–371F, 24°46'S, 35°18'E, 110 m, 1 specimen, USNM 91762; *Anton Bruun* 7–372J, 25°07'S, 34°34'E, 106 m, 28 specimens, USNM 91763.**Description.** The anthocyathus has straight, rounded thecal edges, having an edge angle of 39–60°; the face angle ranges from 22–28°. The largest specimen has a GCD of 26.5 mm, whereas the holotype measures 23.4 × 11.2 in calicular diameter, 24.5 mm in height, and 5.3 mm in greater scar diameter. The GCD:LCD ratio is 1.4–2.2; the H:GCD is 1.0–1.4; the GSC:GCD is 0.19–0.26, with the GSD up to 6.9 mm in length. One pair of very short (rarely more than 1 mm long) and often broken and worn thecal edges spines occur near the basal scar; another pair often is present more distally. The thecal faces bear low ribbing corresponding to the C1–3. The corallum, although worn, sometimes has a blackish color. The septa are arranged in five cycles: S1–3>S4>S5, mature coralla having 96 septa. The lower axial septal edges are highly sinuous, and merge into a rudimentary elongate columella. The upper outer septal edges are not notched. The fossa is deep and narrow, although almost all coralla examined were partially damaged, making observations of the septa and fossa tentative.

Anthocauli are rare, only four of the 262 (1.5%) specimens representing this juvenile stage. It is small, only about 4.1 mm in height with a circular attached pedicel 2 mm in diameter, and a distal calice 5–6 mm in greater diameter corresponding to the scar diameter of the anthocyathus. It has three cycles of septa.

Distribution. Off southern Mozambique, 106–112 m.

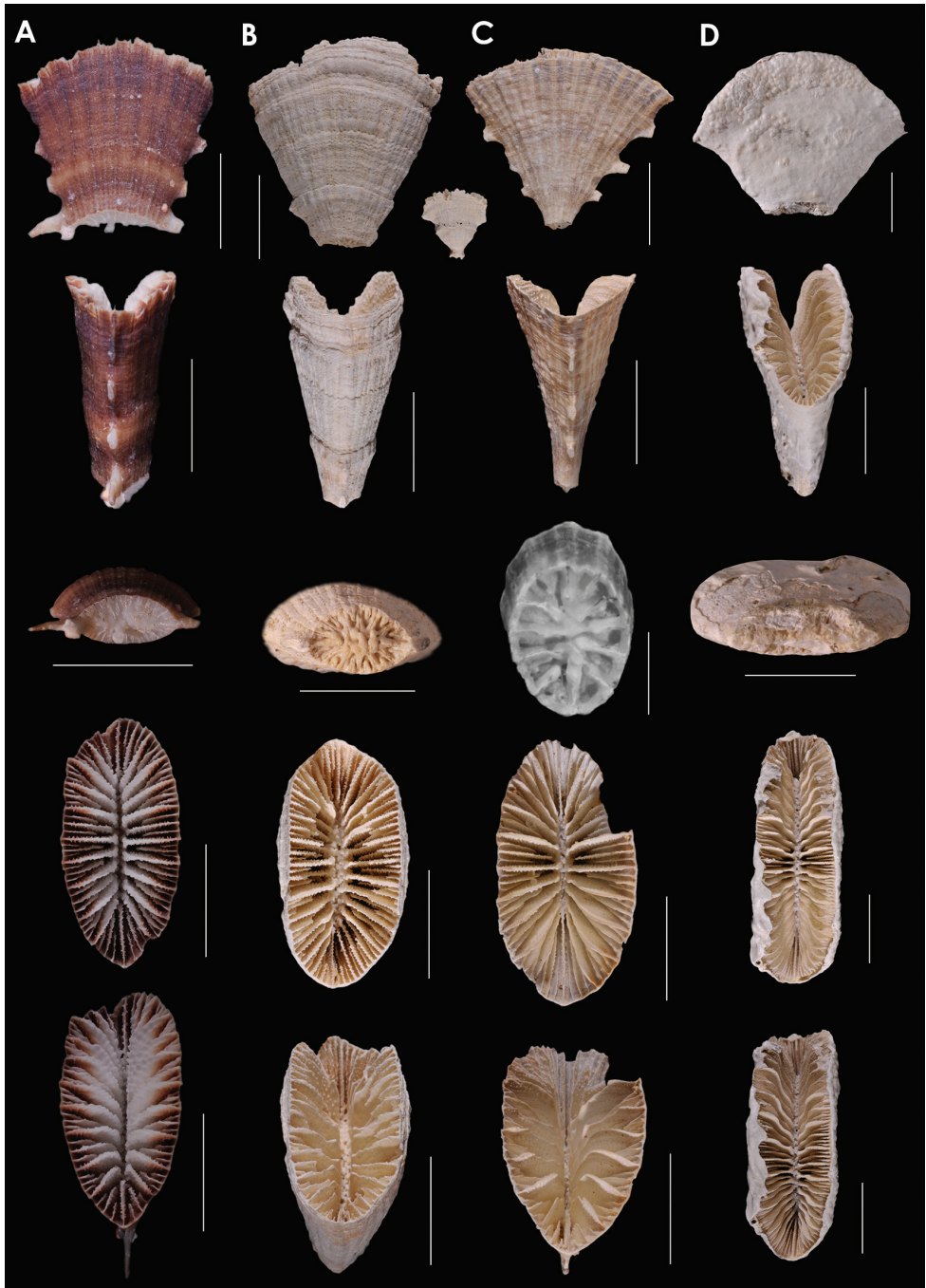


Figure 7. **A** *Truncatoflabellum martensii*, USNM 98908, MUSORSTOM 8 1085, Vanuatu **B** *T. mozambiquensis*, holotype, USNM 91764, and anthocaulus, *Anton Bruun* 372L, Mozambique **C** *T. vigintifarium*, paratype, USNM 98900, MUSORSTOM 1018, Vanuatu **D** *T. spheniscus*, syntype, USNM 92, Singapore. Scale bars: all 10 mm, except for basal scar of C, which is 5 mm.

Remarks. As suggested by the key, *T. mozambiquensis* is most similar to *T. martensii*, but can be distinguished by its smaller basal scar, higher H:GCD ratio, rounded thecal edges, and tendency to have one (or occasionally two) pairs of thecal edge spines vs. three pairs for *T. martensii* (Table 2).

Etymology. Named for the country from which it was found.

***Truncatoflabellum vigintifarium* Cairns, 1999**

Fig. 7C

Truncatoflabellum vigintifarium Cairns, 1999: 121–122, figs 2c–f; 2004, 309.

Distribution. Vanuatu, New Caledonia, off Queensland, 179–1050 m.

***Truncatoflabellum spheniscus* (Dana, 1846)**

Fig. 7D

Euphyllia spheniscus Dana, 1846: 160–161, pl. 6, figs 1a–e.

Flabellum sumatrense Milne Edwards & Haime, 1848: 271.

Flabellum debile Milne Edwards & Haime, 1848: 274, pl. 8, fig. 2.

Flabellum affine Milne Edwards & Haime, 1848: 274, pl. 8, fig. 10.

Flabellum bairdi Milne Edwards & Haime, 1848: 274–275.

Flabellum profundum Milne Edwards & Haime, 1848: 276.

Flabellum elongatum Milne Edwards & Haime, 1848: 275, pl. 8, fig. 7.

Flabellum crenulatum Milne Edwards & Haime, 1848: 277.

Flabellum variabile: Gerth, 1921: 401, pl. 57, fig. 30.—Cairns 1989b: Table 6, pl. 33, pl. 33a.

Flabellum rubrum debile: Yabe & Eguchi, 1941: 269, figs 5–6.

Truncatoflabellum bairdi: Cairns 1989b: 66–67, Table 6, pl. 33k, 34a–c.

Truncatoflabellum profundum: Cairns 1989b: 67, Table 6, pl. 34d–h.

Truncatoflabellum spheniscus: Cairns 1989b: 65–66, pl. 32g–k (synonymy); 1994: 76, pl. 33a–d (synonymy); 1999: 399, Table 4; 2004: 309.

New records. *Albatross* 5483, 10°27'30"N, 125°19'15"E, 135 m, 4 specimens, USNM 1130688; *Albatross* 5593, 4°02'20"N, 118°11'20"E, 69 m, 1 specimen, USNM 1130687.

Distribution. Pliocene: Java (Gerth 1921; Yabe and Eguchi 1941). Holocene: Japan, Indonesia, circum-Australia, 2–174 m.

Remarks. The name *spheniscus*, Latin for small wedge, is treated as a noun in apposition and thus does not match gender with the genus.

***Truncatoflabellum cumingi* (Milne Edwards & Haime, 1848)**

Fig. 8A

Flabellum cumingii Milne Edwards & Haime, 1848: 275, pl. 8, fig. 11.*Flabellum irregulare* Tenison-Woods, 1878b: 313 (junior homonym of *F. irregulare* Semper, 1872).*Truncatoflabellum cumingi*: Cairns 1989b: 69, Table 6, pl. 35f–i (neotype designated, synonymy); 2004: 309 (synonymy).**Distribution.** Philippines, Indonesia, off New South Wales and Western Australia, 46–132 m.***Truncatoflabellum vanuatu* (Wells, 1984)**

Fig. 8B

Flabellum vanuatu Wells, 1984: 215, figs 4 (11–12), 5 (1).*Truncatoflabellum vanuatu*: Cairns 1989b, Table 6, 69, pl. 36c; 1999: 123.*Truncatoflabellum* sp. A: Kitahara et al. 2010: fig. 1.*Truncatoflabellum* sp. B: Kitahara et al. 2010: fig. 1.**New records.** Kere River, Espiritu Santo, Vanuatu, Late Pleistocene, USGS 25715, 25717, and 27718, 35 specimens, USNM 100195, 99485, and 73972, respectively.**Distribution.** Late Pleistocene: Vanuatu. Holocene: Vanuatu, Wallis and Futuna, New Caledonia, 240–335 m.***Truncatoflabellum duncani* sp. n.**<http://zoobank.org/67F30A3A-308C-46E9-8A1C-755DA0D9920B>

Fig. 8C

Flabellum candeanum: Duncan 1864: 163; 1870: 300, pl. 20, fig. 1.*Truncatoflabellum candeanum*: Cairns 1989b: 61, pl. 36i–j.**Types.** Holotype: USGS 10809, Mornington, Balcombe's Bay, Victoria, Balcombian (Middle Miocene), USNM M353592. Paratypes: Muddy Creek, Victoria, Balcombian (Middle Miocene), 3 specimens, USNM 67959; Torquay, Balcombe's Bay, Victoria, Janjukian (Late Oligocene), 1 specimen, USNM 1295618; 3 miles (=4.8 km) west of river Gellibrand, Otway's region, Victoria, "Murray Tertiaries" (probably Middle Miocene) (specimen reported by Duncan, 1864, 1870), BM.**Description.** The anthocyathus has straight rounded thecal edges, with an edge angle of 54–72° and face angle of about 27°. The holotype is 30.8 × 18.1 mm in calicular diameter and 28.5 mm in height, with a greater scar diameter of 8.7 mm,

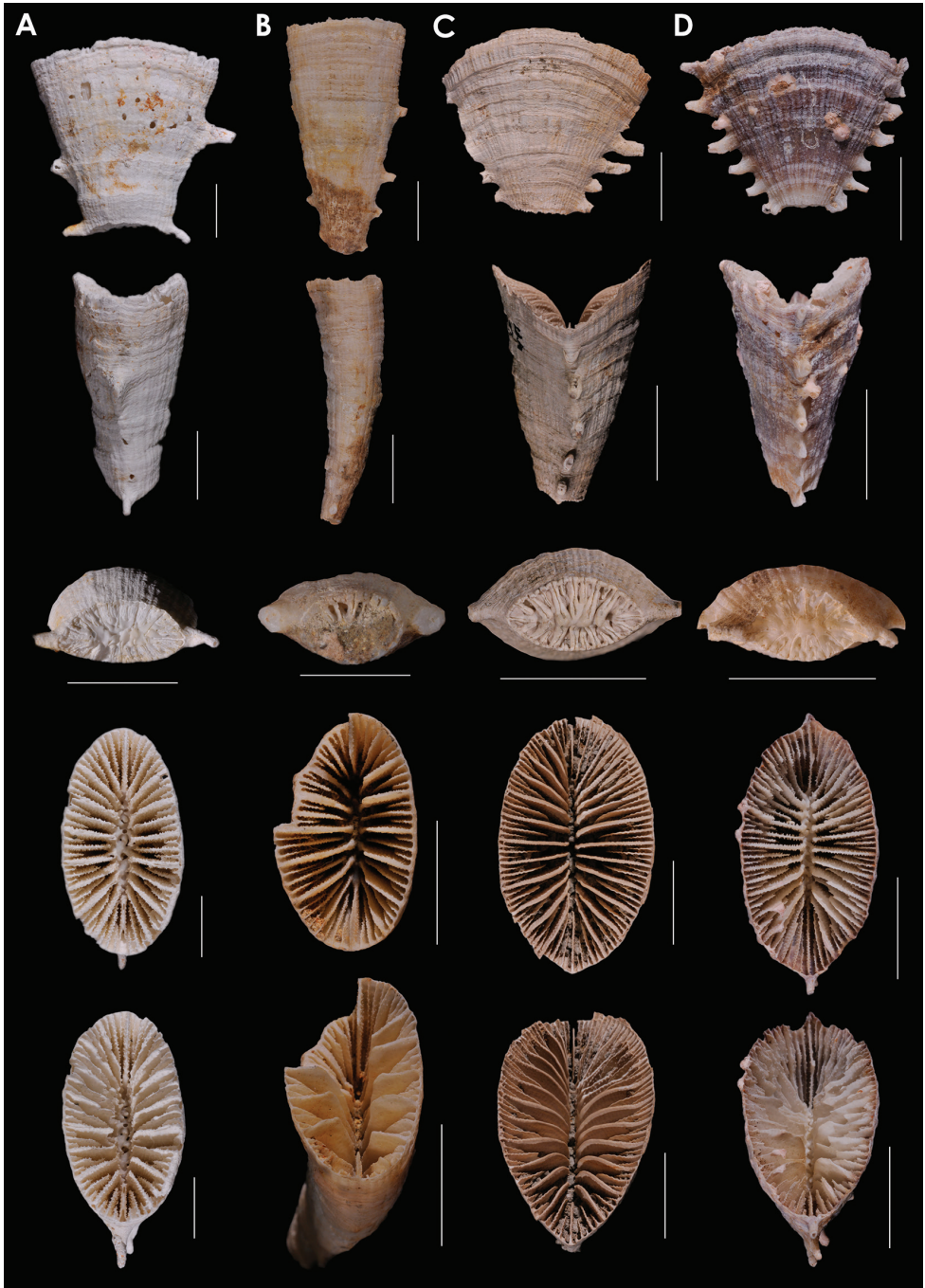


Figure 8. **A** *Truncatoflabellum cumingi*, neotype, USNM 81976, *Te Vega* 1-54, Indonesia **B** *T. vanuatu*, holotype, USNM 71860, Pleistocene of Vanuatu **C** *T. duncani*, paratype, USNM M353592, Balcombe's Bay, Victoria (Balcombian = Middle Miocene) **D** *T. multispinosum*, paratype, USNM 91741, South Africa. Scale bars: all 10 mm, except for basal scar views of **B** and **C**.

similar in size to the specimen reported by Duncan. The GCD:LCD ratio is 1.5–2.1; the H:GCD = 0.95–1.05; and the GSD:GCD is about 0.27, with the scar reaching as long as 12 mm. Four or five pairs of prominent flattened thecal edge spines are present. The septa are quite regularly arranged in five cycles (S1–3>S4>S5), with one pair of S6 in each of the four end half-systems, resulting in 104 septa. The lower axial edges of the larger septa are only slightly sinuous, whereas the upper outer edges are gracefully attenuate, meeting the upper theca as low lamellae. The fossa is open, bordered by the axial edges of the wide S1–3. The anthocaulus is unknown.

Distribution. Late Oligocene to Middle Miocene, Victoria.

Remarks. As suggested by the key, *T. duncani* is remarkably similar to *T. multispinosum*, but can be distinguished by its attenuated upper septal margins. It is also known only from the Oligocene to Miocene of Australia, whereas *T. multispinosum* is restricted to the Holocene and Late Pleistocene.

Etymology. Named in honor Peter M. Duncan, who first discovered specimens belonging to this species.

Truncatoflabellum multispinosum Cairns in Cairns & Keller, 1993

Fig. 8D

Truncatoflabellum multispinosum Cairns in Cairns & Keller, 1993: 268, 272, figs 11H, 12A–C.

New record. USGS 25718, Kere River, Espiritu Santo, Vanuatu, Late Pleistocene, 2 specimens, USNM 100183.

Distribution. Late Pleistocene: Vanuatu. Holocene: western Indian Ocean from South Africa to Tanzania, New Caledonia, 62–183 m.

Truncatoflabellum paripavoninum (Alcock, 1894)

Fig. 9A

Flabellum pari-pavoninum Alcock, 1894: 187.

Flabellum paripavoninum: Alcock 1898: 21, pl. 2, fig. 3a–b.

Truncatoflabellum paripavoninum: Cairns 1989b: 72–73, Table 6, pls. 37j–l, 38a (synonymy); 1995: 113–114, pl. 37d–e.—Cairns and Zibrowius 1997: 169, fig. 22f.—Cairns 1998: 399; 2004: 309.

Distribution. Philippines, Indonesia, New Caledonia, Kermadec Islands, Western Australia, Laccadive Sea, 394–1450 m.

Remarks. *Truncatoflabellum paripavoninum* belongs to a group of six species that lack thecal edge spines and crests (see Key: couplets 28–32). Except for *T. inconstans*, known only from limited material from 23–130 m, these species have the greatest

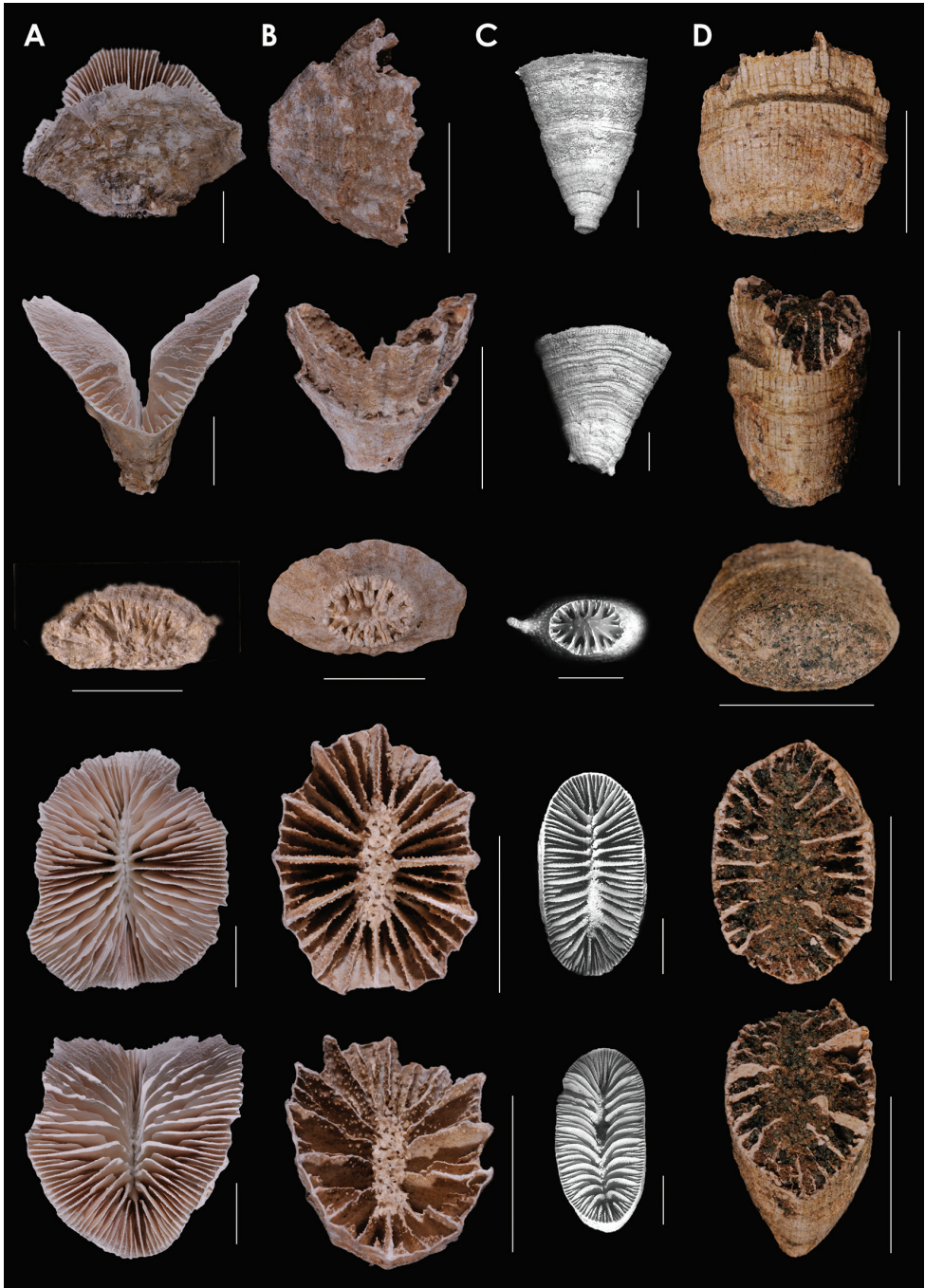


Figure 9. **A** *Truncatoflabellum paripavoninum*, USNM 96650, Soela 1/84/77, Western Australia **B** *T. stabile*, USNM 98886, off Madeira **C** *T. corbicula*, USNM 67939, NZGS GS1341, Waitaki Valley, New Zealand (Duntroonian = Lower Oligocene) **D** *T. inconstans*, syntypes, Valdivia 100, Zoologisches Museum Berlin. Scale bars: all 10 mm, except for basal scar views of **B** and **C**.

depth ranges of all the species in the genus often occurring deeper than 1000 m, suggesting that spines are less necessary for life at great depths. This begs the question of the function of the thecal edge spines. Even the relatively shallow species that have edge spines live at hundreds of meters of depth, far below the level at which surface turbulence would affect them. Thus the function of the thecal spines still remains unresolved.

***Truncatoflabellum stabile* (Marenzeller, 1904)**

Fig. 9B

Flabellum stabile Marenzeller, 1904: 273–274, pl. 17, figs 12a–b.—Zibrowius 1980: 150 (types lost).

Truncatoflabellum stabile: Cairns 1989b: 61.—Zibrowius and Gili 1990: 39.—Cairns 1999: 119, figs 19i–j (synonymy).

Truncatoflabellum sp. cf. *T. stabile*: Cairns and Keller 1993: 264–265, figs 10C, F.

Truncatoflabellum sp. A Cairns, 1994: 75, 79, pl. 34c–e.

Distribution. Ryukyu Islands, Vanuatu, off Mozambique, Cape Verde, Madeira, 786–3010 m.

Remarks. This is the deepest living *Truncatoflabellum* as well as the most geographically widespread.

***Truncatoflabellum inconstans* (Marenzeller, 1904)**

Fig. 9D

Flabellum inconstans Marenzeller, 1904: 277–280, pl. 17, fig. 11a–h.—Boshoff 1981: 34–35.

Flabellum harmeri: Boshoff 1981: 35 (in part).

Truncatoflabellum inconstans: Cairns 1989b: 61.—Zibrowius and Gili 1990: 39 (comparison to other species).—Cairns and Keller 1993: 220 (listed).

Additional record. AFR 985c, 34°47'S, 20°19'E, 80 m, 5.4.1948, 1, SAM .

Distribution. Known only from off southern South Africa, 23–130 m.

Remarks. It is tempting to include Zibrowius and Gili's (1990) *Truncatoflabellum* sp. A form Walvis Ridge (1152 m) as an aberrant *T. inconstans*, but as they say, their unique specimen has many fewer septa, a smaller basal scar, and is found much deeper than typical *T. inconstans*. Their unidentified specimen is thus not assigned to a species.

Very rarely a pair of very small basal thecal spines may be present, but the species is considered to lack spines for the purpose of the key.

***Truncatoflabellum corbicula* (Tenison-Woods, 1880)**

Fig. 9C

Flabellum corbicula Tenison-Woods, 1880: 13, figs 10a–b.—Squires 1958: 66 (lectotype designated).

Truncatoflabellum corbicula: Cairns 1989b: 61.

New record. NZGS 1341, Wharekuri Greensand, Wharekuri, Waitaki Valley, New Zealand, S117/492, Duntroonian (Lower Oligocene), 1 specimen, USNM 67939.

Distribution. Port Hills, Nelson, and Waitaki Valley, New Zealand (Duntroonian =Lower Oligocene).

Remarks. The name *corbicula*, Latin for small basket, is treated as a noun in apposition and thus does not match gender with the genus.

***Truncatoflabellum truncum* (Cairns, 1982)**

Fig. 10A

Flabellum truncum Cairns, 1982: 46, pl. 14, figs 5–8.

Truncatoflabellum truncum: Cairns 1994: 114.—Cairns et al. 2005: 17 (listed).—Cairns and Polonio 2013: 60 (listed).

Distribution. Peru to southern Chile, Falkland Islands, 595–1896 m.

Remarks. This species is known only from its original description.

***Truncatoflabellum trapezoideum* (Keller, 1981)**

Flabellum trapezoideum Keller, 1981: 28, 31, pl. 1, figs 2a–b.

Truncatoflabellum trapezoideum: Cairns 1989b: Table 6; 1994: 79; 1995: 114.

Distribution. Marcus-Necker Ridge, central North Pacific, 1630 m.

Remarks. The species is known from only one specimen. It is very similar to *T. truncum* Cairns, 1982 (see Key and Table 2). Nomenclaturally, this species is similar to *Flabellum trapezoidale* Osasco, 1895, a true *Flabellum* known only from the Pliocene of Italy.

***Truncatoflabellum formosum* Cairns, 1989b**

Fig. 10B

Truncatoflabellum formosum Cairns, 1989b: 69–70, Table 6, (in part: not *Alb* 5137, 5162, 5483, 5484), pl. 35j–k, 36a–b (synonymy).—Cairns and Keller 1993: 264, 265, figs 10I, 11A.—Cairns 1994: 77, pl. 33 g–h.—Cairns and Zibrowius 1997: 169–170.—Cairns 2004: 309.

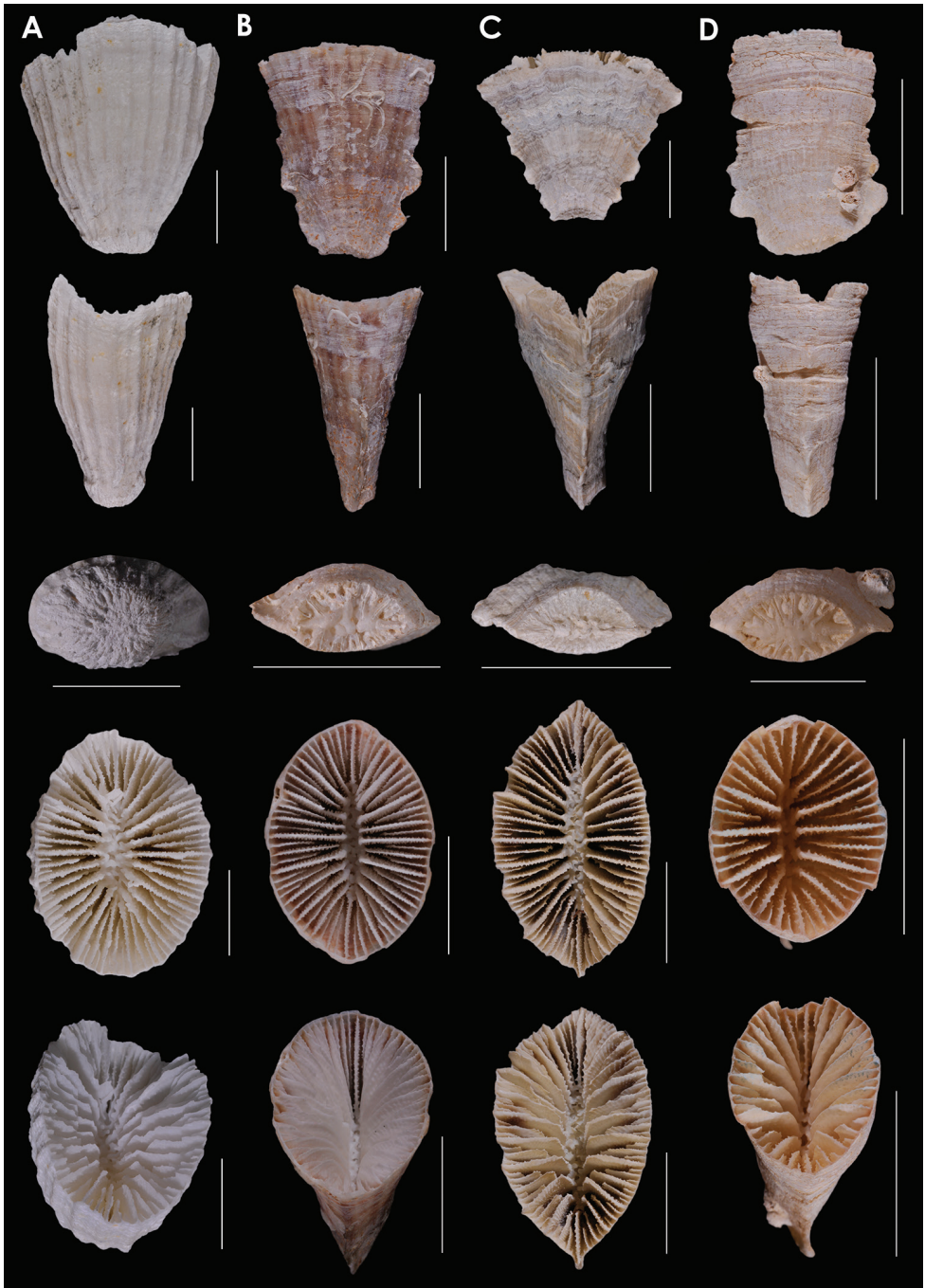


Figure 10. **A** *Truncatoflabellum truncum*, holotype, *Eltanin* 283, Strait of Magellan **B** *T. formosum*, USNM 91757, *Vityaz* 2635, off Mozambique **C** *T. carinatum*, USNM 92806, Taiwan **D** *T. gardineri*, USNM 91736, holotype, *Anton Bruun* 7-3905, South Africa. Scale bars: all 10 mm.

Truncatoflabellum sp. Cairns, 1989b: 73 (undescribed decamerale).

Distribution. Philippines, Indonesia, Japan, Korea Strait, New Caledonia, western Australia, southwest Indian Ocean, 42–933 m.

***Truncatoflabellum carinatum* Cairns, 1989b**

Fig. 10C

?*Flabellum variabile* forma *alta* Gerth, 1921: 401, pl. 57, fig. 16.—Cairns 1989b: pl. 38f.

Flabellum rubrum: Yabe and Eguchi 1942a: 96–98 (in part: pl. 8, figs 6–12, 20).—

Umbgrove 1950: 641, in part: pl. 81, figs 5–6.—Cairns 1989b: pl. 38d.

Truncatoflabellum carinatum Cairns, 1989b: 73–74, Table 6, pl. 38b–e (synonymy); 1994: 77–78, pl. 33j–k.

Flabellum transversale: Hu 1987: pl. 3, figs 1–2.

Flabellum rubrum stokesii: Hu 198: 150, in part: pl. 2, figs 12–14.

New records. *Anton Bruun* 7, 372-J and L, 25°07'S, 34°34'E, 105–112 m, 9 specimens, USNM 1279595 and 127 9596. Plio-Pleistocene, Ryukyu Islands, Okinawa, 4 specimens, USNM 88445.

Distribution. ?Pliocene of Java (Gerth 1921); Pliocene of Ryukyu Islands (Yabe and Eguchi 1942b); Pliocene Taiwan (Hu 1987, 1988); Pleistocene (Java) (Umbgrove 1950); Holocene: South China Sea, Indonesia, off Mozambique, 30–274 m.

Remarks. If Gerth's (1921) forma *alta* is conspecific, it would have nomenclature priority as *Truncatoflabellum altum*.

***Truncatoflabellum gardineri* Cairns in Cairns & Keller, 1992**

Fig. 10D

Truncatoflabellum gardineri Cairns in Cairns & Keller, 1993: 266–267, figs 11B–D.—

Cairns 1994: 78–79, pl. 34a–b.

Distribution. Off South Africa, Japan, 100–144 m.

***Truncatoflabellum arcuatum* Cairns, 1995**

Fig. 11A

Truncatoflabellum arcuatum Cairns, 1995: 116, pl. 38g–i.

Distribution. Norfolk and Kermadec Ridges, 350–364 m.

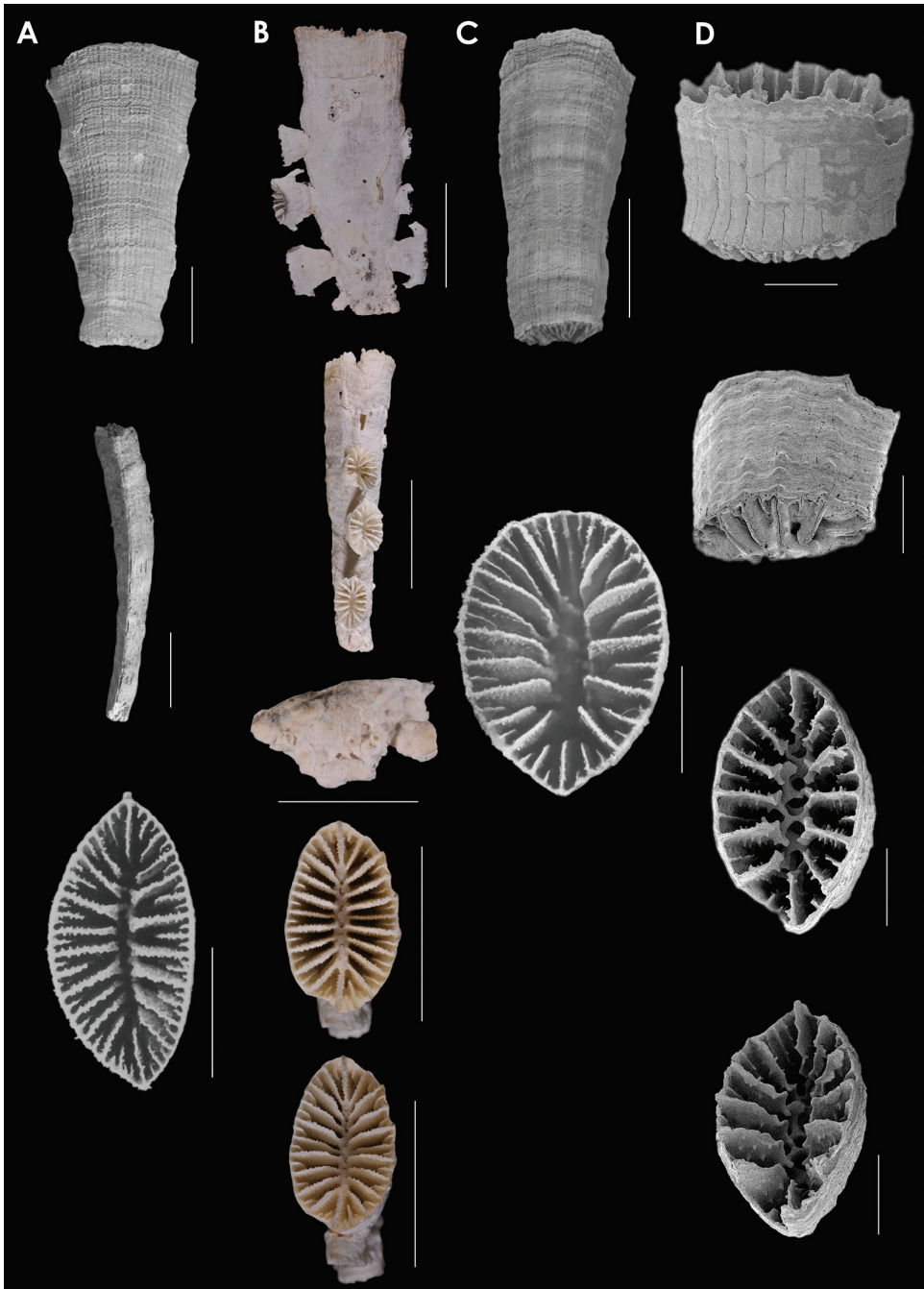


Figure 11. **A** *Truncatoflabellum arcuatum*, lateral and calicular views, holotype, NZOI H633, Norfolk Ridge; edge view, paratype, USNM 94280, Norfolk Ridge **B** *Blastotrochus nutrix*, USNM 97553, *Siboga*, Indonesia **C** *Placotrochides scaphula*, USNM 94273, NZOI G941, New Zealand **D** *P. minuta*, holotype, Australian Museum G16747, Flores Sea. Scale bars: 10 mm (**A–C**), except for calice of **A** and basal scar of **B**, which are 5 mm; 1 mm (**D**).

Genus *Blastotrochus* Milne Edwards & Haime, 1848

Blastotrochus Milne Edwards & Haime, 1848: 284–285.—Cairns 1989a: 645; 1989b: 74 (synonymy, discussion).—Cairns and Kitahara 2012: 14 (key to genus).

Flabellum (*Blastotrochus*): Duncan 1884: 14.

Flabellum: Vaughan and Wells 1943: 226 (in part).—Wells 1956: F432 (in part).—Zibrowius 1974: 19–20 (in part: part of group 2).

Diagnosis. Like *Truncatoflabellum*, but also producing asexual buds (anthoblasts) from thecal edges of anthocyathus. Thecal edges rounded, have a low edge angle, and bear one pair of basal edge spines.

Discussion. The mode of asexual reproduction employed by *Blastotrochus*, described and illustrated by Cairns (1989a) as the anthoblast mode (also called bud shedding), differs slightly from transverse division of *Truncatoflabellum* by its potential to produce many more simultaneous clonemates from its thecal edges (instead of one at a time as with *Truncatoflabellum*), leading to a potentially exponential increase in clonemates instead of a gradual one. This was considered as a key innovation by Cairns (1989a), worthy of generic distinction from *Truncatoflabellum*. A second species was described in this genus, *B. proliferus* d'Archiardi, 1866 (Miocene, Italy), but was reassigned to *Cladocora* (see Pfister 1980). *Blastotrochus* thus remains a monophyletic genus and has rarely been collected.

Distribution. Philippines, Indonesia, 11–62 m.

Type species. *Blastotrochus nutrix* Milne Edwards & Haime, 1848, by monotypy.

***Blastotrochus nutrix* Milne Edwards & Haime, 1848**

Fig. 11B

Blastotrochus nutrix Milne Edwards & Haime, 1848: 284–285, pl. 8, Fig. 14.—Semper 1872: 238–241, pl. 16, figs 1–6.—Chevalier 1961: 379.—Cairns 1989a: 643, 645, fig. 1 (upper); 1989b: 74–75, pl. 38i–m, 39a–b (synonymy).—Cairns and Zibrowius 1997: 173–174.—Cairns and Kitahara 2012: pl. 23A–B.

Distribution. As for the genus.

Genus *Placotrochides* Alcock, 1902

Placotrochides Alcock, 1902: 33.—Zibrowius 1974: 20, 23, 26.—Cairns 1989b: 78 (synonymy, discussion); 1995: 116; 2004: 307 (key to species).—Cairns and Kitahara 2012: 13 (key to genus).

Flabellum: Vaughan and Wells 1943: 226 (in part).

Diagnosis. Asexual reproduction by apical transverse division of corallum, resulting in distal anthocyathus and basal anthocaulus. Corallum usually laterally compressed and subcylindrical, having a low edge angle; thecal edges rounded and do not bear spines or crests; calicular outline often asymmetrical. Columella absent or represented by a fusion of the lower, axial edges of the larger septa. Anthocaulus stereome-reinforced.

Discussion. *Placotrochides* differs from *Truncatoflabellum* by having a non-spinose compressed-cylindrical corallum and a stereome-reinforced anthocaulus.

Distribution. Western and central Pacific, southwestern Indian Ocean, northern and southwestern Atlantic, 80–1628 m.

Type species. *P. scaphula* Alcock, 1902, by subsequent designation (Wells 1936).

Key to the species of *Placotrochides* (characters pertain to the anthocyathus stage)

- 1 GCD > 12 mm.....*P. scaphula* (Fig. 11C)
- 1' GCD < 7 mm.....**2**
- 2 S1>S2; GCD:LCD = 1.07–1.16 (close to circular)*P. cylindrica* (Fig. 12A)
- 2' S1=S2; GCD:LCD = 1.19–2.0 (more elliptical)**3**
- 3 GCD rarely greater than 3.5 mm; GCD:LCD = 1.6–2.0; Indo-West Pacific ...
.....*P. minuta* (Fig. 11D)
- 3' GCD about 5 mm; GCD:LCD = 1.2–1.5; amphi-Atlantic
.....*P. frustum* (Fig. 12B)

Placotrochides scaphula Alcock, 1902

Fig. 11C

Placotrochides scaphula Alcock, 1902: 34, pl. 4, figs 32, 32a.—Cairns 1989b: 45, 78–79, pls. 40l, 41a–e (synonymy).—Cairns and Parker 1992: 48–49, figs 15h–i.—Cairns and Keller 1993: 272–273, figs 12D, G.—Cairns 1994: 79–80, pl. 34f–h; 1995: 116–117, pls. 38j, 39a.—Cairns and Zibrowius 1997: 174; 2004: 307.—Cairns and Kitahara 2012: pl. 20, figs N–O.

Flabellum elongatum Hu, 1987: 44, pl. 3, figs 4, 7–8 (also a junior homonym of *F. elongatum* Milne Edwards & Haime, 1848: 275).

Distribution. Plio-Pleistocene: southern Taiwan (Hu 1987). Holocene: off Japan, Philippines, Indonesia, New Caledonia, New Zealand, off Victoria and Queensland, Australia, southwest Indian Ocean, 80–1628 m.

Remarks. A replacement name for junior primary homonym *Flabellum elongatum* Hu, 1987 is not necessary, as the senior homonym is considered to belong to *Truncatoflabellum* and Hu's species to *Placotrochides*.

***Placotrochides cylindrica* Cairns, 2004**

Fig. 12A

Placotrochides cylindrica Cairns, 2004: 305, 307 (key), figs 10B–D.

Distribution. Known only from seamounts off northeastern Australia, 1117–1402 m.

***Placotrochides minuta* Cairns, 2004**

Fig. 11D

Placotrochides sp. n. Feinstein & Cairns, 1998: 81, 83, fig. 10.

Placotrochides minuta Cairns, 2004: 305–307 (key), figs 10E–H.

Placotrochides minima: Cairns 2006: 52 (*lapsus calumni*).

Distribution. Marion Plateau of Queensland, Indonesia, Hawaii, 119–458 m.

***Placotrochides frustum* Cairns, 1979**

Fig. 12B

Placotrochides frusta Cairns, 1979: 152–153, pl. 29, figs 4–6, 8–9, map 43.

Placotrochides frustra: Zibrowius 1980: 159–161, pl. 81E–M.

Placotrochides frustum: Cairns 2004: 307 (key, nom. correct.).

New records. CRYOS, *Balgim* CP85, 34°24'N, 7°39'W, 1378 m, 15 specimens, MNHN; *Professor Logachev* 37L 165, 16°54.014'N, 46°34.842'W, 2646–2705 m, 6 Mar 2015, 1, USNM 1295415, 1, IOM Moscow; *Professor Logachev* 37L 188, 17°08.470'N, 46°23.443'W, 2291–2327 m, 12 Mar 2015, 1, IOM Moscow.

Distribution. Lesser Antilles, off northeastern Brazil, mid-Atlantic Ridge at latitude of Lesser Antilles, off Morocco, 497–2646 m.

Remarks. The specimens reported herein from the mid-Atlantic Ridge are much larger than any previously reported, having a GCD up to 10.2 mm and a height of 13.9 mm, the calice having corresponding more septa, i.e., S1-2>S3>S4, 12:12:12, or 36 septa. The largest previously known specimen was only 5.0 mm in GCD and had 26 septa. They also represent a considerable depth range extension.

Genus *Placotrochus* Milne Edwards & Haime, 1848

Placotrochus Milne Edwards & Haime, 1848: 282.—Duncan 1884: 16 (in part: not fossil records).—Vaughan and Wells 1943 227 (in part: not fossil records).—Wells

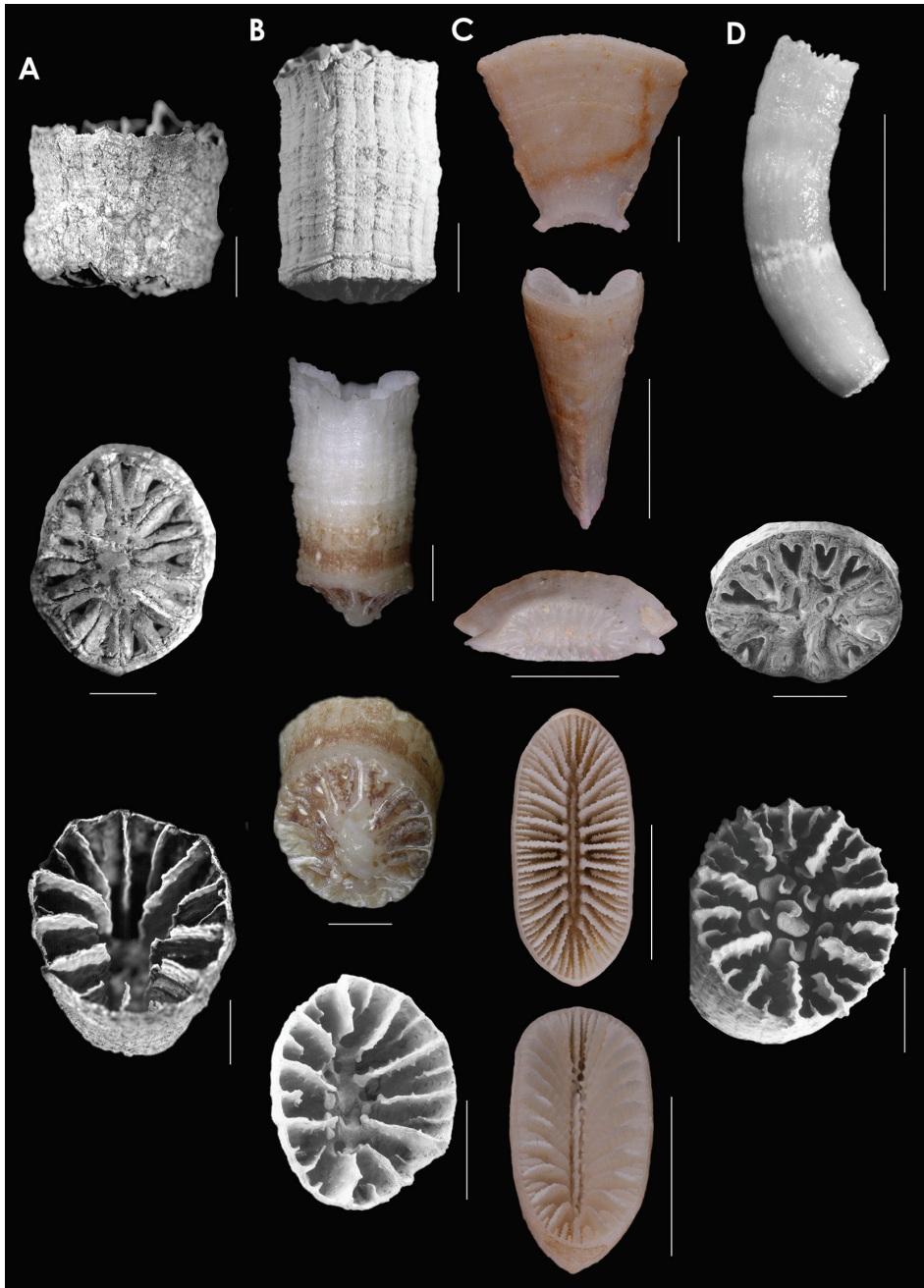


Figure 12. **A** *Placotrochides cylindrica*, holotype, Museum of Tropical Queensland G55627, off Queensland **B** *P. frustum*, holotype, USNM 36451, Lesser Antilles; paratype, NMC, Hudson 4B, Lesser Antilles **C** *Placotrochus laevis*, USNM 81994, Great Barrier Reef, Australia **D** *Falcatoflabellum raoulensis*, upper image, holotype, Museum of New Zealand, CO 258, Kermadec Ridge; lower images, paratype, USNM 94313, Kermadec Ridge. Scale bars: 1mm (**A**); 2 mm (**B**); 10 mm (**C**), except for basal scar, which is 5 mm; 1 mm (**D**), except latera view, which is 5 mm.

1956: F432.—Zibrowius 1974: 21, 26.—Cairns 1989: 45, 75 (synonymy).—Cairns and Kitahara 2012: 13 (key to genus).

Diagnosis. Asexual reproduction by apical transverse division of corallum, resulting in distal anthocyathus and basal anthocaulus. Corallum laterally compressed and fan shaped, having rounded thecal edges with one pair of basal thecal edge spines. Columella lamellar. Anthocaulus not stereome-reinforced.

Discussion. Seven species of *Placotrochus* were described from the Australian Eocene-Miocene by Duncan (1864), Dennant (1899, 1903, 1904), and Tenison-Woods (1878a), but these species are not transversely dividing and thus should be assigned to a different genus (Cairns in prep.). *Placotrochus* is a monotypic genus.

Distribution. Western Pacific, eastern Indian Ocean, 6–289 m.

Type species. *Placotrochus laevis* Milne Edwards & Haime, 1848, by subsequent designation (Milne Edwards and Haime 1850: xviii).

Placotrochus laevis Milne Edwards & Haime, 1848

Fig. 12C

Placotrochus laevis Milne Edwards & Haime, 1848: 283, pl. 8, figs 15, 15a.—Semper 1872: 251–252, pl. 18, figs 11–13.—Bourne 1905: 200–201, pl. 1, fig. 5.—Cairns 1989b: 75–76, pl. 39c–g (synonymy).—Cairns and Zibrowius 1997: 175.—Cairns 2004: 307 (synonymy).—Cairns and Kitahara 2012: pl. 20, figs I–J.

Placotrochus candeanus Milne Edwards & Haime, 1848: 283–284.

Placotrochus pedicellatus Tenison-Woods, 1879: 134–135, pl. 13, figs 7, 7a.

New record. *Alpha Helix* M-21: 8°45'S, 144°05.8'E, 55 m, 1 specimen, USNM 1130681.

Distribution. As for genus.

Genus *Falcatoflabellum* Cairns, 1995

Falcatoflabellum Cairns, 1995: 117–118.—Cairns and Kitahara 2012: 14 (key to genus).

Diagnosis. Asexual reproduction by apical transverse division of corallum, resulting in distal anthocyathus and basal anthocaulus. Corallum compressed-cylindrical, often slightly curved, with rounded thecal edges that lack spines and crests. Columella fascicular; paliform lobes occasionally present before S2. Anthocaulus unknown.

Discussion. *Falcatoflabellum* is easily distinguished from all other flabellids by its fascicular columella and paliform lobes (P2). The genus is monotypic.

Distribution. Kermadec Islands, 366–402 m.

Type species. *Falcatoflabellum raoulensis* Cairns, 1995, by original designation.

***Falcatoflabellum raoulensis* Cairns, 1995**

Fig. 12D

Falcatoflabellum raoulensis Cairns, 1995: 118, pl. 39b–g.—Cairns and Kitahara 2012: pl. 20, figs K–M.

Distribution. As for genus.

Remarks. Known only from the type series of 21 specimens from the type-locality.

Acknowledgements

I would like to thank Robert H. Ford for taking most of photographs for figures 2–12 and arranging them in logical order. I also thank Marianna Terezow (GNS Science, Lower Hutt, New Zealand) for the photographs of *T. sphenodeum*; Frank Holmes (National Museum of Victoria, Melbourne) for the images of *T. gippslanicum*; and Helmut Zibrowius for the images of the syntypes of *F. inconstans*. I also thank Georgia Tschen for drafting Figure 1. Tina Molodtsova graciously provided additional samples of *T. frustum*.

References

- Alcock A (1894) On some new and rare corals from deep waters of India. *Journal of the Asiatic Society of Bengal* 2(62): 186–188.
- Alcock A (1898) An account of the deep-sea Madreporaria collected by the royal Indian Marine Survey Ship “*Investigator*”. *Indian Museum, Calcutta*, 1–29. doi: 10.5962/bhl.title.11313
- Alcock A (1902) Report on the deep-sea Madreporaria of the *Siboga*-Expedition. *Siboga*-Expedition 16a: 1–52.
- Bell KN (1981) A list of the Tertiary coral types in the National Museum of Victoria. *Fossil Cnidaria* 10(1): 9–11.
- Boshoff PH (1981) An annotated checklist of southern African Scleractinia. South African Association for Marine Biological Research, Oceanographic Research Institute, Durban, Investigational Report 49: 1–45.
- Bourne G (1905) Report on the solitary corals collected by Professor Herdman, at Ceylon, in 1902. *Ceylon Pearl Oyster Fisheries, Supplementary Report* 29: 187–242.
- Cairns SD (1979) The deep-water Scleractinia of the Caribbean and adjacent waters. *Studies on the Fauna of Curaçao and Other Caribbean Islands* 57(180): 1–341.
- Cairns SD (1982) Antarctic and Subantarctic Scleractinia. *Antarctic Research Series* 34(1): 1–74.
- Cairns SD (1989a) Asexual reproduction in solitary Scleractinia. *Proceedings of the 6th International Coral Reef Symposium, Townsville, Australia* 2: 641–646.
- Cairns SD (1989b) A revision of the ahermatypic Scleractinia of the Philippine Islands and adjacent waters, Part 1: Fungiacyathidae, Micrabaciidae, Turbinoliinae, Guyniidae, and Flabellidae. *Smithsonian Contributions to Zoology* 486: 1–136. doi: 10.5479/si.00810282.486

- Cairns SD (1994) Scleractinia of the temperate North Pacific. *Smithsonian Contributions to Zoology* 557: 1–150. doi: 10.5479/si.00810282.557.i
- Cairns SD (1995) The marine fauna of New Zealand: Scleractinia (Cnidaria: Anthozoa). *New Zealand Oceanographic Institute Memoir* 103: 1–210.
- Cairns SD (1998) Azooxanthellate Scleractinia (Cnidaria: Anthozoa) of Western Australia. *Records of the Western Australian Museum* 18: 361–417.
- Cairns SD (1999) Cnidaria Anthozoa: deep-water azooxanthellate Scleractinia from Vanuatu, and Wallis and Futuna Islands. *Mémoires du Muséum national d’Histoire Naturelle* 180: 31–167.
- Cairns SD (2004) The azooxanthellate Scleractinia (Coelenterata: Anthozoa) of Australia. *Records of the Australian Museum* 56: 259–329. doi: 10.3853/j.0067-1975.56.2004.1434
- Cairns SD (2006) New records of azooxanthellate Scleractinia from the Hawaiian Islands. *Bishop Museum Occasional Papers* 87: 49–53.
- Cairns SD, Zibrowius H (1997) Cnidaria Anthozoa: Azooxanthellate Scleractinia from the Philippine and Indonesian regions. *Mémoires du Muséum national d’Histoire Naturelle* 172(2): 27–243.
- Cairns SD, Kitahara MV (2012) An illustrated key to the genera and subgenera of the Recent azooxanthellate Scleractinia (Cnidaria, Anthozoa), with an attached glossary. *ZooKeys* 227: 1–47. doi: 10.3897/zookeys.227.3612
- Cairns SD, Keller NB (1993) New taxa and distributional records of azooxanthellate Scleractinia (Cnidaria, Anthozoa) from the tropical south-west Indian Ocean, with comments on their zoogeography and ecology. *Annals of the South African Museum* 103(5): 213–292.
- Cairns SD, Parker SA (1992) Review of the Recent Scleractinia (Stony Corals) of South Australia, Victoria and Tasmania. *Records of the South Australian Museum, Monograph Series* 3: 1–82.
- Cairns SD, Häussermann V, Försterra G (2005) A review of the Scleractinia (Cnidaria: Anthozoa) of Chile, with the description of two new species. *Zootaxa* 1018: 15–46.
- Cairns SD, Polonio V (2013) New records of deep-water Scleractinia off Argentina and the Falkland Islands. *Zootaxa* 3691(1): 58–86. doi: 10.11646/zootaxa.3691.1.2
- Chevalier J-P (1961) Recherches sur les Madréporaires et les formations récifales Miocènes de la Méditerranée Occidentale. *Mémoires de la Société Géologique de France (new series)* 40(93): 1–562.
- d’Archiadi A (1866) Corallarj fossili del terreno nummulitico dell’ Alpi Venete. Part 1. *Memorie della Società Italiana di Scienze Naturali* 2(4): 1–53.
- Dana JD (1846) Zoophytes In: *United States Exploring Expedition during the Years 1838, 1839, 1840, 1841, 1842 under the Command of Charles Wilkes, 7. Lea and Blanchard, Philadelphia*, vi + 1–740. doi: 10.5962/bhl.title.70845
- Dennant J (1899) Descriptions of new species of corals from the Australian Tertiaries. Part 1. *Transactions of the Royal Society of South Australia* 23: 112–122.
- Dennant J (1903) Descriptions of new species of corals from the Australian Tertiaries. Part 6. *Transactions of the Royal Society of South Australia* 27: 208–15.
- Dennant J (1904) Recent corals from the South Australian and Victorian coasts. *Transactions of the Royal Society of South Australia* 28: 1–11.

- Duncan PM (1864) A description of some fossil corals and echinoderms from the south-Australian Tertiaries. *The Annals and Magazine of Natural History* (3)14(81): 161–168.
- Duncan PM (1870) On the fossil corals (Madreporaria) of the Australian Tertiary deposits. *Quarterly Journal of the Geological Society of London* 26: 284–318. doi: 10.1144/GSL.JGS.1870.026.01-02.27
- Duncan PM (1884) A revision of the families and genera of the Sclerodermic Zoantharia Ed. and H., or Madreporaria (M. Rugosa excepted). *Journal of the Linnean Society of London, Zoology* 18(104–105): 1–204.
- Feinstein N, Cairns SD (1998) Learning from the collector: a survey of azooxanthellate corals affixed by *Xenophora* (Gastropoda: Xenophoridae), with an analysis and discussion of attachment patterns. *The Nautilus* 112(3): 73–83.
- Felix JP (1927) Anthozoa Miocaenica. In: Diener C (Ed.) *Fossilium Catalogus, I: Animalia*. W. Junk, Berlin, part 35, 297–488.
- Fitzgerald E, Schmidt R (year unknown) Fossils of Beaumaris. Museum of Victoria.
- Gerth H (1921) Anthozoa. In: Martin K (Ed.) *Die Fossilien von Java. Sammlungen des Geologischen Reiches-Museum, Leiden* 1(1–2), 387–445.
- Hayward BW (1977) Lower Miocene corals from the Waitakere Ranges, North Auckland, New Zealand. *Journal of the Royal Society of New Zealand* 7(1): 99–111. doi: 10.1080/03036758.1977.10419340
- Hoeksema B, Cairns S (2015) Scleractinia. Accessed through: World Register of Marine Species at <http://www.marinespecies.org/aphia.php?p=taxdetails&cid=1363> [on 2016-01-11]
- Hu C-H (1987) Unusual fossil corals from Hengchun Peninsula, southern Taiwan. *Memoir of the Geological Society of China* 8: 31–48.
- Hu C-H (1988) Some solitary fossil corals and paleoecology of the Tunghsaio and Lungkang Formations of Miaoli region, northern Taiwan. *Proceedings of the Geological Society of China* 31(1): 140–153.
- Keller NB (1981) The solitary madreporarian corals In: Kuznetsov AP, Mironov AN (Eds) *Benthos of the Submarine Mountains Marcus-Necker and adjacent Pacific Regions*. P. P. Shirshov Institute of Oceanology, Moscow, 28–39.
- Lamarck JBPA d' (1816) *Histoire Naturelle des Animaux sans Vertèbres*. Volume 2. Les Polypes. Verdière, Paris, 1–569.
- Lamarck JBPA d' (1827) *Tableau Encyclopedique et Méthodique des Trois Règnes de la Nature*, 3. Paris, pl. 483
- Marenzeller E von (1904) Steinkorallen. *Wissenschaftliche Ergebnisse der Deutschen Tiefsee-Expedition auf dem Dampfer "Valdivia" 1898–1899* 7(3): 261–318.
- Milne Edwards H, Haime J (1848) Recherches sur les Polypiers, deuxième mémoire: Monographie des Turbinolides. *Annales des Sciences Naturelles, Zoologie* (3)9: 211–344.
- Milne Edwards H, Haime J (1850) Introduction. In: *A Monograph on the British Fossil Corals*. Part 1. Palaeontographical Society, London, 1–85.
- Moseley HN (1881) Report on certain hydroid, alcyonarian, and madreporarian corals procured during the voyage of H. M. S. *Challenger*, in the years 1873–1876. Report on the Scientific Results of the Voyage of H. M. S. *Challenger* during the Years 1873–76, *Zoology* 2: 1–248.

- Ogawa K, Takahashi K (2006) A revision of Japanese ahermatypic corals around the coastal region with guide to identification – XII. *Truncatoflabellum*, *Placotrochus* and *Placotrochides*. Nankiseibutu, The Nanki Biological Society 48(1): 13–20.
- Osasco E (1895) Di alcuni Corallari pliocenici del Piemonte e della Liguria. Atti della Regia Accademia delle scienze di Torino 31: 225–237.
- Pfister T (1980) Systematische und paläoökologische Untersuchungen an oligozänen Korallen der Umgebung von San Lucas (Provinz Vicenza Norditalien). Schweizerische Paläontologische Abhandlungen 103: 3–121.
- Roberts JM, Wheeler AJ, Freiwald A, Cairns SD (2009) Cold-Water Corals: the Biology and Geology of Deep-Sea Coral Habitats. Cambridge University Press, Cambridge, 334 pp.
- Scheer G, Pillai SG (1974) Report on the Scleractinia from Nicobar Islands. Zoologica 42(122): 1–75
- Squires DF (1958) The Cretaceous and Tertiary corals of New Zealand. New Zealand Geological Survey, Paleontology Bulletin 29: 1–107.
- Squires DF (1963) *Flabellum rubrum* (Quoy and Gaimard). New Zealand Oceanographic Institute Memoir 20: 1–43.
- Tenison-Woods JE (1878a) On some Australian Tertiary corals. Proceedings of the Royal Society of New South Wales 11: 183–195.
- Tenison-Woods JE (1878b) On the extratropical corals of Australia. Proceedings of the Linnean Society of New South Wales 2: 292–341.
- Tenison-Woods JE (1879) On some new extratropical corals. Proceedings of the Linnean Society of New South Wales 3: 131–135. doi: 10.5962/bhl.part.22226
- Tenison-Woods JE (1880) New Zealand fossil corals. Palaeontology of New Zealand, Part 4. Corals and Bryozoa of the Neozoic Period in New Zealand. G. Didsbury, Government Printer, Wellington, 7–33.
- Tokuda Y, Ikeno T, Goto SG, Numata H (2010) Influence of different substrates on the evolution of morphology and life-history traits of azooxanthellate solitary corals (Scleractinia: Flabellidae). Biological Journal of the Linnean Society 101: 184–192. doi: 10.1111/j.1095-8312.2010.01479.x
- Umbgrove JHF (1938) Corals from an elevated marl of Talaud (East Indies). Zoologische Mededelingen 20: 263–274.
- Umbgrove JHF (1950) Corals from the Putjangan Beds (Lower Pleistocene) of Java. Journal of Paleontology 24(6): 637–651.
- Vaughan TW, Wells JW (1943) Revision of the Suborders Families, and Genera of the Scleractinia. Geological Society of America Special Paper 44, 1–363. doi: 10.1130/SPE44-p1
- Wells JW (1936) The nomenclature and type species of some genera of Recent and fossil corals. American Journal of Science (5)31(182): 97–134. doi: 10.2475/ajs.s5-31.182.97
- Wells JW (1956) Scleractinia. In: Moore RC (Ed.) Treatise on Invertebrate Paleontology, Part F: Coelenterata. Geological Society of America and University of Kansas Press, Lawrence, Kansas, F90–F106.
- Wells JW (1984) Notes on Indo-Pacific scleractinian corals. Part 10. Late Pleistocene ahermatypic corals from Vanuatu. Pacific Science 38(3): 205–219.

- Yabe H, Eguchi M (1941) On some simple corals from the Neogene of Java. Proceedings of the Imperial Academy of Japan 17(7): 269–273.
- Yabe H, Eguchi M (1942a) Fossil and Recent *Flabellum* from Japan. Scientific Reports of the Tôhoku Imperial University Sendai, Japan, second series (Geology) 22(2): 87–103.
- Yabe H, Eguchi M (1942b) Fossil and Recent simple corals from Japan. Scientific Reports of the Tôhoku Imperial University, Sendai, Japan, second series (Geology) 22(2): 105–178.
- Zibrowius H (1974) Révision du genre *Javania* et considérations générales sur les Flabellidae (Scléactiniaires). Bulletin de l'Institute Océanographique, Monaco 71(1429): 1–48.
- Zibrowius H (1980) Les Scléactiniaires de la Méditerranée et de l'Atlantique Nord-Oriental. Mémoires de l'Institut Océanographique, Monaco 11: 1–284.
- Zibrowius H, Gili J-M (1990) Deep-water Scleractinia (Cnidaria: Anthozoa) from Namibia, South Africa, and Walvis Ridge, southeastern Atlantic. Scientia Marina 54(1): 19–46.

Unexpected diversity and a new species of *Epizoanthus* (Anthozoa, Hexacorallia) attached to eunicid worm tubes from the Pacific Ocean

Hiroki Kise¹, James Davis Reimer^{1,2}

1 *Molecular Invertebrate Systematics and Ecology Laboratory, Graduate School of Engineering and Science, University of the Ryukyus, 1 Senbaru, Nishihara, Okinawa 903-0213, Japan* **2** *Tropical Biosphere Research Center, University of the Ryukyus, 1 Senbaru, Nishihara, Okinawa 903-0213, Japan*

Corresponding author: *Hiroki Kise* (hkm11sea@yahoo.co.jp)

Academic editor: *B. W. Hoeksema* | Received 18 August 2015 | Accepted 25 November 2015 | Published 10 February 2016

<http://zoobank.org/9A5B29AC-14D1-4879-8C55-DD8515557548>

Citation: Kise H, Reimer JD (2016) Unexpected diversity and a new species of *Epizoanthus* (Anthozoa, Hexacorallia) attached to eunicid worm tubes from the Pacific Ocean. Title. ZooKeys 562: 49–71. doi: 10.3897/zookeys.562.6181

Abstract

Epizoanthus species are generally found in association with other marine invertebrates such as hermit crabs and gastropods. Although *Epizoanthus* spp. are relatively common, there is limited information about their diversity and ecology due to their habitats or hosts, often being below the depths of SCUBA diving (>~50 m). In particular, the *Epizoanthus* fauna of the Indo-Pacific Ocean remains poorly understood. In this study, the diversity of *Epizoanthus* species associated with eunicid worm tubes from shallow waters in the Pacific Ocean we investigated using molecular analyses (mitochondrial cytochrome oxidase subunit 1 = COI, mitochondrial 16S ribosomal DNA = mt 16S-rDNA, nuclear internal transcribed spacer region of ribosomal DNA = ITS-rDNA) combined with morphological and ecological data. The combined data set leads us to describe two new species; *Epizoanthus inazuma* **sp. n.** and *Epizoanthus beriber* **sp. n.** Both new species are found in low-light environments: *E. inazuma* **sp. n.** on mesophotic coral reef slopes and reef floors, or on the sides of overhangs; *E. beriber* **sp. n.** has only been found in caves. Morphological characteristics of these two new species are very similar to *E. illoricatus* Tischbierek, 1930 but the two new species are genetically distinct. Mesentery numbers and coloration of polyps may be useful diagnostic characteristics among eunicid-associated *Epizoanthus* species. These results demonstrate that there is high potential for other potentially undescribed zoantharian species, particularly in underwater cave habitats.

Keywords

Eunicidae, cryptic species, mesophotic, molecular analyses, underwater cave, zoantharian

Introduction

The order Zoantharia is currently separated into two suborders (Haddon and Shackleton 1891): Macrocnemina and Brachycnemina. The suborders are distinguished by differences in the fifth pair of mesenteries from the dorsal directive, which are complete in the suborder Macrocnemina and incomplete in the suborder Brachycnemina. The suborder Macrocnemina is currently composed of five families: Epizoanthidae, Hydrozoanthidae, Microzoanthidae, Nanozoanthidae, and Parazoanthidae. Most species of Macrocnemina to the exception of Microzoanthidae and Nanozoanthidae are often found in association with other marine invertebrates. The family Epizoanthidae can be distinguished from other macrocnemic zoantharians by the presence of a simple mesogloea sphincter muscle.

The family Epizoanthidae consists of three genera: *Epizoanthus*, *Palaeozoanthus*, and *Thoracactis*. The genus *Palaeozoanthus* has not been found or examined in detail since its original description (Carlgren 1924), while *Thoracactis topsenti* Gravier, 1918 is the sole representative of its genus and is an epibiont on sponges at 800–1100 meters around the Cape Verde Islands (Gravier 1918). The type genus of Epizoanthidae, *Epizoanthus*, includes species that have epibiotic associations with hermit crabs (Muirhead et al. 1986; Ates 2003; Reimer et al. 2010a; Schejter and Mantelatto 2011), molluscs (Rees 1967), eunicid worms (Sinniger et al. 2005), or the stalks of glass sponges (hexactinellids) (Beaulieu 2001). *Epizoanthus* spp. have been reported worldwide, including from the northeast Atlantic (Muirhead et al. 1986), the Caribbean Sea (Duerden 1898), and both the eastern (Carlgren 1899; Philipp and Fautin 2009; Sinniger et al. 2009) and western Pacific (Haddon and Shackleton 1891; Reimer et al. 2010a).

Although *Epizoanthus* spp. are relatively common, little research has been conducted on the ecology and taxonomy of this genus (Ates 2003). Many *Epizoanthus* species are known from below the depth limits safe for SCUBA diving (>50 m), making collection and observation difficult. *Epizoanthus* species are also often difficult to identify due to lack of external diagnostic characteristics, and data are often limited to polyp size, oral disk color, and tentacle count (Reimer et al. 2010a). It is often difficult to observe zoantharian internal morphology due to sand encrustation in their epithelial/endodermal tissue, making thin cross sections difficult without compromising histology (Reimer et al. 2010b). Molecular phylogenetic analyses have been used to overcome these issues and to help understand zoantharian diversity and taxonomy (e.g. Burnett 1997; Reimer et al. 2006; Sinniger et al. 2008; Fujii and Reimer 2011). For example, *Epizoanthus* species diversity in Japan has been preliminarily investigated by using molecular methods and potentially undescribed species were found (Sinniger et al. 2009; Reimer et al. 2010a). Thus, molecular methods are an effective tool to help clarify the taxonomy and diversity of *Epizoanthus* species.

There are several described *Epizoanthus* species which are free-living, carcinoecium-forming, or epizoic on gastropods or glass sponges from the Pacific Ocean, such as *E. paguriphilus* Verrill, 1883 from the East China Sea; *E. stellaris* Hertwig, 1888 from the Philippines; *E. patagonichus* Carlgren, 1899 from Chile; *E. indicus* (Lwowsky, 1913) from the East China Sea; *E. illoricatus* Tischbierek, 1930 from Manila; *E. ramosus* Carlgren, 1936 from the East China Sea; *E. scotinus* Wood, 1957 from the Pacific Northwest; *E. sabulosus* Cutress, 1971 from Australia; *E. giveni* Philipp & Fautin, 2009 from California, and *E. fiordicus* Sinniger & Haussermann, 2009 from Chile. For *Epizoanthus* spp. attached to zig-zag shaped eunicid worm tubes, all have been identified as *E. illoricatus* since the species' original description. Eunicid worms are distributed in marine benthic environments around the world and are especially common in shallow tropical waters (Fauchald 1992). The family Eunicidae is currently composed of eight valid genera and ~330 species (Zanol et al. 2013), some of which are known to have associations with various marine invertebrates such as cnidarians, sponges and mollusks (Martin and Britayev 1998; Neves and Omena 2003). Recently, Reimer et al. (2014) investigated the diversity of zoantharians in the central Indo-Pacific and suggested that there are may be at least two species within *E. illoricatus*. However, no taxonomic conclusions were reached in this study.

In the current study the diversity of *Epizoanthus* species attached to eunicid worm tubes we investigated via molecular phylogenetic analyses utilizing three DNA markers; nuclear internal transcribed spacer of ribosomal DNA (ITS-rDNA), mitochondrial 16S ribosomal DNA (mt 16S-rDNA), and cytochrome oxidase subunit I (COI), and nuclear internal transcribed spacer of ribosomal DNA (ITS-rDNA). We then combined molecular results with morphological data (polyp dimensions, polyp arrangement and density within colonies, external colony and oral disk color, cnidae analyses, mesenterial patterns and numbers). The combined results of this research indicated the presence of two phylogenetically distinct and previously undescribed species of *Epizoanthus* associated with eunicid worm tubes in the Pacific Ocean, which we formally describe herein.

Materials and methods

Specimen collection

Epizoanthus specimens were collected from three localities in Okinawa, Japan, seven localities in Palau, and one location each in New Caledonia and Papua New Guinea (Figure 1). In total 70 specimens were collected, of which 69 specimens were collected by SCUBA at 10 to 40 m depth, with one additional specimen collected using the Japan Agency for Marine-Earth Science and Technology (JAMSTEC)'s ROV Hyper-Dolphin from 114 m during a research cruise in southern Japan in 2012. Collected specimens were preserved in 70–99.5% ethanol for molecular analyses and/or fixed in 5–10% seawater formalin and then later preserved in 70% ethanol for morphological analyses.

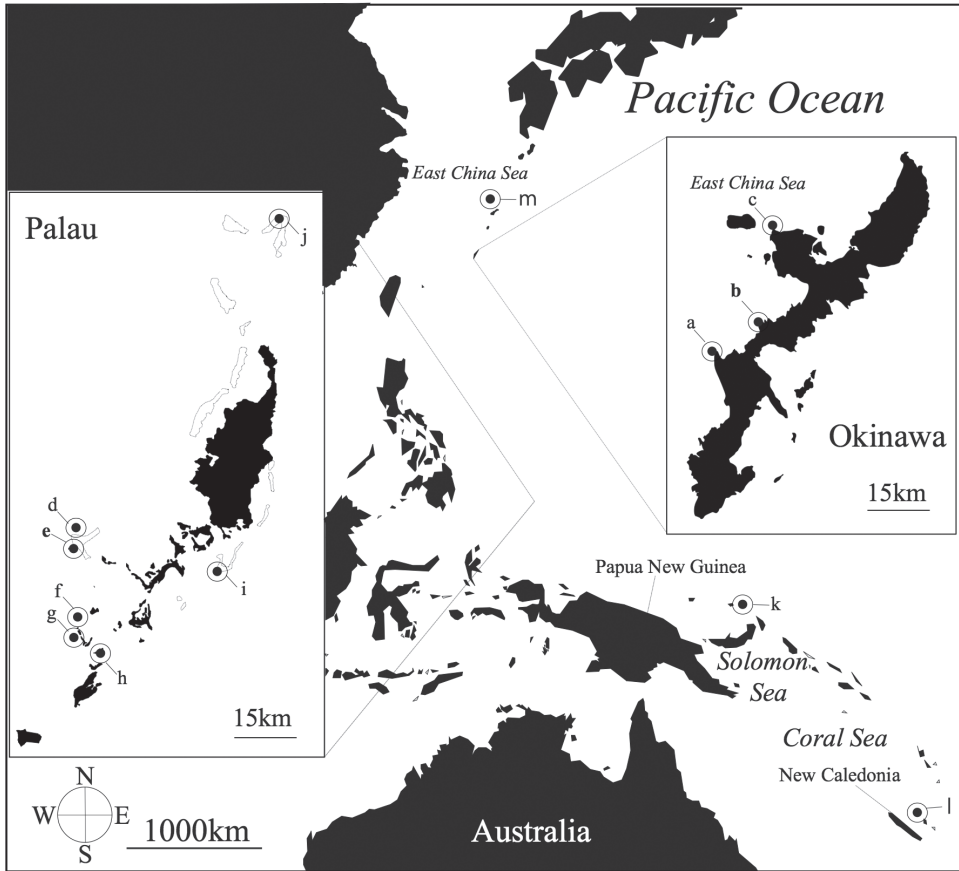


Figure 1. Sampling location in the Pacific Ocean of specimens used in this study. Location of specimens collected in this study represented by closed symbols. **a** Cape Zanpa **b** Cape Manzamo **c** Bise **d** Siaes Corner **e** Siaes Tunnel **f** Blue Hole **g** Blue Corner **h** Turtle Cove **i** Short Drop-off **j** Ngeruangel **k** Mascot Channel **l** Loyalty Islands **m** Kodakara Islands. Location in bold indicate type localities as follows: **b** (Cape Manzamo, Onna, Okinawa, Japan) = *E. inazuma* sp. n. **e** (Turtle Cove, Palau) = *E. beriber* sp. n.

Morphological analyses

The lengths and diameters of individual polyps, tentacle lengths and numbers, color of polyps, and diameters of oral disks were measured using in situ images or a dissecting microscope. Additionally, polyp densities of colonies attached to identically sized eunicid worm tubes (9 cm in length) were calculated using a counter under a dissecting microscope. For internal morphological analyses, some specimens' polyps were cut into 7 μ m cross-sections using a microtome after paraffin embedding following Reimer et al. (2010b), and these sections were subsequently stained with hematoxylin and eosin. Specimens to examine were selected from each phylogenetic clade ($n = 3/\text{clade}$) recovered in the molecular analyses.

Cnidae

Cnidae classification basically followed England (1991) and Ryland and Lancaster (2004). However, Schmidt (1974), Hidaka et al. (1987), Hidaka (1992), Fujii and Reimer (2011), and Montenegro et al. (2015) have referred to basitrichs and microbasic b-mastigophores as the same type of nematocysts and therefore in this study, these two types were pooled together. We used a Nikon Eclipse80i stereomicroscope (Nikon, Tokyo) to count and examine undischarged cnidae, which were measured using ImageJ software (National Institute of Health, Bethesda, Maryland, Nikon Eclipse80i, Nikon, Tokyo). Specimens to be examined were selected from each phylogenetic clade recovered from the molecular analyses.

DNA extraction, PCR amplification and sequence

DNA was extracted from tissue preserved in 99.5% ethanol by following a guanidine extraction protocol (Sinniger et al. 2010) or using a spin-column DNEasy Blood and Tissue Extraction kit (Qiagen, Tokyo). PCR amplification using Hot Star Taq Plus Master Mix Kit (Qiagen, Tokyo) was performed for each of ITS-rDNA (nuclear internal transcribed spacer region of ribosomal DNA), mt 16S-rDNA (mitochondrial 16S ribosomal DNA), and COI (cytochrome oxidase subunit I). The ITS-rDNA region was amplified using the specific primer set ITSf (5'-CTA GTA AGC GCG AGT CAT CAG C-3') and ITSr (5'-GGT AGC CTT GCC TGA TCT GA-3') (Swain 2009). mt 16S-rDNA was amplified using the universal primer 16Sar (5'-CGC CTG TTT ATC AAA AAC AT-3') (Palumbi et al. 1996) and the specific primer 16SBmoH (5'-CGA ACA GCC AAC CCT TGG-3') (Sinniger et al. 2005). The COI gene was amplified using the universal primer set LCO1490 (5'-GGT CAA CAA ATC ATA AAG ATA TTG G-3') and HCO2198 (5'-TAA ACT TCA GGG TGA CCA AAA AAT CA-3') (Folmer et al. 1994). All DNA markers were amplified following the thermal-cycle conditions described in Fujii and Reimer (2011). PCR products were checked using 1.0% agarose gel electrophoresis. The positive PCR products were cleaned using shrimp alkaline phosphatase (SAP) and Exonuclease I (Takara Bio Inc., Shiga, Japan), and then sequenced by Fasmac (Kanagawa, Japan).

Phylogenetic analyses

Obtained DNA sequences were initially checked using the Basic Local Alignment Search Tool (BLAST, National Center for Biotechnology Information). Obtained nucleotide sequences for the COI gene, mt 16S-rDNA and ITS-rDNA were aligned by CLUSTAL W ver. 1.83 (Thompson et al. 1994) on default settings supplied by Bioedit ver. 7.0.9.0. (<http://www.mbio.ncsu.edu/Bioedit/page2.html>). The alignments were inspected by eye and manually edited in Bioedit. Sequences belonging

to the family Hydrozoanthidae were used as outgroups. In this manner three aligned datasets were generated. All sequence datasets are available upon request from the corresponding author.

For the phylogenetic analyses of ITS-rDNA, mt 16S-rDNA and COI, the same methods were independently applied. The neighbor-joining (NJ) method (Saitou and Nei 1987) was performed using MEGA6 (Tamura et al. 2013), with 1000 replicates of bootstrapping. Maximum-likelihood (ML) analyses were performed using PhyML online (Guindon and Gascuel 2003). PhyML was performed using an input tree generated by BIONJ with the general time-reversible model (Rodriguez et al. 1990) of nucleotide substitution incorporating invariable sites and a discrete gamma distribution (eight categories) (GTR+I+C). The proportion of invariable sites, a discrete gamma distribution, and base frequencies of the model were estimated from the dataset. PhyML bootstrap trees (1000 replicates) were constructed using the same parameters as the individual ML trees. Bayesian trees were constructed in Mr Bayes 3.1.2 (Ronquist and Huelsenbesk 2003) under the GTR + I + I- model. One cold and three heated Markov chain Monte Carlo (MCMC) chains with temperature of 0.2 were run for 1,500,000 generations, subsampling frequency of 200 and a burn in length of 700,000 for all alignments.

Results

Systematics

Phylum Cnidaria Hatschek, 1888

Class Anthozoa Ehrenberg, 1831

Subclass Hexacorallia Haeckel, 1896

Order Zoantharia Gray, 1832

Suborder Macrocnemina Haddon & Shackleton, 1891

Family Epizoanthidae Delage & Hérouard, 1901

Genus *Epizoanthus* Gray, 1867

Epizoanthus Gray, 1867

Type species. *Epizoanthus papillosus* Johnston, 1842.

Synonym. *Epizoanthus incrustatus* (Dueben & Koren, 1847) (ICZN 1991: case 2750).

Remark. Herein, we choose to use the ordinal name Zoantharia Gray, 1832 as in the World Register of Marine Species (Hoeksema and Reimer, 2015). Although Zoantharia Gray, 1832, has identical spelling with the supraordinal name Zoantharia de Blainville, 1830, the latter name has fallen from common use—Hexacorallia Haeckel, 1896, being favoured.

***Epizoanthus inazuma* sp. n.**

<http://zoobank.org/0B91DB0E-A5AC-41CB-B78F-C8E7B8D44C2A>

Material examined. Holotype. NSMT-Co1574 (MISE-HK54), 26°30'18.3"N, 127°51'02.3"E, Cape Manzamo, Onna Village, Okinawa, Japan, depth 24 m, collected by Hiroki Kise, July 21, 2014, divided in two pieces, one portion fixed in 99.5% EtOH and the other in 5–10% saltwater formalin, deposited in National Museum of Nature and Science, Tokyo, Japan. Paratype 1. RMNH 42100 (MISE-HK9) 26°30'18.3"N, 127°51'02.3"E, Cape Manzamo, Onna Village, Okinawa, Japan, depth 25 m, collected by James D. Reimer, October 21, 2008, fixed in 99.5% EtOH, deposited in Naturalis Biodiversity Center, Leiden, The Netherlands. Paratype 2. USNM 1296757 (MISE-HK66) 26°26'26.5"N, 127°42'43.7"E Cape Zanpa, Yomitan Town, Okinawa, Japan, depth 34 m, collected by Hiroki Kise, August 5, 2014, fixed in 99.5% EtOH, deposited in Smithsonian Institution National Museum of Natural History, Washington, D.C., USA. Other material. MISE-HK43 26°30'18.3"N, 127°51'02.3"E, Cape Manzamo, Onna Village, Okinawa, Japan, depth 30 m, collected by Hiroki Kise, April 5, 2014, fixed in 99.5% EtOH.

Description of holotype. Colony of approximately 140 polyps connected by thin, under-developed coenenchyme on eunicid worm tubes. The tubes are made of a chitin-like substance. Polyps approximately 0.7 to 1.2 mm high (=length) from coenenchyme, and 1.0 to 1.65 mm in diameter. Polyps were attached from base to proximal extremity of zig-zag shaped tubes of eunicid worms, and attached to not only bent sections but also to other locations. Polyp external coloration black, oral disk light brown to brown, lighter nearer the oral opening and darker around oral disk edges. Polyps encrusted with sand and silica particles in their coenenchyme and ectodermal tissue; with few sand particles in the mesoglea.

Diagnosis. *Morphology.* Polyps connected by thin, under-developed coenenchyme on eunicid worms belonging to family Eunicidae. Maximum diameter of polyps approximately 4 mm, maximum height approximately 5 mm in situ. *Epizoanthus inazuma* sp. n. has 20–22 tentacles that are cylindrical and either as long or longer in comparison to oral disk diameter.

Internal anatomy. While the 5th mesentery from dorsal directive is obviously a complete mesentery (macrocnemic arrangement), the 6th mesentery is also a complete mesentery (Figure 2b). Azooxanthellate. Mesogleal thickness approximately 75 µm.

Cnidae. Holotrichs, basitrichs, microbasic p-mastigophores, spirocysts (see Table 1 into this paper, Figure 3).

Etymology. *Epizoanthus inazuma* sp. n. is named after the Japanese word 'inazuma' meaning 'lightning', as colonies of this species are attached to eunicid worm tubes, and the worm tube shape resembles a classic lightning-bolt shape. *Common Japanese name.* 'Inazuma-yadori-sunaginchaku' (new Japanese name).

Distribution and habitat. *Epizoanthus inazuma* sp. n. is found in low-light environments such as on mesophotic coral reef slopes and reef floors, or on the sides of overhangs. Specimens were collected from 10 to 40 m depth.

Table 1. Cnidae types and sizes of *Epizoanthus inazuma* sp. n., *Epizoanthus beriber* sp. n. and *Epizoanthus illorricatus*. Frequency: relative abundance of cnidae type in decreasing order; numerous, common, occasional, rare (N = number of specimens found/total specimens examined).^{a)}

| | <i>Epizoanthus inazuma</i> sp. n. | | <i>Epizoanthus beriber</i> sp. n. | | <i>Epizoanthus illorricatus</i> | |
|-----------------------|-----------------------------------|------------------|-----------------------------------|------------------|---------------------------------|--------------------------------|
| | Length × Width (µm) | Frequency | Length × Width (µm) | Frequency | Length × Width (µm) | Frequency |
| Tentacles | | | | | | |
| Spirocysts | 8–20 × 1–4 | Numerous (3/3) | 8–21 × 2–5 | Numerous (3/3) | 9–20 × 2–4 | Numerous (3/3) |
| Bastrichs | 6–19 × 1–5 | Common (3/3) | 9–18 × 2–4 | Common (3/3) | 10–23 × 2–5 | Common (3/3) |
| Holotrichs small | 4–9 × 2–4 | Occasional (2/3) | 5–7 × 2–4 | Rare (1/3) | 5–9 × 2–5 | Occasional (2/3) |
| Column | | | | | | |
| Holotrichs small | 5–8 × 3–4 | Common (3/3) | 5 × 4 | Rare (1/3) | 5–8 × 2–4 | Occasional (1/3) |
| Holotrichs medium | 10–17 × 4–9 | Numerous (3/3) | 11–19 × 4–9 | Numerous (3/3) | 10–19 × 3–9 | Numerous (3/3) |
| Holotrichs large | - | - | 20–23 × 7–11 | Occasional (3/3) | 24–32 × 10–15 | Occasional (1/3) |
| Actinopharnx | | | | | | |
| P-mastigophores | 11–20 × 3–5 | Common (3/3) | 17–25 × 4–6 | Common (3/3) | 12–19 × 3–5 | Occasional (2/2) ^{b)} |
| Bastrichs | - | - | 14–19 × 2–4 | Occasional (2/3) | 9–20 × 1–4 | Occasional (2/2) ^{b)} |
| Holotrichs small | 4–9 × 1–6 | Common (3/3) | - | - | 6–9 × 2–4 | Occasional (1/2) ^{b)} |
| Holotrichs medium | 10–19 × 4–6 | Occasional (3/3) | - | - | 11–16 × 5–8 | Common (2/2) ^{a)} |
| Holotrichs large | - | - | 20–25 × 8–12 | Occasional (2/3) | 30 × 8 | Rare (1/2) ^{a)} |
| Mesenteries filaments | | | | | | |
| Bastrichs | - | - | 16–20 × 3–4 | Occasional (2/3) | 16–26 × 2–4 | Occasional (1/3) |
| P-mastigophres | 15–22 × 3–6 | Common (3/3) | 15–21 × 4–7 | Common (3/3) | 7–21 × 3–6 | Common (3/3) |
| Holotrichs small | 5–9 × 3–5 | Common (3/3) | 8 × 3 | Rare (1/3) | - | - |
| Holotrichs medium | 10–20 × 3–7 | Common (3/3) | 10–17 × 3–6 | Occasional (3/3) | 10–18 × 3–7 | Common (3/3) |
| Holotrichs large | - | - | 23–30 × 7–13 | Occasional (2/3) | 25–34 × 5–9 | Occasional (1/3) |

^{a)} Tissue of actinopharynx could be obtained from only two specimens due to specimen condition.

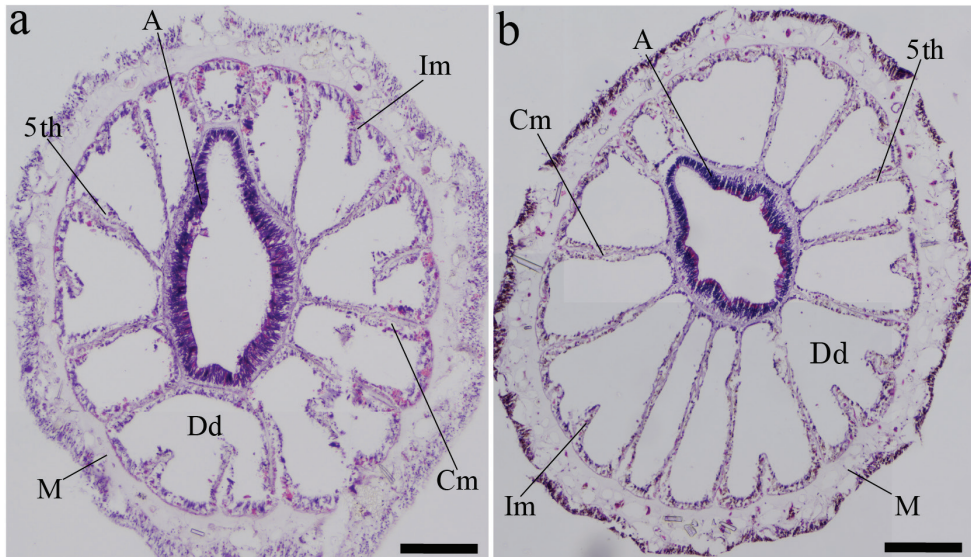

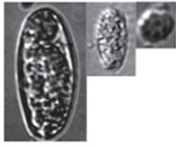
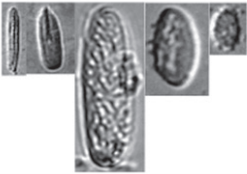




Figure 2. Cross-sections of *Epizoanthus illoricatus* and *E. inazuma* sp. n. **a** *E. illoricatus*; 6th mesentery is incomplete from dorsal directive **b** *E. inazuma* sp. n. 6th mesentery is complete from dorsal directive. **Dd** dorsal directive **A** actinopharynx **Im** incomplete mesentery **Cm** complete mesentery **M** mesoglea; 5th, 5th mesentery from dorsal directive. Scale bars: 200 μ m.






Epizoanthus inazuma sp. n. is currently known only from Okinawa (Figure 1). However, it may be distributed in other locations in the Pacific Ocean, as it is likely this species has been confused with *E. illoricatus* and/or *E. beriber* sp. n. in the past due to their similar external morphology. *E. illoricatus* has been found in many areas of the western Pacific Ocean such as in New Caledonia (Sinniger 2006; Sinniger et al. 2009), the Yellow Sea, China (Pei 1999), Papua New Guinea (BW Hoeksema, pers. comm.), Australia (Lindsay et al. 2012), Taiwan (Reimer et al. 2013), and Palau (Reimer et al. 2014), and *E. inazuma* sp. n. may be similarly distributed.

Remarks. *Epizoanthus inazuma* sp. n., *E. beriber*, and *E. illoricatus* can be distinguished from most other *Epizoanthus* species by their specific substrate (eunicid worm tubes) in the Pacific Ocean. *Acrozoanthus australiae* (family Zoanthidae) is also associated with eunicid worm tubes, but *E. inazuma* sp. n. can be distinguished from *A. australiae* due to its mesenterial arrangement (the family Zoanthidae is within the sub-order Brachycnemina), as well as by many obvious external features such as coloration, polyp size, and by being azooxanthellate (*A. australiae* is zooxanthellate). *E. inazuma* sp. n. is very similar to *E. illoricatus* (Figure 4a, b, c, f), but can be distinguished by differing mesenterial arrangement (6th mesentery is complete as opposed to 6th mesentery being incomplete in *E. illoricatus*) (Figure 2). *Epizoanthus inazuma* sp. n. has different coloration than *E. beriber* sp. n., which is pale white. *Epizoanthus inazuma* sp. n. and *E. illoricatus* can have the same external coloration (black), but the cnidomes of these two species are different; *E. illoricatus* has large holotrachs in the column, pharynx

Epizoanthus illoricatus

| Tentacles | | | Column | | | Pharynx | | | | | Filaments | | | | |
|---|---|----|---|----|----|---|---|----|----|----|--|---|----|----|---|
| S | B | HS | HL | HM | HS | B | P | HL | HM | HS | B | P | HL | HM | |
|  | | |  | | |  | | | | |  | | | |  |

Epizoanthus inazuma

| Tentacles | | | Column | | Pharynx | | | Filaments | | | |
|---|---|----|---|----|---|----|----|---|----|----|---|
| S | B | HS | HM | HS | P | HM | HS | P | HM | HS | |
|  | | |  | |  | | |  | | |  |

Epizoanthus beriber

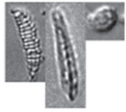

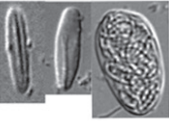
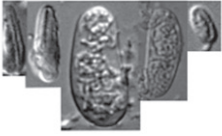

| Tentacles | | | Column | | | Pharynx | | | Filaments | | | | | |
|---|---|----|---|----|----|---|---|----|---|---|----|----|----|--|
| S | B | HS | HL | HM | HS | B | P | HL | B | P | HL | HM | HS | |
|  | | |  | | |  | | |  | | | | |  |

Figure 3. Cnidae in tentacles, column, pharynx, filaments of *Epizoanthus illoricatus*, *E. inazuma* sp. n. and *E. beriber* sp. n. respectively. **HL** holotrichs large **HM** holotrichs medium **HS** holotrichs small **B** basitrichs **pM** microbasic p-mastigophores **S** spirocysts.

and mesenterial filaments, while *E. inazuma* sp. n. does not have any large holotrichs in the column, pharynx, or mesenterial filaments. As well, there are also differences in sizes of some nematocyst types of these two species (e.g. basitrichs in the pharynx or mesenterial filaments). The cnidome composition of *E. inazuma* sp. n. is different from *E. beriber* sp. n. and *E. illoricatus*, and *E. beriber*'s sp. n. cnidome is similar to that of *E. illoricatus* (see Table 1; Figure 3).

All Indo-Pacific *Epizoanthus* species that are obligate epibionts on eunicid worm tubes until now have been identified as *E. illoricatus*, which was originally described

from Manila, the Philippines. The type specimens of *E. illoricatus* were likely lost during World War II when the Zoologische Staatssammlung Museum in München was burned down. Additionally, no specific type locality was given except 'Manila' in the original description and Manila is now a very altered environment compared to 1930. Therefore, it is difficult to find and identify *E. illoricatus*' exact type locality. However, *E. illoricatus* can be clearly separated from *E. inazuma* sp. n. and *E. beriber* sp. n. by both morphological and molecular data.

***Epizoanthus beriber* sp. n.**

<http://zoobank.org/7F0A1F6F-4922-4C2C-AF62-33948394AC97>

Material examined. Holotype. NSMT-Co1575 (MISE-HK129), 7°5'01.0"N, 134°15'80.0"E, Turtle Cove, Palau, depth 20 m, collected by Hiroki Kise, May 6, 2015, divided in two pieces, one portion fixed in 99.5% EtOH and the other in 5–10% saltwater formalin, deposited in National Museum of Nature and Science, Tokyo, Japan. Paratype 1. RMNH 42101 (MISE-HK126), 7°8'29.4"N, 134°13'23.3"E, Blue Hole, Palau, depth 36 m, collected by Hiroki Kise, May 5, 2015, divided in two pieces, one portion fixed in 99.5% EtOH and other in 5–10% saltwater formalin, deposited in Naturalis Biodiversity Center, Leiden, The Netherlands. Paratype 2. USNM 1296758, USNM 1296759 (MISE-HK113), 7°18'54.8"N, 134°13'13.3"E, Siaes Tunnel, Palau, depth 30 m, collected by Hiroki Kise, April 28, 2015, divided in two pieces, one portion fixed in 99.5% EtOH and other in 5–10% saltwater formalin, deposited in Smithsonian Institution National Museum of Natural History, Washington, D.C., USA. Other material. MISE-HK112, 7°18'54.8"N, 134°13'13.3"E, Siaes Tunnel, Palau, depth 37 m, collected by Hiroki Kise, April 28, 2015, divided in two pieces and fixed in 99.5% EtOH and 5–10% saltwater formalin, respectively; MISE-HK116, 7°18'54.8"N, 134°13'13.3"E, Siaes Tunnel, Palau, depth unknown, collected by Hiroki Kise, April 28, 2015, divided in two pieces and fixed in 99.5% EtOH and 5–10% saltwater formalin, respectively; MISE-HK117, 7°18'54.8"N, 134°13'13.3"E, Siaes Tunnel, Palau, depth unknown, collected by Hiroki Kise, April 28, 2015, fixed in 99.5% EtOH; MISE-HK118, 7°18'54.8"N, 134°13'13.3"E, Siaes Tunnel, Palau, depth unknown, collected by Hiroki Kise, April 28, 2015, fixed in 99.5% EtOH; MISE-HK119, 7°18'54.8"N, 134°13'13.3"E, Siaes Tunnel, Palau, depth 19 m, collected by Hiroki Kise, April 28, 2015, fixed in 99.5%; MISE-HK120, 7°18'54.8"N, 134°13'13.3"E, Siaes Tunnel, Palau, depth unknown, collected by Hiroki Kise, April 28, 2015, fixed in 99.5% EtOH; MISE-HK124, 8°19'00.0"N, 134°63'00.0"E, Negruangel, Palau, depth 27 m, collected by Hiroki Kise, April 29, 2015, fixed in 99.5% EtOH; MISE-HK125, 7°8'29.4"N, 134°13'23.3"E, Blue Hole, Palau, depth 32 m, collected by Hiroki Kise, May 5, 2015, divided in two pieces and fixed in 99.5% EtOH and 5–10% saltwater formalin, respectively; MISE-HK127 7°8'29.4"N, 134°13'23.3"E, Blue Hole, Palau, depth 36 m, collected by Hiroki Kise, May 5, 2015, fixed in 99.5% EtOH; HK128

7°8'12.3"N, 134°13'16.5"E, Blue Corner, Palau, depth 29 m, collected by Hiroki Kise, May 5, 2015, fixed in 99.5% EtOH.

Description of holotype. Colony of approximately 75 polyps connected by moderately developed coenenchyme on eunicid worm tubes. Polyps were attached to from base to proximal extremity of zig-zag shaped tubes of eunicid worms, and attached to not only bent sections but also to other locations. Polyps approximately 1.4 to 1.9 mm high from coenenchyme, and 0.7–1.0 mm in diameter. Azooxanthellate. Polyp external coloration is white, oral disk solid in color, ranging from light brown to brown (Figure 4d). Tentacles are transparent and approximately 20–22 in number.

Diagnosis. *Morphology.* Polyps connected by moderately developed coenenchyme on eunicid worm tubes belonging to the genus *Eunice*, as are *Epizoanthus illoricatus* and *E. inazuma* sp. n. Polyps are either circular cones or cylindrical, and approximately 0.5 to 2.1 mm high from coenenchyme (=length) and 1.1 to 2.1 mm diameter (in 5–10% seawater formalin). Maximum diameter of polyps is approximately 3 mm, maximum height approximately 5 mm in situ. Polyps have 20–22 tentacles that are longer than oral disk diameter. In addition, polyp external color is white while oral disk is light brown to brown.

Internal anatomy. Mesogleal thickness approximately 80 µm. We could not obtain cross-sections or images to observe mesentery arrangement due to heavy sand encrustation.

Cnidae. Holotrichs, basitrichs, microbasic p-mastigophores, spirocysts (see Table 1, Figure 3).

Etymology. *Epizoanthus beriber* sp. n. is named after the legendary Beriber of Palauan folklore, who lived in a cave at Oikuul in Airai State, as this species has been found only in caves. *Common Japanese name.* ‘Ziguzagu-yadori-sunaginchaku’ (new Japanese name).

Distribution and habitat. *Epizoanthus beriber* sp. n. is found only on the floor or sides of caves, and always in association with eunicid worm tubes (Figure 4d, e). Specimens were collected from 20–40 m in this study. *E. beriber* sp. n. is known from Palau and Papua New Guinea (Figure 1). However, it may be distributed around the Pacific Ocean as we have speculated for *E. inazuma* sp. n.

Remarks. *Epizoanthus beriber* sp. n. can be distinguished from *E. illoricatus* and *E. inazuma* sp. n. by habitat and coloration. *E. beriber* sp. n. was found only in caves while *E. inazuma* sp. n. and *E. illoricatus* were found on reef slopes or flat reef floors. *E. beriber* sp. n. has white colonial polyps with a moderately developed coenenchyme (Figure 4d, e) while *E. inazuma* sp. n. has black colonial polyps with a well-developed coenenchyme and *E. illoricatus* has gray, yellow or black colonial polyps with a either poorly developed or well-developed coenenchyme (Figure 4a–c, f).

The holotype of *E. illoricatus* was presumably collected by dredging or net as there was no SCUBA in the 1930s; and it can be inferred that the holotype of *E. illoricatus* lived in a location where it could be collected by such a method, such as on a reef flat or reef slope. *E. inazuma* sp. n. is also found in such areas. However, *E. beriber* sp. n. is only known from underwater caves that cannot be easily accessed from the surface.

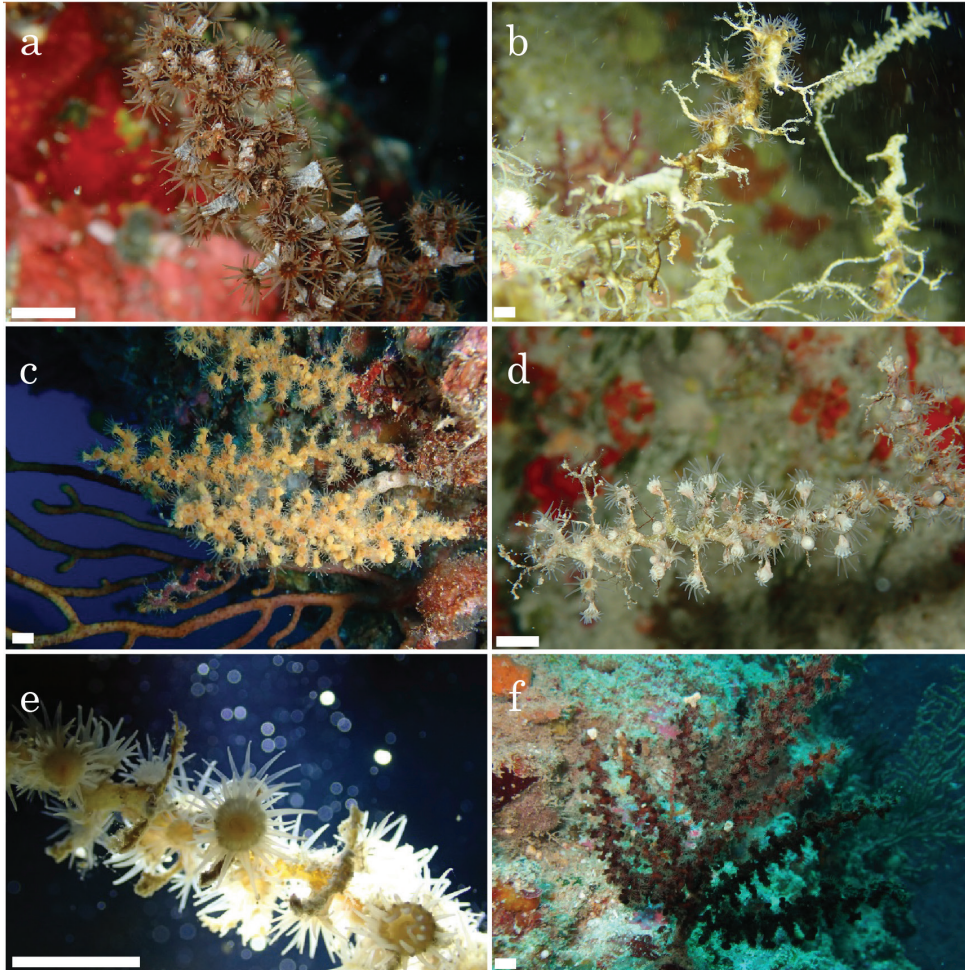


Figure 4. In situ images of *Epizoanthus illoricatus*, *E. inazuma* sp. n. and *E. beriber* sp. n. **a** *E. illoricatus*; with highly developed coenenchyme and high density of polyps. Image taken on September 12, 2014, at Siales Tunnel, Palau. Specimen number HK67. Image taken by J. D. Reimer **b** *E. illoricatus*; with poorly developed coenenchyme and low density of polyps. Image taken on July 19, 2014, at Cape Manzamo, Okinawa, Japan. Specimen number HK53 **c** *E. illoricatus*; yellow colored colonies. Image taken on November 21, 2015, at Cape Manzamo, Okinawa, Japan. Specimen number HK100 **d** *E. beriber* sp. n.; with low density polyps. Image taken on May 6, 2015, at Turtle Cove, Palau. Specimen number HK129 (holotype) **e** *E. beriber* sp. n.; open polyps. Image taken on April 28, 2015, at Siales Tunnel, Palau. Specimen number HK113 **f** *E. inazuma* sp. n.; black colored colony. Image taken on April 5, 2014, at Cape Manzamo, Okinawa, Japan. Specimen number HK54 (holotype). All images excepting specimen number HK67 taken by H. Kise. Scale bars: 3 cm.

Phylogenetic analyses

Sequences from *Epizoanthus* spp. specimens attached to eunicid worm tubes formed a large monophyletic clade along with other *Epizoanthus* spp. in the phylogenetic tree of all three DNA markers (Figures 5–7). The phylogenetic trees' topologies were very similar for all three DNA markers.

Although the morphological features of *Epizoanthus inazuma* sp. n. and *E. beriber* sp. n. were generally very similar to those of *E. illoricatus*, sequences were clearly separated into three monophyletic clades in the ITS-rDNA tree (Figure 5); all sequences of *E. inazuma* sp. n. were contained in a monophyletic clade with very strong support (ML = 99%; NJ = 100%; Bayes = 1), and all sequences of *E. beriber* sp. n. were also contained in another monophyletic clade with very strong support (ML = 100%;

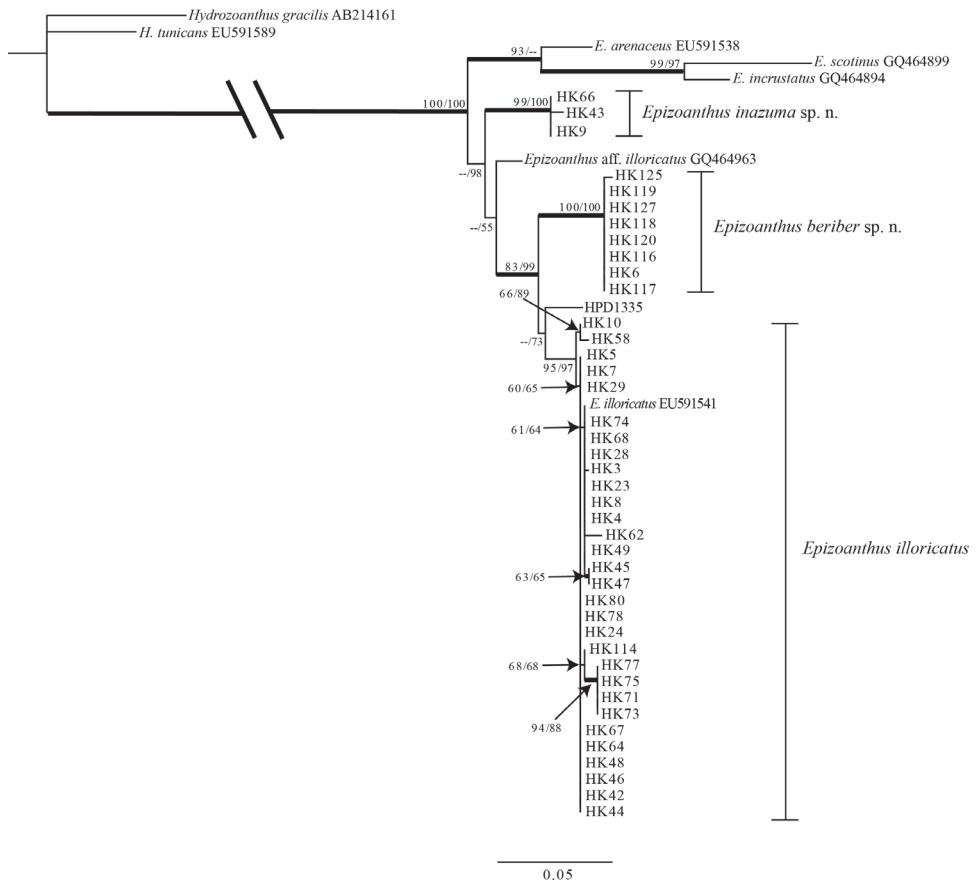


Figure 5. Maximum likelihood (ML) tree based on internal transcribed spacer region of ribosomal DNA sequence. Numbers on nodes represent ML and neighbor-joining (NJ) bootstrap values (> 50% are shown). Bold branches indicate high supports of Bayesian posterior probabilities (> 0.95). Sequences obtained from GenBank are shown with accession numbers.

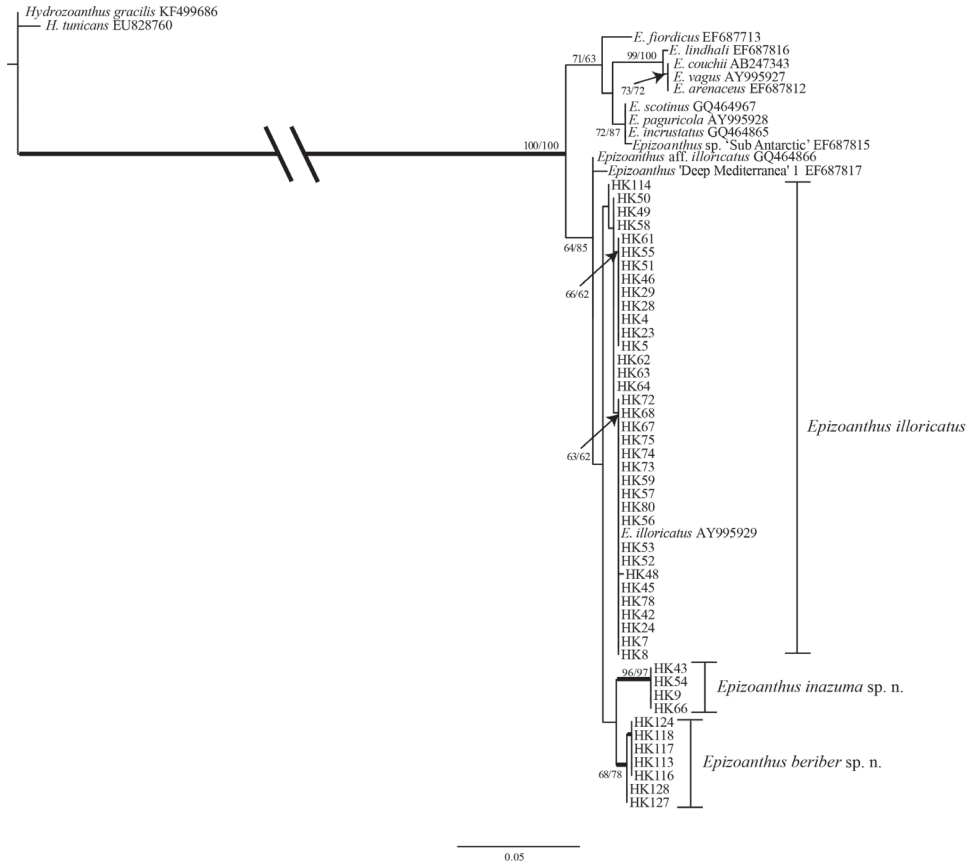


Figure 6. Maximum likelihood (ML) tree based on mitochondrial 16S ribosomal DNA sequence. Numbers on nodes represent ML and neighbor-joining (NJ) bootstrap values (> 50% are shown). Bold branches indicate high supports of Bayesian posterior probabilities (> 0.95). Sequences obtained from GenBank are shown with accession numbers.

NJ = 100%; Bayes = 1). All sequences of *E. illoricatus*, including previously reported sequences from GenBank, were contained in another monophyletic clade with strong support (ML = 95%; NJ = 97%; Bayes = 0.86).

The resulting trees from mt 16S-rDNA and COI sequences from specimens in this study also demonstrated that all three species were different (Figures 6-7, respectively); *E. inazuma* sp. n. and *E. beriber* sp. n. were each contained in monophyletic clades with moderate to strong support (COI: ML = 98%; NJ = 100%; Bayes = 1; and ML = 84%; NJ = 75%; Bayes = 0.97; mt 16S-rDNA: ML = 96%; NJ = 97%; Bayes = 0.99; and ML = 68; NJ = 78; Bayes = 0.98; respectively). There were 5-6 bp differences between *E. beriber* sp. n. and *E. illoricatus* in the each of the mt 16S-rDNA and COI regions.

Previously reported sequences of *Epizoanthus* aff. *illoricatus* (ITS-rDNA: GQ464895; mt 16S-rDNA: GQ464866) from Station M, Monterey Bay, California,

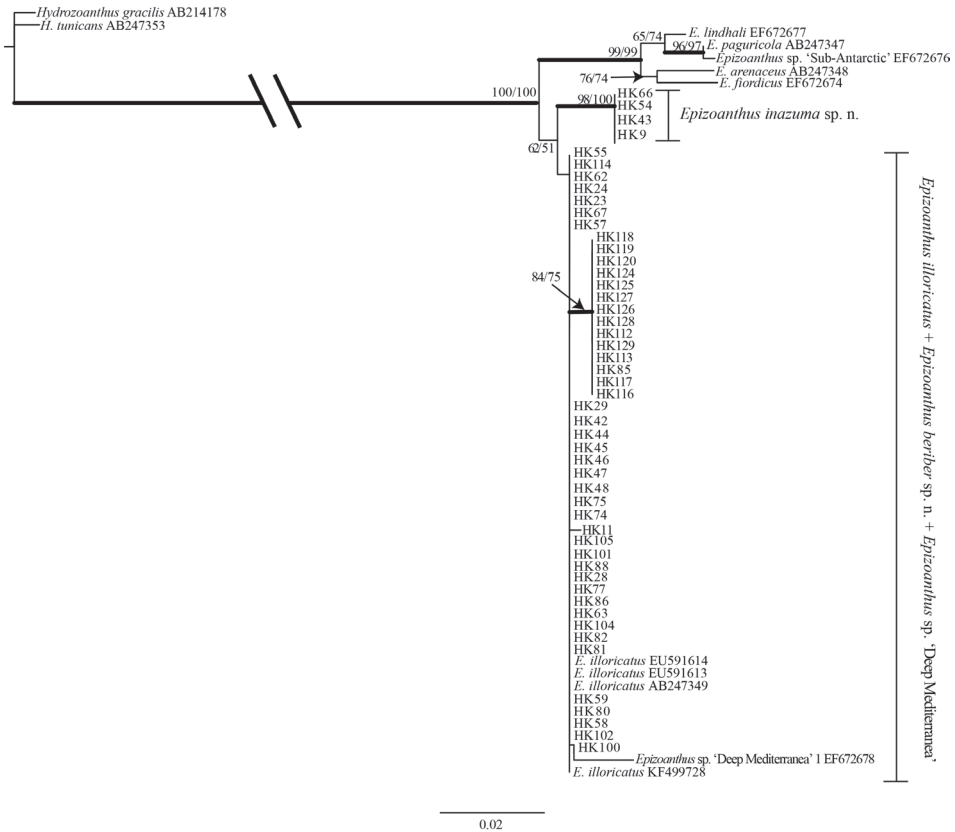


Figure 7. Maximum likelihood (ML) tree based on mitochondrial cytochrome oxidase subunit I sequence. Numbers on nodes represent ML and neighbor-joining (NJ) bootstrap values (> 50% are shown). Bold branches indicate high supports of Bayesian posterior probabilities (> 0.95). Sequences obtained from GenBank are shown with accession numbers.

USA were also contained within the clade of *Epizoanthus* spp. attached to eunicid worm tubes (Figures 5–6), although it is not clear which host this specimen was attached to (T. Swain, MorphBank collection number 477931 [MorphBank 2015]). In the ITS-rDNA tree, the sequence from this specimen was sister to a clade consisting of *E. illoricatus* and *E. beriber* sp. n. sequences with poor support (ML = < 50%; NJ = 55%; Bayes = 0.79) (Figure 5), and was sister to the large *E. illoricatus*+*E. inazuma* sp. n. +*E. beriber* sp. n. clade in the mt 16S-rDNA tree (Figure 6). Previously reported sequences of *Epizoanthus* sp. 'Deep Mediterranean' 1 (mt 16S-rDNA: EF672678; COI: EF687817) were also contained in the clade of *Epizoanthus* spp. attached to eunicid worm tubes (Figures 6–7), although this specimen was apparently not associated with any living substrate (F. Sinniger, personal communication). This sequence was sister to a large, moderately well supported clade of *E. illoricatus*, *E. inazuma* sp. n., and *E. beriber* sp. n. (ML = 64%; NJ = 85%; Bayes = 0.55) in the mt 16S-rDNA tree (Figure 6), and was contained in a clade with *E. illoricatus* sequences in the COI tree (Figure 7).

Discussion

Shallow *Epizoanthus* species associated with eunicid worm tubes are relatively common in the Pacific Ocean. However, until now there has been limited information about their diversity, and overall *Epizoanthus* species diversity is still relatively unknown and may be higher than has been originally thought (Reimer et al. 2010a). In this study two new species have been described, *E. inazuma* sp. n. and *E. beriber* sp. n. Based on these and previous findings (Sinniger et al. 2009; Reimer et al. 2010a), we believe there is a high potential of undescribed species being contained within already described *Epizoanthus* species. In this study, *E. beriber* sp. n. was only found in caves. Similarly, two *Palythoa* species that live in similar habitats have recently been described from Okinawa (Irei et al. 2015), and an azooxanthellate scleractinian coral species was also discovered in similar habitats in various Indo-West Pacific localities, including Palau (Hoeksema 2012). Such findings indicate that there may be high potential of the existence of more undescribed species in underwater caves or other 'cryptic' environments associated with coral reefs, and continued investigations of such environments are needed.

Distinguishing characters of different *Epizoanthus* species attached to eunicid worm tubes

Epizoanthus illoricatus has high levels of intraspecific morphological variation of some characters, such as external coloration, coenenchyme thickness, and polyp density (Figure 4a-c). Therefore, it may be easy to mistake different morphotypes as undescribed or potentially novel species by basing decisions only on morphological analyses, as has been suggested in other zoantharians (e.g. Burnett et al. 1997). In fact, although we collected some *E. illoricatus* specimens that had poorly developed coenenchymes with a low density of polyps, other specimens had a thin, highly developed coenenchyme with a high density of polyps (Figure 4a-b), and these two different morphotypes were not consistently recovered in different phylogenetic clades. Thus, although these two morphotypes had recently been speculated to be different species (Reimer et al. 2014), this does not appear to be an accurate delineation of species. Additionally, *E. inazuma* sp. n. looks very similar externally to *E. illoricatus*. Thus, *E. illoricatus* and *E. inazuma* sp. n. may be easily mistaken for each other due to these similar morphological characteristics.

However, phylogenetic analyses clearly showed that *E. illoricatus* and *E. inazuma* sp. n. are clearly distinct and each is within a well-supported monophyly (Figures 5-7), with genetic distances of 0.4% to 1.3% in mt 16S-rDNA and COI regions separating them. Previous literature has shown such genetic distances to be in line with interspecific differences among other zoantharian congeners (Reimer et al. 2006, 2010a; Sinniger et al. 2008; Irei et al. 2015).

Between *E. illoricatus* and *E. inazuma* sp. n. we found notable differences in mesenteriel arrangements (Figure 2) and in cnidae; and in particular clear differences based

on the presence/absence of large holotrichs (Table 1, Figure 3). Mesenterial arrangement is usually used as a taxonomic character to divide suborders, however our morphological analyses in this study indicate that mesenterial arrangement is an unreliable indicator of suborder. The results of our study also suggest that in some cases mesenterial arrangement may be useful for species-level identification when combined with molecular analyses and data from other morphological characteristics.

Epizoanthus beriber sp. n. can be easily distinguished from *E. illorricatus* and *E. inazuma* sp. n. by habitat and polyp coloration (Figure 4a–f). In general, species identification based on coloration has been thought of as not generally reliable for brachycnemic zoantharians as much intraspecific variation is present (Burnett et al. 1995, 1997; Reimer et al. 2004), while it has been supposed that coloration may be considered useful for identification of some macrocnemic zoantharians (Sinniger et al. 2009, 2010). Here, we consider coloration of polyps as a potentially useful taxonomic characteristic in these *Epizoanthus* species when utilized in combination with habitat data and molecular analyses.

Relationship between *Epizoanthus* spp. and eunicid worm tubes

Epizoanthus illorricatus, *E. inazuma* sp. n. and *E. beriber* sp. n. are obligate epibionts on eunicid worms. Members of Eunicidae that host these *Epizoanthus* spp. make chitin-like zigzag tubes (Tischbierck 1930), and some colonies of *E. illorricatus* completely covered this substrate. In this study, we observed no *E. illorricatus* attached to tubes that did not have living eunicid worms inside. This means that *E. illorricatus* apparently has some kind of association with living eunicid worms; commensalism, mutualism, or parasitism. To understand this relationship, observations of the survival rate of *Epizoanthus* colonies with or without eunicid worms in both controlled laboratory settings and in situ are necessary. *E. illorricatus* and the two new species in this study do not produce tube-like structures such as a carcinoecium (Figure 4a–f), which is a corneous shell-like structure that has been observed in other *Epizoanthus* species' associations (e.g. hermit crabs; Schejter and Mantelatto 2011). In addition, because there are few morphological differences despite clearly distinct phylogenetic signals between *E. illorricatus* and *E. inazuma* sp. n., it is possible that the substrate consisting of eunicid worm tubes may be made by different host taxa (genus/species). Further research using molecular and morphological analyses of not only *Epizoanthus* but also of the *Eunice* host species are needed to understand these relationships better.

Acknowledgements

The first author would like to thank all members of the Molecular Invertebrate Systematics and Ecology Laboratory (MISE) at the University of the Ryukyus (UR) for

their help in fieldwork and data collection. C. Timmons (MISE) proofread an earlier version of this manuscript. Dr. J. Lorion, G. Mereb and A. Mereb at Palau International Coral Reef Center (PICRC) are thanked for logistical support. We also thank Dr. B.W. Hoeksema (Naturalis Biodiversity Center), Dr. T. Fujii (Kagoshima University) for providing invaluable specimens utilized in this study. Dr. F. Sinniger (UR) and Dr. T. Swain (Chicago Field Museum) kindly provided specimen information. Sampling in Palau was supported by the SATREPS P-CoRIE Project, funded by the Japan Science and Technology Agency and the Japan International Cooperation Agency in cooperation with PICRIC and Palau Community College. The senior author was also funded by the International Research Hub Project for Climate Change and Coral Reef/Island Dynamics at UR, and by a Japan Society for the Promotion of Science 'Zuno-Junkan' grant entitled 'Studies on origin and maintenance of marine biodiversity and systematic conservation planning'. Reviewer comments by Dr. J. Ryland, Dr. S. Stampar, and M. Risi greatly improved the manuscript. This is contribution PCoRIE Biodiversity #5.

References

- Ates RML (2003) A preliminary review of zoanthid-hermit crab symbioses (Cnidaria; Zoantharia/Crustacea, Paguridea). *Zoologische Verhandlungen* 180: 303–378.
- Beaulieu SE (2001) Life on glass houses: sponge stalk communities in the deep sea. *Marine Biology* 138: 803–817. doi: 10.1007/s002270000500
- Burnett WJ, Benzie JAH, Beardmore JA, Ryland JS (1995) Patterns of genetic subdivision in populations of a clonal cnidarian, *Zoanthus coppingeri*, from the Great Barrier Reef. *Marine Biology* 122: 665–673. doi: 10.1007/BF00350688
- Burnett WJ, Benzie JAH, Beardmore JA, Ryland JS (1997) Zoanthids (Anthozoa, Hexacorallia) from the Great Barrier Reef and Torres Strait, Australia: systematics, evolution and a key to species. *Coral Reefs* 16: 55–68. doi: 10.1007/s003380050060
- Carlgren O (1899) Zoantharien. *Hamburger Magalhaensische Sammelreise* 4: 1–48.
- Carlgren O (1924) Die Larven der Ceriantharien, Zoantharien und Actiniarien. *Deutsche Tiefsee-Expedition*, 132–136.
- Carlgren O (1934) Über einige ostasiatische Zoantharien. *Arkiv för Zoologi* 28A: 1–11.
- Cutress CE (1971) Corallimorpharia, Actiniaria and Zoanthidea. *Memoirs of the National Museum of Victoria (Melbourne)* 32: 83–92.
- Duerden JE (1898) Jamaican Actiniaria. Part I. Zoantheae. *Royal Dublin Society* 6: 330–332.
- England KW (1991) Nematocysts of sea anemones (Actiniaria, Ceriantharia and Corallimorpharia: Cnidaria): nomenclature. *Hydrobiologia* 216/217: 691–697. doi: 10.1007/BF00026532
- Fauchald K (1992) A review of the genus *Eunice* (Polychaeta: Eunicidae) based upon type material. *Smithsonian Contributions to Zoology* 523: 1–422. doi: 10.5479/si.00810282.523
- Folmer O, Black M, Hoeh W, Lutz R, Vrijenhoek R (1994) DNA primers for amplification of mitochondrial cytochrome oxidase subunit I from diverse metazoan invertebrates. *Molecular Marine Biology and Biotechnology* 3: 294–299.

- Fujii T, Reimer JD (2011) Phylogeny of the highly divergent zoanthid family Microzoanthidae (Anthozoa, Hexacorallia) from the Pacific. *Zoologica Scripta* 40: 418–431. doi: 10.1111/j.1463-6409.2011.00479.x
- Gravier C (1918) Note sur une actinie (* *Thoracactis** n. g., **topsenti** n. sp.) et un annélide polychète (* *Hermadion Fauveli** n. sp.), commensaux d'une éponge siliceuse (* *Sa-rostegia oculata** Topsent). *Bulletin de l'Institut Océano-graphique (Monaco)* 344: 1–20. doi: 10.1093/sysbio/syq010
- Guindon S, Dufayard JF, Lefort V, Anishimova M, Hordijk W, Gascuel O (2010) New algorithms and methods to estimate Maximum-likelihood phylogenies: Assessing the performance of PhyML 3.0. *Systematic Biology* 59(3): 307–321.
- Haddon AC, Shackleton AM (1891) Actiniae: I. Zoantheae. Reports on the Zoological Collections Made in the Torres Straits by Professor A.C. Haddon, 1888–1889. *Scientific Transactions of the Royal Dublin Society, Ser. 2*, 4(13): 673–658.
- Hertwig R (1888) Report on the Actiniaria dredged by H.M.S, Challenger during years 1873–1876. *Reports Scientific Results Voyager Challenger (Zoology)* 26: 39–41.
- Hidaka M (1992) Use of nematocyst morphology for taxonomy of some related species of scleractinian corals. *Galaxea* 11: 21–28.
- Hidaka M, Miyazaki I, Yamazato K (1987) Nematocysts characteristic of the sweeper tentacles of the coral *Galaxea fascicularis* (Linnaeus). *Galaxea* 6: 195–207.
- Hoeksema BW (2012) Forever in the dark: the cave-dwelling azooxanthellate reef coral *Leptoseris troglodyta* sp. n. (Scleractinia, Agariciidae). *ZooKeys* 228: 21–37. doi: 10.3897/zookeys.228.3798
- Hoeksema BW, Reimer JD (2015) Zoantharia. In: Fautin, Daphne G. (2011) *Hexacorallians of the World*. Accessed through: World Register of Marine Species at <http://www.marinespecies.org/aphia.php?p=taxdetails&id=607338> on 2015–11–05.
- International Commission of Zoological Nomenclature [ICZN] (1991) Case 2750. *Epizoanthus* Gray, 1867 (Cnidaria, Anthozoa): proposed conservation. *Bulletin of Zoological Nomenclature* 48: 19–21.
- Irei Y, Sinniger F, Reimer JD (2015) Descriptions of two azooxanthellate *Palythoa* species (Subclass Hexacorallia, Order Zoantharia) from the Ryukyu Archipelago, southern Japan. *ZooKeys* 478: 1–26. doi: 10.3897/zookeys.478.8512
- Lindsay DJ, Uemura T, Yamamoto H, Ishibashi S, Nishikawa J, Reimer JD, Beaman RJ, Fitzpatrick R, Fujikura K, Maruyama T (2012) The untethered remotely operated vehicle PICASSO-1 and its deployment from chartered dive vessels for deep sea surveys off Okinawa, Japan, and Osprey Reef, Coral Sea, Australia. *Marine Technology Society Journal* 46: 4. doi: 10.4031/MTSJ.46.4.3
- Lwowsky FF (1913) Revision der gattung *Sidisia* (*Epizoanthus* auct.), ein beitrag zur kenntnis der Zoanthiden. *Zoologische Jahrbuecher Systematik* 34: 557–613.
- Martin D, Britayev TA (1998) Symbiotic polychaetes: review of known species. *Oceanography and Marine Biology: an Annual Review* 36: 217–340.
- Montenegro J, Sinniger F, Reimer JD (2015) Unexpected diversity and new species in the sponge-Parazoanthidae association in southern Japan. *Molecular Phylogenetics and Evolution* 89: 73–90. doi: 10.1016/j.ympev.2015.04.002

- Morphbank: Biological Imaging (<http://sky.www.morphbank.net/>, 13 December 2015). Florida State University, Department of Scientific Computing, Tallahassee, FL 32306-4026 USA
- Muirhead A, Tyler PA, Thurston MH (1986) Reproduction biology and growth of the genus *Epizoanthus* (Zoanthidea) from the north-east Atlantic. *Journal of the Marine Biological Association of the United Kingdom* 66: 131–143. doi: 10.1017/S0025315400039709
- Neves G, Omena E (2003) Influence of sponge morphology on the composition of the polychaete associated fauna from Rocas Atoll, northeast Brazil. *Coral Reefs* 22: 123–129. doi: 10.1007/s00338-003-0295-4
- Palumbi SR (1996) Nucleic acids II: the polymerase chain reaction. *Molecular Systematics*, 205–247.
- Pei Z (1999) *Fauna Sinica Coelenterata Actiniaria Ceriantharia Zoanthidae*. Science Press, 202–203.
- Philipp NA, Fautin DG (2009) Three new species of shallow water yellow zoanths (Hexacorallia: Zoanthidea: Epizoanthidae) from southern California, USA, and southern Australia. *Zootaxa* 2058: 53–61.
- Rees WJ (1967) A brief survey of the symbiotic associations of Cnidaria with Mollusca. *Journal of Molluscan Studies* 37: 213–231.
- Reimer JD, Ono S, Fujiwara Y, Takishita K, Tsukahara J (2004) Reconsidering *Zoanthus* spp. diversity: molecular evidence of conspecificity within four previously presumed species. *Zoological Science* 21: 517–525. doi: 10.2108/zsj.21.517
- Reimer JD, Ono S, Iwama A, Takishita K, Tsukahara J, Maruyama T (2006) Morphological and molecular revision of *Zoanthus* (Anthozoa: Hexacorallia) from southwestern Japan, with descriptions of two new species. *Zoological Science* 23: 261–275. doi: 10.2108/zsj.23.261
- Reimer JD, Hirose M, Nishikawa T, Sinniger, Itani G (2010a) *Epizoanthus* spp. associations revealed using DNA markers: a case study from Kochi, Japan. *Zoological Science* 27: 729–734. doi: 10.2108/zsj.27.729
- Reimer JD, Nakachi S, Hirose M, Hirose E, Hashiguchi S (2010b) Using hydrofluoric acid for morphological investigations of zoanths (Cnidaria: Anthozoa): a critical assessment of methodology and necessity. *Marine Biotechnology* 12: 605–617. doi: 10.1007/s10126-009-9249-3
- Reimer JD, Irei Y, Fujii T, Yang SY (2013) Molecular analyses of shallow-water zooxanthellate zoanths (Cnidaria: Hexacorallia) from Taiwan and their *Symbiodinium* spp. *Zoological Studies* 52: 38. doi: 10.1186/1810-522X-52-38
- Reimer JD, Polisenio A, Hoeksema BW (2014) Shallow-water zoantharians (Cnidaria, Hexacorallia) from the Central Indo-Pacific. *ZooKeys* 444: 1–57. doi: 10.3897/zookeys.444.7537
- Rodriguez F, Oliver JL, Marin A, Medina JR (1990) The general stochastic model of nucleotide substitution. *Journal of Theoretical Biology* 142: 485–501. doi: 10.1016/S0022-5193(05)80104-3
- Ronquist F, Huelsenbeck JP (2003) MrBayes 3: Bayesian phylogenetic inference under mixed models. *Bioinformatics* 19: 1572–1574. doi: 10.1093/bioinformatics/btg180
- Ryland JS, Lancaster JE (2004) A review of zoanthid nematocyst types and their population structure. *Hydrobiologia* 530/531: 179–187. doi: 10.1007/s10750-004-2685-1

- Saitou N, Nei M (1987) The neighbor-joining method: a new method for reconstructing phylogenetic trees. *Molecular Biology Evolution* 4: 406–425.
- Schejter L, Mantelatto FL (2011) Shelter association between the hermit crab *Sympagurus dimorphus* and the zoanthid *Epizoanthus paguricola* in the southwestern Atlantic Ocean. *Acta Zoologica* 92: 141–149. doi: 10.1111/j.1463-6395.2009.00440.x
- Schmidt H (1974) On evolution in the Anthozoa. *Proceedings of the 2nd International Coral Reef Symposium, Brisbane* 1: 533–560.
- Sinniger F (2006) Zoanthids of New Caledonia. In: Payri C, Richier de Forges B (Eds) *Compendium of marine species from New Caledonia*. IRD Editions, Noumea, 127–128.
- Sinniger F, Häussermann V (2009) Zoanthids (Cnidaria: Hexacorallia: Zoantharia) from shallow waters of the southern Chilean fjord region, with descriptions of a new genus and two new species. *Organisms, Diversity and Evolution* 9: 23–36. doi: 10.1016/j.ode.2008.10.003
- Sinniger F, Montoya-Burgos JI, Chevallon P, Pawlowski J (2005) Phylogeny of the order Zoantharia (Anthozoa, Hexacorallia) based on the mitochondrial ribosomal genes. *Marine Biology* 147: 1121–1128. doi: 10.1007/s00227-005-0016-3
- Sinniger F, Reimer JD, Pawlowski J (2008) Potential of DNA sequences to identify zoanthids (Cnidaria: Zoantharia). *Zoological Science* 25: 1253–1260. doi: 10.2108/zsj.25.1253
- Sinniger F, Reimer JD, Pawlowski J (2010) The Parazoanthidae (Hexacorallia: Zoantharia) DNA taxonomy: description of two new genera. *Marine Biodiversity* 40: 57–70. doi: 10.1007/s12526-009-0034-3
- Swain TD (2009) Phylogeny-based species delimitations and the evolution of host associations in symbiotic zoanthids (Anthozoa, Zoanthidea) of the wider Caribbean region. *Zoological Journal of the Linnean Society* 156: 223–238. doi: 10.1111/j.1096-3642.2008.00513.x
- Swain TD, Schellinger JL, Strimaitis AM, Reuter KE (2015) Evolution of anthozoan polyp retraction mechanisms: convergent functional morphology and evolutionary allometry of the marginal musculature in order Zoanthidea (Cnidaria: Anthozoa: Hexacorallia). *BMC Evolutionary Biology* 15: 123. doi: 10.1186/s12862-015-0406-1
- Tamura K, Stecher G, Peterson D, Filipski A, Kumar S (2013) MEGA6: Molecular Evolutionary Genetics Analysis Version 6.0. *Molecular Biology and Evolution* 30: 2725–2729. doi: 10.1093/molbev/mst197
- Thompson JD, Higgins DG, Gibson TJ (1994) CLUSTAL W: Improving the sensitivity of progressive multiple sequence alignment through sequencing weighting, position-specific gap penalties and weight matrix choice. *Nucleic Acids Research* 22: 4673–4680. doi: 10.1093/nar/22.22.4673
- Tischbirek H (1930) Zoanthiden auf Wurmrohren. *Zoologischer Anzeiger* 91: 91–95.
- Verrill AE (1882) Notice of the remarkable marine fauna occupying the outer banks off the southern coast of New England. *American Journal of Science* (3) 23: 135–142. doi: 10.2475/ajs.s3-23.134.135
- Wood RL (1958) Identification and microanatomical study of a new species of *Epizoanthus* (Zoanthidea). *Dissertation, University of Washington, Seattle*.
- Zanol J, Halanych KM, Fauchald K (2013) Reconciling taxonomy and phylogeny in the bristleworm family Eunicidae (Polychaeta, Annelida). *The Norwegian Academy of Science and Letters* 43: 79–100.

Supplementary material 1

GenBank accession number, name and details of the sequences used in phylogenetic analyses of COI, mt 16S-rDNA and ITS-rDNA in this study

Authors: Hiroki Kise, James Davis Reimer

Data type: GenBank accession numbers

Copyright notice: This dataset is made available under the Open Database License (<http://opendatacommons.org/licenses/odbl/1.0/>). The Open Database License (ODbL) is a license agreement intended to allow users to freely share, modify, and use this Dataset while maintaining this same freedom for others, provided that the original source and author(s) are credited.

Supplementary material 2

List of examined specimens, and GenBank accession numbers

Authors: Hiroki Kise, James Davis Reimer

Data type: GenBank accession numbers

Copyright notice: This dataset is made available under the Open Database License (<http://opendatacommons.org/licenses/odbl/1.0/>). The Open Database License (ODbL) is a license agreement intended to allow users to freely share, modify, and use this Dataset while maintaining this same freedom for others, provided that the original source and author(s) are credited.

Review of the South American leafhopper genus *Parandanus* (Hemiptera, Cicadellidae, Deltocephalinae)

Yani Duan¹, Christopher H. Dietrich², Micael D. Webb³, Yalin Zhang⁴

1 School of Plant Protection, Anhui Agricultural University, Hefei, Anhui Province 230036, China **2** Illinois Natural History Survey, Prairie Research Institute, University of Illinois at Urbana-Champaign, 1816 S. Oak St., Champaign, IL 61820, USA **3** The Natural History Museum, London, UK, SW7 5BD **4** Key Laboratory of Plant Protection Resources and Pest Management of the Ministry of Education, Entomological Museum, Northwest A & F University, Yangling, Shaanxi Province 712100, China

Corresponding author: Yalin Zhang (yalinzh@nwsuaf.edu.cn)

Academic editor: B. Price | Received 11 December 2015 | Accepted 7 January 2016 | Published 10 February 2016

<http://zoobank.org/04853D6C-EDFF-4C0F-8A9E-8E169B4DE870>

Citation: Duan Y, Dietrich CH, Webb MD, Zhang Y (2016) Review of the South American leafhopper genus *Parandanus* (Hemiptera, Cicadellidae, Deltocephalinae). ZooKeys 562: 73–83. doi: 10.3897/zookeys.562.7478

Abstract

The South American leafhopper genus *Parandanus* Linnavuori & DeLong (Deltocephalinae: Deltocephalini) is reviewed and four of its six species are illustrated and male genital characters are provided. Three new species from Peru, *Parandanus longistylus* Duan, **sp. n.**, *Parandanus nigricephalus* Duan, **sp. n.** and *Parandanus paracruciatus* Duan, **sp. n.** are described. A key to species is also provided.

Keywords

Auchenorrhyncha, morphology, taxonomy, new species

Introduction

The South American grassland leafhopper genus *Parandanus* Linnavuori & DeLong (Deltocephalinae: Deltocephalini) was established by Linnavuori and DeLong (1976) for two species from Peru, *P. hilaris* and *P. ornatus* (the type species). Later, Linnavuori and DeLong (1979) described *P. cruciatus* from Bolivia. Zahniser and Dietrich (2013) included the genus in tribe Deltocephalini based on the linear connective fused to the

aedeagus. Members of this genus can be recognised by the following combination of characters: frontoclypeus with pale median longitudinal stripe, anal tube membranous and aedeagus with pair of basal or subbasal appendages. In this paper, *Parandanus* are reviewed with description of three new species from Peru. All species of the genus are listed and a key to males is provided.

Materials and methods

The material studied here is deposited in the Illinois Natural History Survey (INHS). Morphological terminology follows Zhang (1990) and Dietrich (2005). Digital photographs were taken with a QImaging Micropublisher 3.3 digital camera mounted on an Olympus BX41 stereo microscope and with a Nikon D1x digital SLR camera configured with lenses by Microptics, Digital Lab XLT system. Photographs were modified with Adobe Photoshop CS.

Taxonomy

Parandanus Linnavuori & DeLong

Parandanus Linnavuori & DeLong, 1976: 34. Type species: *Parandanus ornatus* Linnavuori & DeLong, 1976.

Redescription. Overall coloration pale yellow with orange to dark brown markings. Frontoclypeus with pale median longitudinal stripe and indistinct pale lateral arcs. Pronotum with six longitudinal bands. Scutellum with basal triangles and a medial stripe, orange to sordid brown. Forewing veins pale, bordered with fuscous. Mesosternum dark brown. Femora and tibiae with fuscous marks.

Body elongate. Head narrower than pronotum. Crown not or only slightly produced, rounded to face; ocelli next to eyes on anterior margin. Face relatively flat, similar in width to length; frontoclypeus relatively narrow; clypeal sulcus absent; anteclypeus nearly parallel-sided, extended to ventral margin of face; genae broad, insinuated near eyes. Forewing long and narrow, appendix distinct, with four apical and three antepical cells, inner antepical cell open basally. Anal tube membranous.

Male genitalia. Pygofer without processes, with numerous macrosetae in posterior region. Subgenital plate elongate triangular, with few stout to many more slender macrosetae laterally. Style with articulating arm short to very long; apophysis short to long. Connective fused to aedeagus, arms close to each other. Aedeagal shaft slender with pair of basal or subbasal elongate appendages extended posteroventrally along shaft; gonopore apical on dorsal surface.

Distribution. Bolivia, Peru.

Checklist of species of *Parandanus**Parandanus cruciatus* Linnavuori & DeLong, 1979. Bolivia.*Parandanus hilaris* Linnavuori & DeLong, 1976. Peru.*Parandanus longistylus* Duan, **sp. n.** Peru.*Parandanus nigricephalus* Duan, **sp. n.** Peru.*Parandanus ornatus* Linnavuori & DeLong, 1976. Peru.*Parandanus paracruciatus* Duan, **sp. n.** Peru.**Key to species of *Parandanus* (males)**

- 1 Style preapical angle indistinct; apophysis long (Fig. 2D).....**2**
 – Style preapical angle distinct; apophysis short (Fig. 4D)**3**
 2 Style >4× longer than distance between lobes of apodeme (Fig. 2D). Aedeagal appendages terminating well short of aedeagal shaft apex (Fig. 2E–G).....
 ***Parandanus longistyle* Duan, sp. n.**
 – Style <3× longer than distance between lobes of apodeme (Fig. 6D). Aedeagal appendages terminating near aedeagal shaft apex (Fig. 6E–G)
 ***Parandanus nigricephalus* Duan, sp. n.**
 3 Aedeagal appendages not crossing each other ventrally (Linnavuori and DeLong 1976: Fig. 94).....***Parandanus ornatus* Linnavuori & DeLong**
 – Aedeagal appendages crossing each other ventrally (Fig. 4E–F).....**4**
 4 Subgenital plate with lateral margins distinctly emarginate near base (Fig. 8D)..... ***Parandanus hilaris* Linnavuori & DeLong**
 – Subgenital plate with lateral margins nearly straight throughout length (Fig. 4C).....**5**
 5 Aedeagal appendages subbasal and curved posterodorsad (Fig. 4E–F).....
 ***Parandanus paracruciatus* Duan, sp. n.**
 – Aedeagal appendages basal and directed posteroventrad (Linnavuori and DeLong 1979: figs 41–42)..... ***Parandanus cruciatus* Linnavuori & DeLong**

***Parandanus longistylus* Duan, sp. n.**<http://zoobank.org/44D7A960-CB27-44BA-91C4-9D92189D469B>

Figs 1–2

Description. Length. Male: 6.8–7.2 mm.

Anterior margin of crown with two dark brown coalescing spots extending around ocelli, disk with an orange spot anterolaterally, its inner area dark brown, a small dark brown spot adjacent to basal angles of eyes. Pronotum with six broad longitudinal orange brown bands (Fig. 1A).

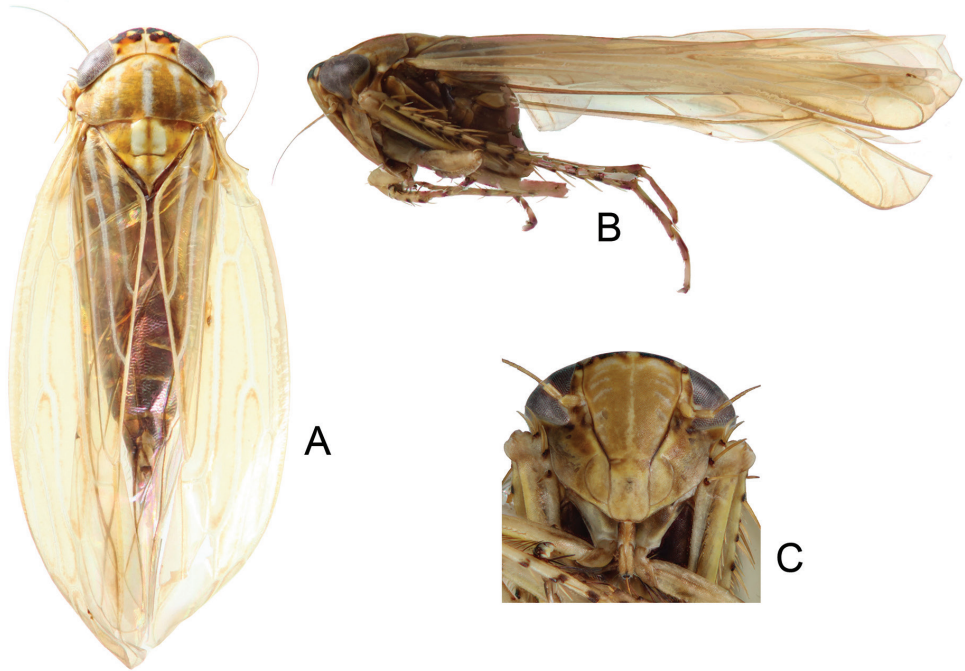


Figure 1. *Parandanus longistylus* Duan, sp. n. **A** habitus, dorsal view **B** habitus, lateral view **C** face.

Crown of near uniform length, $0.43\times$ as long as distance between eyes, $0.43\times$ as long as median length of pronotum (Fig. 1A).

Male genitalia. Pygofer short, sides rounded apically (Fig. 2A–B). Subgenital plate elongate with lateral margins nearly straight, with approximately 17 narrow macrosetae (Fig. 2C). Style articulating arm short; preapical angle indistinct; apophysis very elongate (Fig. 2D). Aedeagus with pair of subbasal parallel appendages, extending to subapex of shaft (Fig. 2E–G).

Material examined. Holotype: male, Peru: Pasco, 3km N Oxapampa, 1700m, $10^{\circ}33.20'S$, $75^{\circ}25.55'W$, 21 Oct 2002, C.H. Dietrich, merc vapor light, 02–31–1 (INHS). Paratypes: 3 males, same data as holotype.

Etymology. This name is based on the style with a long apophysis.

Remarks. This species is similar to *P. paracruciatu*s in color pattern but differs from this and other species by its very long style apophysis.

***Parandanus paracruciatu*s Duan, sp. n.**

<http://zoobank.org/F13969FC-3F84-4092-AAEB-2CB70F7FCDE3>

Figs 3–4

Description. Length. Male: 6.6–7.0 mm.

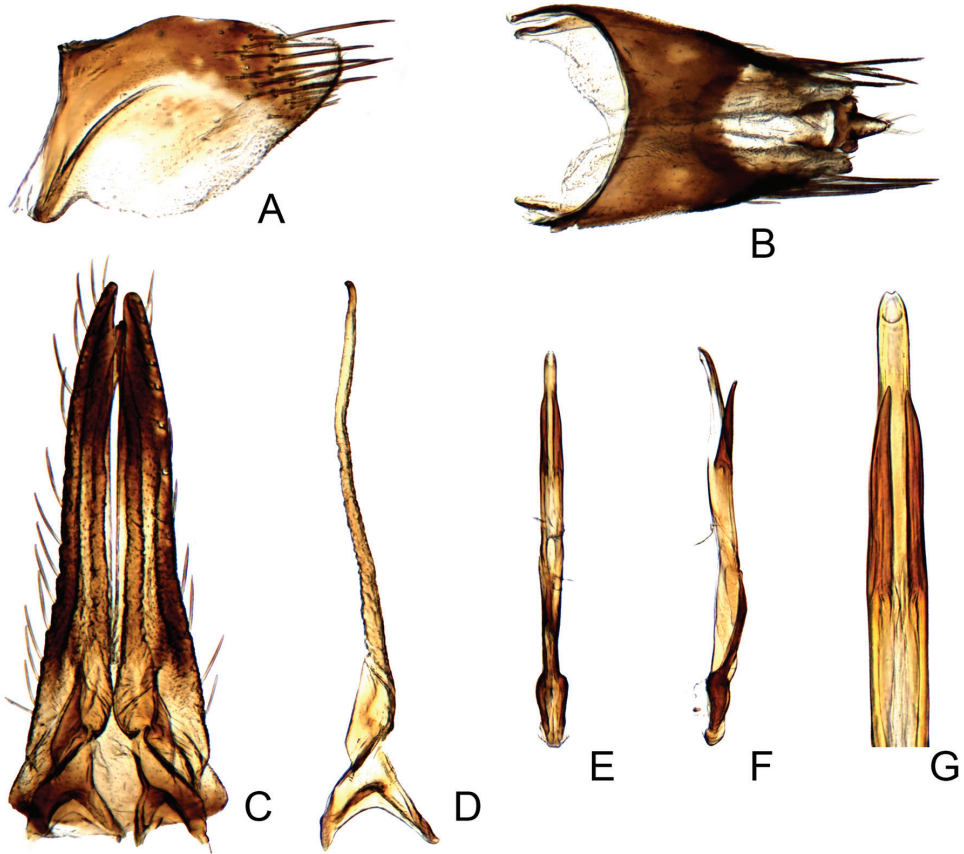


Figure 2. *Parandanus longistylus* Duan, sp. n. **A** male pygofer side, lateral view **B** male pygofer and segments X–XI, dorsal view **C** valve, subgenital plates and styles, ventral view **D** style, dorsal view **E, F** connective and aedeagus, dorsal and lateral view, respectively **G** apex of aedeagus, dorsal view.

Anterior margin of crown with four dark brown spots, disk with an orange spot laterally, its inner area dark brown, a small orange spot adjacent to basal angles of eyes. Pronotum with six narrow longitudinal orange brown bands (Fig. 3A).

Crown of nearly uniform length, 0.48x as long as distance between eyes, 0.47x as long as median length of pronotum (Fig. 3A).

Male genitalia. Pygofer long, sides rounded apically, ventral margin concave (Fig. 4A–B). Subgenital plate with lateral margins nearly straight, with approximately 12 narrow macrosetae (Fig. 4C). Style articulating arm very long; preapical angle distinct; apophysis very short (Fig. 4D). Aedeagus with pair of subbasal crossed appendages, extending to near to apex of shaft (Fig. 4E–F).

Material examined. Holotype: male, Peru: Pasco, 3km N Oxapampa, 1700m, 10°33.20'S, 75°25.55'W, 21 Oct 2002, C.H. Dietrich, merc vapor light, 02–31–1 (INHS). Paratypes: 3 males, same data as holotype.

Etymology. The species name is based on the similarity of the species to *P. cruciatus*.

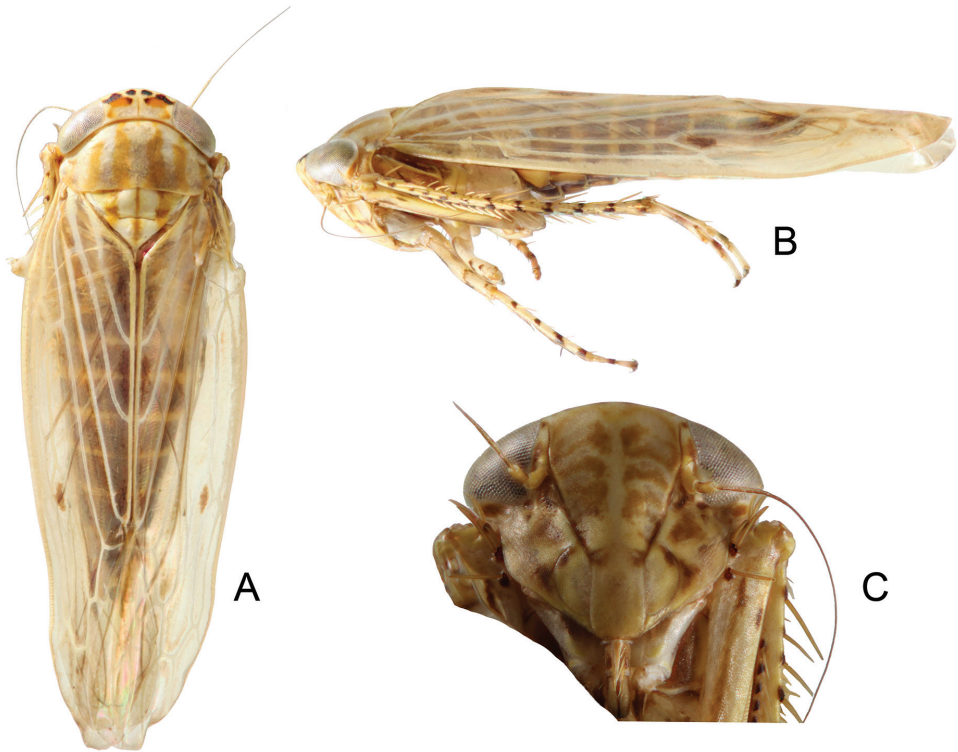


Figure 3. *Parandanus paracruciatus* Duan, sp. n. **A** habitus, dorsal view **B** habitus, lateral view **C** face.

Remarks. This species is similar to *P. longistylus* in color pattern but differs from this and other species by the shape of the style with short apophysis and long articulating arm.

***Parandanus nigricephalus* Duan, sp. n.**

<http://zoobank.org/6EB41ED2-F47A-4CC0-AE6E-5B696F71C04C>

Figs 5–6

Description. Length. Male: 6.6–6.8 mm.

Anterior margin of crown with a dark brown patch extending around ocellus and variably onto disc and to posterior margin, with a medial small yellow spot, a small dark brown spot adjacent to basal angles of eyes (Fig. 5A–B). Face with pronounced brown markings (Fig. 5D). Pronotum with longitudinal bands variably coalescing, sordid orange brown (Fig. 5A–B).

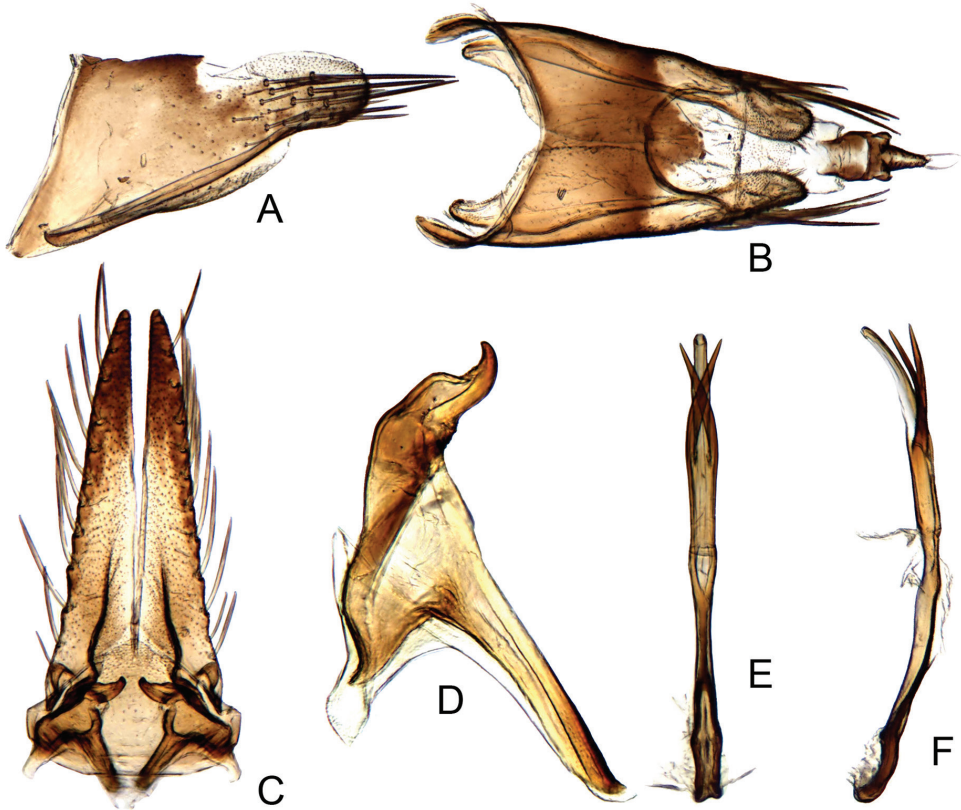


Figure 4. *Parandanus paracruciatius* Duan, sp. n. **A** male pygofer side, lateral view **B** male pygofer and segments X–XI, dorsal view **C** valve, subgenital plates and styles, ventral view **D** style, dorsal view **E, F** connective and aedeagus, dorsal and lateral view, respectively.

Crown of nearly uniform length, $0.36\times$ as long as distance between eyes, $0.38\times$ as long as median length of pronotum (Fig. 5A–B).

Male genitalia. Pygofer short, sides rounded apically (Fig. 6A–B). Subgenital plate with lateral margins nearly straight, with approximately 11 narrow macrosetae (Fig. 6C). Style articulating arm moderately long and robust; preapical angle indistinct; apophysis long (Fig. 6D). Aedeagus with pair of subbasal parallel appendages converging apically, extending near to apex of shaft (Fig. 6E–G).

Material examined. Holotype: male, Peru: Pasco, 3km N Oxapampa, 1700m, $10^{\circ}33.20'S$, $75^{\circ}25.55'W$, 21 Oct 2002, C.H. Dietrich, merc vapor light, 02–31–1 (INHS). Paratypes: 13 males, same data as holotype.

Etymology. This name is based on the vertex with a large dark patch.

Remarks. This species can be distinguished by its pronounced brown head markings and long style apophysis.

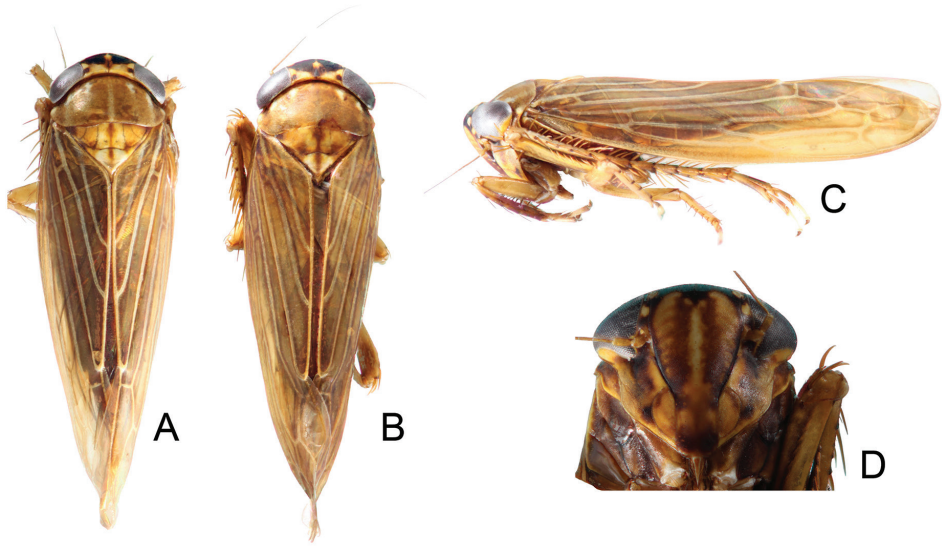


Figure 5. *Parandanus nigricephalus* Duan, sp. n. **A, B** habitus, dorsal view **C** habitus, lateral view **D** face.

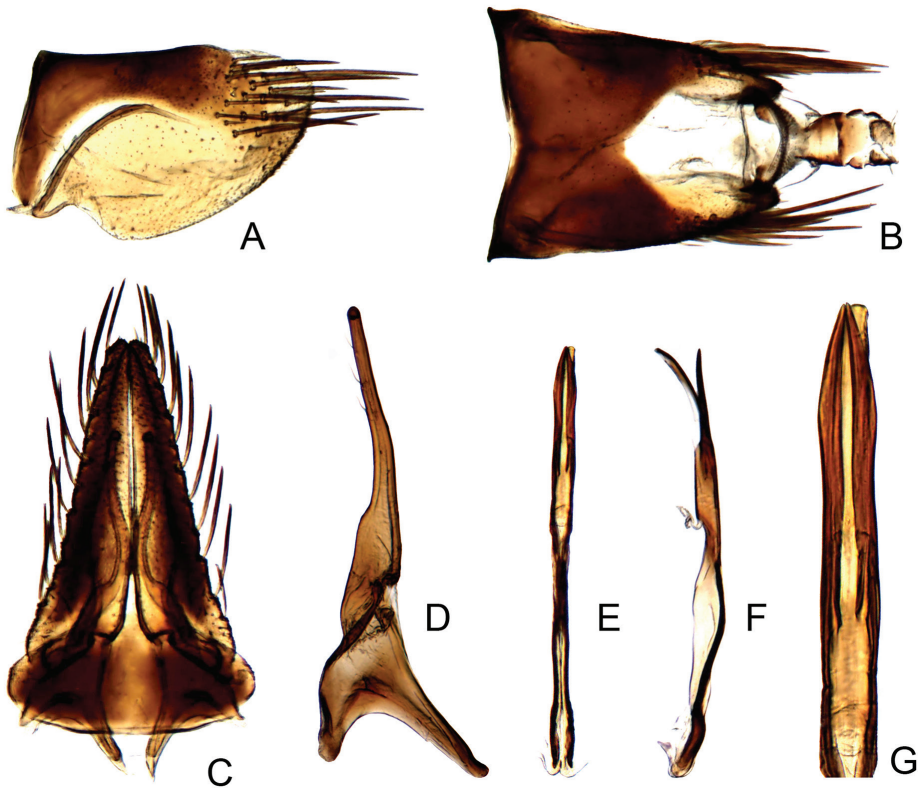


Figure 6. *Parandanus nigricephalus* Duan, sp. n. **A** male pygofer side, lateral view **B** male pygofer and segments X–XI, dorsal view **C** valve, subgenital plates and styles, ventral view **D** style, dorsal view **E, F** connective and aedeagus, dorsal and lateral view, respectively **G** apex of aedeagus, dorsal view.

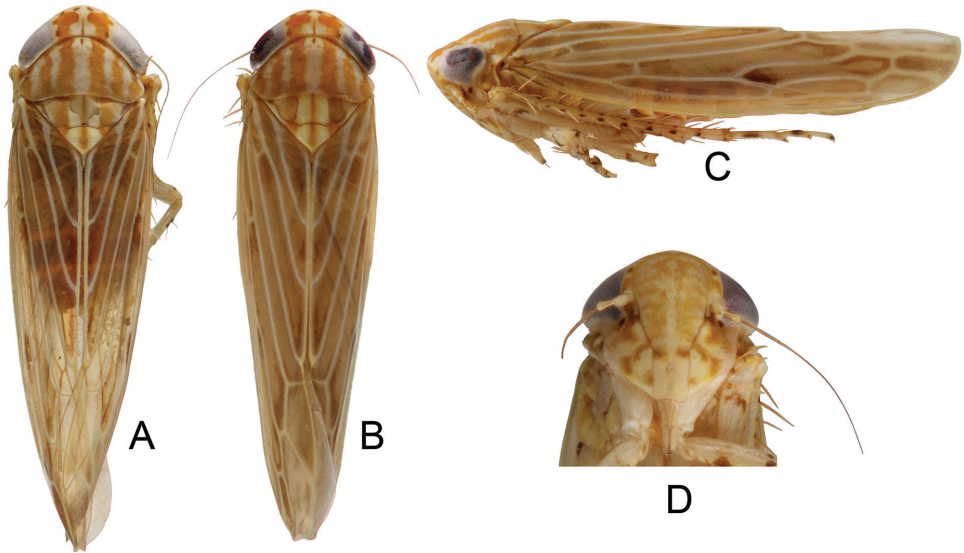


Figure 7. *Parandanus hilaris*. **A, B** habitus, dorsal view **C** habitus, lateral view **D** face.

Parandanus hilaris

Figs 7–8

Parandanus hilaris Linnavuori & DeLong, 1976: 34.

Description. Length. Male: 5.5–5.9 mm.

Anterior margin of crown with six small brown spots, disk with orange patch on each side anteriorly and extending to posterior margin, a small brown spot adjacent basal angles of eyes. Pronotum with six longitudinal narrow orange bands (Fig. 7A–B).

Crown about 1.17× as long medially as next to eyes, 0.67× as long as distance between eyes, 0.56× as long as median length of pronotum (Fig. 7A–B).

Male genitalia. Pygofer short, sides rounded apically (Fig. 8A–B). Subgenital plate with lateral margins distinctly insinuated subbasally, with seven robust macrosetae (Fig. 8D). Style articulating arm moderately long and robust; preapical angle distinct; apophysis very short (Fig. 8E). Aedeagus with pair of relatively robust basal crossed appendages, sinuate in lateral view, extending to middle of shaft (Fig. 8F–G).

Material examined. 2 males, Peru: Huànuco, 5km S Tingo Maria, Pte. Perez, 600m, 9°20.51'S, 75°58.51'W, 25 Oct 2002, C.H. Dietrich, mercury vapor light, 02–41–1 (INHS); 1 male, Peru: Huànuco, 5km S Tingo Maria, Pte. Perez, 600m, 9°20.51'S, 75°58.51'W, 25 Oct 2002, R. A. Rakitov, mercury vapor light, 02–41–2 (INHS).

Distribution. Peru.

Remarks. This species can be distinguished by its relatively longer crown medially, few robust subgenital plate macrosetae, short syle apophysis and shape of the aedeagus.

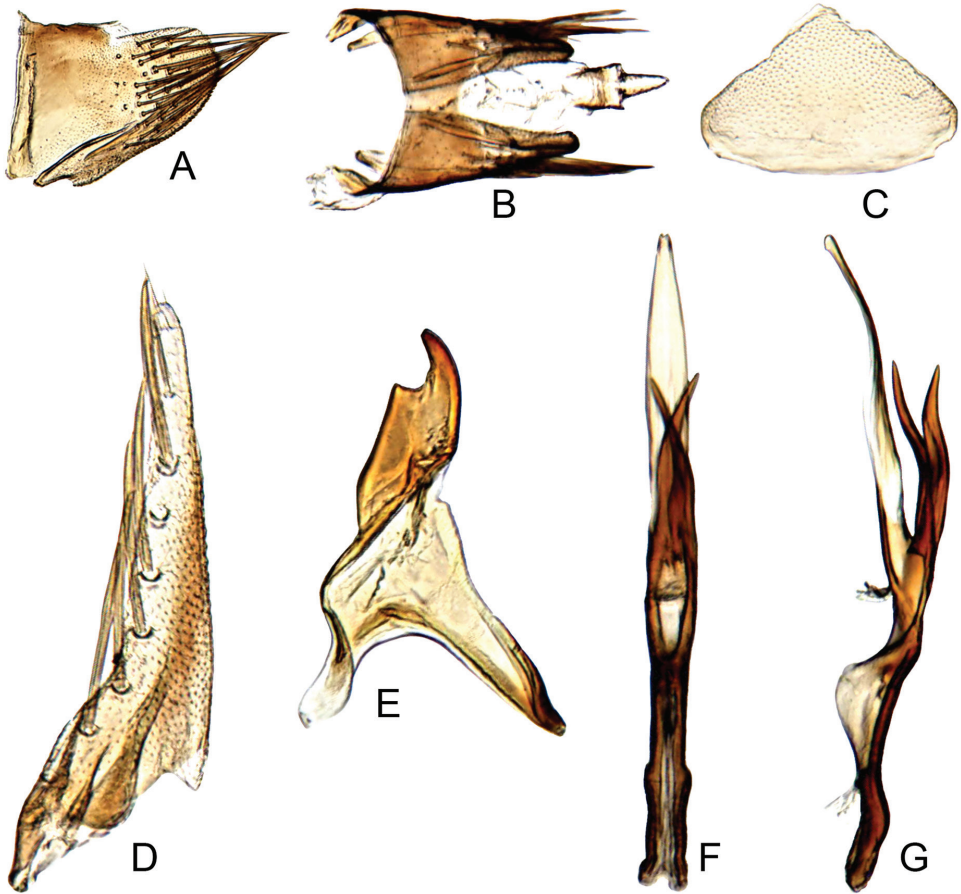


Figure 8. *Parandanus hilaris*. **A** male pygofer side, lateral view **B** male pygofer and segments X–XI, dorsal view **C** valve, ventral view **D** subgenital plate, ventral view **E** style, dorsal view **F, G** connective and aedeagus, dorsal and lateral view, respectively.

Acknowledgements

We express our sincere thanks to J. R. Schrock, Emporia State University, USA for revising this manuscript. We also thank J. N. Zahniser, US Department of Agriculture, San Diego USA for assistance in the identification. This research is supported by the National Natural Science Foundation of China (31000968), Anhui Provincial Natural Science Foundation (1608085MC55) and Anhui Provincial Colleges and Universities Natural Science Foundation (KJ2015A006). The senior author was supported by the National Scholarship Fund of China to pursue his research at the Illinois Natural History Survey, Champaign, USA, from Aug. 2013 to Aug. 2014.

References

- Dietrich CH (2005) Keys to the families of Cicadomorpha and subfamilies and tribes of Cicadellidae (Hemiptera: Auchenorrhyncha). *Florida Entomologist* 88: 502–517. doi: 10.1653/0015-4040(2005)88[502:KTTFOC]2.0.CO;2
- Linnavuori RE, DeLong DM (1976) New Neotropical leafhoppers from Peru and Bolivia (Homoptera: Cicadellidae). *Revista Peruana de Entomologica* 19(1): 29–38.
- Linnavuori RE, DeLong DM (1979) New species of leafhoppers from Central and South America (Homoptera: Cicadellidae: Deltocephalinae, Neobalinae, Xestocephalinae). *Entomologica Scandinavica* 10: 123–138. doi: 10.1163/187631279X00277
- Zahniser JN, Dietrich CH (2013) A review of the tribes of Deltocephalinae (Hemiptera: Auchenorrhyncha: Cicadellidae). *European Journal of Taxonomy* 45: 1–211. doi: 10.5852/ejt.2013.45
- Zhang YL (1990) *A Taxonomic Study of Chinese Cicadellidae (Homoptera)*. Tianze Press, Yangling, Shaanxi, China, 218 pp.

A review of the genera *Gnathochoris* Förster and *Symplecis* Förster of South Korea, with notes on Korean orthocentrines (Hymenoptera, Ichneumonidae, Orthocentrinae)

Andrei E. Humala¹, Jin-Kyung Choi², Jong-Wook Lee²

1 Forest Research Institute, Russian Academy of Sciences, Petrozavodsk, Russia **2** Department of Life Sciences, Yeungnam University, Gyeongsan, South Korea

Corresponding author: Jong-Wook Lee (jwlee1@ynu.ac.kr)

Academic editor: B. Santos | Received 24 November 2015 | Accepted 4 January 2016 | Published 10 February 2016

<http://zoobank.org/F76DF980-33CF-4DE7-AF32-4EF385B07C5F>

Citation: Humala AE, Choi J-K, Lee J-W (2016) A review of the genera *Gnathochoris* Förster and *Symplecis* Förster of South Korea, with notes on Korean orthocentrines (Hymenoptera, Ichneumonidae, Orthocentrinae). ZooKeys 562: 85–104. doi: 10.3897/zookeys.562.7303

Abstract

Two genera of Korean Orthocentrinae, *Gnathochoris* and *Symplecis*, are reviewed, and keys to species of these genera are provided here. Two new species, *Gnathochoris fuscipes* Humala & Lee, **sp. n.** and *G. korensis* Humala & Lee, **sp. n.** are described from South Korea. The current state of the taxonomy of Eastern Palaearctic orthocentrines is briefly discussed.

Keywords

Fauna, ichneumon wasps, keys, Korea, new species, taxonomy

Introduction

Orthocentrinae is a moderately large, cosmopolitan subfamily of small-bodied ichneumon wasps consisting of approximately 500 described species (Yu et al. 2012). Most orthocentrines are koinobiont endoparasitoids of nematoceran Diptera (Sciaroidea), the larvae of which often develop in fungal fruiting bodies (Roman 1923, Askew and Shaw 1986, Humala 2003). Only Orthocentrinae *sensu stricto* (Townes 1971), or the

Orthocentrus genus-group (Wahl and Gauld 1998), is morphologically well defined, comprising a distinctive, monophyletic lineage within the subfamily (Broad 2010), while the remaining genera—for a long time considered a “wastebasket” group among ichneumon wasps, which is the most difficult of the ichneumonid subfamilies to define (Townes 1971)—have significant morphological diversity. The current concept of Orthocentrinae includes most of the genera comprising Townes’s Orthocentrinae and Microleptinae (Helictinae *auct.*) with the exception of some genera. A key to the genera was provided by Townes (1971), but it contained several genera (*Tatogaster* Townes, *Acaenitellus* Morley, *Microleptes* Gravenhorst, *Oxytorus* Förster, *Cylloceria* Schiødte and *Allomacrus* Förster) which were excluded afterwards (Wahl 1986, 1990, Gupta 1988, Wahl and Gauld 1998). Several other genera described by Rossem—*Pantomima* Rossem, *Fetialis* Rossem, *Epitropus* Rossem and *Phosphoriana* Rossem—were synonymized later (Broad 2004, Humala 2007), and *Hyperacmus* Holmgren was transferred to the Cylloceriinae by Quicke et al. (2009).

The subfamily Orthocentrinae remains one of the least known among ichneumonid wasps, and even the European fauna remains relatively unknown. Many genera within this subfamily are in need of modern revisions and potential reclassification, as emphasized by Broad (2010). The Nearctic fauna (excluding Orthocentrinae *s. str.*) was revised by Dasch (1992), the Western Palaearctic fauna was revised by Aubert (1968, 1976, 1977, 1978, 1980, 1981) and Rossem (1981, 1983, 1987, 1988, 1990, 1991, etc.), whereas the Eastern Palaearctic is scarcely covered by taxonomic and faunistic studies (Uchida 1930, 1942; Rossem 1981–1991; Humala 2003, 2007; Kasparyan et al. 2012, etc.). Other regions have not been practically studied yet, with the exception of the Neotropics, where a partial revision of the genus *Orthocentrus* Gravenhorst was recently published (Veijalainen et al. 2014; Zwakhals and Diller 2015).

Two genera of Orthocentrinae in the fauna of South Korea are treated here: *Gnathochorisis* with five species (two of them new to science) and *Symplecis* with two species. Keys to species occurring in South Korea are provided. This paper is the first dealing with orthocentrine ichneumon wasps occurring in South Korea.

Materials and methods

Materials used in this study were collected by sweep nets and Malaise traps, after which they were deposited in the Animal Systematic Laboratory of Yeungnam University (YNU, Gyeongsan, South Korea). Photographs were taken using an AxioCam MRc5 camera attached to a stereo microscope (Zeiss SteREO Discovery. V20), processed using AxioVision SE64 software (Carl Zeiss), and optimized with a Delta imaging system (i-solution, IMT i-Solution Inc.); and a Leica DFC 290 digital camera attached to a Leica MZ9.5 stereomicroscope; images were combined using Helicon Focus Pro software.

The morphological terminology mostly follows Gauld (1991). Note that we use the convenient term ‘temple’ for the upper part of the gena, between the eye and the occipital carina.

Abbreviations are used as follows:

- GW** Gangwon-do;
GG Gyeonggi-do;
CB Chungcheongbuk-do;
CN Chungcheonnam-do;
GB Gyeongsangbuk-do;
GN Gyeongsangnam-do.
AEI American Entomological Institute, Gainesville, Florida, U.S.A. (H. Townes collection)
DEI Deutsches Entomologisches Institut, Eberswalde, Germany.
IZU Instytut Zoologiczny Uniwersytetu, Wrocław, Poland (Gravenhorst collection)
NM Naturhistorisches Museum, Wien, Austria.
ZI Zoologiska Institutionen, Lund, Sweden.

Results

Family Ichneumonidae Latreille, 1802

Subfamily Orthocentrinae Förster, 1869

Genus *Gnathochorisis* Förster, 1869

Gnathochorisis Förster, 1869: 152. Type species: *Gnathochorisis flavipes* Förster, 1871: 113.
Blapticus Förster, 1869: 171. Type species: *Blapticus leucostomus* Förster, 1871: 83.
Laepserus Förster, 1869: 205. Type species: *Blapticus crassulus* Thomson, 1888: 1289.
Acroblapticus Schmiedeknecht, 1911: 2173. Type species: *Blapticus dentifer* Thomson, 1888: 1288.

Diagnosis. Body rather stout. Head transverse; clypeus small, weakly to strongly separated from face by a groove; eye large; temple short; malar space with subocular sulcus; occipital carina complete; antenna long, male antenna lacking tyloids. Mesosoma finely or densely punctate on mesoscutum, polished on mesopleuron. Epicnemial carina complete, dorsally distant from anterior margin of mesopleuron; propodeum polished or matt, usually with carinae complete and strong; often propodeal apophyses somewhat developed. Fore wing with areolet present or absent, when present sessile or short petiolate, rectangular. Hind leg as a rule stout, hind femur 2.85–4.9 times as long as high. First metasomal segment with glymma lacking, sternite fused to tergite and reaching 0.5–0.6 of the segment, with spiracle near middle; second tergite matt or polished, sometimes with longitudinal striae; ovipositor upcurved, with a dorsal subapical notch, 0.5–1.1 times as long as hind tibia.

Remarks. Medium-sized genus, with 13 described species (Yu et al. 2012). Eight species occur in the Nearctic region and seven in the Palearctic region (two species are distributed on both continents). Beyond the Holarctic region, one species of *Gna-*

thochorisis is known in Mexico (Dasch 1992, Humala et al. 2011). The genus was also reported from Australia (Gauld 1984), Ecuador, and Central America (Veijalainen et al. 2012). Five species of *Gnathochorisis*, including two newly described, are presently reported from South Korea here. This is the first record of the genus from this country. In the European part of Russia *G. flavipes* Förster was reared from the fungus gnat *Neoempheria striata* Meigen (Mycetophilidae: Mycomyinae) (Humala 2003), other published host records (Dasch 1992) seem to be doubtful.

Key to species of *Gnathochorisis* occurring in South Korea

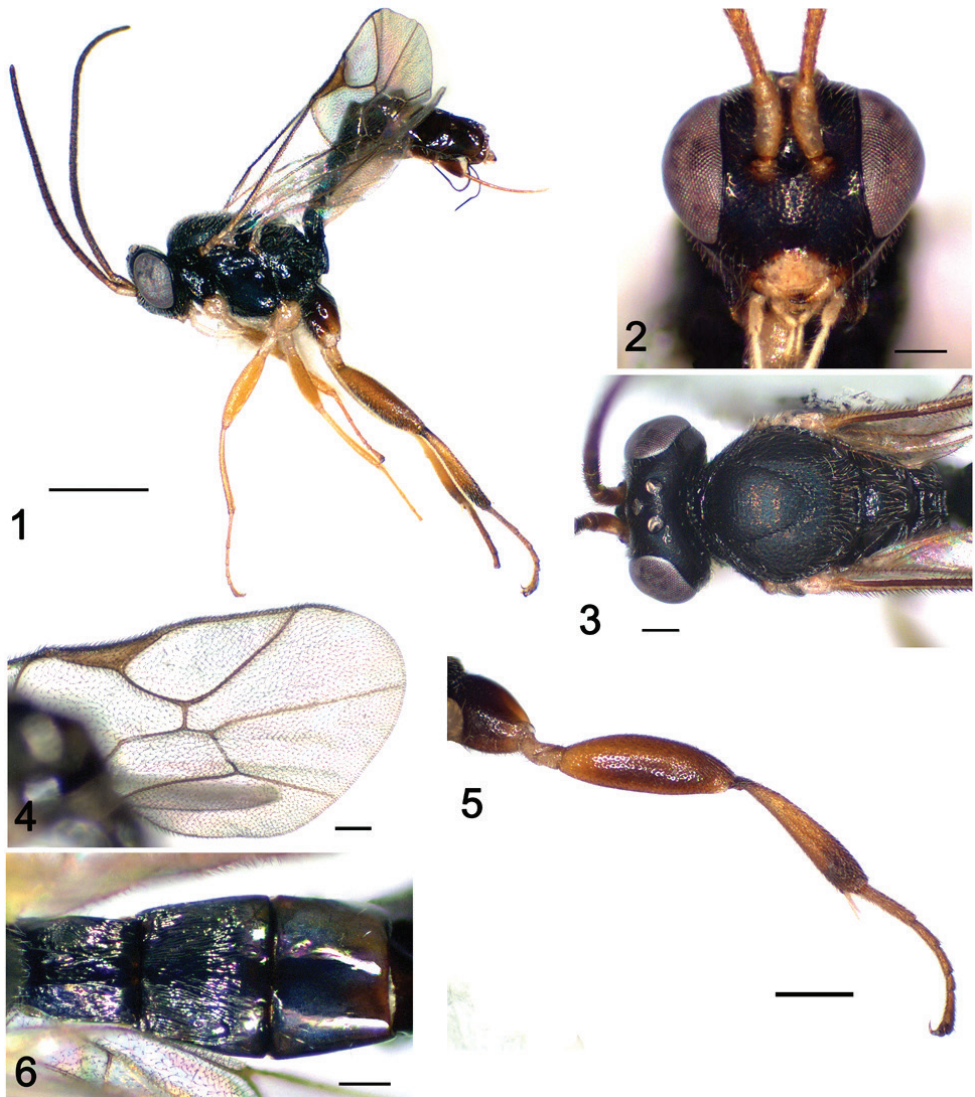
- 1 Fore wing with areolet (Figs 11, 16, 21). Sculpture of the second tergite various..... **2**
- Fore wing without areolet (Figs 4, 28). Second tergite of metasoma polished, longitudinally striate **4**
- 2 Metapleuron coriaceous (Fig. 22); notauli short, developed in anterior 0.3 of mesoscutum. Second tergite coriaceous (Figs 23, 24). Hind femur not strongly inflated, 4.0–4.1 times as long as wide..... ***G. dentifer* Thomson**
- Metapleuron polished and impunctate (Figs 17, 27). Hind femur stout, 3.0–3.8 times as long as high..... **3**
- 3 Second tergite coriaceous, without longitudinal striae (Fig. 18). Female frontal orbits with yellow or pale marks (Fig. 15); notauli developed only in anterior third of mesoscutum. Hind femur 3.5–3.8 times as long as high.....
..... ***G. crassulus* Thomson**
- Second tergite polished, longitudinally striate (Fig. 12). Female frontal orbits fuscous (Fig. 8); notauli well developed, meeting in the centre of mesoscutum (Fig. 9). Hind femur inflated, 3.0 times as long as wide
..... ***G. koreensis* Humala & Lee, sp. n.**
- 4 Female face at the level of antennal fossae 0.47 times as wide as head; face brown near antennal sockets (Fig. 26). Postocellar line equal to maximum diameter of the lateral ocellus. Hind coxa and femur yellow (Fig. 25). Second tergite with yellowish apical band (Fig. 29)..... ***G. flavipes* Förster**
- Female face at the level of antennal fossae 0.53 times as wide as head, face entirely black (Fig. 2). Postocellar line 1.3 times as long as maximum diameter of the lateral ocellus. Hind coxa and femur infuscate (Fig. 1). Second tergite entirely fuscous ***G. fuscipes* Humala & Lee, sp. n.**

***Gnathochorisis fuscipes* Humala & Lee, sp. n.**

<http://zoobank.org/C11D8868-47AF-4B82-B629-859C4B334027>

Figs 1–6

Diagnosis. Closely allied to *G. flavipes* Grav. but differs by its wider and matt face, more matt and rough sculpture of the mesoscutum, the slenderer first and second



Figures 1–6. *Gnathochoris fuscipes* sp. n. (holotype, female); **1** Habitus, lateral view **2** Head and base of antenna, anterior view **3** Head and mesoscutum, dorsal view **4** Fore wing **5** Hind leg, lateral view **6** Metasoma basal tergites, dorsal view. Scale bars: 1.0 mm (**1**); 0.5 mm (**5**); 0.2 mm (**2–4, 6**).

tergites of metasoma; the absence of light apical bands on tergites 2–3, the presence of sclerotized area on second sternite, the stouter flagellomeres, the fuscous hind coxa, and the hind tibia infusate apically and in apical third. Separable from other known Palearctic *Gnathochoris* species by the absence of a closed areolet in the fore wing.

Description. Female (holotype). Fore wing length 3.8 mm.

Head. 1.1 times as wide as high; frons nearly polished with weak microsculpture; face polished with sparse and fine punctures, at the level of antennal fossae 0.5 times as wide as head (Fig. 2). Inner eye orbits slightly divergent ventrally. Clypeus weakly separated from face, approximately 1.9 times as wide as high, edge of clypeus convex; malar space 1.8 times as long as mandible basal width, with subocular sulcus; maxillary palp reaching beyond fore coxa. In dorsal view, head posteriorly deeply concave; occipital carina complete; temples short; ocular-ocellar line 1.3 times as long as maximum diameter of lateral ocellus, equal to postocellar line (Fig. 3). Antenna moderately long, with 21 flagellomeres, basal flagellomere 3.9 times and second flagellomere 3.0 times as long as wide.

Mesosoma. 1.4 times as long as high. Mesoscutum matt with short adpressed dense setae; notauli well developed, meeting in the centre of mesoscutum (Fig. 3); epicnemial carina complete; in profile, scutellum somewhat high, without lateral carinae. Propodeum polished with sparse setae; anterior transverse carina strongly raised; area superomedia transverse, costula present; rounded apophyses of propodeum resulting from crossing lateral longitudinal and posterior transverse carinae developed. Spiracle of moderate size. Most of metapleuron polished with small coriaceous area near base of hind coxa. Fore wing without areolet, with 2rs-m shorter than second abscissa of 1m-cu (Fig. 4); cu-a inclivous, slightly postfurcal. Hind wing with first abscissa of Cu1 inclivous, 2 times as long as cu-a, distal abscissa of Cu1 present. Hind leg stout, coxa and femur polished, tibia and tarsus coriaceous, hind femur inflated, 3.2 times as long as high (Fig. 5). Hind tibia 4.8 times as long as its maximum width, with spine-like setae; hind basitarsus 0.4 times as long as hind tibia.

Metasoma. First metasomal segment moderately arched, 2.2 times as long as its posterior width, polished, with dorsal longitudinal carina strong; postpetiole longitudinally striate. Spiracle at 0.65, sternite at 0.55 of tergite 1 length. Second tergite 0.85 times as long as its posterior width, with small thyridium basally; polished with longitudinal striae, restricted by transverse groove at apical 0.25 (Fig. 6). Remainder tergites polished, metasoma somewhat compressed laterally from tergite 3. Ovipositor upcurved, approximately as long as first metasomal segment, tip with blunt subapical dorsal notch.

Colour. Fuscous. Clypeus, mandible, palpi, tegula, corners of pronotum, wings bases, antenna ventrally, except for brownish flagellomeres in apical 1/3 of flagellum, pale yellow. Legs basically light brown, hind coxa dark brown basally, hind tibia somewhat darkened basally and apically, fore and middle coxae and all trochanters pale yellow. Metasoma from apical third of tergite 3 brown. Wings hyaline, veins and pterostigma brown.

Male. Unknown.

Etymology. Named after the fuscous hind legs.

Material examined. Holotype: female (YNU), Korea: GW, Wonju-si, Socho-myeon, Hakgong-ri, Chiaksan National Park, 37°22'18"N, 128°03'1.84"E, Malaise trap, 9–20 June 2013 (J.W. Lee)

Distribution. South Korea (GW).

***Gnathochorisis koreensis* Humala & Lee, sp. n.**

<http://zoobank.org/49D8B9C9-43D8-4AC9-8800-07B01A46C488>

Figs 7–13

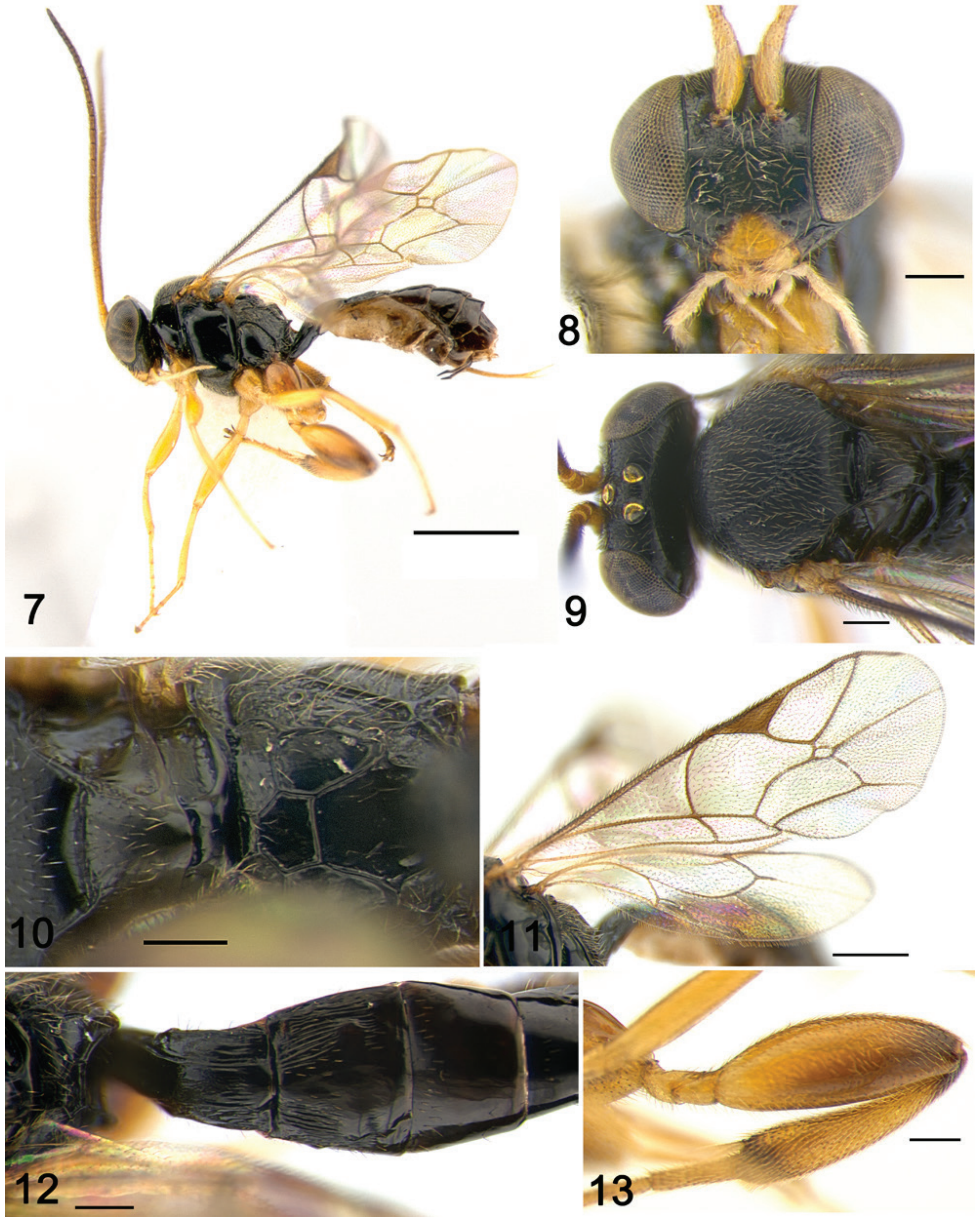
Diagnosis. Fore wing with areolet. Metapleuron polished; notauli well developed, meeting in the centre of mesoscutum. Female frontal orbits fuscous. Second tergite polished, longitudinally striate. Hind femur inflated, 3.0 times as long as wide. From similar Palaearctic *G. flavipes* Grav. it differs by the presence of closed areolet and the absence of light apical bands on tergites 2–3. Separable from other known Palaearctic *Gnathochorisis* species with closed areolet by the polished metapleuron, fine sculpture of mesoscutum, long notauli meeting in the centre of mesoscutum, narrow face, entirely fuscous and polished metasomal tergites with longitudinal striae on tergite 2. From the more closely allied *G. meridionator* Aubert, reported from Russian Far East (Humala 2007), it differs by the wide and entirely fuscous face, strong, distinct notauli meeting in the centre of the mesoscutum, short metasomal tergites, infusate hind coxae, and stouter antennae.

Description. Female (holotype). Fore wing length 3.3 mm.

Head. 1.2 times as wide as high; frons nearly polished with weak microsculpture; face polished, sparsely and finely punctate, at the level of antennal fossae 0.45 times as wide as head (Fig. 8); inner eye orbits subparallel. Clypeus weakly separated from face, approximately 1.8 times as wide as high, edge of clypeus convex; temples short; ocular-ocellar line 1.3 times as long as maximum diameter of lateral ocellus, postocellar line 0.8 times as long as maximum diameter of lateral ocellus (Fig. 9). Antenna moderately long, with 20 (21 in paratype) elongate flagellomeres; basal flagellomere 4.5 times and second flagellomere 3.6 times as high as wide.

Mesosoma. 1.45 times as long as high. Mesoscutum convex, matt with short adpressed dense setae; epomia present; notauli well developed, meeting in centre of mesoscutum (Fig. 9); epicnemial carina complete; in profile scutellum somewhat high, with lateral carinae anteriorly. Most of mesopleuron and metapleuron polished. Propodeum polished with sparse setae; carinae complete and strong; area superomedia slightly transverse (Fig. 10); small propodeal apophyses present; spiracle small. Fore wing with areolet closed, small, short petiolate and slightly longer than high; 3rs-m shorter than 2rs-m (Fig. 11); cu-a inclivous, nearly interstitial. Hind wing with first abscissa of Cu1 inclivous, 2 times as long as cu-a, distal abscissa of Cu1 present but weakly pigmented. Hind leg stout, coxa and femur polished, tibia and tarsus coriaceous; femur inflated, 3.0 times as long as high (Fig. 12); tibia 4.8 times as long as maximum width subapically, with spine-like setae and dense fringe on apex well developed; hind basitarsus 0.35 times as long as hind tibia.

Metasoma. First metasomal segment moderately arched, 2.1 times as long as its posterior width, dorsal longitudinal carina well developed; postpetiole polished, striate laterally; spiracle and end of sternite near middle of tergite length. Second tergite 0.85 times as long as its posterior width, polished with small thyridium basally and oblique longitudinal striae basally and laterally, whereas central and apical parts smooth



Figures 7–13. *Gnathochoris koreensis* sp. n. (holotype, female); **7** Habitus, lateral view **8** Head, anterior view **9** Head and mesoscutum, dorsal view **10** Propodeum, dorsal view **11** Wings **12** Metasoma, basal tergites, dorsal view **13** Hind femur, lateral view. Scale bars: 1.0 mm (**7**); 0.5 mm (**5**); 0.2 mm (**8–10, 12, 13**).

(Fig. 13). Remaining tergites of metasoma polished, somewhat compressed laterally from tergite 3. Ovipositor upcurved, approximately 0.7 times as long as hind tibia.

Colour. Fuscous. Clypeus, mandible, tegula, wings bases, dorsal corner of pronotum, antenna ventrally yellow, palp whitish yellow. Legs mostly light brown, hind coxa reddish

brown, darkened basally, hind femur gradually infuscate to apex, hind tibia somewhat darkened basally and apically. Metasoma fuscous; tergites 2–4 with reddish brown apical bands; thyridium reddish brown. Wings hyaline, veins and pterostigma brown.

Male. Unknown.

Etymology. Named after the type locality, Korea.

Material examined. Holotype female (YNU), Korea: GB, Mungyeong-si, Geaun-eup Wanjang-ri, Songnisan National Park, Beorimigijae, 36°40'59"N, 127°57'07"E, Malaise trap, 12 August–11 September 2013 (J.K. Choi). Paratype female (YNU), Korea: GG, Kwangju-si, Docheong-myeon Mt. Taehwasan, Malaise trap, 15–25 June 2008 (J.K. Choi)

Distribution. South Korea (GG).

Gnathochoris is crassulus (Thomson, 1888)

Figs 14–18

Blapticus crassulus Thomson 1888; type depository: ZI.

Acroblapticus crassulus Thomson (Schmiedeknecht, 1911).

Gnathochoris is crassulus Thomson (Aubert, 1966).

Diagnosis. Inner eye orbits slightly divergent ventrally, face matt, finely punctate; antenna moderately long with 22–24 flagellomeres. Mesosoma finely and densely punctate on mesoscutum and mesosternum, polished on metapleuron. Propodeum polished, carinae complete and strong. Fore wing with areolet short petiolate, rectangular (Fig. 16). Hind femur stout, 3.5–3.8 times as long as high. First tergite with dorsolateral carina strong (Fig. 18); second tergite matt; ovipositor upcurved, 0.95 times as long as hind tibia. Fuscous; pale yellow on frontal orbits, malar space, clypeus, mandibles, palpi, scape and pedicel ventrally, tegula, wing bases, hind corner of pronotum, fore and middle coxae and all trochanters, apical margins of metasomal tergites 2–4. Male with yellow face, inner orbits and malar space; propleuron and lower mesopleuron yellowish.

Material examined. Korea: 1 female, GW, Taebaek-si, Hyeol-dong, Yuilsa, 37°06'N 128°26'E, Malaise trap, 30 June 1991 (J.W. Lee).

Distribution. Holarctic; in Palaearctic region it was reported from Europe, Siberia, Russian Far East (Humala 2003, 2007), Japan (Dasch 1992; no data on the examined material was provided), and South Korea (new record).

Gnathochoris is dentifer (Thomson, 1888)

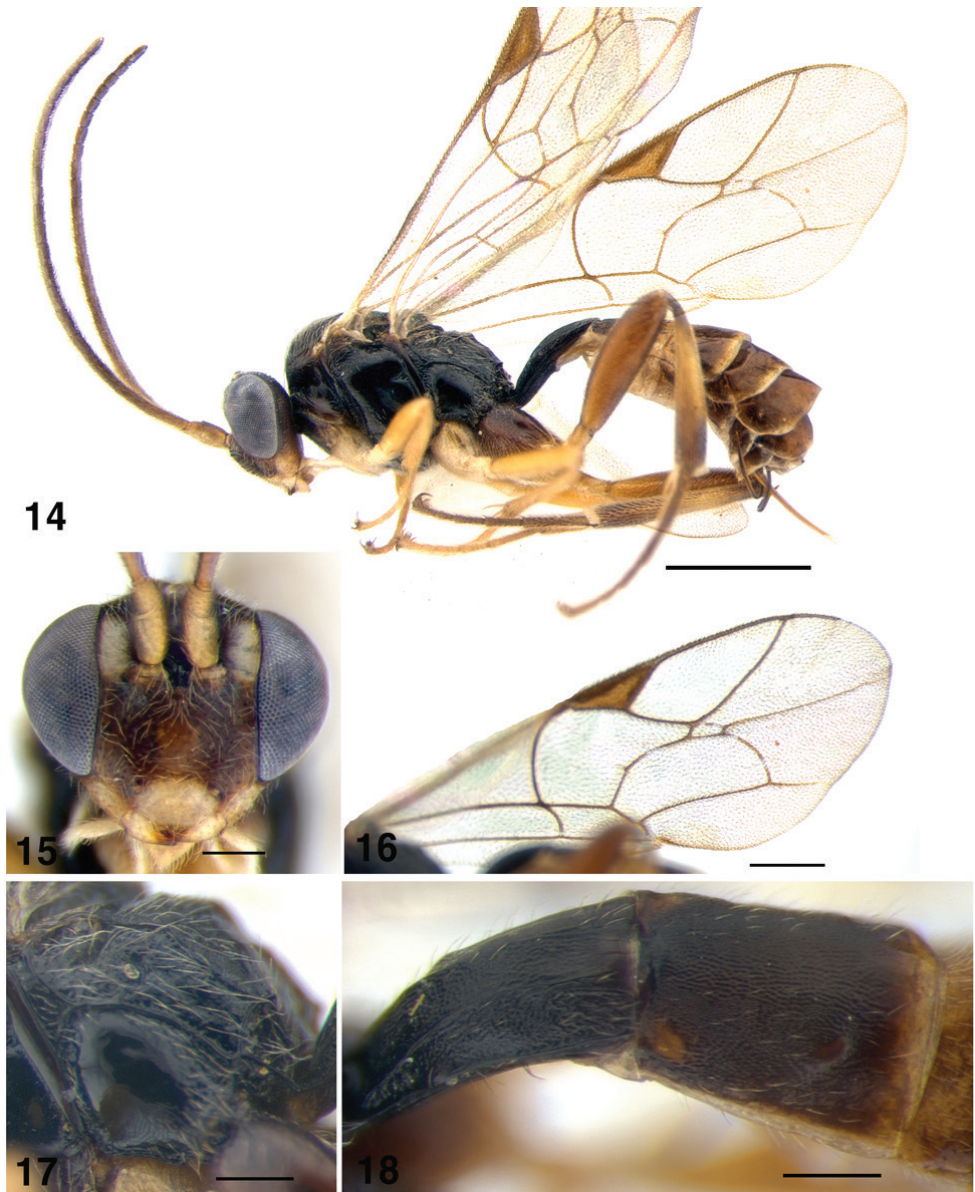
Figs 19–24

Blapticus dentifer Thomson 1888: 1288; type depository: ZI.

Acroblapticus dentifer Thomson (Schmiedeknecht, 1911: 2174).

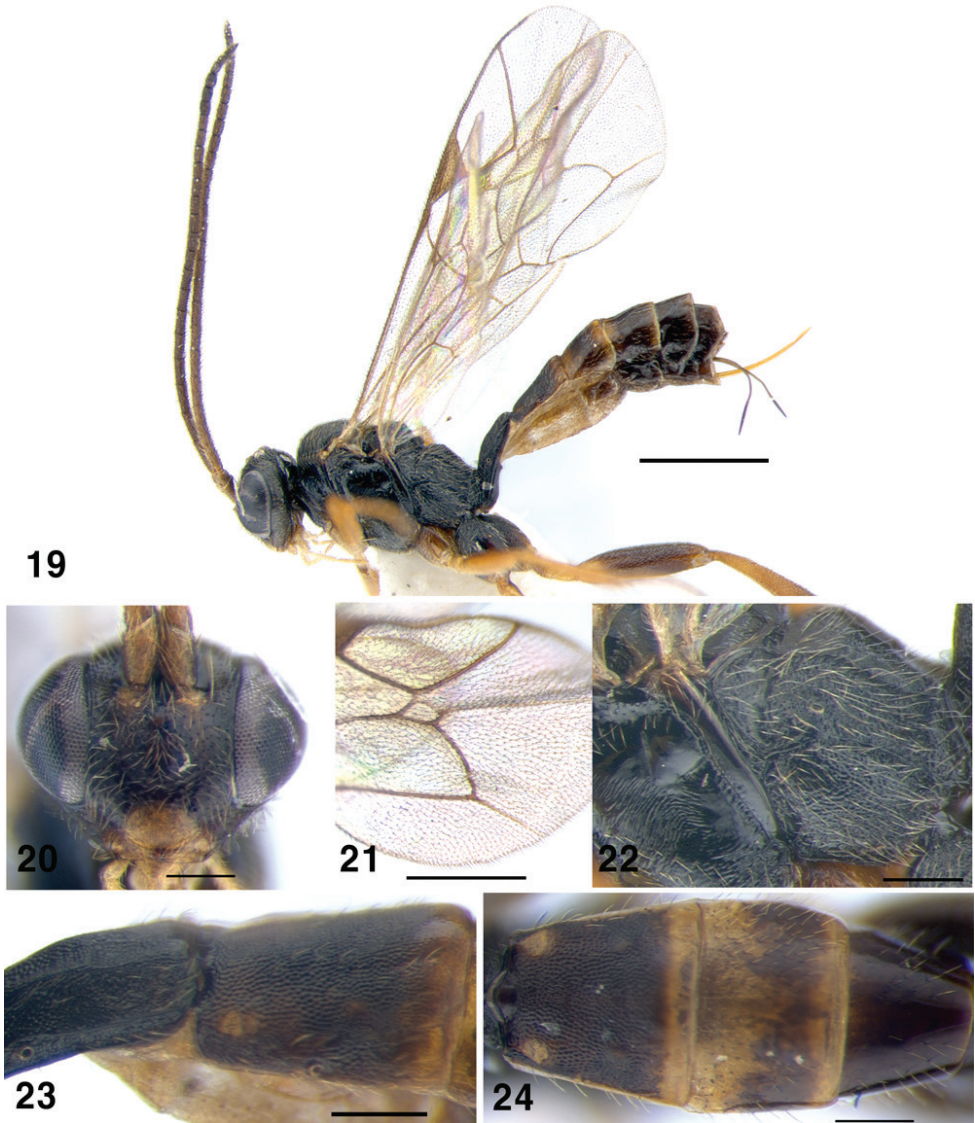
= *Acroblapticus debilis* Schmiedeknecht 1911: 2175; type depository: NM.

Gnathochoris is dentifer Thomson (Aubert 1966: 115–134).



Figures 14–18. *Gnathochorisius crassulus*; **14** Habitus, lateral view; **15** Head of female, anterior view **16** Fore wing **17** Metapleuron, lateral view **18** Metasoma, first and second tergites, dorsolateral view. Scale bars: 1 mm (**14**); 0.5 mm (**16**); 0.2 mm (**15**, **17**, **18**).

Diagnosis. Inner eye orbits slightly divergent ventrally, face lightly matt; antenna moderately long with 22–27 flagellomeres. Mesosoma finely and densely punctate on mesoscutum, coriaceous on metapleurum. Propodeum matt, carinae complete. Fore wing with areolet short petiolate, rectangular (Fig. 21). Hind femur stout, 4.0–4.15



Figures 19–24. *Gnathochorisis dentifer*; **19** Habitus, lateral view **20** Head of female, anterior view **21** Areolet of fore wing **22** Metapleuron, lateral view **23** Metasoma, second tergite, lateral view; **24** Metasoma, second to fourth tergites, dorsal view. Scale bars: 1 mm (**19**); 0.5 mm (**21**); 0.2 mm (**20, 22–24**).

times as long as high. First tergite with dorsolateral carina strong; second tergite matt (Fig. 24); ovipositor 1.0–1.1 times as long as hind tibia. Fuscous, including frontal orbits; pale yellow on clypeus, mandibles, palpi, scape and pedicel ventrally, tegula, wing bases, hind corner of pronotum, fore and middle coxae and all trochanters. Rufous on rest of fore and middle legs, apical margins of metasomal tergites 2–4, and basal margins on tergites 3–6. Male with yellow face, inner orbits and malar space.

Material examined. Korea: 1 female, GW, Donghae-si, Samhwa-dong, Mureung Valley, 37°27'N 129°01'E, Malaise trap, 16 October–25 November 2005 (J.W. Lee) (YNU).

Distribution. Holarctic; in Palaearctic region it was reported from Europe, Siberia, Russian Far East (Humala 2003, 2007, etc.), Japan (Dasch 1992; no data on the examined material was provided), and South Korea (new record).

Gnathochorisis flavipes Förster, 1871

Figs 25–29

= *Gnathochorisis terebrata* Strand 1918: 159; type depository: DEL.

Gnathochorisis flavipes Förster 1871: 113.

Blapticus (*Gnathochorisis*) *flavipes* Förster (Thomson 1888: 1291).

Gnathochorisis flavipes Förster (Schmiedeknecht 1911: 2181).

Diagnosis. Female face at the level of antennal fossae 0.47 times as wide as head; clypeus rather small, weakly separated from face by a groove, flattened; maxillary palp long, almost reaching middle coxae; malar space with distinct subocular sulcus; antenna moderately long with 20–21 flagellomeres. Mesosoma slightly matt and finely punctate on mesoscutum, polished on pronotum, mesopleuron and metapleuron (Fig. 27). Notaulus reaching centre of mesoscutum. Propodeum polished, carinae complete and strong, propodeal apophyses present; area superomedia transverse. Fore wing areolet absent (Fig. 28). Hind leg stout, femur 2.8–3.3 times as long as high; second tergite polished with distinct longitudinal striae (Fig. 29), apical margin polished; ovipositor 0.5–0.6 times as long as hind tibia. Fuscous, pale on clypeus, mandible, palpi, scape and pedicel ventrally, tegula, wing bases, hind corner of pronotum, fore and middle coxae and trochanters. Apical margins of metasomal tergites 2 and 3 and rest of legs yellowish-rufous. Female face brown, paler close to antennal sockets, male with face, inner eye orbits, scape, and malar space yellow.

Material examined. Korea: 2 females, GW, Wonju-si, Socho-myeon, Hakgong-ri, Mt. Chiaksan, 37°22'18"N, 128°03'1.84"E, Malaise trap, 1–22 August 2013 (J.W. Lee); 2 females, GW, Wonju-si, Heungeup-myeon, Maeji-ri, Yonsei Univ., 20 July–28 August 2013 (H.Y. Han); 1 female, GW, Donghae-si, Samhwa-dong, Mureung Valley, 37°27'52"N, 129°01'26"E, Malaise trap, 5–18 August 2007 (J.W. Lee); 1 female, GW, Donghae-si, Samhwa-dong, Mureung Valley, 10–20 September 2006 (J.W. Lee); 2 females, CB, Chungju-si, Suanbo-myeon, Samun-ri, Woraksan National Park, 35°49'46"N, 128°04'05"E, 17 July–12 August 2013 (J.K. Choi); 1 female, CN, Seosan-si, Haemi-myeon, Daedok-ri, Hanseo Univ., 16 July–3 August 2013 (J.K. Kim); 1 female, GB, Cheongdo-gun, Unmun-myeon, Unmunsan, 6 June–1 July 2008 (J.W. Lee); 1 female, GN, Jinju-si, Gajwa-dong, 11–18 November 1987 (J.W. Lee); 1 female, GN, Jinju-si, Gajwa-dong, 12–18 August 1989 (J.W. Lee).

Distribution. Palaearctic; reported from Europe, Siberia and Russian Far East (Primorsky Terr.) (Humala 2003, 2007) and South Korea (new record).

Biology. Reared from *Neoempheria striata* Mg. (Mycetophilidae) (Humala 2003).



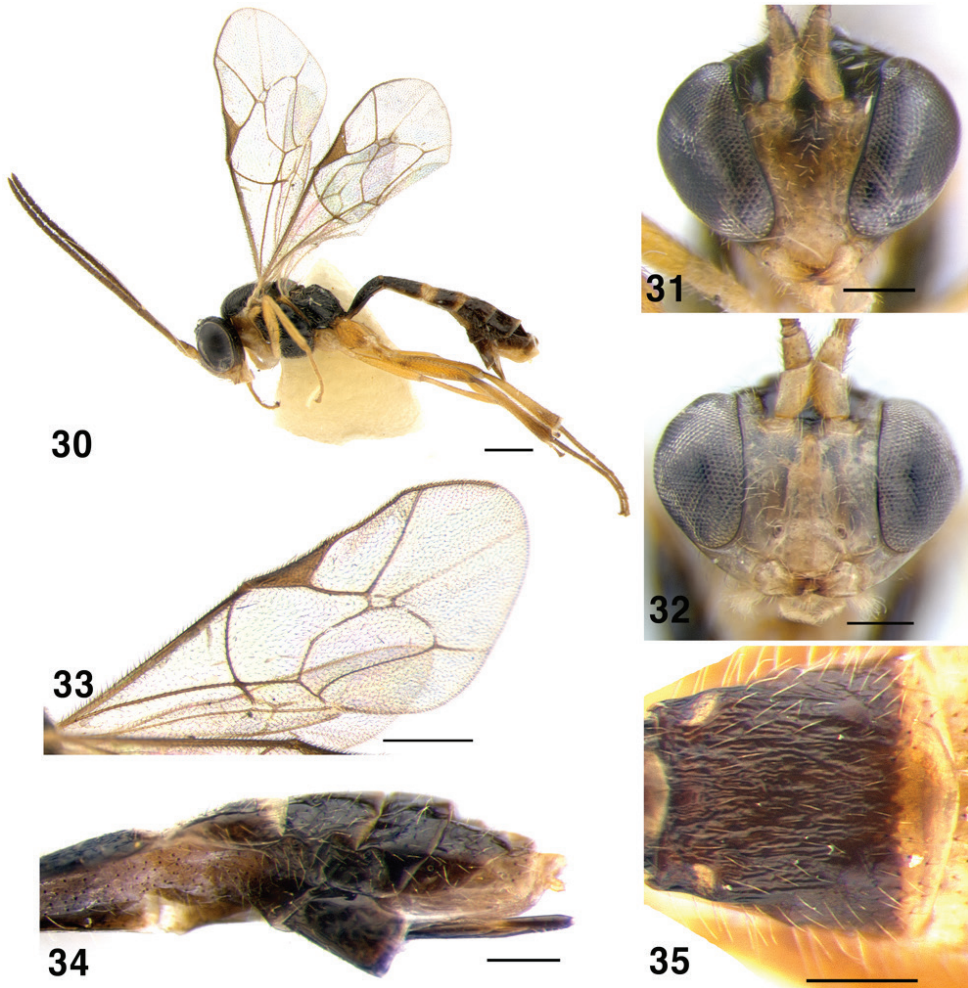
Figures 25–29. *Gnathochoris flavipes*; **25** Habitus, lateral view **26** Head of female, anterior view **27** Metapleuron, lateral view **28** Wings **29** Metasoma, second tergite, lateral view. Scale bars: 1 mm (**25**); 0.5 mm (**28**); 0.2 mm (**26, 27, 29**).

Genus *Symplecis* Förster, 1869

Symplecis Förster 1869: 151. Type species: *Symplecis alpicola* Förster, 1871: 119; Thomson 1888: 1285; Schmiedeknecht 1911: 2169.

Blapticus Förster 1869: 171. Type species: *Blapticus leucostomus* Förster, 1871: 83.

Diagnosis. Inner eye orbits strongly convergent ventrally in female, slightly in male; clypeus small, weakly to more strongly separated from face by a groove; eye large; temple short; malar space very narrow with subocular sulcus; mandible small, usually not twisted; male antenna lacking tyloids. Notaulus short and deep; epicnemial carina complete; carinae of propodeum complete and strong. Fore wing with areolet present



Figures 30–35. *Symplecis bicingulata*; **30** Habitus, lateral view **31** Head of female, anterior view **32** Head of male, anterior view **33** Wings **34** Metasoma, distal tergites, lateral view and ovipositor **35** Metasoma, second tergite, dorsal view. Scale bars: 0.5 mm (**30**, **33**); 0.2 mm (**31**, **32**, **34**, **35**).

or absent, when present sessile or short petiolate, rectangular. First metasomal segment slender, with glymma lacking, its sternite fused to tergite. Second tergite coriaceous, or with longitudinal striae. Ovipositor usually short, almost straight, stout at base, slenderer in apical part, 0.4–0.9 times as long as hind tibia.

Remarks. Medium sized genus with 14 recognized species distributed worldwide: 11 species are known in the Palaearctic region, six in the Nearctic region (Dasch 1992), one in the Neotropical region, one in the Afrotropical region and one in the Oriental region (Yu et al. 2012).

Two species are reported from South Korea in this paper. This is the first record of the genus from this country. Both Korean species of *Symplecis* are Holarctic.

There are two known host records for *Symplecis*, both from Diptera, Sciaroidea: *S. breviscula* Roman was reared from *Diadocidia ferruginosa* Meigen (Diadocidiidae) in Europe (Roman 1923) and *S. matilei* Delobel from *Neoempheria ombrophila* Matile et Matile (Mycetophilidae) in Central Africa (Delobel and Matile 1976).

Key to species of *Symplecis* occurring in South Korea

- 1 Fore wing with areolet (Fig. 33). Ovipositor short, hardly surpassing apex of metasoma (Fig. 34). Second tergite of metasoma longitudinally striate (Fig. 35). Inner eye orbits strongly convergent ventrally in female (Fig. 31), slightly convergent in male (Fig. 32). Area superomedia of propodeum slightly transverse..... ***S. bicingulata* Gravenhorst**
- Fore wing without areolet (vein 3rs-m absent) (Fig. 39). Ovipositor long, 0.8–0.95 times as long as hind tibia. First and second tergites of metasoma coriaceous (Fig. 41). Inner eye orbits strongly convergent ventrally in both sexes (Figs 37, 38). Area superomedia of propodeum longer than wide..... ***S. invisitata* Rossem**

***Symplecis bicingulata* (Gravenhorst, 1829)**

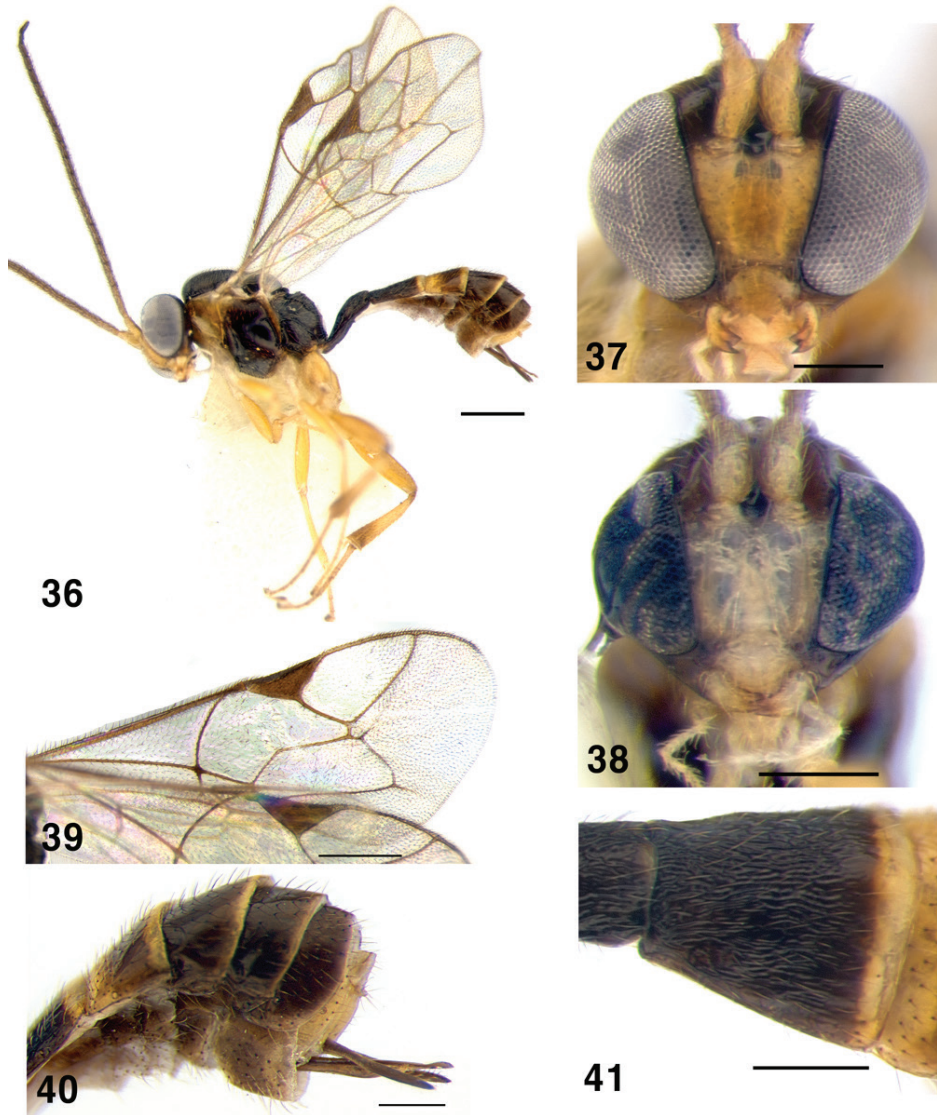
Figs 30–35

Mesoleptus bicingulatus Gravenhorst, 1829: 107; type depository: IZU.

Diagnosis. Inner eye orbits strongly convergent ventrally in female (Fig. 31), face at the level of clypeus 0.41–0.45 times as wide as at the level of median ocellus; slightly convergent in male (Fig. 32). Mesoscutum polished; sternaulus short and deep; epomia lacking. Area superomedia of propodeum slightly transverse. Fore wing with areolet (Fig. 33). First metasomal tergite matt and striate, dorsal carina well developed; second tergite with distinct longitudinal striae (Fig. 35). Ovipositor short, hardly surpassing apex of metasoma (Fig. 34). Face and pronotum usually yellowish; tergites 2–3 apically and 3–4 basally yellow, forming two light bands on dark metasoma (Fig. 30).

Material examined. Korea: 10 females, GW, Donghae-si, Samhwa-dong, Mureung Valley, [9–17 August 2005, 22 June–3 July 2006, 17–28 August 2006, 10–20 September 2006, 20 September–2 October 2006, 9 November 2006] (J.W. Lee); 1 female, ditto, 28 August–9 October 2006 (K.B. Kim); 1 male, GW, Wonju-si, Heungeup-myeon, Yeonse Univ., 22 July–11 August 2007 (J.W. Lee); 2 females, GG, Anyang-si, Manan-gu, Anyang-dong, Kwanagsan, 15–25 July 2008 (J.O. Lim); 1 male, GB, Gyeongsan-si, Daehak-ro, Yeungnam Univ., 22 April–1 May 2006 (J.W. Lee); 1 male, Ulsan-si, Sangbuk-myeon, Gajisan, 11 August 1989 (J.W. Lee).

Distribution. Holarctic; in Palaearctic region reported from Europe, Siberia, Russian Far East (Primorsky Terr., Sakhalin Isl., Kunashir Isl.) (Humala 2007) and Japan (Dasch 1992; no data on the examined material was provided) and South Korea (new record).



Figures 36–41. *Symplecis invisitata*; **36** Habitus, lateral view **37** Head of female, anterior view **38** Head of male, anterior view **39** Wings **40** Metasoma, distal tergites, lateral view and ovipositor **41** Metasoma, second tergite, dorsal view. Scale bars: 0.5 mm (**36**, **39**); 0.2 mm (**37**, **38**, **40**, **41**).

***Symplecis invisitata* Rossem, 1981**

Figs 36–41

Symplecis invisitata Rossem, 1981: 126–127; type depository: AEI.

Diagnosis. Inner eyes orbits strongly convergent ventrally in both sexes (Figs 37, 38), malar space very narrow. Mesoscutum coriaceous, densely punctate; epomia present.

Sternaulus shallow. Area superomedia of propodeum longer than wide. Fore wing without areolet (vein 3rs-m absent) (Fig. 39). First metasomal tergite coriaceous, dorsal carina obsolete; second tergite coriaceous (Fig. 41). Ovipositor long, 0.8–0.95 times as long as hind tibia. Second tergite fuscous with yellow posterior band, third tergite mostly yellow with transverse fuscous band in posterior half (Fig. 36).

Material examined. Korea: 1 female, GW, Donghae-si, Samhwa-dong, Mureung Valley, 9–17 August 2005, (J.W. Lee); 1 male, GW, Hongcheon-gun, Hongcheon-eup, Jangjeonpyeong-ri, Geodungae village, 1–14 July 2006, (J.W. Lee); 1 female, CB, Chungju-si, Suanbo-myeon, Samun-ri, Mt. Woraksan, 35°49'46"N, 128°04'05"E, Malaise trap, 17 July–12 August 2013, (J.K. Choi) (YNU).

Distribution. Holarctic; reported in the Eastern Palaearctic from Kamchatka Peninsula, Primorsky Terr., Sakhalin Isl. (Humala 2007) and South Korea (new record).

Discussion

The fauna of Orthocentrinae of the Eastern Palaearctic and Oriental regions has been extremely poorly studied. There are only six known species of orthocentrine in China and four species in Japan (Yu et al. 2012); nine more species, omitted by Yu et al. (2012), were recorded in Japan resulting from the treatment of Russian collections stored at the Zoological Institute RAS (Humala 2007). In the Catalogue of Ichneumonidae of Russian Far East (Kasparyan et al. 2012) there are 28 genera and 110 species of Orthocentrinae *sensu* Humala (including Microleptinae, Cylloceriinae and Diacri-tinae), though the fauna has been insufficiently studied in the region.

Korean orthocentrines are very poorly known. We have been conducting an inventory of this subfamily since 2014. Up to now only two species of Orthocentrinae from the genera *Proclitus* Fö rster, 1869 and *Eusterinx* Fö rster, 1869 were reported from South Korea (Choi et al. 2014). Besides these genera and two genera reviewed in this publication, during preliminary sorting of large orthocentrine collections stored at the Yeungnam University, thirteen more genera have been found to occur in South Korea, namely *Orthocentrus*, *Picrostigeus* Fö rster, *Stenomacrus* Fö rster, *Batakamacrus* Kolarov, *Plectiscus* Gravenhorst, *Neurateles* Ratzeburg, *Apoclima* Fö rster, *Pantisarthrus* Fö rster, *Aperileptus* Fö rster, *Dialipsis* Fö rster, *Plectiscidea* Viereck, *Helictes* Haliday, and *Megastylus* Schiö dte. The consequent treatment of these materials is planned. All listed 17 genera found by us in South Korea are entirely or predominantly Holarctic and many of them are abundant and species-rich within temperate zones of the Palaearctic. Taking into account that the orthocentrine fauna of Japan and China is practically unstudied, the generic composition of the South Korean Orthocentrinae fauna could be compared with that of the Russian Far East, which contains approximately twice as many genera as Korea (eight Palaearctic genera: *Aniseres* Fö rster, *Atabulus* Rossem, *Entypoma* Fö rster, *Fennomacrus* Humala, *Hemiphanes* Fö rster, *Proelictator* Rossem, *Catastenus* Fö rster and *Terminator* Humala are not registered there). Most Korean species also occur in the Russian Far East (Humala 2007, Kasparyan et al. 2012). However some new species in the genera *Megastylus*,

Eusterinx, *Plectiscus* and *Orthocentrus* have been discovered already, and they will be described in our forthcoming papers, devoted to the Korean fauna of the subfamily.

Acknowledgements

We are deeply grateful to Dr Gavin Broad and Dr Andrey Khalaim for reviewing this manuscript. This work was supported by the 2015 Yeungnam University Research Grant and by a grant from the National Institute of Biological Resources (NIBR), funded by the Ministry of Environment (MOE) of the Republic of Korea (NIBR201501203).

References

- Askew RR, Shaw MR (1986) Parasitoid communities: their size, structure and development. In: Waage JK, Greathead D (Eds) *Insect Parasitoids*. Academic Press, London/Orlando, 225–264.
- Aubert JF (1966) Liste d'identification No.6 (présentée par le service d'identification des Entomophages). *Entomophaga* 11(1): 115–134.
- Aubert JF (1968) Révision du genre *Eusterinx* Först. et descriptions d'autres Ichneumonides Microleptinae inédites. *Bulletin de la Société Entomologique de Mulhouse* 1986(Mai-Juin): 37–41.
- Aubert JF (1976) Révision des *Aperileptus* Först. et *Plectiscidea* Vier. (*Plectiscus* auct.) de Förster et de Strobl (Hymenoptera: Ichneumonidae). *Opuscula Zoologica* 138: 1–8.
- Aubert JF (1977) Révision des Ichneumonides *Proclitus* Först., *Pantisarthrus* Först., *Aniseres* Först. et *Helictes* Hal. *Spixiana* 1(2): 141–149.
- Aubert JF (1978) Révision préliminaire des Ichneumonides Orthocentrinae européennes (Hym. Ichneumonidae). *Eos* 52: 7–28.
- Aubert JF (1980) Notes sur diverse Ichneumonides mal connues ou inédites. *Bulletin de la Société Entomologique de Mulhouse*. Janvier-Mars 1: 1–6.
- Aubert JF (1981) Révision des Ichneumonides *Stenomacrus* sensu lato. *Mitteilungen Münchener Entomologischen Gesellschaft* 71: 139–159.
- Broad GR (2004) Generic synonymies affecting the Orthocentrinae (Hym., Ichneumonidae), with notes on the composition of the subfamily. *Entomologist's Monthly Magazine* 1685/1687: 297–300.
- Broad GR (2010) Status of *Batakomacrus* Kolarov (Hymenoptera: Ichneumonidae: Orthocentrinae), with new generic combinations and description of a new species. *Zootaxa* 2394: 51–68.
- Choi JK, Jeong JC, Lee JW (2014) New Korean record of twenty eight species of the family Ichneumonidae (Hymenoptera). *Animal Systematics, Evolution and Diversity* 30(2): 65–80. doi: 10.5635/ASED.2014.30.2.065
- Dasch CE (1992) The Ichneumon-flies of America North of Mexico: Part 12. Subfamilies Microleptinae, Helictinae, Cylloceriinae and Oxytorinae (Hymenoptera: Ichneumonidae). *Memoirs of the American Entomological Institute* 52: 1–470.
- Delobel A, Matile S (1976) Un nouveau Microleptinae (Hym. Ichneumonidae) parasite de *Neoempheria ombrophila*, n.sp. (Dipt. Mycetophilidae) en République Centrafricaine. *Bulletin de l'Institut Fondamental d'Afrique Noire (A)* 37: 385–394.

- Förster A (1869) Synopsis der Familien und Gattungen der Ichneumoniden. Verhandlungen des Naturhistorischen Vereins der Preussischen Rheinlande und Westfalens 25: 135–221.
- Förster A (1871) Übersicht der Gattungen und Arten der Familie der Plectiscoiden. Verhandlungen des Naturhistorischen Vereins der Preussischen Rheinlande und Westfalens 28: 71–123.
- Gauld ID (1984) An introduction to the Ichneumonidae of Australia. Bulletin of the British Museum (Natural History) 895: 1–413.
- Gauld ID (1991) The Ichneumonidae of Costa Rica 1. Memoirs of the American Entomological Institute 47: 1–539.
- Gravenhorst JLC (1829) Ichneumonologia Europaea. Pars III. Vratislaviae, 1097 pp.
- Gupta VK (1988) Relationships of the genera of the Tryphonine tribe Oedemopsini and a revision of *Acaenitellus* Morley. In: Gupta VK (Ed.) Advances in Parasitic Hymenoptera Research. E.J. Brill, Leiden & New York, 243–258.
- Humala AE (2003) The ichneumonid wasps in the fauna of Russia and adjacent countries. Subfamilies Microleptinae and Oxytorinae (Hymenoptera, Ichneumonidae). Nauka, Moscow, 175 pp. [In Russian]
- Humala AE (2007) Subfamily Orthocentrinae. In: Lelej AS (Ed.) Keys to the Insects of the Russian Far East, Vol. 4. Dal'nauka, Vladivostok, 680–718. [In Russian]
- Humala AE, Ruiz-Cancino E, Coronado-Blanco JM (2011) Orthocentrinae (Hymenoptera: Ichneumonidae) nuevos y poco conocidos de México. Memorias 21 y 22 Encuentro Nacional de Investigación Científica y Tecnológica del Golfo de México (May 2011, Tampico, Tamaulipas, México): 196–200.
- Kasparyan DR, Khalaim AI, Tereshkin AM, Humala AE, Proschalykin MYu (2012) 47. Family Ichneumonidae. In: Lelej AS (Ed.) Annotated Catalogue of the insects of Russian Far East. Vol. 1. Hymenoptera. Dal'nauka, Vladivostok, 210–299. [In Russian]
- Latreille PA (1802) Histoire naturelle, générale et particulière, des Crustacés et des Insectes. Tome troisième. Paris, 468 pp. [Ichneumonidae P. 318–327]
- Quicke DLJ, Laurence NM, Fitton MG, Broad GR (2009) A thousand and one wasps: a 28S rDNA and morphological phylogeny of the Ichneumonidae (Insecta: Hymenoptera) with an investigation into alignment parameter space and elision. Journal of Natural History 43(23–24): 1305–1421. doi: 10.1080/00222930902807783
- Roman A (1923) Ichneumonids reared from Diptera Nematocera. Entomologist's Monthly Magazine 59: 71–76.
- Rossem G van (1981) A revision of some Western Palaearctic oxytorine genera, including two new genera *Phosphorus* and *Ephalinator*. Spixiana 4 (Suppl.): 79–135.
- Rossem G van (1983) A revision of Western Palaearctic oxytorine genera. Part IV Genus *Megastylus* (Hymenoptera, Ichneumonidae). Entomofauna 4: 121–132.
- Rossem G van (1987) A revision of Western Palaearctic oxytorine genera. Part VI Genera: *Hemiphanes*; *Oxytorus*; *Apoclima*; *Cylloceria* (new revision); *Proclitus*; *Pantisarthrus*; *Plectiscidea*; *Gnathochorisis*; *Eusterinx* (new revision); *Helictes*; *Phosphoriana* (nomen novum); *Proelictator* and *Megastylus* (Hymenoptera, Ichneumonidae). Tijdschrift voor Entomologie 130: 49–108.
- Rossem G van (1988) A revision of Palaearctic oxytorine genera. Part VII Genera: *Hemiphanes*; *Hyperacmus*; *Entypoma*; *Atabulus* new genus; *Allomacrus*; *Cylloceria*; *Aniseres*; *Proclitus*;

- Plectiscidea*; *Symplecis*; *Eusterinx*; *Megastylus* and *Microleptes* (Microleptinae) (Hymenoptera, Ichneumonidae). Tijdschrift voor Entomologie 131: 103–112.
- Rossem G van (1990) Key to the genera of the Palaearctic Oxytorinae, with the description of three new genera (Hymenoptera, Ichneumonidae). Zoologische Mededelingen 63(23): 309–323.
- Rossem G van (1991) New Oxytorinae from Siberia, with revised keys to *Plectiscidea* Viereck and *Eusterinx* Foerster s. l. (Hymenoptera: Ichneumonidae). Zoologische Mededelingen 65(3): 25–38.
- Schmiedeknecht O (1911) Opuscula Ichneumonologica. Band. IV. Ophioninae. Blankenburg i. Thur., 2161–2271.
- Strand E (1918) Über W. Horn's litauische entomologische Kriegsausbeute 1916 (Schluss.) Hymenoptera. Entomologische Mitteilungen 7: 149–160.
- Thomson CG (1888) Försök till gruppering af släktet *Plectiscus* (Grav.). Opuscula Entomologica, Lundensis 12: 1266–1318.
- Townes HK (1971) The genera of Ichneumonidae, Part 4. Memoirs of the American Entomological Institute 17: 1–372.
- Uchida T (1930) Vierter Beitrag zur Ichneumoniden-Fauna Japans. Journal of the Faculty of Agriculture, Hokkaido University 25: 243–298.
- Uchida T (1942) Ichneumoniden Mandschukuos aus dem entomologischen Museum der kaiserlichen Hokkaido Universitaet. Insecta Matsumurana 16: 107–146.
- Veijalainen A, Wahlberg N, Broad GR, Erwin TL, Longino JT, Sääksjärvi IE (2012) Unprecedented ichneumonid parasitoid wasp diversity in tropical forests. Proceedings of the Royal Society of London, Series B (Biological Sciences) 279: 4694–4698. doi: 10.1098/rspb.2012.1664
- Veijalainen A, Broad GR, Sääksjärvi IE (2014) Twenty seven new species of *Orthocentrus* (Hymenoptera: Ichneumonidae; Orthocentrinae) with a key to the Neotropical species of the genus. Zootaxa 3768(3): 201–252. doi: 10.11646/zootaxa.3768.3.1
- Wahl DB (1986) Larval structures of oxytorines and their significance for the higher classification of some Ichneumonidae (Hymenoptera). Systematic Entomology 11(1): 117–127. doi: 10.1111/j.1365-3113.1986.tb00171.x
- Wahl DB (1990) A review of the mature larvae of Diplazontinae, with notes on larvae of Acaenitinae and Orthocentrinae and proposal of two new subfamilies (Insecta: Hymenoptera, Ichneumonidae). Journal of Natural History 24(1): 27–52. doi: 10.1080/00222939000770041
- Wahl DB, Gauld ID (1998) The cladistics and higher classification of the Pimpliformes (Hymenoptera: Ichneumonidae). Systematic Entomology 23(3): 265–298. doi: 10.1046/j.1365-3113.1998.00057.x
- Yu DSK, van Achterberg C, Horstmann K (2012) Taxapad 2012, Ichneumonoidea 2011. Database on flash-drive. Ottawa, Ontario, Canada.
- Zwakhals CJ, Diller E (2015) Eight new *Orthocentrus* species from South America (Hymenoptera; Ichneumonidae, Orthocentrinae). Mitteilungen der Münchner Entomologischen Gesellschaft 105: 65–78.

The Knight and the King: two new species of giant bent-toed gecko (*Cyrtodactylus*, Gekkonidae, Squamata) from northern New Guinea, with comments on endemism in the North Papuan Mountains

Paul M. Oliver^{1,2}, Stephen J. Richards³, Mumpuni⁴, Herbert Rösler⁵

1 Division of Evolution, Ecology & Genetics, Research School of Biology, The Australian National University, Canberra, ACT 0200, Australia **2** Department of Zoology, University of Melbourne, Parkville, Victoria 3052, Australia, and Department of Sciences, Museum Victoria, GPO Box 666, Melbourne, Victoria, Australia **3** South Australian Museum, Adelaide, South Australia 5000, Australia **4** Herpetology Division, Museum Zoologicum Bogoriense, Research Center for Biology, Indonesian Institute of Sciences (LIPI), Indonesia **5** Senckenberg Naturhistorische Sammlungen Dresden, Museum für Tierkunde, Dresden, Germany

Corresponding author: Paul M. Oliver (paul.oliver@anu.edu.au)

Academic editor: A. Bauer | Received 22 May 2015 | Accepted 6 November 2015 | Published 10 February 2016

<http://zoobank.org/8879EE2C-19F1-40BF-876C-B9FF656D9B7C>

Citation: Oliver PM, Richards SJ, Mumpuni, Rösler H (2016) The Knight and the King: two new species of giant bent-toed gecko (*Cyrtodactylus*, Gekkonidae, Squamata) from northern New Guinea, with comments on endemism in the North Papuan Mountains. ZooKeys 562: 105–130. doi: 10.3897/zookeys.562.6052

Abstract

The diverse biota of New Guinea includes many nominally widespread species that actually comprise multiple deeply divergent lineages with more localised histories of evolution. Here we investigate the systematics of the very large geckos of the *Cyrtodactylus novaeguinae* complex using molecular and morphological data. These data reveal two widespread and divergent lineages that can be distinguished from each other, and from type material of *Cyrtodactylus novaeguinae*, by aspects of size, build, coloration and male scalation. On the basis of these differences we describe two new species. Both have wide distributions that overlap extensively in the foothill forests of the North Papuan Mountains, however one is seemingly restricted to hill and lower montane forests on the ranges themselves, while the other is more widespread throughout the surrounding lowlands. The taxon endemic to the North Papuan Mountains is related to an apparently lowland form currently known only from Waigeo and Batanta Island far to the west – hinting at a history on island arcs that accreted to form the North Papuan Mountains.

Keywords

Arc accretion, Endemism, Indonesia, lizard, orogeny, Papua New Guinea, Papua Province, Sepik Basin

Introduction

Integrated morphological and molecular investigations of the exceptionally diverse biota of New Guinea are confirming that many nominally widespread species comprise multiple deeply divergent lineages (Donnellan and Aplin 1989; Oliver et al. 2013; Georges et al. 2014). In turn, as estimates of lineage diversity and phylogenetic relationships improve, so too does our understanding of patterns of regional and elevational endemism and turnover, and the processes that have shaped them – most notably the complex geological history and extreme topography of New Guinea (Unmack et al. 2013; Toussiant et al. 2014).

The Bent-toed geckos (*Cyrtodactylus*) are the most species-rich radiation of geckos in the world (Wood et al. 2012; Uetz 2015). *Cyrtodactylus* diversity is concentrated in Indochina, South-east Asia and the Greater Sunda islands, however the clade extends from India and Sri Lanka in the west, the Himalayas in the north, through south-east Asia to the Philippines, Lesser Sundas, New Guinea and into northern Australia (Wood et al. 2012). Within the south-eastern region of this distribution New Guinea and surrounding islands are a centre of diversity, with an endemic radiation of at least 25 species, a majority of which have only been recognised in the last decade (Kraus and Allison 2006; Kraus 2007, 2008; Rösler et al. 2007; Oliver et al. 2008, 2009, 2012; Oliver and Richards 2012). Recent work has also indicated that the main Papuan lineage has evolved in at least one novel direction – it includes several lineages that are significantly larger than other *Cyrtodactylus* (SVL > 160 mm) (Zweifel 1980; Kraus 2007, 2008; Oliver et al. 2008; Bauer 2013; Oliver et al. 2014).

Cyrtodactylus novaeguineae Schlegel (1837) is the largest of these giant *Cyrtodactylus*, with a maximum recorded snout-vent length in excess of 170 mm (Zweifel 1980; Bauer 2013). While the type locality of *Cyrtodactylus novaeguineae* is in the Triton Bay area (now in Papua Barat Province) on the southern edge of the ‘Bird’s Neck’ in western New Guinea (Schlegel 1837), specimens from a wide range of localities both north and south of New Guinea’s Central Cordillera are currently assigned to this species (Brongesma 1934; Zweifel 1980; Kraus 2008) – generally on the basis that they possess enlarged tubercles extending onto and often across the posterior region of the throat (Zweifel 1980; Rosler et al. 2007; Kraus 2008).

Here we present an analysis of genetic and morphological variation within geckos referred to *Cyrtodactylus novaeguineae* from across New Guinea (with a focus on the much better sampled eastern half of the island). These data reveal two genetically and morphologically distinct lineages in northern New Guinea that are not conspecific with this nominal taxon - and which we therefore describe as new taxa. We also review the biogeography of these geckos in the context of recent phylogenetic investigations into the role that orogeny and arc accretion has played in shaping the biota of northern New Guinea.

Materials and methods

Sampling

DNA sequence data was amplified from tissues subsampled from frozen or ethanol collections lodged at the Australian Biological Tissue Collection (ABTC) in the South Australian Museum, the Museum Zoologicum Bogoriense (MZB), and the Bernice P. Bishop Museum (BPBM) (Appendix 1). Comparative material was examined at the following institutions: American Museum of Natural History (AMNH) – New York, Australian Museum (AMS) – Sydney, Bernice P. Bishop Museum (BPBM) – Honolulu, Museum of Comparative Zoology (MCZ) – Harvard University, Cambridge, Museum Zoologicum Bogoriense (MZB) – Bogor, and South Australian Museum (SAMA) – Adelaide (Appendix 2).

Genetics

Sequence data from the NADH dehydrogenase subunit 2 (*ND2*) for 13 nominal *C. novaeguineae* were aligned with a subset of Papuan *Cyrtodactylus* sequence data published elsewhere, and chosen to include all potential close relatives (Oliver et al. 2012). GenBank accession numbers and associated specimen data for newly amplified material are given in Appendix 2. Laboratory protocols largely followed Siström et al. (2009). *ND2* and partial flanking tRNAs were amplified using the primers M112F (5'- AAGCTTTCGGGGCCCATACC-3') and M1123R (5'- GCTTAATTAAAGT-GTYTGAGTTGC -3') designed in the flanking Methionine and Alanine tRNAs.

Our final alignment included up to 987 bp of data and was aligned using the MUSCLE algorithm (Edgar 2004) in Geneious version 6.0.5 (Biomatters 2012), and subsequently checked by eye. Phylogenetic trees were estimated using standard maximum Likelihood (RAxML v7.2.8; Stamatakis 2006) analyses implemented on the CIPRES web portal version 3.1 for online phylogenetic analysis (www.phylo.org/portal2). Data were not partitioned by codon (first, second and third base positions) and analyses were run using the default settings for RAxML on the CIPRES portal - the GTRGAMMA model of sequence evolution and ceasing bootstrapping when MRE-bootstrapping criteria had been reached.

Morphology

Measurements taken with digital calipers to the nearest 0.1 mm largely follow Kraus (2006): snout-vent length (SVL), tail length (from the posterior edge of the vent to the tip of the tail) (TL), total length of original portion of tail (OT), trunk length from posterior edge of axilla to anterior edge of groin with limbs held at right angles (TrK), maximum head width (HW), maximum head height (HH), head length from

tip of snout to anterior margin of ear opening (HL), distance from posterior edge of naris to eye (EN) (used as a proxy for snout-length), transverse diameter of eye (EYE), internarial distance (IN), transverse diameter of ear (EAR), forearm length from base of palm to outer edge of elbow (FA), and crus length from base of heel to outer edge of knee (CS).

We counted left and right enlarged supralabials to both the midpoint of the eye and to the rictus, left and right infralabials to rictus, dorsal tubercle rows between the lateral folds (not including the lateral fold) at the midpoint of body, ventrals at midpoint of the body in transverse series between ventral folds, the number of narrow lamellae distal to the inflection of the digit (not including the claw sheath), the number of wide subdigital lamellae proximal to the inflection of the joint under the first and fourth digits of the left manus and pes, precloacal and femoral pores where present, and postcloacal tubercles. Finally, we also recorded the extent of large tubercles on the lower jaw: absent, extending to the infra-angular region only, or extending across the throat.

Results

Genetics

We identify three major mitochondrial lineages of '*C. novaeguineae*': 'south' – from three sites to the south of the Central Cordillera in Western and Gulf Provinces of Papua New Guinea; 'north 1' – North Papuan Mountains (Foja, Bewani and Torricelli Mountains); and 'north 2' – northern lowlands and foothills of Papua New Guinea from close to the Indonesian border in Sandaun Province east as far as Morobe Province. A clade comprising 'north 1', 'south', and *Cyrtodactylus zugi* from Batanta Island off the western coast of New Guinea is strongly supported. Within this clade there is strong support for the close relationship of *C. zugi* and 'north 1' (Figure 1). The 'north 2' lineage is more divergent, but a clade comprising all members of the *novaeguineae* group and its inferred closest relative *Cyrtodactylus mimikanus* (see Oliver et al. 2012) is supported. Mean levels of *ND2* sequence divergence between these four clades calculated using the Jukes Cantor Model ranges from (13.6–15.7%). There is evidence of additional mitochondrial structure in 'north 1' (mean 4.9%, max 7.5%) and 'north 2' (mean 4.7%, max 8.1%), but low diversity between samples of 'south' (mean 0.01%, max 0.01%).

Morphology

Each of the three genetic lineages shows consistent differences in colour pattern, body size and aspects of scalation (see further details in Table 1, Figures 2–5, and comparisons below). The 'south' lineage is characterised by smaller size, narrow head (Figure 2), low number of ventral scales in transverse series, higher number of and darker and

unbroken dorsal bands (Figure 3), plain venter and unbroken pore series in males. The ‘north 1’ lineage is of intermediate size, has a broad head (Figure 2), higher number of ventral scales, a dorsal colour pattern consisting of three relatively indistinct light brown transverse bands or patches on a light greyish brown background (Figure 4), a relatively plain venter with at most scattered small dark brown maculations, and a widely broken pore series in males. Finally, ‘north 2’ is distinctly larger, has a broad head (Figure 2), high number of ventral scales, a ‘messier’ three toned dorsal colour pattern comprising alternating but indistinctly defined regions of dark brown, medium grey and light grey to dirty off white (Figure 5), extensive amounts of dark-brown barring underneath the throat (Figure 2) and often also on the ventral surfaces of the body, and a generally continuous pore series in the males.

Systematics

Concordant patterns of genetic and morphological variation indicate that at least three evolutionarily distinct lineages (species) have been confounded within *Cyrtodactylus novaeguineae*. No genetic samples are available from the vicinity of the type locality so determining which, if any, of these populations represents true *C. novaeguineae* relies on comparisons of morphology. The two male syntypes of *C. novaeguineae* (RENA (formerly RMNH) 2708A–B) are of relatively small size (SVL 115 and 129 mm) with narrow heads (HW/SVL 0.18 and 0.19), and continuous to near-continuous pore series (divided only by one or two medial scales). This combination of morphological characters clearly distinguishes the types from both of the ‘north’ lineages, but does not distinguish them from the lineage we refer to here as ‘south’.

A colour plate accompanying the description of *C. novaeguineae* (Schlegel, 1834) – presumably of one of the syntypes although this is not clear – shows three continuous and clearly defined brown dorsal bands (Figure 6). Recently collected specimens of ‘south’ also have strong dorsal bands, but usually have four instead of three. Unfortunately the colour patterns illustrated by Schlegel are no longer evident on the types and Schlegel does not report whether the non-illustrated material had a different number of dorsal bands. Nearly one thousand kilometres separates the type locality of *C. novaeguineae* from the nearest locality for genetically typed ‘south’ lineage. Brongersma (1934) lists additional samples from southern New Guinea, especially from around the Lorentz River, however there are again few recent collections from this area and none with matching tissue samples. Given the limited morphological divergence between material from ‘south’ populations and the types of *C. novaeguineae*, and the lack of genetic and colour pattern data for the population from the type locality, we conservatively consider the ‘south’ population to represent easternmost populations of *C. novaeguineae* at this stage.

The populations from southern New Guinea that we here refer to *C. novaeguineae* can be distinguished from other Papuan *Cyrtodactylus* by the following unique combination of characters – moderately large size (SVL to 129 mm), narrow head (HW/SVL

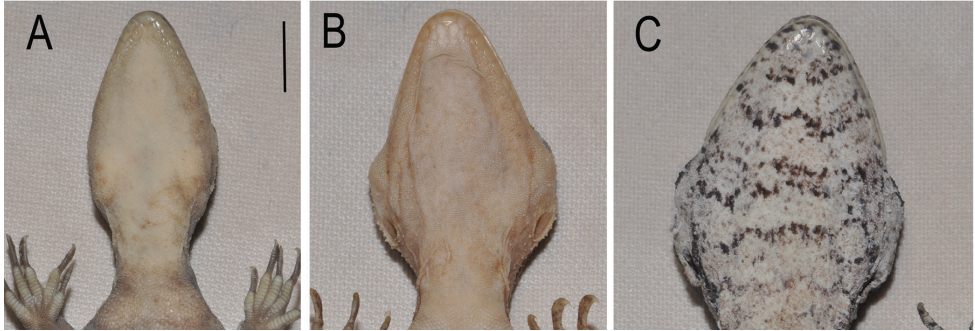


Figure 2. Throats of *Cyrtodactylus novaeguineae* and related species. **A** *Cyrtodactylus novaeguineae* (SJR10490/SAMA R66156) **B** *Cyrtodactylus equestris* sp. n. SJR6134/MZB lace 5436 (paratype), and **C** *Cyrtodactylus rex* sp. n. Scale bar = 1 cm. Note variation in relative width and colouration.



Figure 3. Genotyped *Cyrtodactylus novaeguineae* from southern slopes of the Central Cordillera of New Guinea. Photograph S. Richards.

0.18–0.19), enlarged tubercles on the infra-angular region and often extending across the posterior region of the throat, mid dorsal tubercles in 21 to 22 rows at midpoint of body, subcaudal scales not transversely widened, moderate number of mid-body ventral scales (31–44) and a continuous or near-continuous, relatively straight, row of femoral and preloacal pores in adult males (up to at least 43 pores in total).

The two northern forms ('north 1' and 'north 2') differ from *C. novaeguineae* from southern New Guinea (including the types) in having broader heads and in being of slightly to much larger size (Figure 2). The 'north 1' lineage also has a discontinuous series of femoral and preloacal pores divided by one or two regions of poreless scales. We consider that these characters, coupled with substantial genetic divergence be-

tween the northern lineages and southern *C. novaeguineae*, and between ‘north 1’ and ‘north 2’ are sufficient to differentiate these two lineages and we present their formal descriptions below.

***Cyrtodactylus equestris* sp. n.**

<http://zoobank.org/EF29B95D-5C28-4A26-B6BF-D9A566E79996>

Figures 2, 4

Holotype. AMS R135520 adult male with everted left hemipenis and completely re-grown tail, Papua New Guinea, Sandaun Province, Torricelli Mountains, Mt. Sumbau (3°23'S, 142°31'E, between 1000–1200 m a.s.l.), collected by P. German, 10 March 1990, with frozen tissue at the South Australian Museum (ABTC50282).

Paratypes (n = 6). Papua New Guinea: AMS R119547 Sandaun Province, Torricelli Mtns, Wigote (3°25'S, 142°09'E), collected by T. Flannery, 20 July 1985; BPBM 23314–16 Sandaun Province, Torricelli Mountains, between 2.9–3.2 km east of Mt Sapau summit (3°23'27.0636"S, 142°31'47.028"E, 550–700 m a.s.l.), collected by F. Kraus between 23–25 May 2005. Indonesia: MZB lace 5435–6 Papua Province, Foja Mountains, camp above Marina Valen Village (02°22.230'S, 138°12.753'E; 500 m a.s.l.), collected by S. Richards and B. Tjaturadi between 17–22 July 2004.

Referred material (n = 5). Papua New Guinea: AMNH 100050–1, Sandaun Province, Lumi (~530 m a.s.l.), collected by M. Lorenz; AMNH 100052 Sandaun Province, Mt Menawa, Bewani Mountains, collected by J. Diamond; AMNH 82360 Madang Province, Adelbert Mountains, Maratambu (~700 m a.s.l.), collected by E.T. Gillard; AMNH 103193 Madang Province, Adelbert Mountains, Wanuma (~700 m a.s.l.), collected by A.C. Zeigler. The last two specimens are listed as referred material because of taxonomic uncertainty (see below), while the remainder are relatively poor specimens.

Diagnosis. A large *Cyrtodactylus* (SVL to 139 mm), with a moderately broad head (HW/SVL 0.19–0.22), enlarged tubercles on the infra-angular region and often extending across the posterior throat, mid-dorsal tubercles in 19 to 25 rows at midpoint of body, subcaudal scales not transversely widened, high number of mid-body ventral scale rows (42–59), femoral pores in two separated rows of 9–19, usually with a further medial preloacal row of 6–13 pores (up to 39 pores in total), venter relatively plain brown with at most scattered darker brown maculations, and dorsum with three distinct to indistinct medium-brown transverse bands on relatively plain light brownish-grey background.

Description of holotype. A moderately large (113 mm SVL) and slender gecko. Head large (HL/SVL 0.28), moderately wide (HW/SVL 0.21) and clearly distinct from neck. Snout rounded in dorsal profile, broadly truncate in lateral profile, eye to naris distance longer than eye diameter (EN/EYE 1.4), loreal region slightly inflated, interorbital region and top of snout concave, canthus rostralis rounded, weakly defined. Eyes large (EYE/HL 0.26), pupil vertical, supraciliaries extending from anter-



Figure 4. *Cyrtodactylus equestris* sp. n. in life. Paratype MZB lace 5435 from near Marina Valen Village, Papua Province, Indonesia. Photograph S. Richards.

oventral to posterodorsal edge of orbit, longest at the anterodorsal corner. Ear opening rounded, bordered by distinct dorsal skin fold.

Rostral rectangular, wider than high, with medial suture extending approximately halfway from dorsal edge towards ventral edge, bordered dorsally by two flattened nasals and single tiny internasal. Nares bordered by first supralabial (point contact), rostral, nasal, 2–3 enlarged postnasals and 2–3 tiny granular postnasals. Supralabials generally wider than high, 10 on right, 11 on left, 8 to midpoint of eye. Head, temporal and nuchal scales small and granular, interspersed with numerous enlarged weakly conical tubercles, approximately 3–4 times width of surrounding scales, on temporal and posterior nuchal regions. Enlarged infralabials slightly to much wider than high, 11 on right and 10 on left, bordered by rows of slightly enlarged scales that grade into small granular gular scales. Mental slightly wider than long, broadly triangular, but with distinctly concave edges at contact with postmentals, in contact with first infralabials. Scattered small conical tubercles (approximately twice size of surrounding scales) in the infra-angular regions of the lower jaw only.

Body moderately robust (TrK/SVL 0.44) with distinct ventrolateral folds. Moderately tuberculate, tubercles along lateral fold heterogeneous, up to 3 times larger than surrounding scales. Dorsum with approximately 23 rows (not including lateral fold) of often keeled tubercles up to 4 times width of surrounding granular scales. Ventral scales much larger than dorsal scales, increasing in size medially, arranged in approximately 39 rows at midpoint of body. Several continuous rows of enlarged femoral scales, posterior row extending almost to knee, distinctly larger and contrasting against granular posterior femorals. Precloacal pores in a series of 8, femoral pores in individual series of 15–16, respective series separated by 7 poreless scales.

Limbs moderately robust, forelimbs (FA/SVL 0.14) shorter and less robust than hindlimbs (CS/SVL 0.19). Lateral and dorsal surfaces of antebrachium and crus with numerous conical tubercles. Digits long and well developed, inflected at basal interphalangeal joints; subdigital lamellae smooth, rounded and expanded proximal to digital inflection (8-12-11-13-11 manus; 9-12-15-15-13 pes); narrow distal to digital inflection (9-10-11-11-11 manus; 7-12-12-14-13 pes) (counts not including ventral claw sheath); large recurved claws sheathed by a dorsal and ventral scale.

Tail almost completely regrown, scalation heterogeneous and irregular. Cloacal sacs swollen and prominent, each with 3 rounded cloacal spurs at anterior edge.

Measurements of holotype (in mm). SVL 113, TL 97, OT 13, TrK 49.5, HW 23.4, HH 13.1, HL 32.2, EN 11.6, IN 4.2, EYE 8.3, EAR 2.0, FA 15.3, CS 21.5.

Color in ethanol. Dorsal pattern consisting of alternating light brown and medium brown regions. Nuchal band medium brown, posterior edge triangular with thin continuous dark brown margin and extending along dorsum to level of forelimb insertion, anterior edge deeply notched and less clearly margined. Nuchal dark band bordered posteriorly by a deeply notched light brown band with distinct thin dark brown edging on medial anterior and posterior edges, and extending anteriorly onto lower jaw. Subsequent dark bands not deeply notched and less distinctly margined, but generally with at least some dark brown edging at their midpoint. Dorsal surface

of head medium brown, darker anteriorly, without pattern, with the exception of a pair of small curved dark brown lines on the nape. Lower lateral region of head whitish brown, strongly demarcated against upper lateral and dorsal brown colouration. Ventral colouration dirty brown with scattered darker brown maculations on the throat and across the venter. Limbs medium brown dorsally, slightly lighter ventrally, largely unpatterned except for scattered dark maculations and very small blotches on the hindlimbs. Stub of original tail medium brown dorsally with a pair of smeared very dark brown markings. Regrown tail plain light brown on all surfaces.

Variation. The type series includes 4 adult males (with fully expressed pore series) varying from 113–129 mm SVL, two adult females both of 139 mm, and one juvenile male of 104 mm. Mensural data for the type series are summarized in Table 2. Supralabials to center of eye 8–10, to rictus of jaw 11–15, Infralabials 10–13. Fourth toe wide lamellae 11–13, fourth toe narrow lamellae 11–13, mid-belly scale rows 39–59, and maximum number of dorsal tubercle rows 19–23. Cloacal spurs 3–4, expressed pre-cloacal pores from 6–8, femoral pore series from 8–15, total number of pores 24–35.

Dorsum generally with alternating transverse regions of light and medium brown, however the width and distinctiveness of these region varies. Some variation in the intensity of colouration may be ontogenetic. On the largest specimens the medium brown regions are relatively narrow, and not or only weakly defined by dark brown edging, giving the overall impression of a somewhat faded pattern. On smaller specimens the transverse bands are more distinct and strongly defined. An indistinct trace of medium brown mottling or barring is also sometimes apparent on the dorsal and lateral surfaces of the hindlimbs. Venter medium to light brown, sometimes with very scattered darker brown maculations. Original tails with alternating medium-brown dorsal blotches and light-brown to creamish regions, border between colours often sharply defined by dark-brown edging. Regrown tails creamish or light brown with at most a few very indistinct light brownish streaks and patches. Iris in life deep chestnut brown with dark brown vermiculations (Figure 4).

Comparisons. *Cyrtodactylus equestris* sp. n. can be distinguished from most other *Cyrtodactylus* by its large size (males to 129 mm, females to 139 mm), including all species from west of Lydekker's Line (maximum size <130 mm). It can be differentiated from the other large Papuan taxa as follows. *Cyrtodactylus equestris* sp. n. differs from *Cyrtodactylus lorae* and *Cyrtodactylus serratus* in having enlarged tubercles on the infra-angular region and often extending across the throat (vs. absent), a lower number of pores (up to 39 vs. up to 81) in a discontinuous series (vs. continuous), and in lacking enlarged tubercles extending the length of the tail (vs. *C. serratus* only). *Cyrtodactylus equestris* sp. n. differs from members of the *C. lousiadensis* group (*C. epiroticus*, *C. klugei*, *C. lousiadensis*, *C. murua*, *C. robustus*, *C. salomonensis* and *C. tripartitus*) in its smaller subcaudal scales, in having tubercles on the infra-angular region and throat, and in its more poorly defined light-brown bands or blotches on the dorsum (vs. strongly defined and unbroken transverse brown banding). *Cyrtodactylus equestris* sp. n. differs from *C. zugii* in its smaller size (139 vs. 159 mm SVL), more extensive tuberculation that usually extends across the throat (vs. on infra-angular region only), and dorsal

Table 2. Measurements for the type series of *Cyrtodactylus equestris* sp. n.

| | AMS R135520 | BPBM 23314 | BPBM 23316 | BPBM 23315 | MZB lace 5436 | MZB lace 5435 | AMS R119547 |
|-----|-------------|------------|------------|------------|---------------|---------------|-------------|
| Sex | m | m | M | m | f | f | juv |
| SVL | 113 | 129 | 129 | 125 | 139 | 139 | 104 |
| TL | 97 | 148 | 104 | 151 | 119 | 129 | 135 |
| OT | 13 | 148 | 18 | 151 | 22 | 69 | 135 |
| TrK | 49.5 | 57.7 | 57.1 | 56.7 | 60.8 | 61.0 | 51.3 |
| HW | 23.4 | 26.5 | 26.8 | 24.4 | 26.8 | 29.7 | 20.6 |
| HH | 13.1 | 14.2 | 15.0 | 13.9 | 16.1 | 17.1 | 13.1 |
| HL | 32.2 | 34.1 | 35.3 | 32.7 | 34.8 | 39.1 | 27.6 |
| EN | 11.6 | 12.4 | 13.1 | 11.6 | 11.4 | 4.5 | 10.4 |
| IN | 4.2 | 5.2 | 5.1 | 4.7 | 4.8 | 5.1 | 3.7 |
| EYE | 8.3 | 7.7 | 7.9 | 8.1 | 7.8 | 8.7 | 7.7 |
| EAR | 2.0 | 1.8 | 1.1 | 1.7 | 2.1 | 1.7 | 1.7 |
| FA | 15.3 | 19.5 | 19.7 | 19.1 | 20.0 | 19.9 | 14.9 |
| CS | 21.5 | 22.1 | 23.1 | 22.2 | 23.0 | 25.5 | 18.7 |

colour pattern on torso consisting of light-brown transverse bands on a plain greyish-brown background (vs. alternating dark brown blotches on a mottled dark-grey and off-white background). *Cyrtodactylus equestris* sp. n. differs from *C. irianjayaensis* by its smaller size (139 vs. 163 mm SVL), the presence of enlarged tubercles usually extending across the throat (vs. infra-angular region only) and its higher number of femoral and preloacal pores (24–39 vs. 7–16). *Cyrtodactylus equestris* sp. n. differs from other populations of *Cyrtodactylus* here referred to *C. novaeguineae* (both syntypes and genotyped material) in its wider head (HW/SVL 0.19–0.23 vs. 0.18–0.19), larger size (SVL 139.0 vs. 129.0) and tripartite femoral and preloacal pore arrangement (vs. continuous or at most one poreless intervening scales).

Distribution and natural history. Known from scattered localities in the Foja, Torricelli and possibly the Adelbert Ranges (see below) of northern New Guinea (Figure 7). Specimens for which detailed information is available were collected in relatively undisturbed hill or lower montane forest between 500–1200 m a.s.l.

Etymology. *Equestris* latin for knight, in reference to the relative size of this species – large for the genus, but still subordinate to some of its near relatives.

Comments. The referred material include two specimens in the American Museum of Natural History (AMNH 82360, AMNH 103193) from separate localities in the Adelbert Ranges, Morobe Province. These specimens have plain venters and two-toned brown and light brown dorsal colouration. On this basis they do not conform with ‘north 2’ (the only other member of the *C. novaeguineae* complex from northern New Guinea) and are tentatively assigned to *Cyrtodactylus equestris* sp. n. However these localities are separated from the other localities in the North Papuan Mountains by the low swampy country around the Sepik River, and the single male from this region has a bipartite pore arrangement (vs. clearly tripartite). Fresh material and genetic samples are required to confirm the taxonomic status of these easternmost populations.

***Cyrtodactylus rex* sp. n.**

<http://zoobank.org/10AED2AF-65E2-43FF-ACE8-A3A29AF6B9E7>

Figures 2, 5

Holotype. SAMA R67636 (Field number SJR13190), Papua New Guinea, East Sepik Province, un-named camp in Sepik River basin, (4°24'14"S, 142°17'33"E, 55 m a.s.l.), adult female, collected by S. Richards, 1 March 2011, tissue stored in ethanol at the South Australian Museum ABTC114693.

Paratypes (n = 19). Papua New Guinea: SAMA R67637 (SJR13011) Sandaun Province, Sepik River Basin, un-named camp (4°43'39"S, 141°47'08"E, 425 m a.s.l.), collected by S. Richards on 20 February 2010; BPBM 11522 Morobe Province, Oomsis Forestry Camp (6°41'54.1278"S, 146°48'56.412"E, 400 m a.s.l.), collected by A. Allison 3 March 1988; BPBM 18655 Morobe Province, 8.4 km W of Mt Shungol summit (6°47'40.56"S, 146°40'49.98"E, 420 m a.s.l.), collected by F. Kraus 23 October 2003; BPBM 34719 Madang Province, Samorek village (4°42'38.0412"S,



Figure 5. *Cyrtodactylus rex* sp. n. in life. **A** adult female holotype SAMA R67636 from the Sepik River Basin, East Sepik Province **B** juvenile paratype SAMA R67637 from Sepik River Basin, Sandaun Province. Photographs S. Richards.



Figure 6. Reproduction of plate of *Cyrtodactylus novaeguineae* from the original description (plate published in 1844, several years after original description of 1837).

145°24'51.3714"E, 690 m a.s.l.), collected by F. Kraus 1 October 2009; BPBM 34747 East Sepik Province, Joromba River, 16.25 km W of Wewak (3°34.732'S, 143°30.020'E, 227 m a.s.l.), collected by F. Kraus 25 September 2009; AMS R13025 Morobe Province, Lae (6°44'S, 147°00'E), collected by E.L. Troughton 18 May 1945; AMS R31940 Morobe Province, Lae Botanic Gardens (6°44'S, 147°00'E), collected by E.L. Troughton 5 September 1969; AMS R129290 East Sepik Province, Maprik (3°25'S, 143°02'E), collected by W.H. Ewers 5 November 1964; AMS R119548–50 Sandaun Province, Torricelli Mts, Wigote (3°39'S, 142°09'E), collected by T. Flannery 22 July 1985; AMNH 92341–2 Morobe Province, Oomsis Creek (6°41'S, 146°48'E), collected by H.M. Van Deusen April 1959; AMNH 95165–8 Morobe Province, Lae (6°44'S, 147°00'E); AMNH 95169 Morobe Province, Busu River, 8 mi. N of Lae; AMNH 95170 Morobe Province, 13 mi. N of Lae, previous six specimens collected by R. Zweifel & G. Sluder July–August 1964.

Referred material (n = 7). Papua New Guinea. AMNH 95171 East Sepik Province, Maprik (3°38'S, 143°03'E); AMNH 100048–9 Sandaun Province, Lumi (3°28'S, 142°02'E); AMNH 104871 Madang Province, Alexishafen (5°05'S, 145°48'E); AMNH 103194 Madang Province, Kaibugu (4°54'S, 144°57'E); MCZ 142462 Madang Province, 4 mi. S Madang; MCZ 96201 Morobe Province, Morobe town (7°45'S, 147°36'E).

Diagnosis. A very large *Cyrtodactylus* (SVL to 172 mm), with a very broad head (HW/SVL 0.20–0.24), enlarged tubercles across the infra-angular region and often extending across the throat, mid-dorsal tubercles in 21 to 27 rows at midpoint of body, subcaudal scales not transversely widened, high number of mid-body ventral scales in transverse series (49–60), moderate number of femoral and preloacal pores (20–38) in

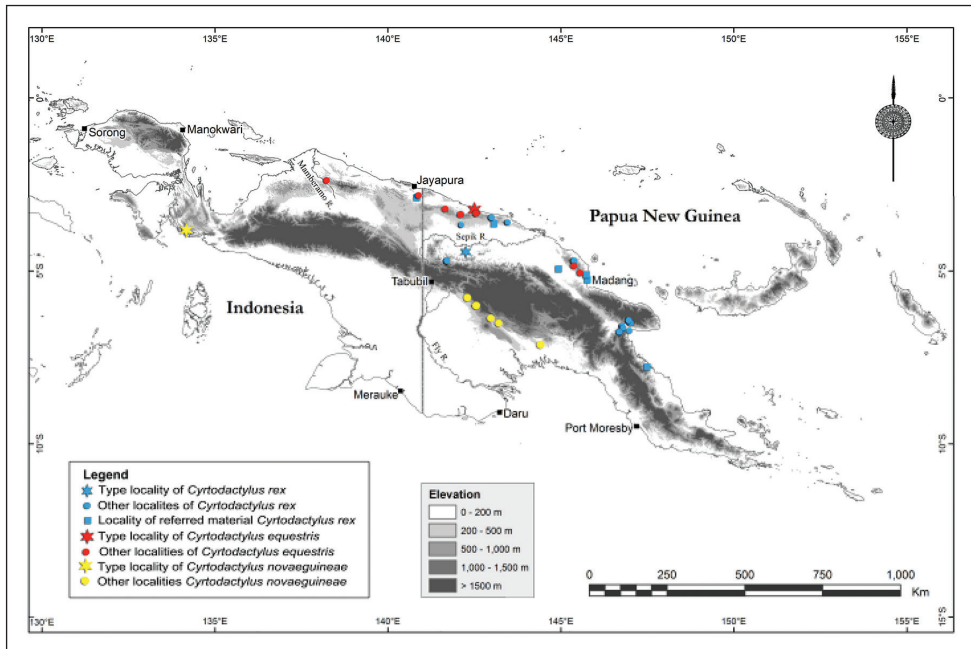


Figure 7. Distribution map for *Cyrtodactylus novaeguineae*, *Cyrtodactylus equestris* sp. n. and *Cyrtodactylus rex* sp. n.

a nearly continuous chevron, narrow dark brown barring on the throat, labials and often venter, and dorsal colour pattern on torso including indistinctly defined alternating dark-brown, medium-brown and whitish regions.

Description of holotype. A very large (169 mm SVL) and robust gecko. Head very large (HL/SVL 0.27), very wide (HW/SVL 0.23) and clearly distinct from neck. Snout longer than eye diameter, eye to naris distance longer than the eye (EN/EYE 1.4), curved in dorsal profile, broadly truncate in lateral profile, mid-loreal region slightly inflated, interorbital region and top of snout slightly concave, canthus rostralis weakly defined. Oval patch of skin missing from top of snout. Eyes large (EYE/HL 0.24), pupil vertical, supraciliaries extending from anteroventral to posterodorsal edge of orbit, longest at the anterodorsal edge. Ear opening roughly circular, bordered by distinct dorsal skin fold.

Rostral broadly rectangular, approximately 1.5 times wider than high with medial suture extending approximately 60% from dorsal edge towards ventral edge, bordered dorsally by two nasals and three smaller internasals. Nares bordered by first supralabial (point contact), rostral, nasal, and series of five to eight granular postnasals. Supralabials generally slightly wider than high, 13 right, 14 left, 10 to midpoint of eye. Head, temporal and nuchal scales small and granular with conical tubercles approximately 2–3 times width of surrounding scales densely distributed across the temporal and nuchal regions. Enlarged infralabials to rictus 14 right, 13 left, anterior infralabials higher than wide, posterior infralabials wider than high,

infralabials bordered by rows of enlarged scales that grade into small granular gular scales. Mental triangular, approximately as wide as long, bordered by first infralabials and two pentagonal postmentals. Numerous wide flat tubercles present across posterior region of throat.

Body robust (TrK/SVL 0.43) with distinct ventrolateral folds. Skin heavily tuberculate dorsally and laterally, 33–34 prominent enlarged tubercles along lateral folds, dorsum with up to 23 rows (not including lateral fold) of enlarged conical tubercles up to four times width of surrounding small and granular scales. Ventral scales larger than dorsal scales, increasing in size medially, arranged in approximately 54 rows at mid-point of body, one or two poorly defined rows of enlarged ventral tubercles present just inferior to the lateral fold. Enlarged precloacal and femoral scales in three rows, posterior row longest (47 scales) and extending laterally approximately two thirds length of femur, medial scales distinctly larger.

Limbs robust, forelimbs shorter (FA/SVL 0.15) and less robust than hindlimbs (CS/SVL 0.17). Lateral and dorsal surfaces of hindlimbs with numerous enlarged conical tubercles. Digits long and well developed, inflected at basal interphalangeal joints; subdigital lamellae smooth, rounded and expanded proximal to joint inflection (11–12–13–15–11 manus; 10–14–14–15–9 pes); narrow distal to digital inflection (7–9–10–10–11 manus; 8–8–12–11–11 pes) (not including ventral claw sheath); large recurved claws sheathed by a dorsal and ventral scale.

Tail original, partially fractured approximately halfway from base, long and moderately robust, numerous low conical tubercles on dorsal and lateral surfaces close to base, but not extending beyond anterior third of tail, subcaudal scales enlarged, not wider than long, arranged in series 2–4 scales wide, 4 rounded cloacal spurs.

Measurements of holotype (in mm). SVL 169, TL 177, OT 177, TrK 72.7, HW 38.1, HD HH 24.3, HL 45.1, EN 14.7, IN 6.4, EYE 10.6, EAR 3.2, FA 26.1, CS 29.3.

Color in ethanol. Dorsum consists of alternating regions of dark greyish-brown, medium grey, and light-grey to dirty off-white. Four dark-brown regions most clearly defined, and consisting of three paired sets of oval, pentagonal and triangular blotches between fore- and hindlimbs, and an additional distinct dark-brown triangular nuchal patch anterior to insertion of forelimbs, and extending antero-laterally as a stripe through eye and along dorsal edge of supralabials. Ventro-lateral regions of head with wide off-white stripe extending to lower edge of supralabials. Supraciliaries and dorsal tip of snout dark brown. Limbs and toes dirty grey with broad indistinct dark-brown bands on upper and lateral surfaces. Ventral ground colouration off-white with brownish tinge and extensive dark-brown flecks, often covering just a single scale, but also coalescing to form four distinct sets of jagged transverse bars on throat, and less prominent bars and ocelli on torso. Dorsal and lateral surfaces of tail dirty grey with four indistinctly edged dark-brown blotches or bands, and extensive smaller dark brown maculations, stripes or blotches. Subcaudal surfaces dark-brown with scattered lighter grey spots.

Variation. The type series of 20 specimens includes five adult males with expressed pores (SVL 152–165 mm), 10 females (128–172 mm), and five juveniles or subadults

Table 3. Measurements for the type series of *Cyrtodactylus rex* sp. n.

| | Males (n = 5) | | Females (n = 10) | | Immatures (n = 5) | |
|-----|---------------|-------|------------------|-------|-------------------|------|
| | Range | Mean | Range | Mean | Range | Mean |
| SVL | 127–165 | 153 | 128–172 | 154.3 | 73–111 | 89.3 |
| TL | 16–162 | 118.0 | 23–177 | 122.9 | 74–112 | 94.0 |
| OT | 11–137 | 40.6 | 11–142 | 37.2 | 74–112 | 94.0 |
| TtK | 54.9–78.2 | 70.0 | 47.0–87.2 | 69.8 | 34.4–53.7 | 42.4 |
| HW | 27.1–35.0 | 32.5 | 28.6–38.1 | 33.4 | 15.1–23.1 | 18.9 |
| HH | 16.6–21.8 | 19.8 | 15.5–24.3 | 19.7 | 9.3–14.0 | 11.7 |
| HL | 36.5–43.3 | 41.1 | 35.6–45.6 | 41.4 | 20.6–29.9 | 25.2 |
| EN | 12.2–14.5 | 13.6 | 12.1–15.1 | 13.8 | 7.1–10.7 | 8.7 |
| IN | 4.9–6.4 | 5.8 | 5.2–6.4 | 5.9 | 2.8–4.4 | 3.7 |
| EYE | 8.7–10.4 | 9.5 | 8.1–10.9 | 9.9 | 4.8–7.4 | 6.4 |
| EAR | 1.5–3.9 | 2.4 | 1.8–4.2 | 2.6 | 1.0–1.7 | 1.5 |
| FA | 20.5–24.2 | 23.0 | 18.6–26.1 | 22.3 | 9.9–16.4 | 12.8 |
| CS | 23.6–29.5 | 27.2 | 22.8–31.0 | 27.0 | 11.8–18.7 | 15.0 |

(72–127 mm). Mensural data for the type series are summarized in Table 3. Supralabials counted to center of eye vary from 8–12, to angle of jaw 10–15, infralabials vary from 11–14, fourth toe wide lamellae 10–19, fourth toe narrow lamellae 8–16, mid-belly scale rows 39–60, number of rows of dorsal tubercles 20–27, cloacal spurs 2–6, and expressed femoral and precloacal pores in continuous or near continuous series of 28–38 (males only).

Dorsal pattern always consists of indistinctly defined alternating regions of dark grey brown, medium brown and dirty off-white. Dark grey-brown markings usually most clearly defined, but showing extensive variation in shape and size - usually less than half width of torso, but occasionally wider and varying in shape from small diamonds, transverse bands to paired blotches or triangles. Dark brown ventral barring always present, but on some specimens restricted to throat only, while in others forming a network across throat and venter. All specimens with at least some indistinct dark brown barring on toes and four or five dark brown longitudinal blotches or bands on original tails. Iris in life brick red with extensive fine brown vermiculations (Figure 5).

All specimens heavily tuberculate with usually several indistinct rows of large tubercles extending as much as 10 mm inferior to lateral fold at midpoint of torso. Throat tuberculation varies in extent from a broad band spanning the posterior throat to concentrated in infra-angular regions and largely absent from the throat.

Comparisons. *Cyrtodactylus rex* sp. n. is readily distinguished from most other *Cyrtodactylus* by its very large size (SVL up to 172 mm vs generally < 130mm). It further differs from the relatively small number of other large Papuan species as follows. *Cyrtodactylus rex* sp. n. differs from *C. loriae* and *C. serratus* in having enlarged tubercles on the infra-angular region and often extending onto and across the throat (vs absent from both regions), a lower number of pores (up to 38 vs. up to 81), and in lacking

enlarged tubercles extending the length of the tail (vs. *C. serratus* only). *Cyrtodactylus rex* sp. n. differs from members of the *C. lousiadensis* group (*C. epiroticus* (with which it is sympatric in Morobe Province), *C. klugei*, *C. lousiadensis*, *C. murua*, *C. robustus*, *C. salomonensis* and *C. tripartitus*) by its much smaller subcaudal scales, the presences of extensive tubercles on infra-angular region and often the throat, and in its much more poorly defined dark bands or paired blotches on the dorsum (vs. distinctly edged, unbroken transverse light and dark-brown bands). *Cyrtodactylus rex* sp. n. differs from *C. zugi* by the presence of dark-brown barring on the throat and venter, tuberculation often extending across the throat (vs. on infra-angular region only), and dorsal colour pattern on torso consisting of alternating indistinct dark-brown, medium brown and whitish regions (vs. alternating dark-brown and off-white). *Cyrtodactylus rex* sp. n. differs from *C. irianjayaensis* by the presence of dark-brown barring on the throat and venter (vs. plain and unpatterned), tubercles often extending across the throat (vs. infra-angular region only), dorsal colour pattern on torso consisting of alternating indistinct dark-brown, medium brown and whitish regions (vs. very wide brown transverse blotches on a lighter greyish brown ground colour), and higher number of femoral and precloacal pores (21–38 vs. 7–16). *Cyrtodactylus rex* sp. n. differs from all populations referred to *C. novaeguineae* in its wider head (HW/SVL 0.21–0.24 vs. 0.18–0.19) and larger size (SVL 172 vs. 129 mm), and differs from *C. equestris* sp. n. in its larger size (SVL 172 vs. 139 mm), in having a continuous (or nearly so) row of femoral and precloacal pores, presence of dark barring on the throat and ventral surfaces of body (vs. absent), and ‘messier’ dorsal colouration of alternating indistinct dark-brown, medium brown and whitish regions (vs. light-brown transverse bands or blotches on relatively plain light brownish-grey background).

Distribution and natural history. Widespread in northern Papua New Guinea, extending from Sandaun Province in the west to Morobe Province in the east (Figure 7). Photographs of a specimen from the vicinity of Senggi Village to the south of Jayapura in West Papua Province (kindly provided by Burhan Tjaturadi), indicate that this species also occurs in adjacent parts of Indonesian New Guinea.

The holotype was collected on a low ridge in Sago-dominated swamp forest. Other specimens were collected in lowland and foothill forest at altitudes ranging from near sea level up to 690 m a.s.l.

Etymology. From the latin for king as it is the largest of the over 200 species of *Cyrtodactylus*, and amongst the largest of all known geckos (Bauer 2013).

Discussion

The complex geological history of New Guinea has played a major role in shaping Papuan biodiversity (Toussaint et al. 2014). The high Central Cordillera is the dominant mountain complex in New Guinea, however the lower and smaller upland regions of the North Papuan Mountains also have an endemic biota that remains poorly understood (Helgen 2007; Richards et al. 2009; Kraus and Myers 2012). The North Papuan

Mountains are derived from the (ongoing) accretion of formerly isolated island arcs onto the northern edge of New Guinea (Polhemus 2007). One key question is the extent to which endemism in these ranges is attributable to dispersal from other (relatively distant) montane habitats, persistence of a previously insular biota of terranes, or localised in situ transitions from surrounding lowland habitats (Toussaint et al. 2014).

The two new geckos described here have overlapping, yet somewhat complementary distributions: *Cyrtodactylus equestris* sp. n. is seemingly restricted to hill and lower montane forests on the North Papuan Mountains themselves, while *C. rex* sp. n. is more widespread throughout the surrounding lowlands (Figure 7). *Cyrtodactylus equestris* sp. n. is the second *Cyrtodactylus* that has only been recorded from hill and low montane forest on the North Papuan Mountains – the other being *Cyrtodactylus boreoclivus* from the Foja, Torricelli and Bewani Mountains (Oliver et al. 2011). Sampled populations of both of these apparent North Papuan Mountain endemics show levels of mitochondrial genetic diversity (< 10%) consistent with the hypothesis that they represent single (ableit structured) species and suggest some degree of historical connectivity between the ranges that comprise the North Papuan Mountains (Oliver et al. 2012, this study). The as yet ungenotyped populations referred to *Cyrtodactylus equestris* sp. n. from the Adelbert Mountains in the east may prove to be an exception to this.

In contrast to their broadly overlapping intraspecific distribution, the distribution of sister lineages to these two North Papuan Mountain *Cyrtodactylus* differs. On the one hand *C. boreoclivus* is closely allied to *C. medioclivus*, an allopatric lower montane form currently known only from a small area of the Central Cordillera (Oliver et al. 2012). On the other hand, records of the inferred relatives of the newly described *Cyrtodactylus equestris* sp. n. (*C. novaeguineae*, *C. rex* sp. n. and *C. zugi*) are concentrated in lowland habitats spanning New Guinea, and suggest that the upland habitat association of this taxon is derived. The putative sister taxon *C. zugi* is currently known only from other still discrete northern terranes – the islands of Batanta and probably Waigeo (Oliver et al. 2008). Batanta and especially Waigeo have moved significantly westward through the Miocene and Pliocene (Polhemus 2007) – highlighting the possibility that the evolutionary history of the clade comprising *C. equestris* sp. n. and *C. zugi* may be linked to the northern arc islands.

The contrasting distribution of sister lineages in the North Papuan Ranges suggests endemism is accumulating through multiple processes - colonisation by taxa already associated with hill and lower montane habitats from the older Central Cordillera (eccentric endemism), accretion of pre-existing island arc biotas, and potentially even de novo shifts up elevational gradients within otherwise lowland lineages (centric endemism) (Merckx et al. 2015) and complements recent work addressing the same question in water beetle (Toussaint et al. 2014).

Cyrtodactylus is also an exceptionally species rich genus of lizards with over 200 recognised species (Uetz 2015), however, how potentially key factors such as competition, ecological diversification, isolation and dispersal, have shaped the evolution of this diversity remain largely untested. Within New Guinea a number of lineages have larger body sizes than elsewhere, with the giant *Cyrtodactylus rex* sp. n. sitting at the

apex of this trend. It has been suggested that this is indicative of a unique trajectory of ecological evolution in the Papuan region – potentially linked to either competitive and/or predatory release (Oliver et al. 2014). The ongoing elucidation of a suite of apparently lower montane and hill forest species suggests that altitudinal segregation has also played some role in mediating the accumulation of regional diversity in this lineage (Oliver et al. 2013; this paper), at least within the exceptionally complex orogeny of New Guinea, and potentially also other topographically variable tropical regions (Grismer et al. 2012).

Acknowledgements

Specimens examined included material collected over the course of numerous independent field trips in Papua New Guinea and Papua Province, Indonesia, but we particularly thank the numerous staff and major donors to Conservation International for work in Indonesia and Papua New Guinea, and to WWF Papua New Guinea for facilitating work in the Kikori region. We thank the PNG National Research Institute and especially Jim Robins for assisting with SJR's Research Visas, and the PNG Department of Environment and Conservation and especially Barnabas Wilmott for issuing relevant visas and export approvals. The following individuals provided access for specimens, tissues and other data: David Kizirian and Edward Stanley (AMNH), Ross Sadlier and Glenn Shea (AMS), Allen Allison (BPBM), Fred Kraus, José Rosado (MCZ), Mark Hutchinson and Carolyn Kovach (SAMA), and Aaron Bauer and Todd Jackman (Villanova University). This work was funded by a grant from the Australian Pacific Science Foundation to Paul Oliver, Stephen Richards and Mike Lee, and Paul Oliver was also supported by a McKenzie Postdoctoral Fellowship from the University of Melbourne.

References

- Bauer AM (2013) *Geckos: The Animal Answer Guide*. Johns Hopkins University Press, Baltimore, 159 pp.
- Brongersma LD (1934) Contributions to Indo-Australian herpetology. *Zoologische, Mededelingen* 17: 161–251.
- Donnellan SC, Aplin KP (1989) Resolution of cryptic species in the New Guinea lizard, *Sphenomorphus jobiensis* (Scincidae) by electrophoresis. *Copeia* 1989: 81–88. doi: 10.2307/1445608
- Edgar RC (2004) MUSCLE: multiple sequence alignment with high accuracy and high throughput. *Nucleic Acids Research* 32: 1792–1797. doi: 10.1093/nar/gkh340
- Georges A, Zhang X, Unmack PJ, Reid BN, Le M, Mccord WP (2014) Phylogeography of an endemic New Guinea freshwater turtle reflects geological events during the Miocene. *Biological Journal of the Linnean Society* 111: 192–208. doi: 10.1111/bij.12176

- Grismer L, Wood JR, Quah ESH, Anuar S, Muin MA, Sumontha M, Ahmad N, Bauer AM, Wangkulangkul S, Grismer J, Pauwels SGO (2012) A phylogeny and taxonomy of the Thai-Malay Peninsula Bent-toed Geckos of the *Cyrtodactylus pulchellus* complex (Squamata: Gekkonidae): combined morphological and molecular analyses with descriptions of seven new species. *Zootaxa* 3520: 1–55.
- Helgen K (2007) A Taxonomic and geographic overview of the mammals of Papua. In: Marshall A, Beehler B (Eds) *The Ecology of Papua*. Periplus Editions, Singapore, 689–749.
- Kraus F (2007) A new species of *Cyrtodactylus* (Squamata: Gekkonidae) from western Papua New Guinea. *Zootaxa* 1425: 63–68. doi: 10.11646/zootaxa.1425.1.8
- Kraus F (2008) Taxonomic partitioning of *Cyrtodactylus louisiadensis* (Lacertilia: Gekkonidae) from Papua New Guinea. *Zootaxa* 1883: 1–27.
- Kraus F, Allison A (2006) A new species of *Cyrtodactylus* (Lacertilia: Gekkonidae) from Papua New Guinea. *Zootaxa* 1247: 59–68.
- Kraus F, Myers S (2012) New species of *Hypsilurus* (Squamata: Agamidae) from Papua New Guinea. *Journal of Herpetology* 46: 396–401. doi: 10.1670/11-159
- Merckx VSFT, Hendriks KP, Beentjes KK, Mennes CB, Becking LE, Peijnenburg KTC a., Afendy A, Arumugam N, de Boer H, Biun A, Buang MM, Chen P-P, Chung AYC, Dow R, Feijen F a. a., Feijen H, Soest CF, Geml J, Geurts R, Gravendeel B, Hovenkamp P, Imbun P, Ipor I, Janssens SB, Jocqué M, Kappes H, Khoo E, Koomen P, Lens F, Majapun RJ, Morgado LN, Neupane S, Nieser N, Pereira JT, Rahman H, Sabran S, Sawang A, Schwallier RM, Shim P-S, Smit H, Sol N, Spait M, Stech M, Stokvis F, Sugau JB, Suleiman M, Sumail S, Thomas DC, van Tol J, Tuh FYY, Yahya BE, Nais J, Repin R, Lakim M, Schilthuizen M (2015) Evolution of endemism on a young tropical mountain. *Nature*. doi: 10.1038/nature14949
- Oliver LA, Rittmeyer EN, Kraus F, Richards SJ, Austin CA (2013) Phylogeny and phylogeography of *Mantophryne* (Anura: Microhylidae) reveals cryptic diversity in New Guinea. *Molecular Phylogenetics and Evolution* 67: 600–607. doi: 10.1016/j.ympev.2013.02.023
- Oliver PM, Tjaturadi B, Mumpuni, Krey K, Richards S (2008) A new species of large *Cyrtodactylus* (Squamata: Gekkonidae) from Melanesia. *Zootaxa* 1894: 59–68.
- Oliver PM, Krey K, Mumpuni, Richards SJ (2011) A new species of bent-toed gecko (*Cyrtodactylus*, Gekkonidae) from the North Papuan Mountains. *Zootaxa* 2930: 22–32.
- Oliver PM, Richards SJ (2012) A new species of small bent-toed gecko (*Cyrtodactylus*, Gekkonidae) from the Huon Peninsula, Papua New Guinea. *Journal of Herpetology* 46: 488–493. doi: 10.1670/11-101
- Oliver PM, Siström M, Richards S (2012) Phylogeny and systematics of Melanesia's most diverse gecko lineage (*Cyrtodactylus*, Gekkonidae, Squamata). *Zoologica Scripta* 41: 437–454. doi: 10.1111/j.1463-6409.2012.00545.x
- Oliver PM, Skipwith P, Lee MSY (2014) Crossing the line: shifting body size optima in a trans-Wallacean lizard radiation. *Biology Letters* 10: 20140479. doi: 10.1098/rsbl.2014.0479
- Polaszek A, Alonso-Zarazaga M, Bouchet P, Brothers DJ, Evenhuis NL, Krell FT, Lyal CHC, Minelli A, Pyle RL, Robinson N, Thompson FC, van Tol J (2005) ZooBank: the open-access register for zoological taxonomy: Technical Discussion Paper. *Bulletin of Zoological Nomenclature* 62: 210–220.

- Polhemus D (2007) Tectonic Geology of Papua. In: Marshall A, Beehler B (Eds) *The Ecology of Papua*. Periplus Editions, Singapore, 137–164.
- Richards SJ, Oliver PM, Krey K, Tjaturadi B (2009) A new species of *Litoria* (Amphibia: Anura: Hylidae) from the foothills of the Foja Mountains, Papua Province, Indonesia. *Zootaxa* 2277: 1–13.
- Rösler H, Günther R, Richards SJ (2007) Remarks on the morphology and taxonomy of geckos of the genus *Cyrtodactylus* Gray, 1827, occurring east of Wallacea, with description of two new species (Reptilia: Sauria: Gekkonidae). *Salamandra* 43: 193–230.
- Schlegel H (1837) *Abbildungen neuer oder unvollständig bekannter Amphibien, nach der Natur oder dem Leben entworfen*. Arnz & Comp, Düsseldorf, i-xiv + 141 pp.
- Sistrom MJ, Hutchinson MN, Hutchinson RG, Donnellan SC (2009) Molecular phylogeny of Australian *Gehyra* (Squamata: Gekkonidae) and taxonomic revision of *Gehyra variegata* in south-eastern Australia. *Zootaxa* 2277: 14–32.
- Stamatakis A (2006) RaxML-VI-HPC: Maximum Likelihood-based Phylogenetic Analyses with thousands of taxa and mixed models. *Bioinformatics* 22: 2688–2690. doi: 10.1093/bioinformatics/btl446
- Toussaint EFA, Hall R, Monaghan M, Sagata K, Ibalim S, Shaverdo HV, Vogler AP, Pons J, Balke M (2014) The towering orogeny of New Guinea as a trigger for arthropod megadiversity. *Nature Communications* 5: 4001. doi: 10.1038/ncomms5001
- Wood JR, Heinicke MP, Jackman TR, Bauer AM (2012) Phylogeny of bent-toed geckos (*Cyrtodactylus*) reveals a west to east pattern of diversification. *Molecular Phylogenetics and Evolution* 65: 992–1003. doi: 10.1016/j.ympev.2012.08.025
- Uetz P (2015) TIGR reptile database. Available via <http://www.reptile-database.org> [accessed 10 February 2015]
- Unmack PJ, Allen GR, Johnson JB (2013) Phylogeny and biogeography of rainbowfishes (Teleostei: Melanotaeniidae). *Molecular Phylogenetics and Evolution* 67: 15–27. doi: 10.1016/j.ympev.2012.12.019
- Zweifel RG (1980) Results of the Archbold Expeditions. No. 103. Frogs and lizards from the Huon Peninsula, Papua New Guinea. *Bulletin of the American Museum of Natural History* 165: 387–434.

Appendix I

Registration numbers, GenBank numbers and localities for material included in genetic analyses.

Ingroup. *Cyrtodactylus equestris*: BPBM 23316, JX440547, Papua New Guinea, 2.9–3.2km E of Mt Sapau summit; AMS R135520, KT835458, Papua New Guinea, Sandaun Province, Torricelli Mountains, Mt. Sumbau; AMS R119547, KT835457, Papua New Guinea, Sandaun Province, Torricelli Mtns, Wigote; MZB lace 5436, KT835459, Indonesia, Papua Province, Foja Mountains, Marina Valen Village; *Cyrtodactylus novaeguineae*: SAMA R62648, JQ820302, Papua New Guinea, Southern Highlands Province, Libano; AMS R122410, JQ820301, Papua New Guinea, Southern Highlands Province, Waro; SAMA R66153, JQ820304, Papua New Guinea, Western Province, upper Strickland basin; SAMA R66154, JQ820303, Papua New Guinea, Western Province, upper Strickland basin; *Cyrtodactylus rex*: SAMA R67637, KT835460, Papua New Guinea, Sandaun Province, Sepik River basin; SAMA R67636, KT835461, Papua New Guinea, Sandaun Province, Sepik River basin; AMS R119548, KT835462, Papua New Guinea, Sandaun Province, Torricelli Mts, Wigote; ABTC 44201 (no voucher), KT835463, Papua New Guinea, Sandaun Province, Torricelli Mts, Wigote; BPBM 18655, KT835463, Papua New Guinea, Morobe Province, 8.4km W of Mt Shungol summit.

Outgroups. *Cyrtodactylus adorus*: QM J86979, HQ401166, Australia, Queensland, Pascoe River; *Cyrtodactylus arcanus*: AMS R124559, JQ820314, Papua New Guinea, Madang Province, Bundi; *Cyrtodactylus arcanus*: (paratype) AMS R124560, JQ820319, Papua New Guinea, Madang Province, Bundi; *Cyrtodactylus epiroticus*: BPBM 18653, HQ401195, Papua New Guinea, Milne Bay Province, Mt Shungol; *Cyrtodactylus hoskini*: QM J86950, HQ401119 Australia, Queensland, Iron Range National Park; *Cyrtodactylus mcdonaldii*: QM J88027, HQ401150, Australia, Queensland, Parrot Creek Falls; *Cyrtodactylus mimikanus*: MZB lace 5343, JQ820316, Indonesia, Papua Province, Foya Mtns; SJR9807, KT835456, Indonesia, Papua Province, Foya Mtns; *Cyrtodactylus tuberculatus*: QM J87024, HQ401086, Australia, Queensland, Cooktown, Finch Bay; QM J87025, HQ401087, Australia, Queensland, Cooktown, Finch Bay; QM J87010, HQ401090, Australia, Queensland, Cooktown, Jensen's Crossing; *Cyrtodactylus zugi*: MZB lace 5575, JQ820306, Indonesia, Papua Barat Province, Raja Ampat Archipelago, Batanta Island; MZB lace 5573, JQ820305 Indonesia, Papua Barat Province, Raja Ampat Archipelago, Batanta Island.

Appendix 2

Material examined for morphological comparisons.

Institutional abbreviations are as follows: Australian Museum (AMS), American Museum of Natural History (AMNH), British Museum of Natural History (BMNH), Museum für Naturkunde, Berlin (ZMB), Museum of Comparative Biology, Harvard (MCZ), Museum Zoologicum Bogoriense (MZB), Naturalis, Amsterdam (RMNH), South Australian Museum (SAMA) and Western Australian Museum (WAM).

Cyrtodactylus aaroni: ZMB 62275 (holotype), ZMB 62273–4, ZMB 622737, ZMB 62756–7 (paratypes) Indonesia, Papua Barat Province, Wondiwoi Mountains; *Cyrtodactylus arcanus*: AMS R124599 (holotype), AMS R124599 (paratype) Papua New Guinea, Madang Province, Bundi; *Cyrtodactylus boreoclivus*: AMS R135519 (holotype) Papua New Guinea, Sandaun Province, Torricelli Mountains, Kukumbau area of Mount Sapau; MZB lace 7474–7475, SJR13593–13613 (field numbers, currently at MZB, to be lodged at South Australian Museum) Indonesia, Papua Province, Foja Mountains; *Cyrtodactylus capreoloides*: SAMA R62634 (holotype) Papua New Guinea, Southern Highlands Province, Moro; AMS R122412–122414 Papua New Guinea, Southern Highlands Province, Namosado; *Cyrtodactylus darmadvillei*: MZB lace 2005 Indonesia, Komodo National Park, Loh Liang; MZB lace 5297 East Flores, Mt Egon; *Cyrtodactylus derongo*: AMNH 103910 (paratype) Papua New Guinea, Western Province, Derongo Area, Alice River system; *Cyrtodactylus deveti*: MZB lace 6036 Indonesia, North Maluku Province, west Halmahera, Weda Village; MZB lace 6037 Indonesia, North Maluku Province, Halmahera, Toso Village; *Cyrtodactylus halmahericus*: MZB lace 6086 Indonesia, North Maluku Province, southern Ternate Island, Gambesi Village; MZB lace 6088, 6091–6092 Indonesia, North Maluku Province, Ternate Island, Faramadiahi Village; MZB lace 6095 Indonesia, North Maluku Province, east Halmahera, 17km from Lolobato National Park; MZB lace 1899 Indonesia, Maluku Province, Seram, Manusela National Park, Sasarata; MZB lace 2360 Seram, Kanike; MZB lace 2359, 2361 Seram, Solea; MZB lace 2362, 2363 Seram, Saunulu, Waikawa. *Cyrtodactylus irianjayensis*: MZB lace 5765 Indonesia, Papua Barat Province, Salawati Island. *Cyrtodactylus* cf. *irianjayensis*: MZB lace 2297 (seven specimens), 2298 (five specimens) Indonesia, Papua Barat Province, Sorong (from dealers' premises); *Cyrtodactylus jellesmae*: MZB lace 4647–4651 Indonesia, Southeast Sulawesi Province, Pulau Buton, Sungai Ladungkula, Kakenauwe Village; *Cyrtodactylus loriae*: SAMA R62635 Papua New Guinea, Kikori Basin, Darai Plateau; SAMA R62636 Papua New Guinea, Eastern Highlands Province, Crater Mountain Wildlife Management Area, Herowana Village; SAMA R62637 Papua New Guinea, Southern Highlands Province, Moro; SAMA R8305, 8369, WAM R67688–676889 Papua New Guinea, Chimbu Province, Karimui Village. *Cyrtodactylus medioclivus*: SAMA R66091 (holotype) Papua New Guinea, Southern Highlands Province, Wanakipa Village; AMS R122441 (paratype), Papua New Guinea, Southern Highlands Province,

Bobole; *Cyrtodactylus mimikanus*: BMNH 1946.8.23.5 (syntypes) Indonesia, Papua Province, Mimika River region; MZB lace 3561–3564, Indonesia, Papua Province, Cyclops Mountains, Yongsu; MZB lace 3565–3566 Indonesia, Furu River; MZB lace 2303 (2 specimens) Indonesia, Papua Province, Wapoga River Basin, Siewa. *Cyrtodactylus minor* SAMA R65954 (holotype), SAMA R65953 (paratype) Papua New Guinea, Morobe Province, Huon Peninsula, Tarona Camp, 0.5 km S of Yuwong Village, YUS Tree Kangaroo Conservation Project area; *Cyrtodactylus novaeguineae*: RMNH 2708A–B (cotypes) Indonesia, Papua Province, Triton Bay area; SAMA R66153–4, SJR10338 (field number, currently at SAMA, to be lodged at PNG National Museum) Papua New Guinea, Western Province, upper Strickland basin; SAMA R66156 Papua New Guinea, Western Province, Liddel River; AMS R122410, Papua New Guinea, Southern Highlands Province, Waro; SAMA R62648–9 Papua New Guinea, Gulf Province, Libano; *Cyrtodactylus nuaulu*: MZB lace 2326 (holotype), MZB lace 2325, 2327–2329 (paratypes) Indonesia, Maluku Province, Seram Island, Manusela National Park; *Cyrtodactylus salomonensis*: SAMA R56879 (holotype), SAMA R56780 (paratype) Solomon Islands, Isabel Province, Santa Isabel Island, Kolopakisa; *Cyrtodactylus serratus*: SAMA R62635 Papua New Guinea, Gulf Province, Darai Plateau; SAMA R66155 Papua New Guinea, Western Province, upper Strickland basin; *Cyrtodactylus sermowaiensis*: SAMA R62653 Papua New Guinea, Madang Province, Ramu River basin; *Cyrtodactylus tuberculatus*: SAMA R12058, SAMA 14002 Australia, Queensland, Cooktown; *Cyrtodactylus tripartitus*: SAMA R62638–62644 Papua New Guinea, Milne Bay Province, Misima Island; *Cyrtodactylus zugi*: MZB lace 5574 (holotype), MZB lace 5573, 5575 (paratypes) Indonesia, Papua Barat Province, south coast of Batanta Island; MZB lace 7310 Indonesia, Papua Barat Province, Batanta.

The desert tortoise trichotomy: Mexico hosts a third, new sister-species of tortoise in the *Gopherus morafkai*–*G. agassizii* group

Taylor Edwards^{1,2}, Alice E. Karl³, Mercy Vaughn⁴, Philip C. Rosen¹,
Cristina Meléndez Torres⁵, Robert W. Murphy⁶

1 School of Natural Resources and the Environment. The University of Arizona, Tucson, AZ 85721 USA
2 University of Arizona Genetics Core, University of Arizona, Tucson, AZ 85721 USA **3** P.O. Box 74006, Davis, CA 95617 USA **4** Paso Robles, CA 93446 USA **5** Comisión de Ecología y Desarrollo Sustentable del Estado de Sonora, Sonora, México **6** Royal Ontario Museum, Toronto M5S 2C6, Canada

Corresponding author: Robert W. Murphy (bob.murphy@utoronto.ca)

Academic editor: J. Penner | Received 16 June 2015 | Accepted 6 January 2016 | Published 10 February 2016

<http://zoobank.org/CF7F89A2-7021-470F-8DE6-35221708017C>

Citation: Edwards T, Karl AE, Vaughn M, Rosen PC, Torres CM, Murphy RW (2016) The desert tortoise trichotomy: Mexico hosts a third, new sister-species of tortoise in the *Gopherus morafkai*–*G. agassizii* group. ZooKeys 562: 131–158. doi: 10.3897/zookeys.562.6124

Abstract

Desert tortoises (Testudines; Testudinidae; *Gopherus agassizii* group) have an extensive distribution throughout the Mojave, Colorado, and Sonoran desert regions. Not surprisingly, they exhibit a tremendous amount of ecological, behavioral, morphological and genetic variation. *Gopherus agassizii* was considered a single species for almost 150 years but recently the species was split into the nominate form and Morafka's desert tortoise, *G. morafkai*, the latter occurring south and east of the Colorado River. Whereas a large body of literature focuses on tortoises in the United States, a dearth of investigations exists for Mexican animals. Notwithstanding, Mexican populations of desert tortoises in the southern part of the range of *G. morafkai* are distinct, particularly where the tortoises occur in tropical thornscrub and tropical deciduous forest. Recent studies have shed light on the ecology, morphology and genetics of these southern 'desert' tortoises. All evidence warrants recognition of this clade as a distinctive taxon and herein we describe it as *Gopherus evgoodei* **sp. n.** The description of the new species significantly reduces and limits the distribution of *G. morafkai* to desertscrub habitat only. By contrast, *G. evgoodei* **sp. n.** occurs in thornscrub and tropical deciduous forests only and this leaves it with the smallest range of the three sister species. We present conservation implications for the newly described *Gopherus evgoodei*, which already faces impending threats.

Keywords

Gopherus agassizii, *Gopherus morafkai*, Sinaloa, Sonora, Testudinidae, *Xerobates*

Introduction

Desert tortoises (genus *Gopherus*: *G. agassizii* group) occupy a large geographic range throughout the Mojave and Colorado deserts and in the Sonoran desert region of the United States and mainland Mexico (Fritts and Jennings 1994; Berry et al. 2002) (Figure 1). *Gopherus morafkai* (Murphy et al. 2011) was described as a species separate from *G. agassizii* (Cooper 1861) based on ecological, behavioral and genetic differences. Murphy et al. (2011) noted that the full diversity of *G. morafkai* had not yet been defined. Lamb et al. (1989) reported deeply divergent mitochondrial DNA (mtDNA) haplotypes in the southern portion of the range of *G. morafkai*. Edwards et al. (2015) conducted a detailed genetic analysis of *G. morafkai* in Mexico. They found that this southern “Sinaloan lineage” constituted a species distinct from northern congeners.

Ecological and morphological characteristics distinguish the northern “Sonoran” and southern “Sinaloan” lineages of tortoises found in thornscrub and tropical deciduous forest of southern Sonora and northern Sinaloa from those occurring further north in Sonoran Desertscrub (Bogert and Oliver 1945; Loomis and Geest 1964; Hardy and McDiarmid 1969; Germano 1993; Fritts and Jennings 1994; Berry et al. 2002; Bury et al. 2002; Legler and Vogt 2013). The three biomes, including Sonoran Desertscrub (SDS), Sinaloan Thornscrub (STS), and Tropical Deciduous Forest (TDF), occur in the area known broadly as the Sonoran Desert region (*sensu* Brown et al. 1979; Brown 1994; Martin et al. 1998). Whereas the Sonoran lineage of *G. morafkai* ranges throughout SDS in Sonora, Mexico and Arizona, USA, the Sinaloan lineage occurs solely in TDF and STS environments (Figure 1; Edwards et al. 2015). The two lineages occur sympatrically in a relatively narrow ecotone between the SDS and STS and limited hybridization occurs only in this region. No obvious geographic barrier limits introgression yet the two groups of tortoises are deeply diverged genetically and they maintain their unique identities (Edwards et al. 2015, 2016). Because the Sinaloan lineage is genetically, ecologically and morphologically distinct from its congeners, below we describe it as a new species.

Materials and methods**Genetics**

Edwards et al. (2015) assessed the population genetic structure of desert tortoises in the Sonoran Desert region by sampling 233 wild desert tortoises consisting of both Sonoran and Sinaloan lineages of *G. morafkai*. They sampled their known distributions in each of the three major biomes where tortoises occur. They reconstructed

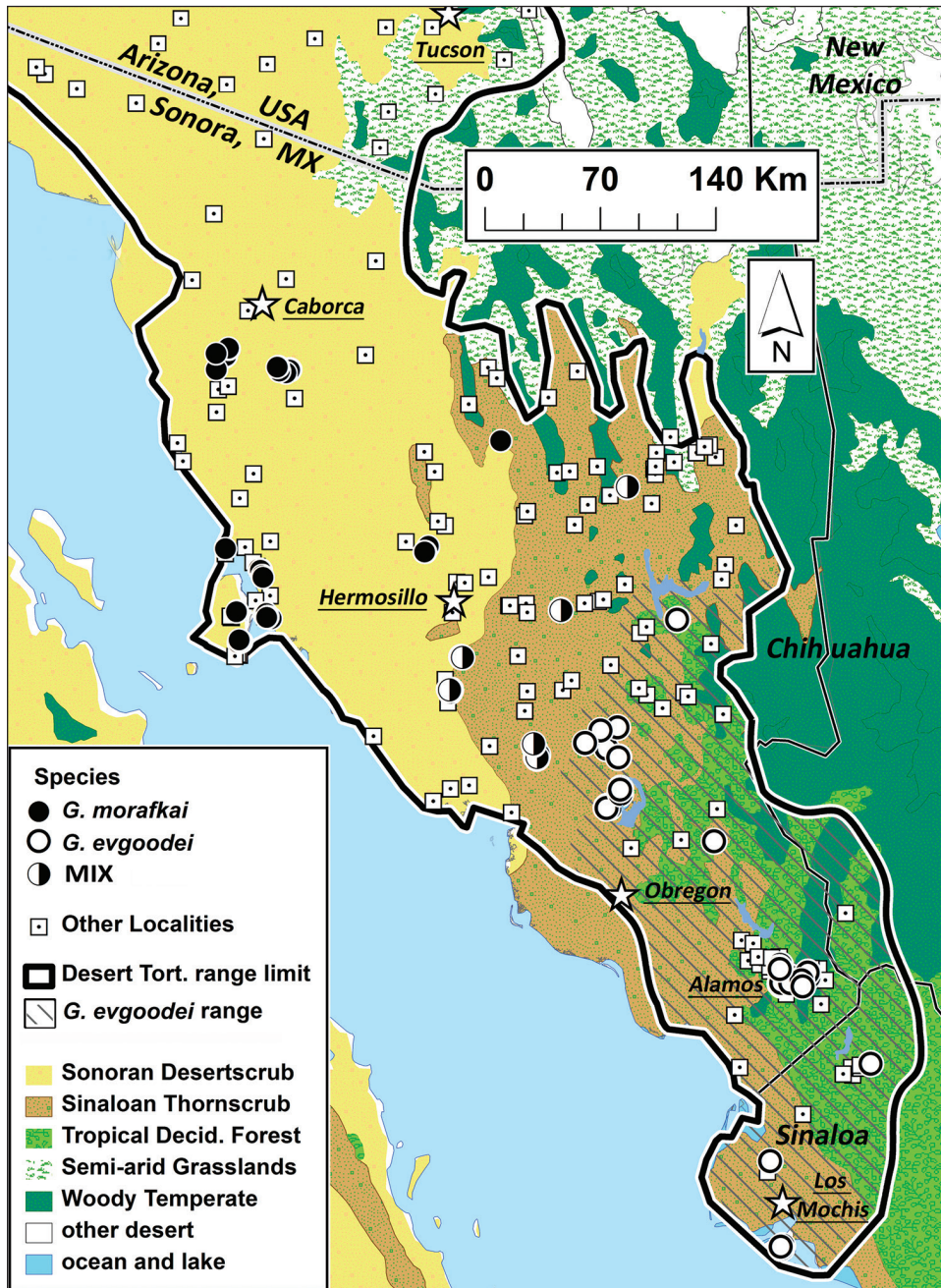


Figure 1. Conservative estimate of the distribution of *G. evgoodei* in Mexico indicated by diagonal lines. Desert tortoise range limit, modified based on our field sampling, from Germano et al. (1994). Squares indicate museum and literature records of occurrence of *G. spp.* Circles are sample locations from Edwards et al. (2015) for both *G. morafkai* (black) and *G. evgoodei* (white). Localities in the Sinaloan thornscrub-Sonoran deserts scrub ecotone indicated by split circles, which indicate the occurrence of both *G. evgoodei* and *G. morafkai* genotypes and/or hybrids.

matrilineal relationships using mtDNA sequences and employed 25 microsatellites (STRs) to perform Bayesian analyses of gene flow. They also conducted clinal analyses using both mtDNA and STRs to determine the position and amount of introgression where lineages co-occur. Further, Edwards et al. (2016) used mtDNA and four nDNA loci to perform a multi-locus phylogenetic analysis to estimate the species-tree among desert tortoise lineages. They also tested for ancestral lineage admixture with RNA-seq data based on diffusion approximation for demographic inference using the software package $\partial A\partial I$ (Gutenkunst et al. 2009).

Herein, to assist direct comparison with previous data, we add mtDNA divergence estimates for cytochrome *b* (*Cytb*) as well as the standard barcoding locus cytochrome oxidase subunit I (*COI*) for species discrimination within the Cold Code project (Murphy et al. 2013). For *Cytb*, we used primers H16464 and L14724 to amplify an approximately 1,500 bp fragment following the methods developed for *Gopherus* by Osentoski and Lamb (1995). We generated sequences across the entire amplicon by sequencing with both the amplification primers and with internal sequencing primers CytbF2 and CRR3 developed by Clostio et al. (2012). We then aligned these sequences to available sequences in GenBank for *G. agassizii* (Accession AY434562.1) to generate a 1,140 bp sequence for each sample. For *COI*, we used primers L-turtCOIc and H-turtCOIc and followed protocols developed by Stuart and Parham (2004). For both loci, we generated sequences for *G. agassizii* ($n = 4$; sampled from Nevada and California), Sonoran lineage of *G. morafkai* ($n = 4$; sampled from Arizona, USA and Sonora, MX) and the Sinaloan lineage of *G. morafkai* ($n = 2$; from Sonora and Sinaloa, Mexico). In addition, we included their closest outgroup based on Lamb et al. (1989), *G. berlandieri* (Agassiz) ($n = 2$), for comparison. We estimated divergence among the species of *Gopherus* using DNASP (v.5.10.01; Librado and Rozas 2009).

Morphology

Bogert and Oliver (1945) first recognized the distinct morphology of the southern, Sinaloan lineage of *G. morafkai*, but they were unable to quantify it due to very small sample sizes. Other studies have also noted morphological characteristics that distinguish the Sinaloan lineage but did not provide a quantitative analysis (Loomis and Geest 1964; Hardy and McDiarmid 1969; Germano 1993; Fritts and Jennings 1994; Berry et al. 2002; Bury et al. 2002; Legler and Vogt 2013). We observed distinct morphological characters in 23 tortoises in the vicinity of Alamos, Sonora in 2005. To this, we added anecdotal observations and measurements of several preserved specimens of Sonoran and Sinaloan lineages of *G. morafkai* and *G. agassizii* in the University of Arizona herpetological collection and data from McLuckie et al. (1999). Consequently, we developed a suite of measurements and qualitative factors that morphologically diagnose the Sinaloan lineage. Measurements (in mm) included the following 37 variables: mid-carapace length (MCL); maximum width; maximum width at 3/4 marginal scute seam; maximum width at mid-6th marginal; maximum

width at 7/8 marginal scute seam; width of C-truss 1 (left); width between anal tips; rear foot-pad greatest width; maximum height; height at 2nd vertebral scute; height at 3rd vertebral scute; height at 4th vertebral scute; maximum plastron length from tip of gular horn to tip of anal scutes; length of plastron truss (left); length of plastron shortest diagonal; length of right pectoral scute; length of left pectoral scute; average midline length of abdominal scutes; average midline length of femoral scutes; average midline length of anal scutes; depth of male concavity; distance of posterior shell opening from anal tip to carapace; distance of supracaudal scute to anal notch; distance of mid-9th marginal to inner femoral; distance of mid-9th marginal to outer femoral; distance of anterior shell opening; distance of nuchal to plastron; distance of mid-2nd marginal to humeral (inner and outer); distance of gular straight-line length; distance of curved length; head length from tip of rostrum to anterior corner of the eye; width of tympanum; height of bridge from 6th marginal to abdominal scutes; shortest bridge length; distance of anterior bridge opening to inner 2nd/3rd marginal scute seam; distance of anterior bridge opening to outer 2nd/3rd marginal scute seam; and distance from bridge to inguinal point of attachment. We took straight-line measurements only. We also assessed the following 13 qualitative characters: shape of rear feet (flat/rounded); presence of spur at humeral junction; shape of anterior and posterior armoring scales (rounded/pointed); spikiness of rear and front legs (high/moderate/low); lateral profile of shell (flat/domed); profile of pre-frontals; wear-class of shell; carapace color; plastron color; integument color; annuli distinct (yes/no); and tail length (shorter or same as *G. agassizii*).

Measurements were taken on most tortoises that we encountered during field trips in Sonora and northern Sinaloa from 2006 through 2012. These animals served as the genetic resources for Edwards et al. (2015). From this larger dataset, we analyzed a subset of tortoises whose genetic lineage was verified using molecular diagnostics, including 62 individuals of Sonoran (*G. morafkai*; n=16) and Sinaloan lineages (n=36) sampled in Mexico, as well as 10 tortoises of mixed lineage. We compared these tortoises to three populations of *G. agassizii* in the Mojave and Colorado deserts of California (n=109). Populations near Algodones Dunes in eastern Imperial County (n=19) and near California City in eastern Kern County (n=64) were at the southeastern and northwestern geographic limits of the range of *G. agassizii* in California, respectively. A third population from 55 km southeast of Barstow, San Bernardino County (n=26) was from central Mojave Desert in California.

A comprehensive analysis of morphological characters for these desert tortoises does not exist. Thus, our taxonomic evaluation was based on a statistical analysis of the following variables that appeared to us to consistently diagnose the species by exhibiting little intraspecific variation: shell color; integument color; tail length; depth of male plastron concavity; presence of a spur at the radial-humeral joint; and roundness of carapace (e.g. dome-shape vs. flat) based on the ratio of the height at the 3rd vertebral scute to carapace length, while accounting for depth of plastron concavity in males. Shell and integument highlights and hues were coded based on the following wavelengths of colors (Encycolorpedia 2015): orange, 605 nm; yellow,

580 nm; olive, 570 nm; and brown and grey, 539 nm. These six variables were compared between groups that consisted of lineage/location using the ANOVA function in SYSTAT ver. 13 (Systat Software, Inc., San Jose, California). Analyses accounted for interactions by size and sex. Tukey's post-hoc pairwise comparison was used to identify among-site differences.

Area of occurrence

We estimated the area of occurrence for the Sinaloan lineage by using the web-based tool GEOCAT (<http://geocat.kew.org/what>). Due to having few data points and a hybrid zone, we did not calculate the area of occupancy. Estimated values for *G. morafkai* and *G. agassizii* were taken from U.S. Fish and Wildlife Service (2015).

Results

Edwards et al. (2015) estimated a 5.7 Ma divergence between matrilineal lineages of *G. morafkai*. Strong genetic differentiation occurred across the STR loci. Analyses indicated that *G. morafkai* consisted of two genetically and geographically distinct species (referred to as “Sonoran” and “Sinaloan” lineages). Both lineages occurred in a relatively narrow zone of overlap in STS where limited introgression occurred (Fig. 1). Bimodal genetic clines for both mtDNA and nDNA coincided with ecological features where the lineages came into contact. Clinal analysis revealed a strong coincidence of slope and concordance of centers for the mtDNA and nDNA markers. These occurrences dismissed cytonuclear discordance as an explanation for the observations (Toews and Brelsford 2012). The shifting ecotone between STS and SDS biomes may have acted as an ephemeral boundary that fostered adaptations in each lineage, and resulted in a largely parapatric distribution. Despite incomplete reproductive isolation, the two lineages of *G. morafkai* maintained separate evolutionary trajectories.

Edwards et al. (2016) presented a species-tree reconstructed using a multi-locus Bayesian species delimitation analysis reconstructed from mtDNA and four nDNA loci. The tree depicted Sonoran and Sinaloan tortoises as sister lineages and together they formed the sister to *G. agassizii*. Nodes of the tree had overlapping standard deviations. This tree topology was consistent with that of an independent analysis of 15 nuclear loci performed by Spinks et al. (P. Spinks, University of California Los Angeles; *personal communication*). In their RNA-seq analysis, Edwards et al. (2016) also characterized 20,126 synonymous variants from 7,665 contigs in six individuals, two representing each of the three lineages. The best-fit model observed from the $\partial A\partial I$ analysis was concordant with their multilocus species tree but more clearly elucidated the relative divergence times among the lineages. This result suggested that the Sonoran/Sinaloan split occurred only a short time after (or possibly even simultaneous with) divergence of *G. agassizii*. Thus, the three lineages formed a trichotomy with relatively

equal levels of divergence from each other. The $\partial A \partial I$ analysis also failed to detect evidence of gene flow during divergence among the three lineages. Analyses revealed that divergence among the lineages occurred in the absence of gene flow, whether through physical allopatry or ecological niche segregation. The results further validated species-level differentiation among the three lineages.

MtDNA sequence divergence

We generated a 761 bp sequence of mtDNA that encodes part of the gene encoding *COI* and identified seven unique haplotypes in our sample set (GenBank accession numbers; KR610436–KR610442). Divergence at *COI* between *G. agassizii* and Sonoran *G. morafkai* was 4.1%, between Sinaloan lineage tortoises and *G. agassizii* 3.6%, and between Sinaloan lineage tortoises and Sonoran *G. morafkai* 3.4%. Divergence between all three species/lineages of desert tortoise with *G. berlandieri* averaged 6.1%. For *Cytb*, we generated 1140 bp sequences and identified six haplotypes (GenBank Accession No. KT956833–KT956838). We included GenBank sequences from *G. agassizii* (Accession No. AY434562.1) in our alignment and analyses. Divergence at *Cytb* between *G. agassizii* and Sonoran *G. morafkai* was 4.5%, between Sinaloan lineage tortoises and *G. agassizii* 3.7%, and between Sinaloan lineage tortoises and Sonoran *G. morafkai* 4.2%. Divergence between all three species/lineages of desert tortoise with *G. berlandieri* averaged 5.9%.

Morphology

All species of *Gopherus* shared the following morphological characteristics with other members of the family Testudinidae (Ernst and Barbour 1989): 11 marginal scutes on both right and left edges of the carapace; five toenails on each forelimb and four toenails on each elephantine hind limb. Within the desert tortoises and like *G. agassizii* and *G. morafkai*, the Sinaloan lineage tortoise was sexually dimorphic with mature males having a slightly longer tail, enlarged gular horn, a concave plastron, a tucked supracaudal scute and prominent chin glands. However, several characteristics generally distinguished the Sinaloan lineage from other desert tortoises. Sinaloan tortoises had a very flat carapace (Fig. 2) that was highly significantly flatter than the conspicuously domed carapaces of *G. agassizii* and Mexican *G. morafkai* ($F_{5,162} = 6.789$; $p < 0.0005$). All Sinaloan tortoises (100% of 37 adults) had prominent, pointed scale(s) (spurs) at the humeral/radial joint (Fig. 3). *Gopherus morafkai* and *G. agassizii* also had spurs, but less consistently, and they were rarely prominent or pointed in *G. agassizii*. Only 25% of Mexican *G. morafkai* ($n=16$) and 15.9% of *G. agassizii* from the Colorado Desert had spurs ($n=19$). Interestingly, 73.9–74.6% of the tortoises ($n=86$) from the Mojave Desert had spurs. There were too few small tortoises to detect an association between size and presence of spurs. The occurrences of spurs did not differ between sexes.



Figure 2. The flat shell profile/shape of carapace generally distinguishes *G. evgoodei* from other species of desert tortoises. Live, wild-caught individuals from (i–iv) Rancho Las Cabras and (v–vi) Rancho La Sierrita near Alamos, Sonora, Mexico (in Tropical Deciduous Forest).

While male *Gopherus* have longer tails than females in all species, Sinaloan lineage tortoises differed highly significantly from the other desert tortoises in having a very short tail in both sexes ($F_{5,153} = 56.044$; $p < 0.0005$) (Fig. 4). The tails of female Sinaloan tortoises were frequently little more than nubs (2–8 mm) and those of males and female *G. agassizii* were the same size (<13 mm).

Subdued shell mottling and spotting differed highly significantly in Sinaloan lineage tortoises (orange hues) versus *G. agassizii* and Sonoran *G. morafkai* ($F_{5,162} = 49.118$; $p < 0.0005$) (Fig. 5); the shells of both *G. morafkai* and *G. agassizii* were medium to dark

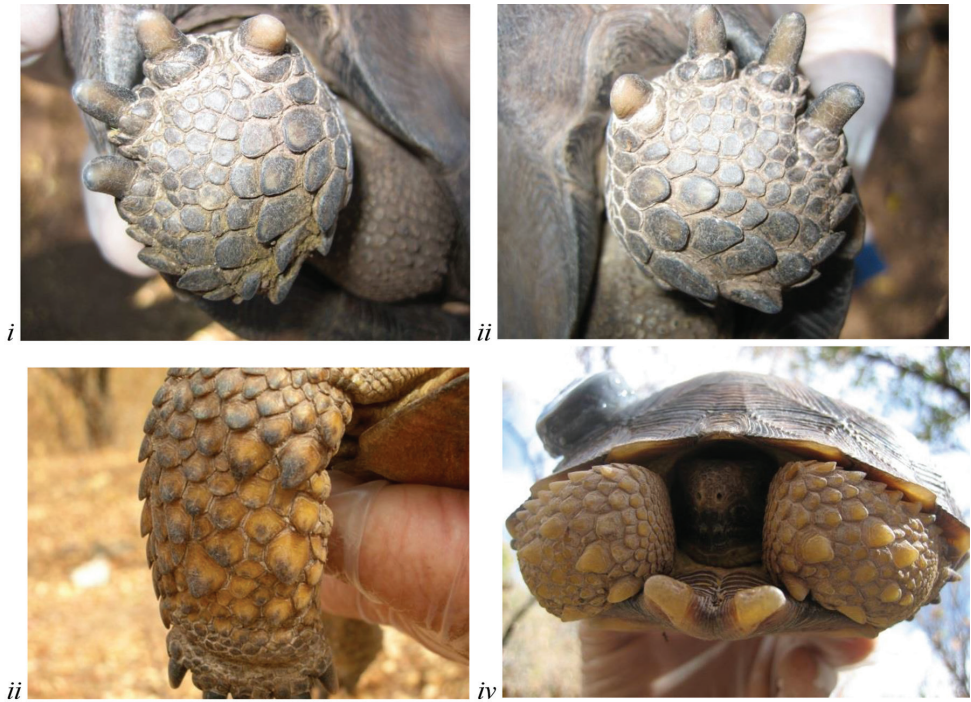


Figure 3. The rounded ventral surface of the rear feet (i–ii) and multiple enlarged, raised scales present on surface of forelegs generally (iii–iv) diagnose *G. evgoodei* in relation to other species of desert tortoises. i–ii same individual in Figure 2 from Rancho Las Cabras near Alamos, Sonora, Mexico (in Tropical Deciduous Forest) iii–iv two individuals from Rancho Las Cabras.

brown or dark gray, sometimes with a subtle greenish hue and generally dark gray to dark brownish-gray near scute interfaces. The integument of *G. morafkai* and *G. agassizii* tortoises was dark gray to brownish-gray and this differed highly significantly from the dark tan to medium-brownish coloration, with a distinctly orange cast, in Sinaloan lineage tortoises ($F_{5,152} = 58.137$; $p < 0.0005$).

The concavity on the plastron of male Sinaloan lineage tortoises was similar to that of *G. morafkai* yet highly significantly shallower than that of *G. agassizii* ($F_{5,77} = 17.885$; $p < 0.0005$). Several other morphological characters appeared to consistently diagnose the Sinaloan lineage tortoises. Sinaloan lineage tortoises typically displayed rounded pads on the rear feet (Fig. 3) while the pads of *G. agassizii* in the northern Mojave Desert were generally flat. Whereas the Sinaloan lineage tortoises were distinctly bulbous over the pre-frontal scales in profile, *G. agassizii* in the Sonoran Desert of California was generally rounded (Fig. 6), and Mexican *G. morafkai* was flat to slightly round. The nictitating membrane of tortoises of the Sinaloan lineage was generally pink and enlarged. In *G. morafkai*, and less so in *G. agassizii*, the nictitans may have been enlarged but rarely pink, and, if pink, it indicated an inflammation (USFWS 2013).

Area of occurrence

Analyses using GeoCAT suggested that the distribution of the Sinaloan lineage encompassed roughly 24,000 km². We could not calculate the area of occupancy owing to the limited number of data points.

To varying degrees, some of these morphological differences have been recognized in other studies (Bogert and Oliver 1945; Loomis and Geest 1964; Hardy and McDiarmid 1969; Germano 1993; Fritts and Jennings 1994; Berry et al. 2002; Bury et al. 2002; Legler and Vogt 2013). The new genetic assessments (Edwards et al. 2015, 2016) and our morphological analyses and assessment of habitat preferences suggest that *G. morafkai* is a composite of two species. As such, the current taxonomy may negatively affect efforts to conserve both species. Herewith, we describe the Sinaloan lineage of desert tortoise as a new species.

***Gopherus evgoodei* Edwards, Karl, Vaughn, Rosen, Meléndez Torres & Murphy, sp. n.**
<http://zoobank.org/125138E1-31AC-4FE5-8971-2F3D0A5113B8>

Figs 6–14

Goode's Thornscrub Tortoise

Xerobates agassizii Cooper, 1861 (partim)

Gopherus agassizii (Cooper, 1861) (partim). Generic reassignment by Stejneger (1893)

Scaptochelys agassizii (Cooper 1861) (partim). Generic reassignment by Bramble (1982)

Xerobates lepidocephalus (ex errore) Otlely and Velázquez Solis 1989. In error by Crumly and Grismer (1994)

Gopherus morafkai Murphy, Berry, Edwards, Leviton, Lathrop & Riedle, 2011 (partim)

Holotype. AMNH (American Museum of Natural History) R64160; adult male from Alamos (approximate location 27°02'N, 108°55'W, elevation 433 m), Sonora, Mexico, collected on 27 August–2 September 1942 by Charles M. Bogert and preserved in ethanol (Figs 6–14).

Paratypes. AMNH R64157, an adult male; AMNH R64158, an adult female; and ROM (Royal Ontario Museum) 53301 (formerly AMNH R64159), an adult female; all with same collecting data as the holotype and all preserved in ethanol.

Referred specimens. ASU (Arizona State University, Tempe) 6427, ASU 6543–44, ASU 6605–06, ASU 6620–22, ASU 6702–03, ASU 6769, ASU 8534–39, CAS (California Academy of Sciences) 142243, CM (Carnegie Museum) Herps:62200, CNAR (Colección Nacional de Anfibios y Reptiles)-4002, LACM (Los Angeles County Museum) 105338, LSUMZ (Louisiana State University Museum of Zoology, Baton Rouge) 34925, MSB (Museum of Southwestern Biology) MSB 41497–99, MVZ (Museum of Vertebrate Zoology) 129943, SMNS (Staatliches Museum fuer Naturkunde, Stuttgart) 7367–68, SMNS 7515, TNHC (Texas Memorial Museum) 60607, UAZ (University of Arizona) 28105, UAZ 35405, UAZ 36875–76,

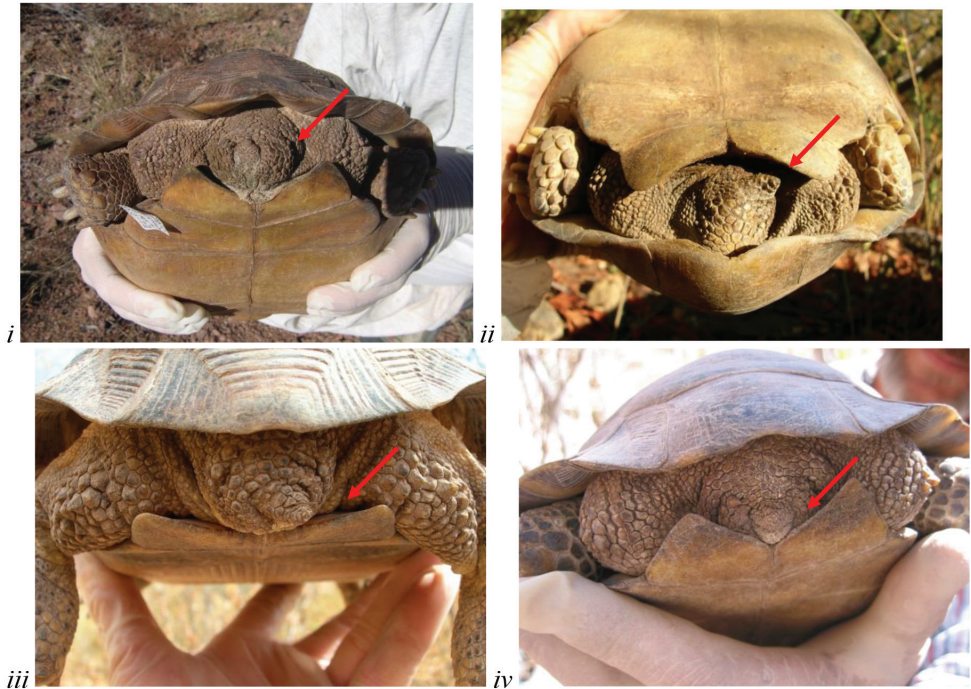


Figure 4. *Gopherus evgoodei* differs from other species of desert tortoises in having a very short tail. **i** Rancho El Chupadero east of Guaymas (in thornscrub habitat); **ii** Rancho Las Cabras; and **iii–i** Rancho La Sierrita near Alamos, Sonora, Mexico (in Tropical Deciduous Forest).

UAZ 56589-PSV, UAZ 56607-PSV, and UIMNH (University of Illinois Museum of Natural History) 85836.

Diagnosis. Molecular data can readily diagnose all species of *Gopherus* and their hybrids (Murphy et al. 2011; Edwards et al. 2016). Morphologically, *G. evgoodei*, *G. agassizii* and *G. morafkai* (the *agassizii* group) can be separated generally from both *G. flavomarginatus* Legler and *G. polyphemus* (Daudin) in having relatively smaller front feet. Whereas the distance from the bases of the first to fourth claws is the same on all feet in the *agassizii* group, in the latter two species the distance from the bases of the first and third claws on the forelimb is about the same as the distance between the bases of the first and fourth claws on the hindlimb (Auffenberg and Franz 1978). Living captive specimens of the *agassizii* group and *G. berlandieri* cannot all be distinguished morphologically because of extensive hybridization (Edwards et al. 2010) and developmental abnormalities in shell, head and limb integument from poor nutrition (Donoghue 2006). However, in native non-hybrid individuals, *G. berlandieri* can be separated from the *agassizii* group in having a wedge-shaped snout when viewed from above in contrast to a rounded snout (Fig. 12) (Auffenberg and Franz 1978). Further, the gular projections of *G. berlandieri* often diverge in large males and the species often exhibits paired axillary scales preceding each bridge. In contrast, the gular projections do not normally diverge in the *agassizii* group and there is a single axillary



Figure 5. *Gopherus evgoodei* differs from other species of desert tortoises in often having yellow/orange integument (skin) and shell. **i** Rancho El Divisadero **ii–iii** Rancho Las Cabras; and **iv–v** Rancho La Sierrita near Alamos, Sonora, Mexico (in Tropical Deciduous Forest).

scale. Morphological characters among the *agassizii* group exhibit overlap (Germano 1993; McLuckie et al. 1999) and characters like coloration in desert tortoises can be highly variable (Legler and Vogt 2013). However, *G. evgoodei* differs from *G. morafkai*



Figure 6. Dorsal view of the holotype of *Gopherus evgoodei*, AMNH R64160. Scale bar 50 mm in 10 mm increments.

and *G. agassizii* (Table 1). *Gopherus evgoodei* is flatter in shell profile (Fig. 2). It has rounded foot pads, multiple enlarged spurs on the radial-humeral joint (Fig. 3). The new species has short tails (Fig. 4), orange tones in the integument (skin) and shell (Fig. 5), and a distinctly shallower concavity on the plastron of males.

Description of holotype (parallels that of *G. morafkai* by Murphy et al. 2011). An adult male, with carapace length at the midline (MCL) = 209 mm; curved carapace length from nuchal scute to supracaudal scute = 254 mm; plastron from tip of gular horn to tip of anal scutes = 219 mm; plastron from gular notch to anal notch = 202 mm; maximum height of shell at 3rd vertebral scute = 83 mm; width at 3rd/4th marginal scute seam = 137 mm; width at 6th marginal scute = 140 mm; greatest width at mid-8th marginal scute = 158 mm; plastron concavity depth = 10.1 mm; head length = 51.3 mm; and tail = 8 mm. Eleven marginal scutes present on both right and left edges of the carapace. Five toenails present on each forelimb and four toenails on each hind limb. The third nail of each hind limb slightly longer than the others. Multiple enlarged, raised scales present on the anterior ventral surface of each foreleg. No scale “spikiness” on the posterior femoral surface of the rear legs. Scales on head smooth and asymmetrical, with two large pre-frontal scales and smaller scales in the temporal area. Shape of head prefrontal profile rounded/bulging. Shell profile/shape of the carapace appearing nearly flat. Shape of ventral surface of rear feet rounded and lacking projecting, enlarged scales on the posterior plantar surface. Areolae and >17 growth

Table 1. Least-square means (LSM) and sample size (N) for ANOVA for five morphometric characters that are highly descriptive for *G. evgoodei* and frequency percentages for one character. Mixed samples from localities in the Sinaloan thornscrub-Sonoran desertscrub ecotone with the occurrence of both *G. evgoodei* and *G. morafkai* genotypes and/or hybrids. Carapace shape measures ‘roundness’ of carapace.

| Lineage (Location) | Variable | | | | | | | | | | | |
|---|-------------|----|------------------|----|-------------|----|-------------------------|----|----------------|----|---------------|----|
| | Shell Color | | Integument color | | Tail length | | Male plastron concavity | | Carapace shape | | Humeral spurs | |
| | LSM | N | LSM | N | LSM | N | LSM | N | LSM | N | % with spurs | N |
| <i>G. evgoodei</i> (Mexico) | 601.686 | 35 | 593.543 | 35 | 0.61 | 33 | 10.185 | 17 | 0.419 | 36 | 100.0 | 37 |
| Mixed <i>G. evgoodei</i> / <i>G. morafkai</i> (Mexico) | 574.8 | 10 | 560.667 | 9 | 0.778 | 9 | 13.8 | 4 | 0.447 | 10 | 62.5 | 8 |
| <i>G. morafkai</i> (Mexico) | 548.25 | 16 | 541.563 | 16 | 0.833 | 12 | 11.35 | 8 | 0.454 | 16 | 25.0 | 16 |
| <i>G. agassizii</i> (Imperial County, California) | 562.706 | 17 | 546.882 | 17 | 0.947 | 19 | 25.312 | 10 | 0.449 | 18 | 15.8 | 19 |
| <i>G. agassizii</i> (San Bernardino County, California) | 549.654 | 26 | 552.882 | 17 | 0.96 | 25 | 19.786 | 8 | 0.461 | 25 | 73.9 | 23 |
| <i>G. agassizii</i> (Kern County, California) | 563.219 | 64 | 543.578 | 64 | 0.934 | 61 | 22.844 | 36 | 0.454 | 63 | 74.6 | 63 |



Figure 7. Ventral view of the holotype of *Gopherus evgoodei*, AMNH R64160. Scale bar 50 mm in 10 mm increments.



Figure 8. Anterior view of the holotype of *Gopherus evgoodei*, AMNH R64160.

laminae present on all carapacial scutes, although areola are diminishing, especially on the anterior scutes. In alcohol, the color of areolae dark, fading to dark brown with orange hue in outer portion of carapacial scutes. Color of areolae on the plastron dark brown and rest of the plastron medium orange brown. Head and neck tan to dark tan with an orange hue. Skin in the axillary and inguinal areas lighter in coloration; light tan fading to medium tan toward axillary. Nails dark brown, lighter brown at the tips.

Coloration of the species in life. *Gopherus evgoodei* may exhibit orange or yellow mottling or spotting on the shell and integument. Because color constitutes a diagnostic feature, these data are given above.

Variation. As with all species of *Gopherus*, substantial variability exists among individuals for most morphological features (Germano 1993; McLuckie et al. 1999). Bogert and Oliver (1945) first recognized the distinct morphology of tortoises at Alamos, but they were unable to quantify it due to small sample sizes. Shell profile is generally flat but may also appear domed in some individuals. Spikiness of scales on forelimbs can vary widely and the shape of the plantar surface of the rear feet, while generally rounded, can be difficult to classify in some cases.

Distribution. The distribution of *G. evgoodei* (Fig. 1) occupies roughly 24,000 km² and corresponds to habitat. The species primarily occurs in tropical deciduous forest (TDF) and relatively mesic Sinaloan thornscrub (STS) in the state of Sonora, Mexico, and its distribution extends southward into TDF and the southern part of the



Figure 9. Posterior view of the holotype of *Gopherus evgoodei*, AMNH R64160.

STS where it still remains intact in northern Sinaloa south of the Río Fuerte (Loomis and Geest 1964; Edwards et al. 2015). It also occurs in the TDF of extreme southwestern Chihuahua (Smith et al. 2004). Thus, *G. evgoodei* occupies both STS and Sinaloan TDF (Fritts and Jennings 1994; Berry et al. 2002). The eastern limit of its known range is the foothills of the Sierra Madre Occidental at elevations of 800–1,000 m where the TDF transitions rather abruptly into oak woodlands (Bury et al. 2002). Although the southern limit of its range remains undetermined, continuous TDF extends along the West Coast of Mexico from Sonora through Sinaloa to Nayarit (>500 km), although it only maintains an average width of 50 km (Krizman 1972). It is unlikely that *G. evgoodei* occurs very much further south in Sinaloa than currently known, or as far south as Nayarit, based on an absence of records for this relatively conspicuous and readily recognizable animal, and presumably due to as yet unidentified environmental limitations (Bury et al. 2002). The northern boundary of *G. evgoodei* corresponds approximately to the transition from STS to SDS (Edwards et al. 2015). Although characteristic thornscrub maintains 100% ground cover, where it grades into desertscrub it becomes patchy (Felger et al. 2001). The transition of TDF and thornscrub to desertscrub dominated by more xeric species often occurs at elevations between 200 and 300 m a.s.l., but with notable exceptions (Van Devender et al. 2000). Broadly, the distribution approaches



Figure 10. Left lateral view of the holotype of *Gopherus evgoodei*, AMNH R64160.



Figure 11. Right lateral view of the holotype of *Gopherus evgoodei*, AMNH R64160.

the boundary of the Sonoran Desert as defined by Brown and Lowe (1980) and Turner (1982). However, this transition zone is patchy, with a mosaic of SDS and STS. Both *G. morafkai* and *G. evgoodei* occur in the more arid, desert-like ecotone-phase of STS, where limited hybridization has been observed (Edwards et al. 2015; Fig. 1). As such, we conservatively estimate the distribution of *G. evgoodei* by excluding sites where *G. evgoodei* and *G. morafkai* come into contact (Fig. 1).

Natural history. *Gopherus agassizii*, *G. morafkai* and *G. evgoodei* appear to have diverged roughly 5.7–5.9 Ma from a common ancestor that was potentially widespread throughout what is now the Mojave, Colorado and Sonoran desert regions (Edwards et



Figure 12. Detail of head scales of the holotype of *Gopherus evgoodei*, AMNH R64160.

al. 2016). *Gopherus agassizii* likely diverged first via allopatric speciation when the Bouse embayment extended northward between 8–4 Ma (Lamb et al. 1989). This waterway (now the Colorado River) created a barrier between the Sonoran and Mojave deserts. About the same time, *G. morafkai* and *G. evgoodei* began to segregate into tropical and arid ecosystems, possibly under a parapatric model of speciation (ecological isolation), although allopatric speciation owing to climatic change and ephemeral isolation can also explain the split. By the end of the Miocene (5.3 Ma) much of the Sonoran region was likely covered in tropical forests or desert thornscrub but orogenesis initiated the drying trend that led to the formation of the current North American deserts. The changing environment would have created new arid niches in the northern portion of the ancestral range of the desert tortoise. This could have started the ecological divergence of the three species.

Microhabitat. Ecologically, *G. evgoodei* occupies hills and low mountains with at least some large boulders or rock outcrops in the TDF, and the TDF–STS ecotone. Its



Figure 13. Detail of the tail of the holotype of *Gopherus evgoodei*, AMNH R64160.



Figure 14. Ventral surface of the right rear foot of the holotype of *Gopherus evgoodei*, AMNH R64160.

distribution differs from *G. morafkai* by its strong association with TDF and STS, as well as its absence from SDS. Similar to *G. morafkai*, *G. evgoodei* often associates with slopes where rock outcrops and boulders are common. In TDF, the tortoise generally

excavates burrows under already existing boulders or enters and modifies existing rock cavities. In flatter areas where boulders are not be available, it digs burrows in soil, although possibly not as extensively as its congeners. During 2012–2013 surveys in Sonora, only 9 of 44 tortoise burrows (20%) in TDF were in soil. In comparison, 56 of 87 burrows (64%) occurred in soil in STS and SDS. Local variation was not surprising. In northern Sinaloa, Vargas V (1994) reported *G. evgoodei* used packrat middens, dry cacti and even burrows dug by other animals (e.g. nine-banded armadillo, *Dasyplus novemcinctus*). Our observations of *G. evgoodei*, as part of an ongoing radio-telemetry study near Alamos, Sonora, suggested that Goode's Thornscrub Tortoise uses several burrows a year and exhibits strong site-tenacity, returning to familiar dens year after year (unpublished data), just like its sister-species.

Activity. Presumably, tortoise activity corresponds with monsoonal rains and vegetation growth (Bury et al. 2002). Goode's Thornscrub Tortoise is active from at least June well into November; we lack data on activity during the dry season. In Sonora, the TDF hugs the western edge of the Sierra Madre Occidental and the biome hosts extremely lush vegetation during periods of summer rainfall (July–September). During dry periods, the TDF is almost entirely leafless, but with many spectacularly blooming trees and large columnar cacti (Krizman 1972; Van Devender et al. 2000).

Little is known about daily activity patterns, reproduction, movements or forage of *G. evgoodei*. Like other species of *Gopherus*, their activity relates to forage availability and ambient temperatures. Van Devender et al. (2002) reported that scat from tortoises near Alamos, Sonora contained many species of plants not found in the Sonoran Desert, suggesting differences in foraging activity and selection, although species-availability might also account for this. We observed adults to begin seasonal activity shortly in advance of the growth of forage, usually in June at the leading edge of the monsoons, and enter winter dens by sometime in December and remain underground during the dry, cool winter season (unpublished data).

Etymology. The new species is a patronym, a noun in the genitive case, in recognition of Eric V. Goode, a conservationist, naturalist, and founder of the Turtle Conservancy. He has contributed generously to the conservation of this species via the preservation of land in Mexico, and he actively pursues the conservation of turtles and tortoises on a global scale. Eric sets an important precedent by complementing this taxonomic description with a tangible action that contributes to the conservation of the new species in its native habitat.

Discussion

Few paratypes

We designate paratypes conservatively to exclude the possibility of hybrid individuals that could confound the identity of *G. evgoodei* (Edwards et al. 2010).

Comparisons

Because of the high level of variability within all species of *Gopherus*, descriptions based on only a few individuals or individuals from few populations should be viewed cautiously. For instance, Germano (1993) calculated that female *G. evgoodei* were larger than female *G. agassizii* from the Mojave Desert, but our larger sample set indicates this is not the case. Legler and Vogt (2013) compared the basic proportions among *G. agassizii*, *G. morafkai* and *G. evgoodei* (as Mojave, Sonoran and Sinaloan tortoises, respectively) and also suggested that *G. evgoodei* was slightly smaller. However, analysis was also generated from a very limited dataset. Populations (sampling localities) of *G. agassizii* differ widely in sizes of adults, with some populations hosting very large animals, including females, such as those in the northwestern Mojave Desert, and some hosting relatively small adult females (A. Karl; unpublished data).

Our divergence estimates for *COI* are consistent with species-level divergence in other chelonians (*Cytb*, 2.8–18.3%; Vargas-Ramirez et al. 2010). Other species of tortoises with large, continuous distributions do not exhibit the deep phylogenetic structure we observe within *G. morafkai* between the Sonoran and Sinaloan lineages; for example within *Gopherus polyphemus* (Daudin) (1.5%, *ND4*; Ennen et al. 2012), *Testudo hermanni* Gmelin (1.48%, *Cytb*; Fritz et al. 2006) and *Stigmochelys pardalis* (Bell) (1.47%, *Cytb*; Fritz et al. 2010). In addition, these studies observed a range of divergences between haplogroups (intermediate haplogroups) in network analyses as opposed to the deeply bifurcating tree that typifies the matrilineal genealogy of *G. morafkai*. Some species of tortoises exhibit distinct matrilineal (mtDNA lineages), such as the *Testudo graeca* Linnaeus complex (mean: 3.35%, *Cytb*; Fritz et al. 2007). However, in many such cases gene flow is maintained across nuclear markers. This condition has been deemed to support the recognition of subspecies (Mashkaryan et al. 2013; Mikulicek et al. 2013). In contrast, Edwards et al. (2015) did not observe cytonuclear discordance between *G. evgoodei* and *G. morafkai*. The Chaco tortoise, *Chelonoidis chilensis* (Gray), of Argentina and Paraguay is perhaps the most appropriate comparison in that it has similar latitudinal range (>1,500 km), exhibits clinal variation, and occupies a variety of arid environments, including plains, deserts and semi-deserts (Fritz et al. 2012). However, the mtDNA sequence divergence in *C. chilensis* is ~1.37% whereas the corresponding mtDNA sequence divergence between *G. evgoodei* and both *G. agassizii* and *G. morafkai* ranges from 3.4% to 4.2%.

Implications for conservation

Desert tortoises command a strong interest in their conservation. A distinct population segment (DPS) of *G. agassizii* was federally listed in 1990 as threatened under the U.S. Endangered Species Act based on its status (USFWS 1990). *Gopherus morafkai* is considered Wildlife of Special Concern in Arizona (AGFD 2012). Mexican populations

of *Gopherus* (including *G. flavomarginatus*) also receive protection as threatened species (Category A “Amenazada” in NOM-059; SEMARNAT 2010).

Additional field work is necessary to assess the conservation status of *G. evgoodei*, as the above summary is primarily based on observations during field work by Edwards et al. (2015) and does not include an extensive examination of population trends or threats. We lack a comprehensive understanding of its ecology and behavior. *Gopherus evgoodei* has a smaller distribution than either of its sister taxa and it occurs in some of the most threatened habitat of any of the desert tortoises (Martin and Yetman 2000). The conversion of native thornscrub to buffelgrass pasture poses the greatest threat to *G. evgoodei* living in STS habitat. Conversion has specifically targeted STS in central and southern Sonora (Búrquez et al. 2002) and in TDF. Of greatest concern, this action potentially effects the operative thermal environment of the tortoise via dramatic heating. Although some parts of the STS have naturally open, desertscrub-like vegetation, the TDF and much of the STS occupied by *G. evgoodei* is naturally shady in summer. The resultant thermal challenge may be especially acute in STS, which is more arid than TDF and occurs at lower elevations, and thus experiences higher temperatures.

Fortunately, successional forces can restore habitat quality for *G. evgoodei* in some buffelgrass pastures in thornscrub and especially in TDF. Upon cessation of slashing and burning, secondary growth of native, woody species can quickly replace buffelgrass, and there is some evidence for this in thornscrub as well. Many local people are aware that tortoises enjoy protection and are part of nature. Their occurrence benefits society by providing employment in ecotourism and natural resource conservation. A positive trend involves the establishment and partial re-purposing of private ranches as hunting and conservation reserves throughout much of the tortoise’s distribution in Mexico. Part of the distribution of *Gopherus evgoodei* includes natural protected areas in Mexico, including Área de Protección de Flora y Fauna Sierra de Álamos-Río Cucujaqui and certificaded área for conservation Reserva Monte Mojino in Sonora, both relatively recent institutions. If these current trends continue, environmental concerns are likely to tip the balance between pasture and native habitats somewhat in favor of tortoises, particularly if the threats to biodiversity are widely understood. However, these and other impacts on the species, such as the fragmentation of habitat, some mining activities and collection, necessitate further research that can better inform conservation and management efforts.

The recognition of *G. evgoodei* reduces the area of occurrence for *G. morafskai* by about 14% from roughly 171 km² (USFWS 2015) to 147 km². This reduction of 24,000 km² is especially critical in Mexico where the distribution of *G. morafskai* changes from 67,340 km² (USFWS 2015) to only 43,340 km², which is a reduction of almost 34%. By comparison, *G. agassizii* occupies 83,124 km² (Murphy et al. 2011). The IUCN considers *G. agassizii* to be vulnerable to extinction (TFTSP 1996). This designation is an umbrella covering the nominate form plus *G. morafskai* and *G. evgoodei*. We encourage the IUCN to prepare updated assessments of the three species of *Gopherus*, as they are likely to meet the criteria for the Threatened category, particularly *G. agassizii* and *G. evgoodei*. Finally, all testudinids enjoy protection at least

in Appendix II of CITES and *G. flavomarginatus* is the only *Gopherus* with Appendix I protection. *Gopherus evgoodei* may also qualify for listing in Appendix I given its highly restricted distribution, our limited knowledge of it, threat from habitat modification and its potential to be targeted for illegal trade as a rare, charismatic animal.

Conclusion

For decades, herpetologists have noted the distinctiveness of Mexican populations of desert tortoises in the southern part of the range of *G. morafkai*, particularly where they occur in STS and TDF. Our review of recent studies sheds light on the ecology, morphology and genetics of these southern populations, which warrant species recognition of this southernmost group. Divergence estimates for *COI* and *Cytb* are consistent with species-level differences in other chelonians. *Gopherus evgoodei* primarily occurs in the state of Sonora, Mexico, extending southward into the northerly extensions of TDF in southern Sonora, northern Sinaloa, and extreme southwestern Chihuahua. The new species occurs only in STS and TDF, leaving it the smallest distribution of the three species of desert tortoises. It is important to define accurately the limits of its distribution, especially because it may occur further south in Mexico. Molecular analyses can easily diagnose all species of *Gopherus* and their hybrids (Edwards et al. 2016). Further, morphologically, *G. evgoodei* is easily distinguished from *G. morafkai* and *G. agassizii* by several characters, among the most obvious of which is the coloration of both the shell and integument. *Gopherus evgoodei* is a dark tan to medium-brownish tortoise with a distinctly orange cast. To assess the conservation status of *G. evgoodei*, additional field work is necessary as very little research on this newly described species exists and a comprehensive understanding of its ecology and behavior must be determined to inform conservation and management initiatives.

Acknowledgments

We obtained Mexican samples through a multinational, collaborative effort including Comisión de Ecología y Desarrollo Sustentable del Estado de Sonora (CEDES) and F.R. Méndez de la Cruz, Instituto de Biología, Universidad Nacional Autónoma de México (UNAM). Permits for Mexican samples were facilitated by Secretaría de Medio Ambiente y Recursos Naturales (SEMARNAT). Special thanks to Delegaciones de SEMARNAT Sonora, Sinaloa y Chihuahua, Procuraduría Federal de Protección al Ambiente (PROFEPA) and for the “Área de Protección de Flora y Fauna Sierra de Álamos-Río Chahujaqui” from Comisión Nacional de Áreas Naturales Protegidas (CONANP). The collection of samples was only made possible by a dedicated field crew of over 50 volunteers over an 8 year period. Special thanks go to K. Berry, S. Bolland, A. Leon, M. Figueroa, L. Smith and P. Woodman. Access to almost all of the collection sites in Mexico was made possible through the generosity of local land owners

and we are extremely grateful for the assistance of ranch hands (vaqueros) who shared their local knowledge with us in the field. S. Dunlap assisted with sequencing *COI* and S. Sotak facilitated sequencing at the University of Arizona Genetics Core. We greatly appreciate the assistance of L. Vonnahme and C. Raxworthy and the AMNH who facilitated our request for specimens. Primary funding for this project came from private donors, the Royal Ontario Museum Foundation, Natural Sciences and Engineering Research Council of Canada Discovery Grant 3148 and the U.S. Fish and Wildlife Service, Science Support Program (SSP). Additional funding and support was received from The Tucson Herpetological Society, Desert Tortoise Council, Arizona Game and Fish Department, University of Florida, University of Arizona Genetics Core, the U.S. Geological Survey, Hyundai Motor America and Natural Resources and Environmental Affairs at the Twentynine Palms Marine Corps Air Ground Combat Center.

References

- Auffenberg W, Franz R (1978) *Gopherus*. Catalogue of American Amphibians and Reptiles 211: 1–2.
- Arizona Game and Fish Department [AGFD] (2012) Arizona's State Wildlife Action Plan: 2012–2022. Arizona Game and Fish Department, Phoenix, Arizona, 245 pp.
- Berry KH, Morafka DJ, Murphy RW (2002) Defining the desert tortoise(s): our first priority for a coherent conservation strategy. *Chelonian Conservation and Biology* 4: 249–262.
- Bogert CM, Oliver JA (1945) A preliminary analysis of the herpetofauna of Sonora. *Bulletin of the American Museum of Natural History* 83: 301–425.
- Bramble DM (1982) *Scaptochelys*: generic revision and evolution of gopher tortoises. *Copeia* 1982: 852–867. doi: 10.2307/1444097
- Brown DE (1994) Biotic communities of the southwestern United States and northwestern Mexico. University of Utah Press, Salt Lake City, Utah, 346 pp.
- Brown DE, Lowe CH (1980) Biotic communities of the Southwest. Map. Rocky Mountain Forest and Range Experiment Station, U.S. Forest Service. General Technical Report RM-78. [Map]
- Brown DE, Lowe CH, Pase CP (1979) A digitized classification system for the biotic communities of North America, with community (series) and association examples for the Southwest. *Journal of the Arizona-Nevada Academy of Science* 14: 1–16.
- Búrquez A, Miller M, Martínez-Yrizar A (2002) Mexican grasslands, thornscrub, and the transformation of the Sonoran Desert by invasive exotic buffelgrass (*Pennisetum ciliare*). In: Tellman B (Ed.) *Invasive Species in Sonoran Desert Communities*. University of Arizona Press, Tucson, Arizona, 126–146.
- Bury RB, Germano DJ, Van Devender TR, Martin BE (2002) The desert tortoise in Mexico. In: Van Devender TR (Ed.) *The Sonoran Desert Tortoise; Natural History, Biology, and Conservation*. Arizona-Sonora Desert Museum and University of Arizona Press, Tucson, AZ, 86–108.
- Clostio RW, Martinez AM, LeBlanc KE, Anthony NM (2012) Population genetic structure of a threatened tortoise across the south-eastern United States: implications for

- conservation management. *Animal Conservation* 15: 623–625. doi: 10.1111/j.1469-1795.2012.00557.x
- Cooper JG (1861) New Californian animals. *Proceedings of the California Academy of Sciences* (ser. 1) 2: 118–123.
- Crumly CR, Grismer LL (1994) Validity of the tortoise *Xerobates lepidoccephalus* Ottley and Velazquez [sic] in Baja California. In: Bury RB, Germano DJ (Eds) *Biology of North American Tortoises*. *Fish and Wildlife Research* 13: 32–36.
- Donoghue S (2006) Nutrition. In: Mader R (Ed.) *Reptile Medicine and Surgery*. 2nd ed. Saunders Elsevier, St. Louis, Missouri, 251–298. doi: 10.1016/b0-72-169327-x/50022-5
- Edwards T, Jarchow CJ, Jones CA, Bonine KE (2010) Tracing genetic lineages of captive desert tortoises in Arizona. *Journal of Wildlife Management* 74: 801–807. doi: 10.2193/2009-199
- Edwards T, Vaughn M, Rosen PC, Meléndez-Torres C, Karl AE, Culver M, Murphy RW (2015) Shaping species with ephemeral boundaries; the distribution and genetic structure of the desert tortoise (*Gopherus morafkai*) in the Sonoran Desert. *Journal of Biogeography*. doi: 10.1111/jbi.12664
- Edwards T, Tollis M, Hsieh PH, Gutenkunst RN, Liu Z, Kusumi K, Culver M, Murphy RW (2015) Assessing models of speciation under different biogeographic scenarios; an empirical study using multi-locus and RNA-seq analyses. *Ecology and Evolution*. doi: 10.1002/ece3.1865
- Encyclopedia (2015) Hex Color Code. <http://encycolorpedia.com> [accessed 30 October 2015]
- Ennen JR, Kreiser BR, Qualls CP, Gaillard D, Aresco M, Birkhead R, Tuberville TD, McCoy ED, Mushinsky H, Hentges TWB, Schrey A (2012) Mitochondrial DNA assessment of the phylogeography of the gopher tortoise. *Journal of Fish and Wildlife Management* 3: 110–122. doi: 10.3996/102011-JFWM-063
- Ernst CH, Barbour RW (1989) *Turtles of the World*. Smithsonian Institution Press, Washington D.C.
- Felger RS, Johnson MB, Wilson MF (2001) *Trees of Sonora, Mexico*. Oxford University Press, New York.
- Fritts TH, Jennings RD (1994) Distribution, habitat use, and status of the desert tortoise in Mexico. In: Bury RB, Germano DJ (Eds) *Biology of North American Tortoises*. *Fish and Wildlife Research* 13, US Dept. of the Interior, National Biological Survey, Washington, DC, 49–56.
- Fritz U, Auer M, Bertolero A, Cheylan M, Fattizzo T, Hundsdorfer AK, Sampayo MM, Pretus JL, Široký P, Wink M (2006) A rangewide phylogeography of Hermann's tortoise, *Testudo hermanni* (Reptilia: Testudines: Testudinidae): implications for taxonomy. *Zoologica Scripta* 35: 531–543. doi: 10.1111/j.1463-6409.2006.00242.x
- Fritz U, Hundsdorfer AK, Široký P, Auer M, Kami H, Lehmann J, Mazanaeva LF, Turkozan O, Wink M (2007) Phenotypic plasticity leads to incongruence between morphology-based taxonomy and genetic differentiation in western Palaearctic tortoises (*Testudo graeca* complex; Testudines, Testudinidae). *Amphibia-Reptilia* 28: 97–121. doi: 10.1163/1568-53807779799135
- Fritz U, Daniels SR, Hofmeyr MD, González J, Barrio-Amorós CL, Široký P, Hundsdorfer AK, Stuckas H (2010) Mitochondrial phylogeography and subspecies of the wide-ranging

- sub-Saharan leopard tortoise *Stigmochelys pardalis* (Testudines: Testudinidae) – a case study for the pitfalls of pseudogenes and GenBank sequences. *Journal of Zoological Systematics and Evolutionary Research* 48: 348–359. doi: 10.1111/j.1439-0469.2010.00565.x
- Fritz U, Alcalde L, Vargas-Ramirez M, Goode EV, Fabius-Turoblin DU, Praschag P (2012) Northern genetic richness and southern purity, but just one species in the *Chelonoidis chilensis* complex. *Zoologica Scripta* 41: 220–232. doi: 10.1111/j.1463-6409.2012.00533.x
- Germano DJ (1993) Shell morphology of North American tortoises. *American Midland Naturalist* 129: 319–335. doi: 10.2307/2426513
- Germano DJ, Bury RB, Esque TC, Fritts TH, Medica PA (1994) Range and habitats of the desert tortoise. In: Bury RB, Germano DJ (Eds) *Biology of North American Tortoises*. U.S. Department of Interior, National Biological Survey, Fish and Wildlife Research 13: 73–84.
- Gutenkunst RN, Hernandez RD, Williams SH, Bustamante CD (2009) Inferring the joint demographic history of multiple populations from multidimensional SNP frequency data. *PLoS Genetics* 5: e1000695. doi: 10.1371/journal.pgen.1000695
- Hardy LM, McDiarmid RW (1969) *The amphibians and reptiles of Sinaloa, Mexico*. University of Kansas Publications, Museum of Natural History 18: 39–252.
- Krizman RD (1972) *Environment and Season in a Tropical Deciduous Forest in Northwestern Mexico*. Ph.D. Dissertation, University of Arizona, Tucson, AZ.
- Lamb T, Avise JC, Gibbons JW (1989) Phylogeographic patterns in mitochondrial-DNA of the desert tortoise (*Xerobates agassizi* [sic]), and evolutionary relationships among the North-American gopher tortoises. *Evolution* 43: 76–87. doi: 10.2307/2409165
- Legler J, Vogt RC (2013) *The Turtles of Mexico: Land and Freshwater Forms*. University of California Press, Oakland, CA, USA.
- Librado P, Rozas J (2009) DnaSP v5: A software for comprehensive analysis of DNA polymorphism data. *Bioinformatics* 25: 1451–1452. doi: 10.1093/bioinformatics/btp187
- Loomis RB, Geest JC (1964) The desert tortoise *Gopherus agassizii* in Sinaloa, Mexico. *Herpetologica* 20: 203.
- Martin PS, Yetman DA, Fishbein M, Jenkins P, Van Devender TR, Wilson RK (Eds) (1998) *Gentry's Río Mayo Plants. The Tropical Deciduous Forest and Environs of Northwest Mexico*. University of Arizona Press, Tucson, Arizona, 558 pp.
- Martin PS, Yetman DA (2000) Introduction and prospect; secrets of a tropical deciduous forest. In: Robichaux RH, Yetman DA (Eds) *The Tropical Deciduous Forest of Alamos: Biodiversity of a Threatened Ecosystem in Mexico*. University of Arizona Press, Tucson, AZ, 3–18.
- Mashkaryan V, Vamberger M, Arakelyan M, Hezaveh N, Carretero MA, Corti C, Harris DJ, Fritz U (2013) Gene flow among deeply divergent mtDNA lineages of *Testudo graeca* (Linnaeus, 1758) in Transcaucasia. *Amphibia-Reptilia* 34: 337–351. doi: 10.1163/15685381-00002895
- McLuckie AM, Lamb T, Schwalbe CR, McCord RD (1999) Genetic and morphometric assessment of an unusual tortoise (*Gopherus agassizii*) population in the Black Mountains of Arizona. *Journal of Herpetology* 33: 36–44. doi: 10.2307/1565541
- Mikulicek P, Jandzik D, Fritz U, Schneider C, Siroky P (2013) AFLP analysis shows high incongruence between genetic differentiation and morphology-based taxonomy in a

- widely distributed tortoise. *Biological Journal of the Linnean Society* 108: 151–160. doi: 10.1111/j.1095-8312.2012.01999.x
- Murphy RW, Berry KH, Edwards T, Leviton AE, Lathrop A, Riedle JD (2011) The dazed and confused identity of Agassiz's land tortoise, *Gopherus agassizii* (Testudines, Testudinidae) with the description of a new species, and its consequences for conservation. *ZooKeys* 113: 39–71. doi: 10.3897/zookeys.113.1353
- Murphy RW, Crawford AJ, Bauer AM, Che J, Donnellan SC, Fritz U, Haddad CFB, Nagy ZT, Poyarkov NA, Vences M, Wang W, Zhang Y-p (2013) Cold Code: the global initiative to DNA barcode amphibians and nonavian reptiles. *Molecular Ecology Resources* 13: 161–167. doi: 10.1111/1755-0998.12050
- Osentoski MF, Lamb T (1995) Intraspecific phylogeography of the gopher tortoise, *Gopherus polyphemus*: RFLP analysis of amplified mtDNA segments. *Molecular Ecology* 4: 709–718. doi: 10.1111/j.1365-294X.1995.tb00271.x
- Ottley JR, Velázquez Solís VM (1989) An extant, indigenous tortoise population in Baja California Sur, Mexico, with the description of a new species of *Xerobates* (Testudines: Testudinidae). *Great Basin Naturalist* 49: 496–502.
- Secretaría de Medio Ambiente y Recursos Naturales [SEMARNAT] (2010) Norma Oficial Mexicana NOM-059-SEMARNAT-2010. Diario Oficial de la Federación (DOF). [jueves 30 de diciembre de 2010]
- Smith HM, Chiszar D, Lemos-Espinal A, Woolrich-Piña JG (2004) Geographic distribution: *Gopherus agassizii*. *Herpetological Review* 35: 284.
- Stejneger L (1893) Annotated list of the reptiles and batrachians collected by the Death Valley Expedition in 1891, with descriptions of new species. *North American Fauna* 7: 159–228. doi: 10.3996/nafa.7.0002
- Stuart BL, Parham JF (2004) Molecular phylogeny of the critically endangered Indochinese box turtle (*Cuora galbinifrons*). *Molecular Phylogenetics and Evolution* 31: 164–177. doi: 10.1016/S1055-7903(03)00258-6
- Toews DPL, Brelsford A (2012) The biogeography of mitochondrial and nuclear discordance in animals. *Molecular Ecology* 21: 3907–3930. doi: 10.1111/j.1365-294X.2012.05664.x
- Turner RM (1982) Sonoran desert scrub. *Desert Plants* 4: 181–221.
- Tortoise and Freshwater Turtle Specialist Group [TFTSG] (1996) *Gopherus agassizii*. The IUCN Red List of Threatened Species 1996: e.T9400A12983037. doi: 10.2305/IUCN.UK.1996.RLTS.T9400A12983037.en
- U.S. Fish and Wildlife Service [USFWS] (1990) Endangered and threatened wildlife and plants: Determination of threatened status for the Mojave population of the desert tortoise. *Federal Register* 55: 12178–12191.
- U.S. Fish and Wildlife Service [USFWS] (2013) Health assessment procedures for the Mojave desert tortoise (*Gopherus agassizii*): a handbook pertinent to translocation. Desert Tortoise Recovery Office, U.S. Fish and Wildlife Service, Reno, Nevada.
- U.S. Fish and Wildlife Service [USFWS] (2015) Species status assessment for the Sonoran desert tortoise. Version 1.0, September 2015. U.S. Fish and Wildlife Service, Southwest Region, Albuquerque, NM.

- Van Devender TR, Sanders AC, Wilson RK, Meyer SA (2000) Vegetation, flora, and seasons of the Río Cuchujaqui, a tropical deciduous forest near Alamos, Sonora, México. In: Robichaux RH, Yetman DA (Eds) The Tropical Deciduous Forest of Alamos: Biodiversity of a Threatened Ecosystem in Mexico. University of Arizona Press, Tucson, AZ, 36–101.
- Van Devender TR, Averill-Murray RC, Esque TC, Holm PA, Dickenson VM, Schwalbe CR, Wirt EW, Barrett SL (2002) Grasses, mallows, desert vine, and more: diet of the desert tortoise in Arizona and Sonora. In: Van Devender TR (Ed.) The Sonoran Desert Tortoise: Natural History, Biology, and Conservation. University of Arizona Press and the Arizona-Sonora Desert Museum, Tucson, AZ, 159–193.
- Vargas VH (1994) Estudio de la densidad poblacional de la tortuga del desierto (*Gopherus agassizii*) en la zona norte del Estado de Sinaloa. Informe final de servicio Social Profesional, Universidad Occidente Unidad Los Mochis, Sinaloa, Mexico.
- Vargas-Ramirez M, Vences M, Branch WR, Daniels SR, Glaw F, Hofmeyr MD, Kuchling G, Maran J, Papenfuss TJ, Siroky P, Vieites DR, Fritz U (2010) Deep genealogical lineages in the widely distributed African helmeted terrapin: evidence from mitochondrial and nuclear DNA (Testudines: Pelomedusidae: *Pelomedusa subrufa*). Molecular Phylogenetics and Evolution 56: 428–40. doi: 10.1016/j.ympev.2010.03.019